MICHIGAN STATE UNIVERSITY

DIVISION OF ENGINEERING RESEARCH

MICHIGAN DEPARTMENT OF STATE HIGHWAYS AND TRANSPORTATION

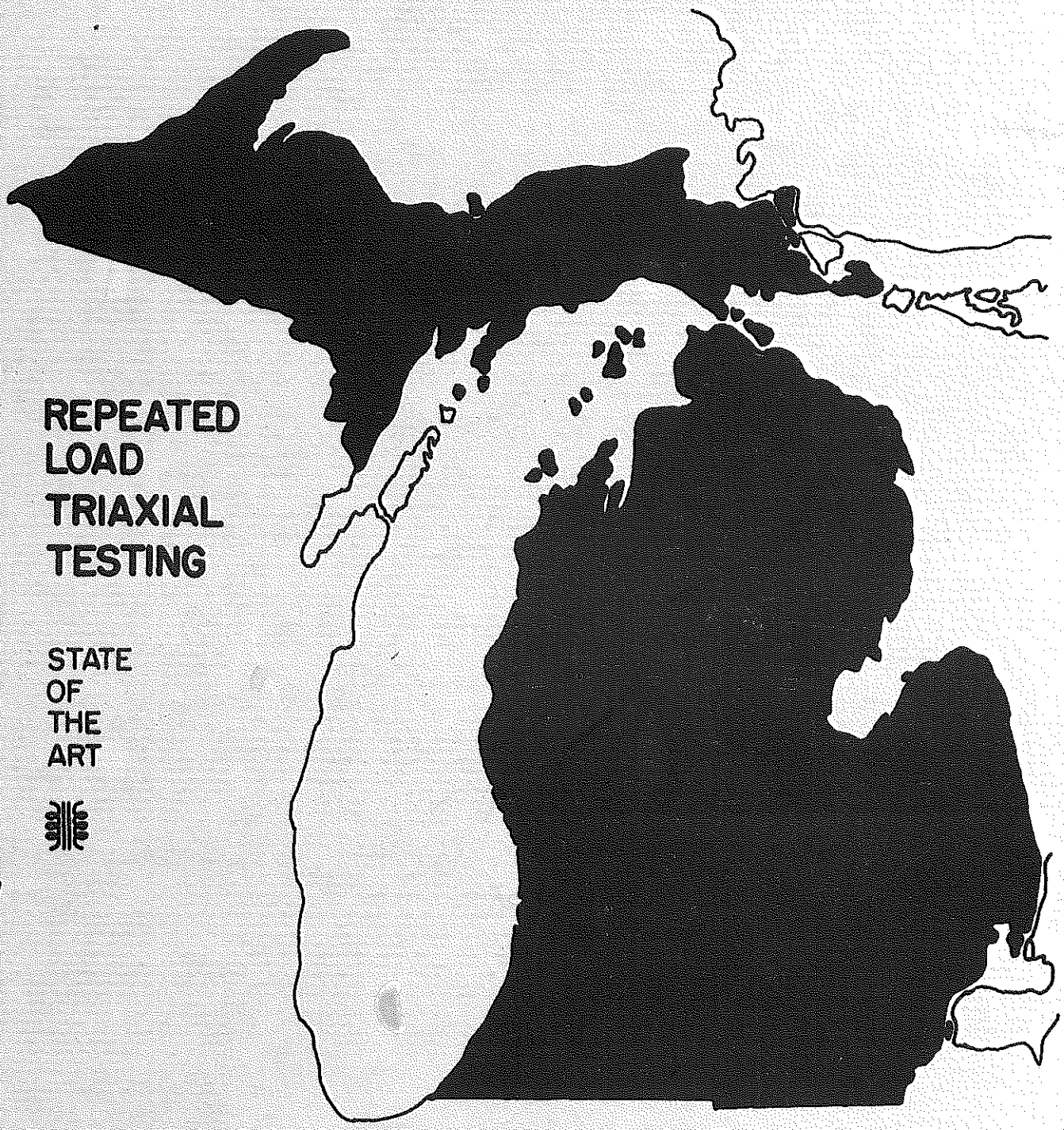

REPEATED LOAD TRIAXIAL TESTING

STATE OF THE ART

M. A. YOUNG and G. Y. BALADI

REPEATED LOAD TRIAXIAL TESTING STATE OF THE ART

by

M. A. Young and G. Y. Baladi

Department of Civil Engineering

STATE OF THE ART REPORT OF RESEARCH CONDUCTED UNDER RESEARCH GRANT 75-1679

RESILIENT MODULUS AND DAMPING RATIO IN CORRELATION TO SOIL SUPPORT VALUE FOR MICHIGAN ROADBED SOILS

SPONSORED BY THE

MICHIGAN DEPARTMENT OF STATE HIGHWAY AND TRANSPORTATION

EAST LANSING, MI.

DIVISION OF ENGINEERING RESEARCH

MICHIGAN STATE UNIVERSITY

EAST LANSING, MICHIGAN 48824

MARCH 1977

ACKNOWLEDGMENTS

The authors are grateful to the Michigan Department of State Highways and Transportation for their support which made this report possible. Also, they express sincere thanks to Professors T. S. Vinson and O. B. Andersland who have contributed to the preparation of this report. To Messrs. T. Boker and S. Clarke for their assistance, and to the Division of Engineering Research personnel for typing the final draft of this report, the authors express their appreciation.

To their parents, the authors express deep gratitude for their encouragement and understanding.

TABLE OF CONTENTS

LIST OF FIGURES

LIST OF TABLES

ABSTRACT

In the past, design and/or rehabilitation of flexible highway pavements were based on a rule of thumb procedure and the accumulated experience of the highway engineer, with the result that severe break-up was a common occurence. Thus, the need for new design methods and improved material characterization techniques were frequently stated. Recently researchers recognized the fact that the action of traffic on highway pavement is a transient one. Consequently, they established a dynamic, repeated load testing technique as a tool for the characterization of highway materials.

In this paper, an attempt is made to review some of the available literature dealing with dynamic testing and the many variables affecting the test output. The subject is presented in seven chapters as outlined in Chapter 1. Appendix A is devoted entirely to test procedure as published in Special Report 162, Transportation Research Board, National Research Council, National Academy of Sciences, Washington, D.C., 1975.

CHAPTER 1

INTRODUCTION

The complexity and variability of pavement-subgrade materials and their interactive mechanism make the design and/or rehabilitation of an existing pavement a major problem. Present design methods are empirical and quasi-rational; they are based on correlation with in-service performance (1, 2, 3 and 4)*. These design procedures consider only a few material descriptors, and cause great difficulties in extrapolating and correlating pavement performance under different loading and environmental conditions. Thus, the need to develop an approach to material characterization, which recognizes the complexity and variability, not only of the individual pavement components and their interaction, but also the conditions that exist throughout the life cycle of the pavement system, has been frequently stated (5,6).

Further, present design of flexible highway pavements has been, for many years, based on the accumulated experience of the highway engineer (3), with the major design consideration being control of permanent deflection. While permanent deflection is one way in which the pavement can fail, there are five other modes of distress which must be considered in the design process. These modes of distress include:

1) fatigue, which occurs in the layers of the flexible pavement structure, is caused by the repeated bending of the layers due to traffic traveling over the pavement surface,
2) rutting, which is caused by cumulative plastic and shear deformations in the subgrade and/or base materials as a result of load repetitions,
3) excessive deflection in the base materials due to compaction by vehicular loads,
4) temporary excessive rebound in the subgrade and base materials (7), and
5) lack of stability in the wearing course (and resistance to fatigue failure).

These failure modes are manifestated by an uneven surface and a pavement can be considered to have failed functionally when deformation of its components are sufficiently large to cause an unacceptable and uneven riding surface, or to cause cracking of the surface material (2).

---

* Figures in brackets indicate references in the Bibliography

In recent years, those in the field of highway design have called for a new improved design method, which will deal with all modes of distress which can deteriorate flexible pavements. This new method of design has often been referred to as the rational design method. It is a more realistic approach to design, based on the mechanical properties of the roadbed and subgrade materials. Efforts to perfect this method of design have been focused in two areas. The first of these is proper characterization of the materials. The second, which is based on the first, is technique whereby deflections of the pavement may be predicted.

The characterization of paving materials and subgrades is a complex task. Formerly, these materials were characterized by their static behavior, i.e., the loads applied to materials being tested were static, even though their magnitudes may have been subject to change during the test. The California Bearing Ratio (CBR), the Hveem stabilometer, and the static triaxial test are representative of this type of test. However, the application of stress to pavement materials by moving wheel loads is a transient one. A more realistic test procedure to characterize these materials should be one in which the loads applied to specimens are also transient. The repeated load triaxial test is one such test. Samples of soil or paving material are placed in the cell and subjected to confining and axial stresses, just as in the static triaxial test. The difference, however, is that the application of stresses to the sample in the cell is cycled or repeated. The repeated application of axial stress does not duplicate applied stresses in the field, but more realistically represents the form of stress applied to roadbed materials by traffic. Some of the drawbacks involved with this test will be discussed later in this paper.

Reliable predictive techniques must be available to implement the rational design method. Though some of the problems in predicting pavement deflections stem from the difficulties in properly characterizing the roadbed materials, still more problems are encountered by trying to select an appropriate theory to make this prediction. Recent investigations employing the transfer function theory seem to have considerable success. Baladi (5), using the transfer function theory and the Kelvin-mass-spring-dashpot model, predicted pavement deflections to within five percent (5%), 0.0005 inch, of the measured deflections for nine different flexible highway and runway pavements.

A new rational design method is sought which deals with the mechanics of the pavement materials on a more elemental level. Researchers believe a more efficient design may be realized through the association of calculated stresses with the mode of failure presented. The development of a new design method has been impeded primarily by two aspects of analysis: accurate material characterization and reliable pavement deflection prediction. The behavior of soils under repeated loading is much different from that under static loading. Accurate material characterization requires that investigators try to simulate field states of stress in testing, or to use full-scale field tests in a rapid nondestructive manner (3, 8, 9, 10, 11, 12, 13, 14, and 15).

This paper will deal with efforts by investigators to characterize roadbed materials through the use of repeated load triaxial testing. The subject will be presented in the following order:

1. Chapter 2 Review of Literature
2. Chapter 3 The Repeated Load Triaxial Test
3. Chapter 4 Factors Affecting the Resilient Modulus
4. Chapter 5 The Stiffness Modulus of Asphalt Treated Mixes
5. Chapter 6 Sample Preparation and Test Procedure
6. Chapter 7 Equipment
7. Appendix A Test Procedures for Characterizing Dynamic Stress-Strain Properties of Pavement Materials (Special Report 162, Transportation Research Board, National Research Council, National Academy of Sciences, Washington, D. C., 1975).

CHAPTER 2

REVIEW OF LITERATURE

In the early stages of development, design and/or rehabilitation of a pavement system consisted of rule-of-thumb procedures based on judgment and past experience. In the 1920's, the U.S. Bureau of Public Roads* developed a soil classification system based upon the observed field performance of soils under highway pavements (16). This system, in conjunction with the accumulated data, helped the highway engineer to correlate performance with subgrade types.

Beginning in the late 1940's engineers were faced with the need to predict the performance of pavement systems subjected to greater wheel loads and frequencies than they had ever before experienced (3,4,17). Thus, a quasi-rational design procedure was introduced in the early 1950's (18); however, severe breakup is still a common phenomenon on some flexible highways and runways (18,19).

An important problem which the highway engineer faces today is that of providing remedial measures to upgrade existing pavements to meet today's traffic loadings and frequencies. This need has led many investigators to agree that a closer look at the materials comprising the pavement structure is a must. Researchers concerned with fatigue failures recognized the need for a testing method which would simulate the action of traffic. This was pointed out by Professor A. Cassagrande who wrote (20):

> "Irrespective of the theoretical method of evaluation of load tests, there remains the important question as to what extent individual static load tests reflect the results of thousands of dynamic load repetitions under actual traffic. Tests have already indicated that various types of soils react differently, and that the results of static load tests by no means bear a simple relation to pavement behavior."

Mitry (36) noted the work of many investigators who first began testing with repeated loads. In 1947, Campen and Smith (55), McLead (56), Phillippe and Hittle (57), and Goetz (58) had all begun investigations of repeated load tests on model pavement sections, with the number of load repetitions on the order of 10. However, due to several disadvantages of the test (time consumption and cost), experimentation with repeated load testing in the conventional triaxial cell was soon recognized as a better test.

---

* The Bureau of Public Roads is now known as the Federal Highway Administration. (3)

The cyclic (repeated) plate load tests could only evaluate the soil parameters under one set of conditions, namely, those that existed at the time of testing. However, critical soil conditions could be reproduced in the triaxial cell. This strengthened the practice of material property determination in the laboratory. The effects of many different parameters such as density, gradation, degree of saturation and others were soon under investigation.

The first efforts in triaxial testing were associated with the evaluation of repeated load characteristics of subgrade materials such as clays and silts. According to Mitry (36), Barber presented data in 1959, which showed that increased fines content in aggregates considerably decreased its permeability. The need for drainage time was recognized, due to the development of excess pore water pressure upon loading. Seed and Chan (6), showed that the resilient modulus of the silts increased as the time of duration of the axial load decreased.

Given the considerable amount of data available from conventional static tests, a correlation between dynamic and static test properties was sought. Seed et al (6) made a comparison between Young's Modulus as determined by the unconfined compression test and the resilient modulus. Figure (2.1) shows that the resilient modulus in all tests was higher than the tangent modulus for tests on silty clays. Ahmed and Larew (21) found just the opposite. In tests on silts and clays, they determined the strength and modulus by conventional tests. They ran repeated load tests using 6 different levels of repeated stress which were less than the determined strength. In all cases, the modulus based on the repeated load test was less than that for the static test as shown in Figure (2.2). The results also show that stiffness and peak strength were less in the repeated load case.

Repeated load tests on poorly graded sand, with a slow cyclic frequency to represent loads due to parking were performed by Trollope (59). In these tests, he found that the resilient modulus increases with increasing dry density (decreasing void ratio) and increasing rate of deformation. Hicks (29) and Mitry (36) acknowledged Biarez (60) as the first investigator to note a logarithmic relationship between the resilient modulus, M_R, and the sum of principal stresses, θ. In tests on uniform sand, a log-log plot

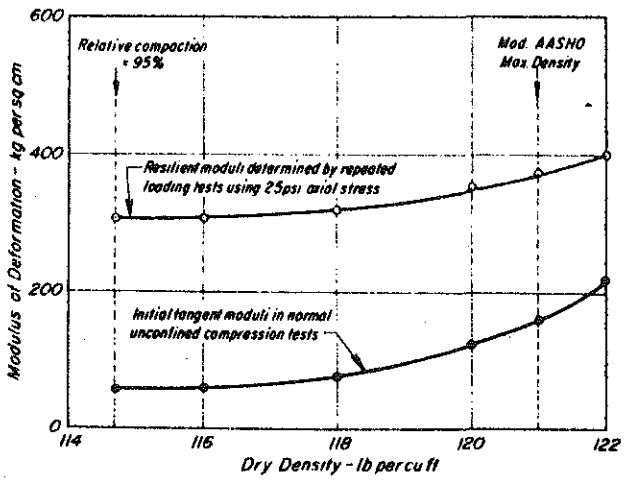

FIGURE 2.1 COMPARISON OF RESILIENT MODULUS AND TANGENT MODULI FOR SILTY CLAY (6).

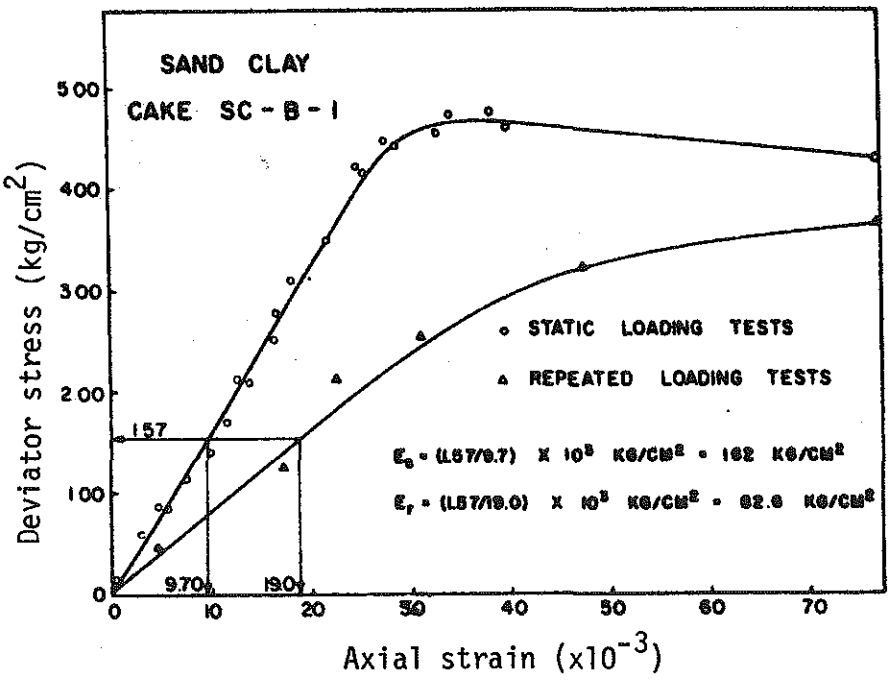

FIGURE 2.2 STRESS STRAIN CURVES (21).

of M_R vs. θ gave a straight line, which could be expressed by the equation:

$$M_R = K \cdot \theta^n \tag{2.1}$$

in which K is a constant, and n is an exponent between 0.5 and 0.6. Dunlap (61) formulated another relation between the resilient modulus and the triaxial stress level as follows:

$$M_R = K_1 + K_2 (\sigma_r + \sigma_\theta) \tag{2.2}$$

in which, K_1 = the unconfined modulus

K_2 = a constant

σ_r = the radial stress

σ_θ = the tangential stress

Mitry (36) performed many tests on untreated base course material. He confirmed the linear relationship, on a log-log scale, between resilient modulus and the confining pressure. He expressed the relationship in terms of the confining pressure as,

$$M_R = K\sigma_3^n \tag{2.3}$$

in which, σ_3 = the confining pressure

K = a constant

n = an exponent between 0.5 and 0.7

He noted the strong effect that the confining pressure has on the resilient modulus, one increasing with the other. He also found that the resilient modulus for saturated gravel under drained conditions was only slightly higher than that for dry specimens, and that the resilient modulus determined under undrained conditions was nearly the same as that of dry aggregate. Seed and others confirmed this in 1967. Coffman (62) showed that the resilient modulus increased with increasing frequency of repeated load.

Morgan (36) conducted tests on uniform sand. He reported that the behavior of freely drained saturated sands is only slightly different from that of the air-dried sands. Morgan found that the resilient modulus is dependent on the magnitude of the deviator stress and confining pressure. Also, he found that the resilient Poisson's ratio was unaffected by changes in either of the test parameters.

Haynes and Yoder (26) carried out repeated load triaxial tests on different kinds of coarse aggregate, gravel and crushed stone. They found that the resilient modulus decreased with the increasing saturation. The

amount of decrease was dependent on the aggregate type; gravel being affected more than the crushed stone. The resilient modulus was found to be only slightly affected by gradation.

Tests made by the Asphalt Institute in 1967 on untreated base course materials also showed that the resilient modulus decreased with increasing saturation. Hicks (29) cites the findings of Kallas and Riley (63), which saw the decrease of K while n remained constant in equation (2.3). In tests run by Kasianchuk (64), the build-up of excess pore water pressure and a corresponding decrease in effective confining pressure, with an increasing number of load applications was reported. These tests were made on saturated sand and appear to be related to the phenomenon of liquefaction. Kasianchuk also confirmed the linear relationship between confining pressure and resilient modulus. For a comparison of these findings, see Table (2.1).

In 1962, Seed showed that the resilient modulus of clay was dependent on axial stress level. Recognizing this fact, the characterization of the subgrade layer becomes very complex. Since the load on the soil varies with horizontal and vertical position, the resilient modulus varies throughout the soil no matter how homogeneous it may be.

The emphasis of researchers seems to have changed at this point. With a great deal of testing having already been done, it was fairly clear how many parameters were affecting the resilient response of highway materials. It was now a matter of determining which test parameters and conditions were most important. Hicks (29) addressed himself to this in work on untreated base course materials at the University of California. He showed that stiffness increased (resilient modulus decreased) with increasing confining pressure, and was relatively unaffected by the deviator stress. Stiffness increased with density, decreasing fines and decreasing saturation. The magnitude of the increase in stiffness was dependent on the type of aggregate tested. The resilient Poisson's ratio increased with decreasing confining pressure and increasing deviator stress. These tests were carried out in a conventional triaxial cell, with repeated axial stress and sustained confining pressure. Axial and radial strains were measured, based on realistic stress histories, load duration and frequency, at stress levels expected in the field.

TABLE 2.1 SUMMARY OF THE COEFFICIENTS K_1, K_2, K_1', K_2', RELATING MODULUS TO CONFINING PRESSURE (σ_3) AND TO THE SUM OF THE PRINCIPAL STRESSES (θ), (27).

REFERENCE	MATERIAL	$M_R(psi) = K_1\sigma_3^{K_2}$		$M_R(psi) = K_1'\theta^{K_2'}$		WATER CONTENT
		K_1	K_2	K_1'	K_2'	
(36)	Dry Gravel	7,000	.55	1,900	.61	-
(112)	Crushed Gravel	13,000	.50	-	-	.20
		9,000	.50	2,800	.59	.07
(64)	Aggregate Base	11,300	.39	3,830	.53	
	Aggregate Subbase	6,310	.43	2,900	.47	
(63)	Aggregate Base and Subbase	10,618	.45			.024
		10,144	.47			.043
		10,019	.47			.063
		8,687	.50			.082
(113)	Aggregate Base			5,400	.50	.027
				2,100	.50	.063

As a result of this work, Hicks and Monismith (28), reported that the effects of stress level on the resilient modulus are greater, than those for other material parameters such as density, gradation, and saturation, which have a lesser importance. Hicks and Monismith also noted a relationship between resilient Poisson's ratio and the principal stress ratio of the form,

$$\nu = A_0 + A_1 (\sigma_1/ \sigma_3) + A_2 (\sigma_1/ \sigma_3)^2 + A_3 (\sigma_1/ \sigma_3)^3 \qquad (2.4)$$

in which A_0, A_1, etc. are regression constants from a least squares curve fitting, and (σ_1/σ_3) is the principal stress ratio.

Barksdale and Hicks (23) suggested a relationship between the measured plastic strain in a repeated load test and rutting of the surface of a flexible pavement. They defined the rut index as "the sum of the average plastic strains occurring in the top and bottom half of the base multiplied by a constant 10,000 so as to give a whole number." They stated that the rut index can be evaluated from the results of two repeated load triaxial tests performed at a confining pressure of 10 psi and deviator stresses of 35 and 60 psi. However, they acknowledged that a more general approach than the rut index must be used to study rutting in pavement structures having different geometries and varying base course materials. To this end, it was apparent that a proper material characterization was still not in hand. Thus, investigators started looking for other methods to determine the stress-strain relationship for asphalt mixes; among these methods are the stiffness modulus, the complex and/or dynamic modulus, and the dynamic stiffness modulus.

Nijboer (65) related asphalt mix stiffness to the ratio of Marshall stability and Marshall flow value. Terrel et al (47) cited the work of other investigators in the correlation of the ultimate tensile strength with the resilient modulus. In the estimation of mix stiffness, Heukelom and Klomp (69) extended the earlier work of Van der Poel (70,71). They presented a semi-empirical equation whereby the volume concentration of aggregates is determined. It should be noted that these equations also make use of the nomographs presented by Van der Poel.

The concept of stiffness modulus was first presented by Deacon (68), based on the results of repeated load beam flexure tests; however, it was Terrel who presented the most noteworthy work in resilient and complex modulus determinations in the triaxial cell in 1967 and again in 1972.

The most significant of his findings is the linear stress-strain behavior of asphalt treated mixes in the range of stresses and temperatures expected in the field, in contrast to the non-linear behavior of untreated soils. Terrel and Awad (47) stressed the continuation of research to develop and refine more realistic test methods, pointing out the failure of conventional testing in newer theoretical techniques with adequate material parameters. Recently, investigators have recognized that pavement deflection is one such technique. Thus, the search was begun for a method whereby an accurate pavement deflection can be made.

In the search for the theoretical basis upon which to predict pavement deflections, Pell and Brown (41) gave further support to linear elastic theory, noting it as the most promising. First, this theory could be modified for use with non-linear material properties, such as exhibited by cohesive and granular soils, through an iterative process. Second, the thickness of the flexible pavement usually insured linear behavior. Interaction between layers, which is a function of the layer thickness and material composition is as important as the behavior of the materials comprising the pavement structure. Furthermore, the use of a linear elastic theory may introduce nonpredictible error. To this end, layered elastic theory was introduced. Seed et al (44) had limited success in prediction of pavement deflection based on layered elastic theory and laboratory determined properties.

In 1970, Harr introduced the transfer function theory as a method whereby pavement parameters could be determined. Ali (72) applied transfer function theory to study flexible pavements under laboratory controlled conditions. He reported: that "Temperature, surface course thickness, and spatial location have their respective influence on the transfer function." Boyer and Harr (73) extended transfer function theory to an in-service pavement system. They used installed linear variable differential transformers (LVDT) gages in the pavement and conducted field tests at Kirtlind Air Force Base, New Mexico. They concluded that the characteristics of flexible pavements could be represented by a "time dependent transfer function" (TDT). Baladi (5) and Ng-A-Qui (74) successfully predicted pavement deflection of various highway and runway sections using the transfer function theory. Also, Baladi succeeded in determining pavement parameters that are needed in the design and/or rehabilitation of flexible pavement structures.

In summary, the effort to develop a new rational design of flexible pavements or to modify existing design methods has been concentrated in two areas: 1) characterization of roadbed and surface materials, and 2) development of a technique whereby an accurate prediction of pavement deflection can be achieved. Most researchers agree that the theoretical techniques for prediction of pavement deflections are far more advanced than our ability to characterize the paving materials. Indeed, the problem of predicting pavement response is primarily related to the lack of adequate material parameters. Due to the complexity and variability of highway materials, and the limitation of our testing ability, much of the work in this area has been of little help in changing and improving methods of design. However, research has increased our knowledge about the problem; the different modes of distress and the mechanics behind them have been identified; the testing procedure has been improved such that field conditions are now being accurately simulated in the laboratory. Further, full-scale field testing is a must in order to modify the laboratory test procedures and consequently to check its results.

CHAPTER 3

THE REPEATED LOAD TRIAXIAL TEST

1. INTRODUCTION

The repeated load triaxial test has been singled out for extensive use by researchers for material characterization. There are several reasons for this:

1) it is considered the best test technique due to the ease with which investigators can control various parameters,

2) low cost, and

3) the ability to give relatively accurate estimations of material properties for pavement deflection analyses.

However, as we shall see, the repeated load triaxial test falls short of truly representing the real in-situ state of stress for the soil element. Before examining the inconsistencies of the state of stress, the repeated load triaxial test itself will be considered.

2. THE TEST

Triaxial testing is concerned with the determination of the stress-strain behavior of soils. Cylindrical soil samples are carefully prepared, most often to represent the in-situ condition of the soil, and these samples are placed in a test chamber or cell. In the cell, the soil sample is subjected to a lateral or radial confining stress, and an axial stress applied by a piston to the end of the sample. In conventional triaxial testing, the sample is subjected to an axial stress which is maintained and steadily increased. Stresses and strains are monitored throughout the test. Repeated load testing is much different in several ways. The soil sample in the cell is still subjected to a confining stress by pressurizing the air or cell fluid in the chamber, but the cell pressure may be pulsated as is the axial stress. The axial stress, which in conventional testing is maintained, is continuously reapplied to the specimen. This repeated loading of the sample is meant to represent the stress pulse felt by a soil element due to moving wheel loads on pavements. If the test confining pressure is pulsed, it is typically pulsed in sequence with the axial load. Thus, many more test parameters require consideration in repeated load testing. Not only must values of the axial and confining stresses be specified, but the conditions of loading such as load frequency, duration, and number of loadings must

also be considered. As might be expected, each of these test parameters has an effect on the response of the material. These effects will be discussed in the next chapter.

3. STATE OF STRESS

To illustrate the manner in which the triaxial test fails to truly represent the state of stress of a soil element in the pavement structure, consider the stresses induced in the element due to the passage of a moving wheel load. Figure (3.1) shows that as the wheel moves along the surface of the pavement, the orientation of the principal stresses which are applied to an element in the pavement structure rotates. At an instant when the load is directly above the element, the principal stresses are oriented horizontally and vertically. Except for this very instant, the major principal stress applied to the in-situ element is at all times greater than the vertical stress. The triaxial test employs application of principal stresses in one orientation only, that of horizontal and vertical, with no possibility for reorientation. Due to the fact that the principal stress applied by the wheel load rotates as the wheel moves, a shear stress, τ, exists on the vertical and horizontal planes of the in-situ element. Figure (3.2) illustrates the normal and shear stresses exerted on the in-situ element. In the figure, the shear stress is zero when the normal stresses are maximum, corresponding to the wheel load located directly above a soil element. The triaxial test can only represent this condition, since it is incapable of applying shear stresses directly to the sample. Deformations of the sample are measured only in the directions of the applied normal stresses, giving an inaccurate and overestimated measure of permanent deformation. However, in relation to the in-situ element, Pell and Brown (41) stated that if the soil is considered to be isotropic, the measured deflection can be considered satisfactory.

In representing the state of stress of an element under the surface of a pavement, the triaxial test falls short of a true representation in two ways:

1) the principal stresses on an element in the field rotate, whereas the repeated load triaxial test applies them in one orientation only, and
2) because of the rotation of the principal stresses, shear stresses

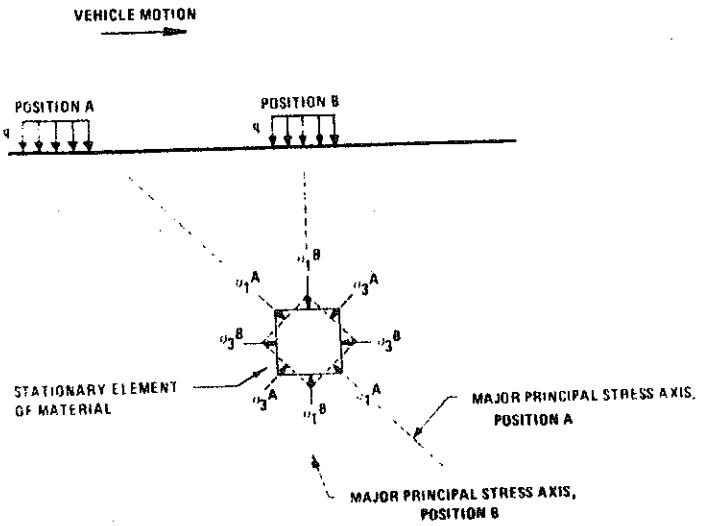

FIGURE 3.1 ROTATION OF PRINCIPAL STRESS AXES OF AN ELEMENT AS A VEHICLE MOVES ALONG THE SURFACE OF A PAVEMENT, (24).

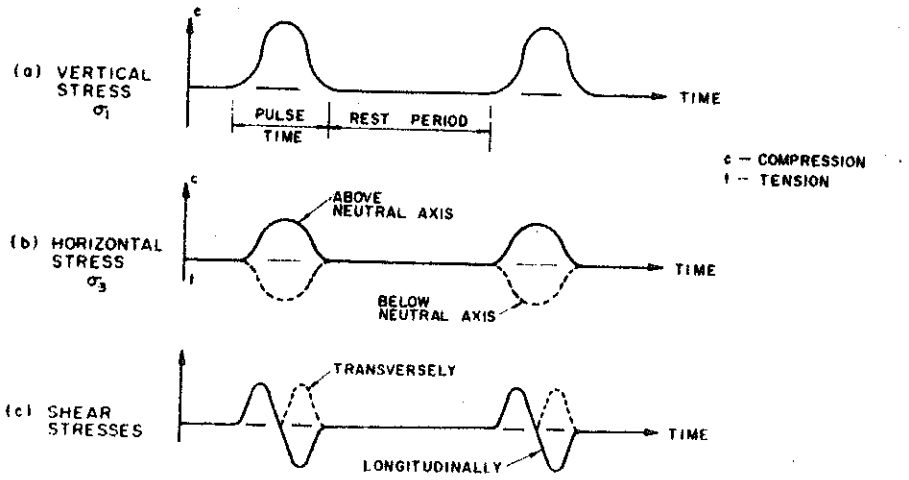

FIGURE 3.2 STRESS VARIATIONS IN A TYPICAL ASPHALT CONCRETE ELEMENT DUE TO A MOVING LOAD, (40).

occur on the horizontal and vertical planes of the element

These shear stresses cannot be applied in triaxial testing.

No one is certain as to the importance of these drawbacks in material characterization, however, it does not appear likely that the repeated load triaxial test will be replaced in the near future. Morgan (39) suggested the use of direct shear testing to supplement triaxial testing characterization, but it is not clear how this would be achieved. Baladi (5) has suggested the use of full-scale field tests in conjunction with repeated load triaxial tests so as to determine the importance of these shortcomings of the triaxial testing. Before looking more closely at the various triaxial test parameters, the definition of some terms may be warranted.

4. RESILIENT PROPERTIES

In the determination of the most important resilient properties, the response of the test specimen is carefully monitored. Axial and radial strains and deformations characterize this response. When the sample is loaded axially it deforms a certain amount, and upon unloading, a portion of this total deformation is recovered. Thus, the total deformation is comprised of an elastic or recoverable deformation and a permanent deformation. These deformations lead to the corresponding total, resilient, and permanent strains defined by them. The two most important resilient properties, the modulus of resilient deformation, M_R, and resilient Poisson's ratio, ν_r, are defined by these strains and the values of the applied stresses.

The resilient modulus M_R is defined as follows:

$$M_R = \frac{\sigma_1 - \sigma_3}{\varepsilon_a} = \frac{\sigma_d}{\varepsilon_a} \qquad (3.1)$$

in which, σ_d = the deviator stress which is the difference between the axial stress, σ_1, and the radial stress σ_3

ε_a = the resilient or recoverable axial strain

This definition applys to a linear elastic, isotropic material under uniaxial stress. It is valid for cohesive and cohesionless soils and has also been adopted to characterize asphalt treated materials. Figure (3.3) shows typical recordings of stress and strain taken for a repeated load triaxial test, and the resilient modulus determined based on them.

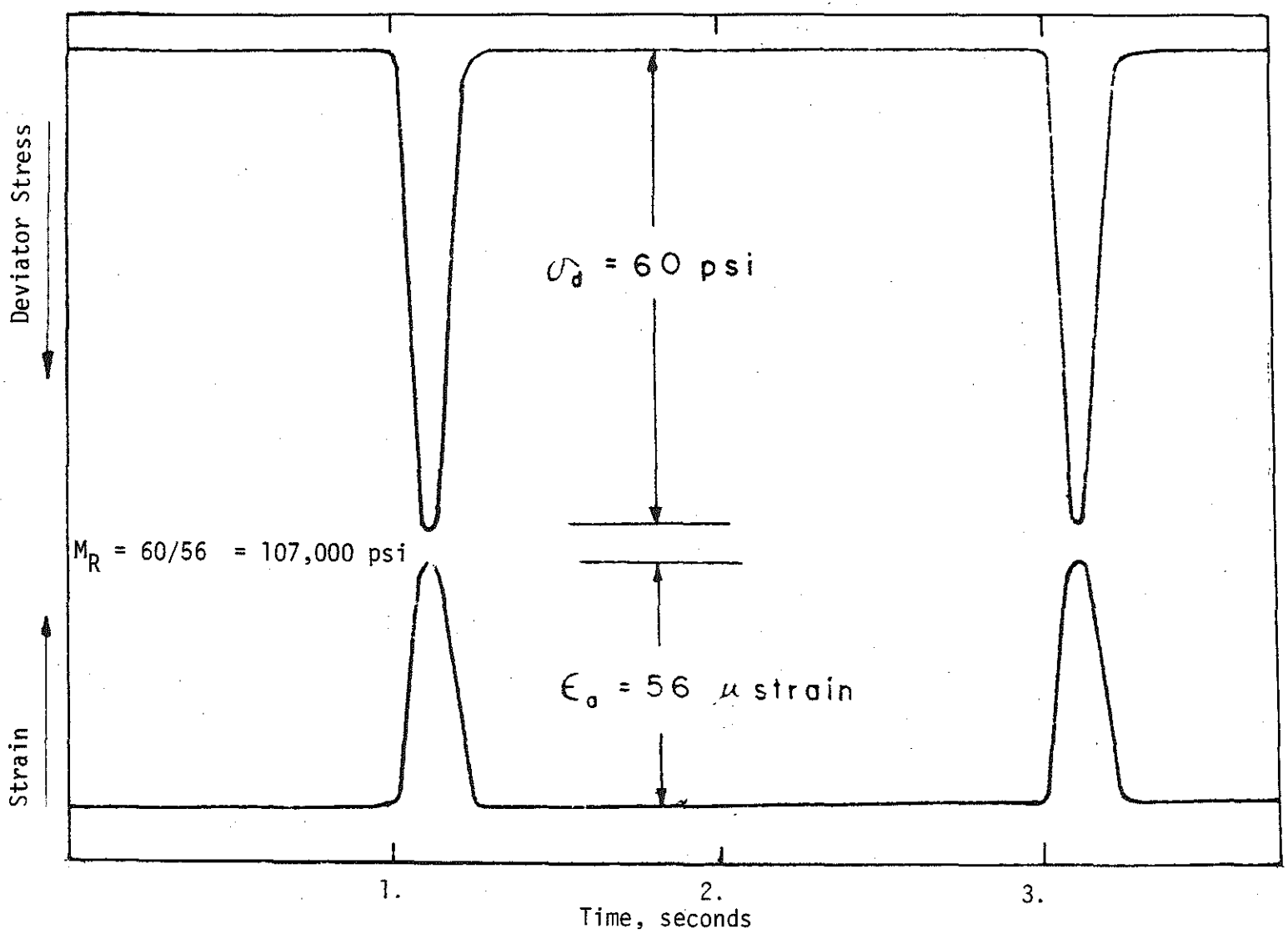

FIGURE 3.3 TYPICAL LOAD-DEFORMATION RECORDING TRACE FOR σ_3=20 psi AND FREQUENCY OF 30 cpm, (31).

The resilient response and M_R for asphalt treated materials are dependent upon many factors. Among these are temperature, mix properties, stress level, load duration and frequency. It is also known that the value of the resilient deformation measured is dependent upon load duration. Under short stress durations and low temperatures, the asphalt treated materials behave almost elastically. However, saturated mixes at high temperatures exhibit little or no resilient response, which leads to an excessively high and misleading value of M_R. Terrel and Awad (48) recognized that M_R was not enough to completely characterize the stiffness or quality of a mix. They introduced the modulus of total deformation, M_T, defined as follows:

$$M_T = \frac{\sigma_d}{\varepsilon_T} \tag{3.2}$$

in which, σ_d = the deviator stress

ε_T = the total strain

They observed that when total strains were used instead of resilient strains, the material properties computed were more consistent. Figure (3.4) shows a typical recording of stress for an asphalt treated material.

The resilient Poisson's ratio, ν_r, for isotropic linear elastic materials under uniaxial stress is defined as follows:

$$\nu_r = \frac{\varepsilon_r}{\varepsilon_a} \tag{3.3}$$

in which, ε_r = the recoverable radial strain

ε_a = the recoverable axial strain

This resilient Poisson's ratio and modulus are defined under the condition of a constant confining pressure. The most recent investigations have been made utilizing a variable confining pressure which pulses with the axial load, and more accurately simulates the stress conditions in the field.

With a variable confining pressure, determination of the resilient modulus as previously defined would ignore the effects of the pulsed radial stress. This change in confining pressure would have an effect on the recoverable axial strain, leading to an overestimate of ν_r based on the constant confining pressure. Allen and Thompson (22) suggested the use of three

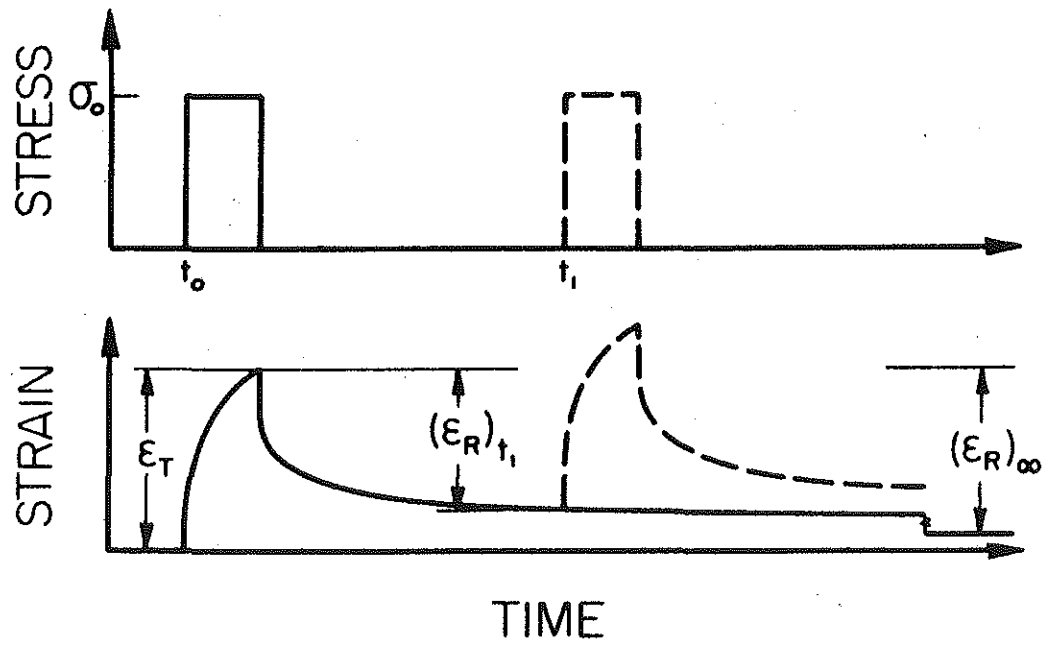

FIGURE 3.4 RESILIENT AND TOTAL STRAINS UNDER REPEATED STRESS, (47).

dimensional stress-strain relationships:

$$\varepsilon_a = \frac{1}{M_R} \quad (\sigma_a - 2\nu_r\sigma_r) \tag{3.4}$$

$$\varepsilon_r = \frac{1}{M_R} \quad [\sigma_a - \nu_r(\sigma_a + \sigma_r)] \tag{3.5}$$

in which, ε_a = the recoverable axial strain
ε_r = the recoverable radial strain
ν_r = the resilient Poisson's ratio
σ_a = the axial stress
σ_r = the radial stress

Terrel et al (48) presented the following equations for strain based on linear elastic behavior

$$\varepsilon_r = B_1\,\sigma_r + B_2\,\sigma_a \tag{3.6}$$

$$\varepsilon_a = B_3\,\sigma_r + B_4\,\sigma_a \tag{3.7}$$

in which, B_1 through B_4 are constants determined from linear fitting of the experimental data. If ε_r and ε_a are resilient strains, then B_1 through B_4 can be used to determine M_R and ν_r as follows:

$$M_r \simeq \frac{2}{B_1 + B_4} + \frac{2}{3}\,\frac{(B_2 + B_3)}{\left[(B_1 + B_4) - \frac{(B_2 + B_3)}{3}\right](B_1 + B_4)} \tag{3.8}$$

$$\nu_r \simeq -\frac{2}{3}\,\frac{(B_2 + B_3)}{(B_1 + B_4) - \frac{(B_2 + B_3)}{3}} \tag{3.9}$$

Again, these relationships are based on linear elastic behavior and, therefore, may only be applied to materials exhibiting this behavior.

5. TEST PARAMETERS

Researchers seek to predict the in-service behavior of the pavement structure based on the results of laboratory tests on its components. It follows that testing in the lab must be performed in such a manner as to simulate the actual field loading and soil conditions. To simulate field conditions, realistic values for the various test parameters must be chosen. The ranges of stress, temperature, number and duration time of loads, etc.,

are chosen so that they fall within service conditions. These parameters will be discussed in the following subsections.

5.1 Load Repetitions

The choice of this parameter for testing is reasonably straight forward. One would expect to subject a test specimen to a number of loads of the same order as that which we would expect in the field. During its lifetime, a typical highway pavement can be subjected to anywhere between 100,000 to 1,000,000 or more 18 kip single axle loads. Indeed, most repeated load triaxial testing is carried out with the number of load applications in the range of 10,000 to 100,000 repetitions. As will be pointed out later, after a certain number of applications, the response of the specimen does not change appreciably. This fact, in conjunction with the excessive time required to apply a realistic number of loads is the reason that investigators use a smaller number of loadings.

5.2. Deviator Stress

It will become evident that changes in the stress level to which test specimens are subjected will affect the resilient properties to a greater extent than changes in any other test condition. The resilient modulus may vary as much as several hundred percent in the range of stresses encountered in the pavement structure. To determine the value of axial load to apply to a specimen, several things must be considered. Of primary importance is load intensity in the field. It is obvious that the intensity of the vertical load applied diminishes with depth, but the level of stress to which an element is subjected is also affected by the geometry of the pavement structure. Computer programs aid researchers in determining the magnitude of load to expect and use for testing for a given material at a given depth in the roadbed. Figure (3.5) shows the variation of stress with time for different depths in the base course for a given vehicle speed and tire pressure. Published data such as this aids investigators in choosing the appropriate axial stress level.

5.3 Load Wave Form

As the axially loading piston moves downward to make contact with the test specimen, the change of applied load with time must be con-

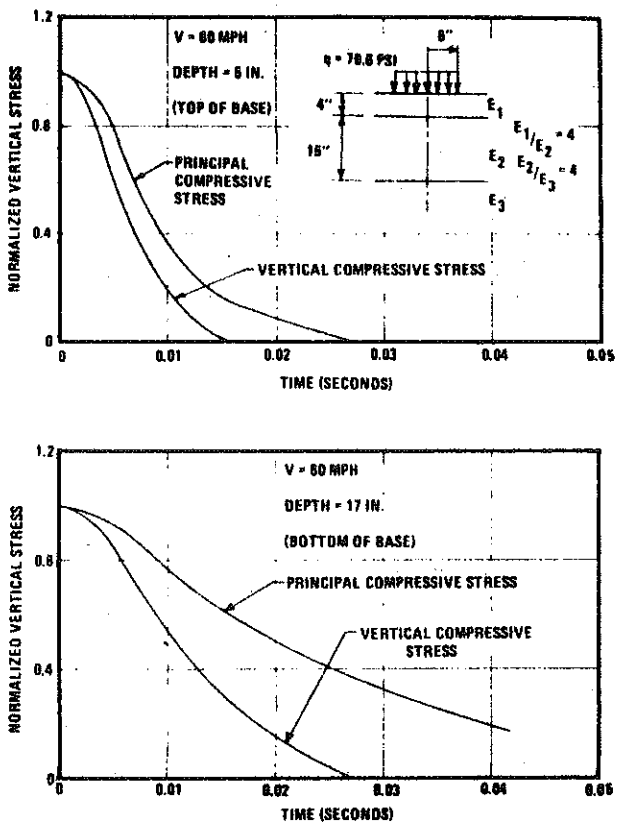

FIGURE 3.5 COMPARISON OF VERTICAL AND PRINCIPAL COMPRESSIVE STRESS PULSES FOR TWO DEPTHS, (4 inch surface and 15 inch base), (24).

sidered. This is typically referred to as the wave form. Figure (3.6) shows some of the wave forms used in past investigations. The most commonly used stress-pulse for many years was the square wave. It was used because analysis of the data was simplified and it was a wave form which was easily achieved with pneumatic loading test systems used in many laboratory studies.

Barksdale (24) found that the form of the stress pulse changed with depth for in-service loadings. He found that the vertical stress pulse varies from a near sinusoidal one near the top of the pavement structure to a more nearly triangular pulse in the lower portions of the base course. Figure (3.7) shows the variation of stress versus time for different depths in the pavement structure. Examination of the figure indicates that a triangular or sinusoidal wave form may be considered as a good approximation. Terrel and Awad (47) were in agreement with these findings. They noted the replacement of sinusoidal waves with other wave forms, by researchers, for ease in analyses.

Allen and Thompson (22) also showed the dependence of stress wave form upon depth. In agreement with Barksdale and Terrel, they described the vertical stress pulse as generally sinusoidal, with a sharper peak near the surface, and a flatter top in deeper portions of the base course. Conversely, they claimed that the radial stress pulse was more or less a flat-topped sinusoidal shape, which became more sharply peaked with depth. For all of their testing, a half-sinusoidal wave form was used since this shape is the most general for all of the different stress distributions, and because it can be produced with standard laboratory function generators.

In work performed by Terrel et al (48) on the effects of different wave forms on specimen response, it was found that no significant difference was observed in the total and resilient strains using either the sinusoidal or triangular wave shapes. Also, an equivalent square pulse can be used if the same stress is applied for 33% of the duration of the equivalent sinusoidal pulse, or if 66% of the sinusoidal stress is applied for the same duration as the sinusoidal pulse. For simplified data analysis, and other reasons, they concluded that a square vertical wave form is a

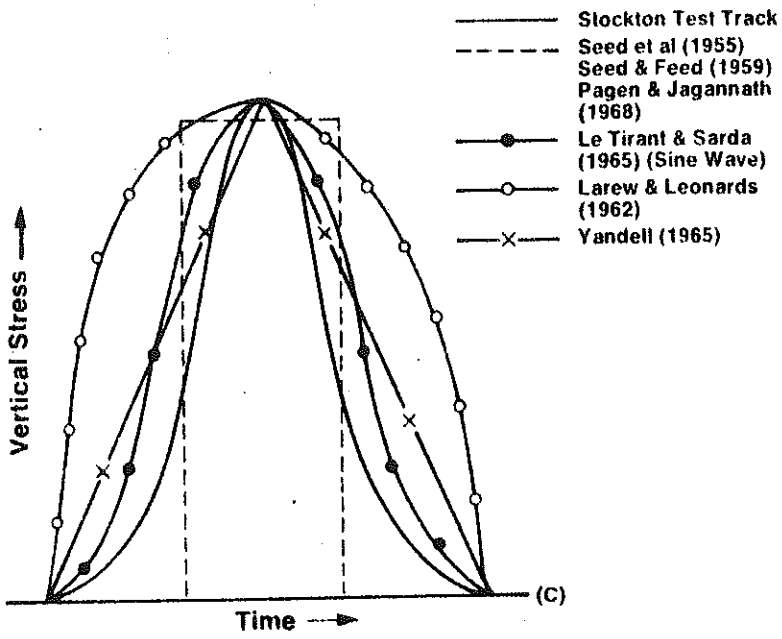

FIGURE 3.6 VERTICAL STRESS FUNCTIONS USED BY DIFFERENT INVESTIGATORS, (45).

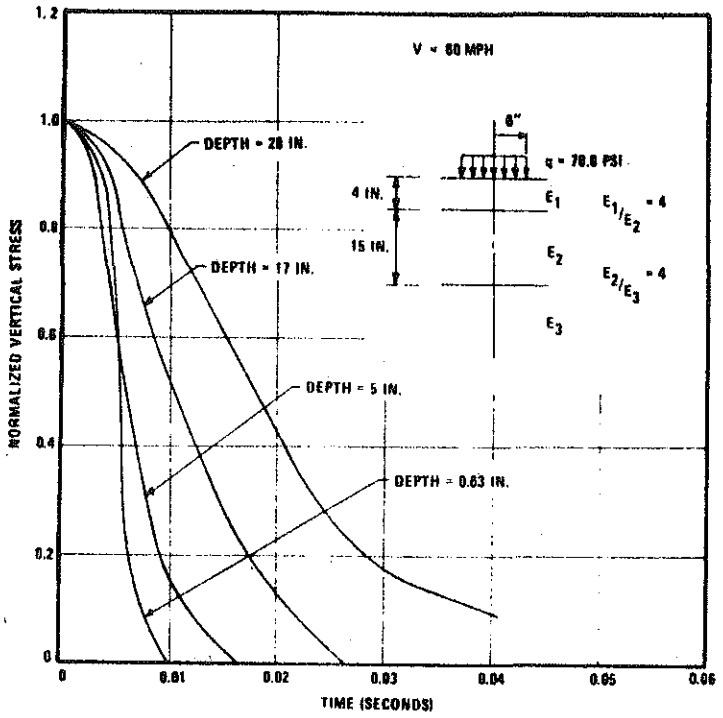

FIGURE 3.7 VARIATION OF CALCULATED VERTICAL COMPRESSIVE STRESS PULSE SHAPE WITH DEPTH, (4 inch surface and 15 inch base), (24).

reasonable approximation of actual conditions. Considering the deficiencies and imperfections of laboratory testing and predictive techniques for deformation, the precise wave was of little importance. They suggested the use of the sinusoidal wave pulse for all testing, which still appears to be the case today.

5.4. Load Frequency and Duration

Under actual in-service conditions, the stress pulse applied by a moving wheel lasts about 0.01 to 0.1 of a second. This duration time is primarily dependent upon the speed of the vehicle and the position of the element under consideration within the pavement structure. The vehicle speed is inversely related with the load duration. As vehicle velocity increases, the duration of loading decreases linearly, and as the velocity decreases, the load duration linearly increases. It is also known that the load duration time increases with depth. For a flexible pavement with 4 inches of surfacing and 15 inches of base course, Barksdale (24) found that the time of load duration increases by a factor of about 2.7 from surface to subgrade.

As was pointed out earlier, the principal stresses applied to the in-situ soil element are always greater than the vertical stress applied, except for the case when they are equal, for the wheel load located directly above the element. Owing to this fact, the duration of the principal stresses applied is also of a larger magnitude than the duration of the vertical stress applied, and the difference in these two durations increases with depth. Figures (3.8) and (3.9) were developed by Barksdale, and give suggested load duration times based on different vehicle speeds and depths, for both the principal and vertical stress pulses. The question arises as to which stress to use, and Barksdale suggests: (1) use the principal stress pulse for determining the dynamic modulus of elasticity, since principal stresses are applied in the triaxial cell, and (2) use the vertical stress pulse for the investigation of plastic properties and rutting, as these are related to the accumulation of vertical strain.

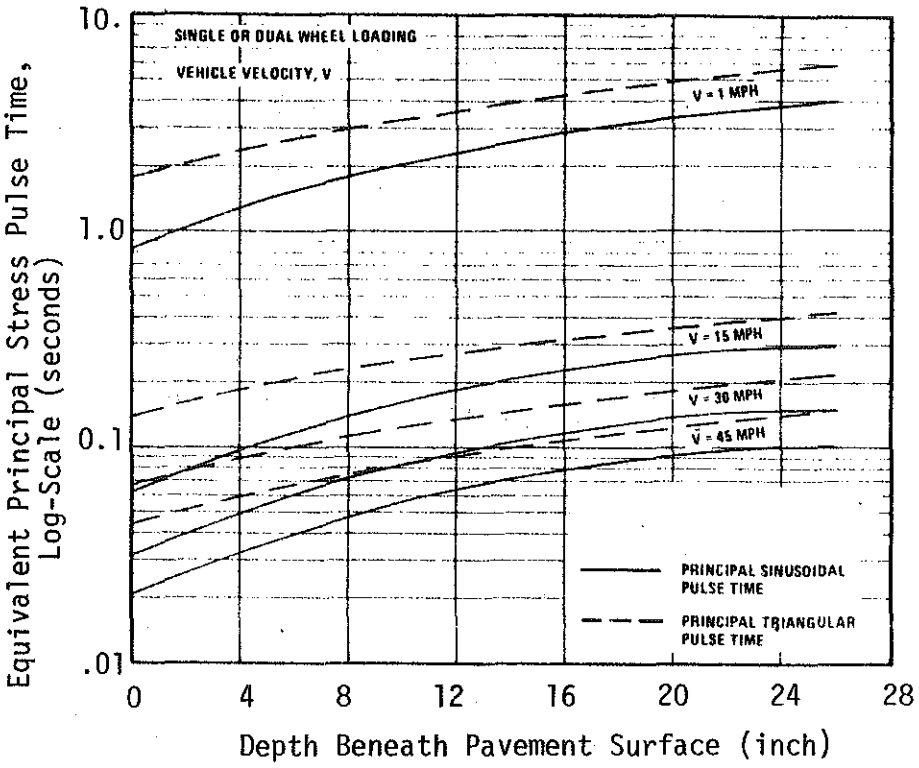

FIGURE 3.8 VARIATION OF EQUIVALENT PRINCIPAL STRESS PULSE TIME WITH VEHICLE VELOCITY AND DEPTH, (24).

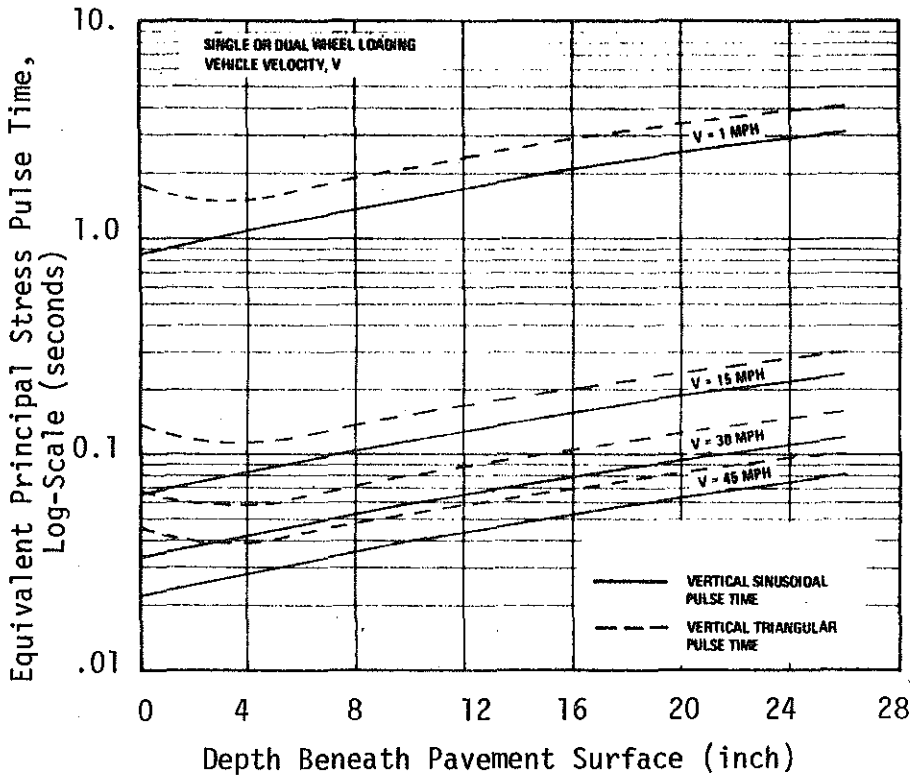

FIGURE 3.9 VARIATION OF EQUIVALENT VERTICAL STRESS PULSE TIME WITH VEHICLE VELOCITY AND DEPTH, (24).

Barksdale (24) also reported another finding in his work which bears mention here. For conventional flexible pavements, including those of deep-strength design, and for spring and summer temperatures, the load duration time is not affected by the pavement geometry or by layer stiffness and thickness. For engineering considerations, the effects of these are negligible.

In general, most repeated load triaxial tests are performed using a load duration of 0.1 second and a frequency of loading of 20 cycles per minute.

5.5. Confining Pressure

Just as the level of axial stress depends on load intensity and depth within the pavement structure, so does the confining or lateral pressure. Allen and Thompson (22) used non-linear finite element analyses for typical pavement sections to establish confining pressure values. Terrel and Awad (47) used a n-layer computer program to plot the variation of confining pressure as a result of moving load.

Recently, investigators have incorporated varying confining pressures which pulse in sequence with the axial load as shown in Figure (3.10). However, there is no general agreement as to the importance of such variation, since pulsating the confining pressure tends to overestimate the resilient properties of the specimen being tested.

6. TYPICAL VALUES OF TEST PARAMETERS

The various test parameters and criteria for choosing the values of test parameters have been presented. Typical values for these parameters are:

Load Frequency:	10 to 30 cpm
Load Duration:	0.04 to 0.25 seconds
No. of Repetitions:	10,000 to 100,000
Confining Pressure	0 to 25 psi
Deviator Stress:	1 to 70 psi
Sample Size:	1.4" x 3" to 4" x 8"
Load Wave Form:	square or sinusoidal

Table (3.1) lists specific values of these test parameters for past investigations, along with the range of resilient modulus values determined.

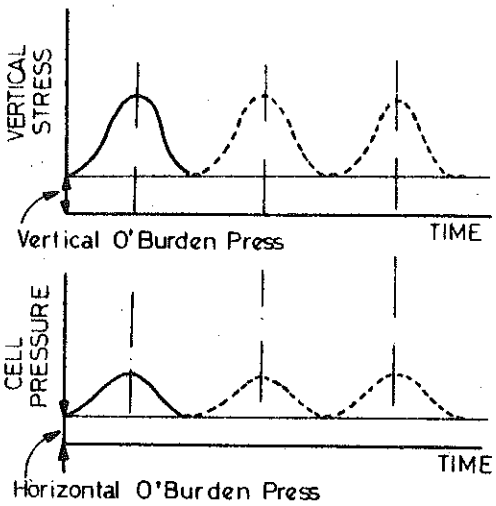

FIGURE 3.10 STRESS REGIME FOR THE REPEATED LOAD TRIAXIAL TEST, (41).

TABLE 3.1 SUMMARY OF LABORATORY TESTS TO EVALUATE THE ELASTIC PROPERTIES OF GRANULAR MATERIALS, (36).

Type of Rep. Loading	Reference	Material Investigated	Factors Investigated	Conf. Press. in p.s.i.	Deviator Stress in p.s.i.	Frequency	Number of Load Applications	Modulus of Resil. Deform. in p.s.i.
A. Triaxial repeated-loading compression tests	A. H. B. Seed and C. K. Chan (1961)	Silty sand	Effect of duration of stress applications	14.7	23.5 and 36.0 36.0 36.0	20/min. for 1/3 sec. 2 min. on, 2 min. off 20 min. on, 20 min. off	10,000	21,300 and 27,300 23,200 22,000
	B. Haynes (1961) Joint highway research project, Purdue University	AASHO base-course mat. Revised gradation, 3/4 in. max. size 1. Gravel 2. Crushed stone	- Percent of fines passing #200 mesh sieve: 6.2, 9.1 and 11.5% -Degree of saturation 70, 85 and 100%	15.0	55	60/min.	100,000	From 28,000 up to 63,000
	C. University of California (1962)	Niles aggregate, fairly rounded 3/4" max. size, 5% passing #200 sieve	-void ratio -confining pressure	15.2 and 29.4	20, 40 and 60	30/min.	10,000	From 16,650 up to 54,500
	L. Jean Biarez ( )	Uniform sand - 0.016 in. in diam. Specimen dimensions 5.4 in. x 5.4 in. x 10 in.	Variation of k with the applied mean	Mean normal stress from 2.2 145 lbs./in.^{2}		Cyclic load - the rate of deformation is not indicated	of the order of 5	1,300 lbs./in.^{2} for mean =2.2 lbs./in^2 and 71,000 lbs./in.^{2} for mean = 145 lbs./in.^{2}
	E. D. P. Trollope, D. K. Lee, and J. Morris (1962)	poorly graded, (dry sand) (Carlston sand)	- Initial dry density (loose and dense) -Rate of deformation from 0.003 to 0.2 in./min. -Lateral pressure at constant stress -Effect of stress level at const. conf. press.	from 15.0 up to 45 p.s.i.	Stress level was varied	Cyclic load - rate of deformation from .003 to .02 in./min.	of the order of 100	From 35,000 up to 95,000 p.s.i.
	F. Texas Transp. Institute, W. A. Dunlap (1963)	Graded material - 1 in. max. size - 4% passing #200 - S.G.S., L.L. 21 Plasticity w.c. 5.5%	Variation of modulus of resil. def. with confin. press.	From 3 up to 30 p.s.i.	30.5 and 51.7 p.s.i.	30/min. - duration 0.2 sec.	130,000 reps	from 31,000 up to 160,000 psi

CHAPTER 4

FACTORS AFFECTING THE RESILIENT RESPONSE

1. COHESIVE SOILS

Unlike other materials which will be discussed, cohesive subgrade materials cannot be accurately characterized without great attention being given to the preparation of the sample. In determining the resilient parameters for clays, the lab samples should be identical in composition to the field. This means that water content, density and the structural arrangement of the particles (which is controlled by the method of compaction used in preparing the sample) must be identical. In this section the effects of the most important soil and test parameters on the repeated load characteristics of clay soils will be discussed.

1.1 Number of Stress Applications

Silt and clay subgrade materials generally exhibit a stiffening behavior with an increasing number of stress applications, N. The total deformation of test specimens increases with increasing N, and the resilient deformation tends to decrease. Most investigators tend to evaluate the resilient properties based on sample response after a relatively small number of applications, of the order of 5,000 or less, and this can present a misleading picture of the resilient behavior.

In tests on stiff clays, Dehlen (75) found that 1,000 stress repetitions were sufficient to condition the sample for testing without significantly altering the specimen response. Conditioning the sample helps to avoid variations in axial deformations caused by end imperfections. He found that once the sample was conditioned, the response obtained at a relatively low number of stress applications (N = 50 to 100) was representative. As long as N was small, testing at many different stress levels was possible, before stiffening behavior became significant. With the number of stress applications on the order of 25,000, the test specimens stiffen and the response is affected, but at N = 100, many different stress levels could be applied, and the resilient properties at these levels could be determined. Tanimoto and Nishi (46) also emphasize the importance of selecting the proper number of stress

applications at which to determine resilient properties.

Seed et al (6) also found that the response of clay samples was dependent on the number of stress applications. In general, they found that compacted clays develop their greatest resilient deformation when N is less than 5000. This resilient deformation was found to decrease significantly at N > 100,000. Permanent deformations continued to increase at this number of applications. Figure (4.1) shows the effect of N on permanent strain with different levels of stress. Larger stresses took fewer load applications to yield excessive permanent strains.

Some question remains as to what number of stress applications is appropriate for the determination of resilient properties. The resilient behavior of cohesive soils is only evident at small numbers of load application; however, these soils are subjected to many more load applications in the field. It appears that the determination of the resilient modulus at lower numbers of stress applications is a conservative measure. It is lowest when resilience is greatest, and increases as the sample stiffens at high numbers of load applications. With N of the order of that expected in the field, the resilient modulus is much greater due to the subsequent stiffening of the soil, meaning increased subgrade support.

1.2. Thixotropy

Investigators have found that the response of cohesive soils can be greatly influenced by the length of time between preparation and testing. The strength increases as the time between preparation and testing (storage time) increased. However, this effect tends to diminish as the number of load applications increased.

Seed et al (6) found the resilient deformation decreased (the resilient modulus increased) as the time between compaction and testing increased. This effect could be seen for N < 40,000, but for N > 40,000, samples of all different ages began to exhibit the same behavior. For a number of load applications of the order of 10, the resilient modulus for 1 day and 50 days storage time may differ by as much as 300 or 400%. Figure (4.2) shows the effect of different storage times on the resilient modulus for a range of number of stress applications. For large value of N, the effects of aging are reduced and the same results are obtained for samples tested immediately after compaction as those tested

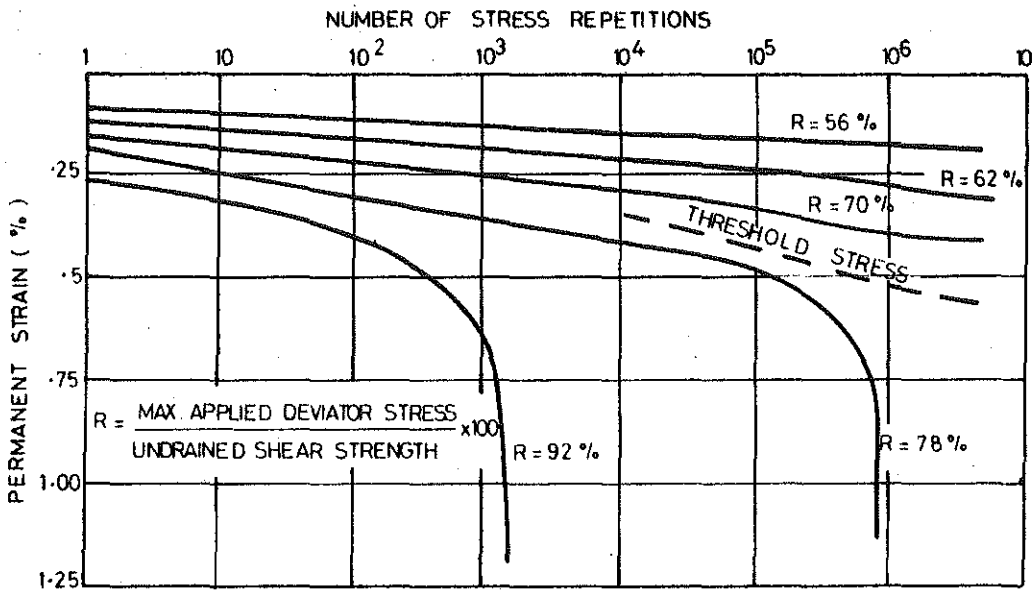

FIGURE 4.1 PERMANENT STRAIN Vs. NUMBER OF LOAD REPETITIONS FOR A SATURATED SILTY CLAY, (41).

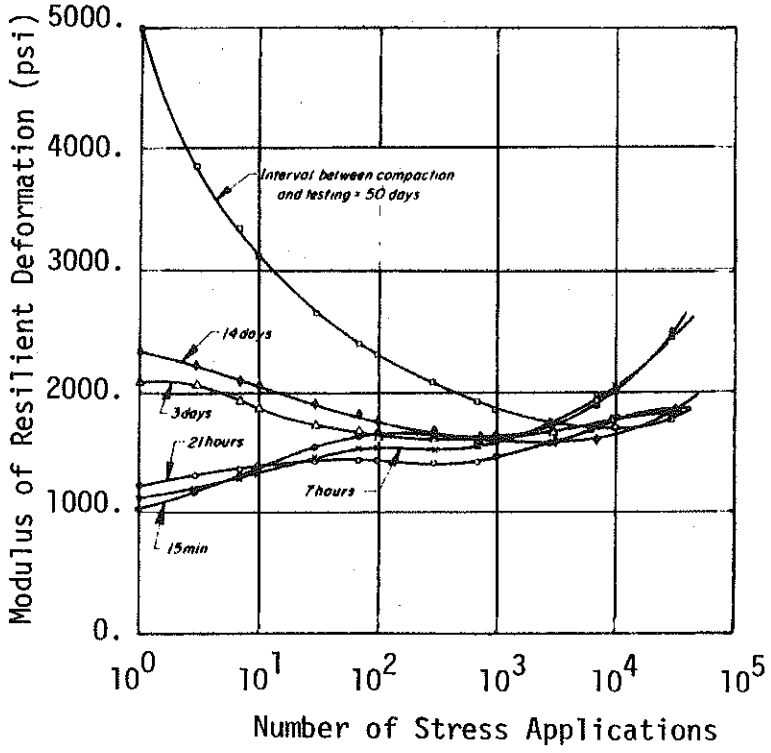

FIGURE 4.2 EFFECT OF THIXOTROPY ON RESILIENCE CHARACTERISTICS, AASHO ROADTEST SUBGRADE SOIL, (6).

after a period of time. Tanimoto and Nishi (46) also found this to be the case, but water content appeared to affect the thixotropic strength gain. At water contents far below or well above the optimum, they found that storage time had little effect on the specimen response. However, at water contents just above optimum this effect is much more pronounced. Again, these effects were destroyed by high numbers of stress applications. Figure (4.3) illustrates this point for a silty clay with an optimum water content of about 18 percent.

The effect of storage time on strength is still uncertain. The number of stress applications used in the lab can be developed usually within one day, whereas the number of stress applications under in-service conditions may take many years to develop. Once again, it appears that lab estimates of strength are conservative due to the much shorter times involved.

1.3 Stress Intensity

In all investigations, the relationship between the resilient modulus and the deviator stress is similar. At low stress levels, the resilient modulus decreases and the deviator stress increases. This is true up to a deviator stress of about 10 psi where the resilient modulus is found to be unaffected or increases only slightly with further increase in deviator stress. Because of this dependence on the deviator stress, it is important that lab tests are conducted at stresses which are expected in the field. Figure (4.4) shows the decrease in M_R as the deviator stress increases from 2 to 10 psi under a constant radial pressure. It also shows that Poisson's ratio is only slightly affected by changes in the deviator stress.

For test on silty clays Mitchell et al (35), using 24,000 load applications, found that the resilient modulus decreased with increasing deviator stress up to 25 psi, above which the resilient modulus increased slightly. Seed et al (6) had also found that the resilient modulus decreased rapidly with a variation of 300 to 400 percent as the deviator stress increased from 3 to 15 psi. Above this range the resilient modulus was observed to increase slightly, as shown in Figure (4.5). This means that as the depth of a soil element

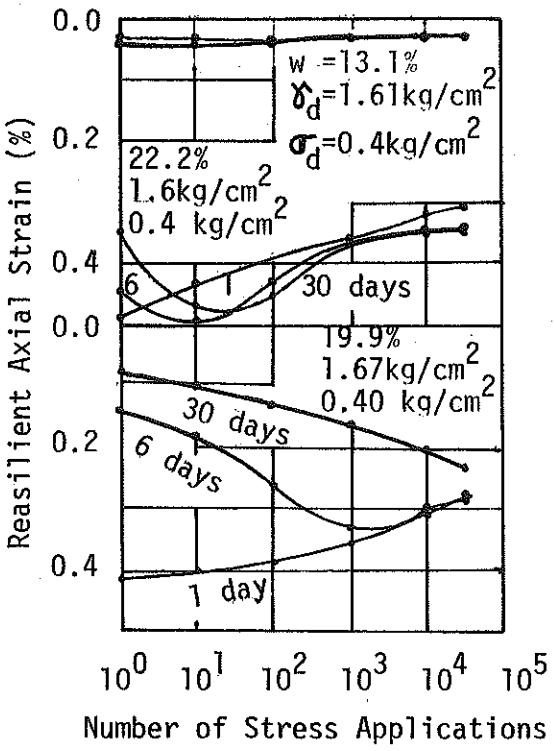

FIGURE 4.3 EFFECT OF STORAGE PERIOD ON RESILIENCE CHARACTERISTICS OF COMPACTED SUBGRADE MATERIAL,(46).

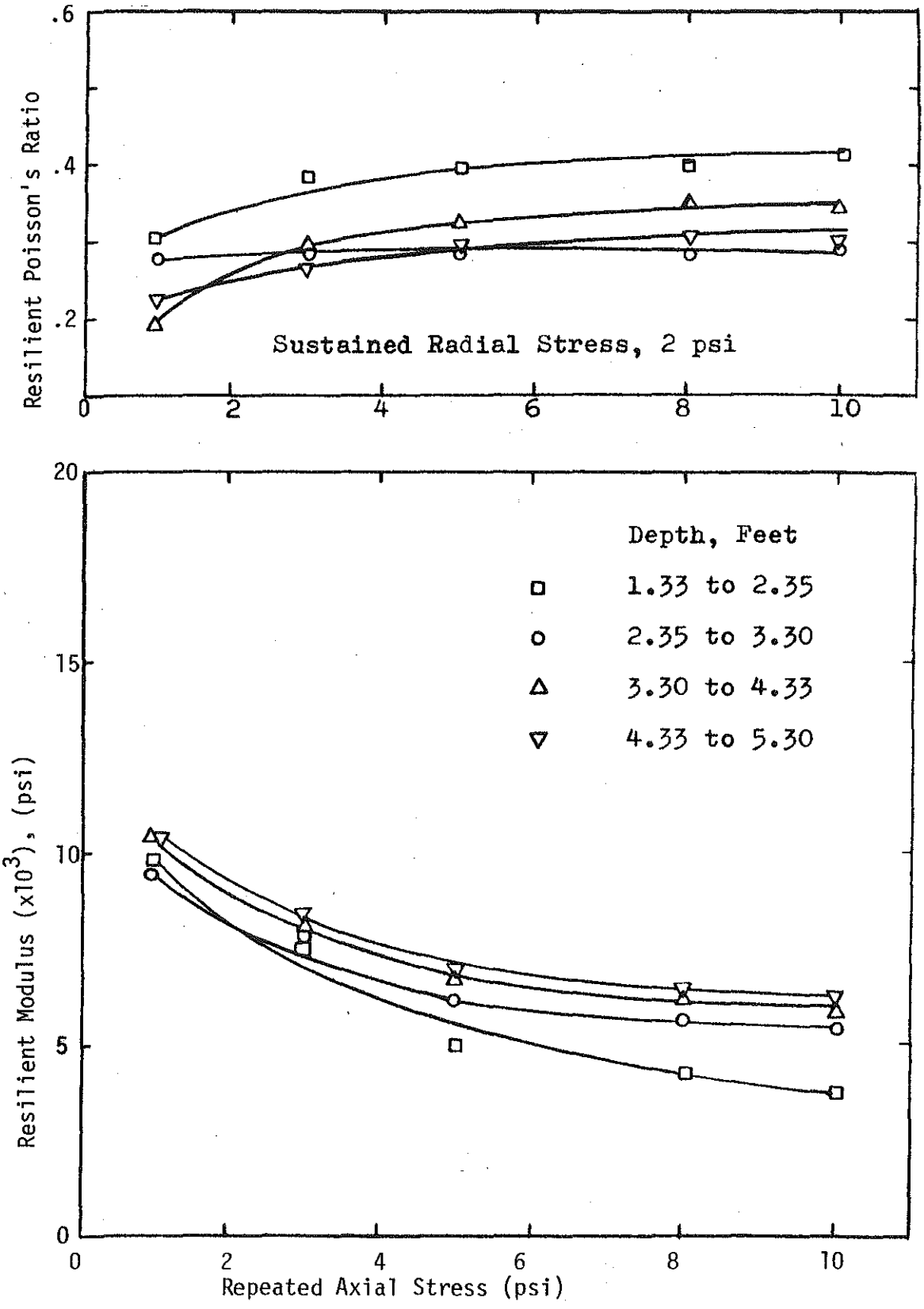

FIGURE 4.4 SECANT MODULUS AND POISSON'S RATIO OF CLAY SUBGRADE AS A FUNCTION OF REPEATED AXIAL STRESS AND DEPTH BENEATH PAVEMENT SURFACE, (29).

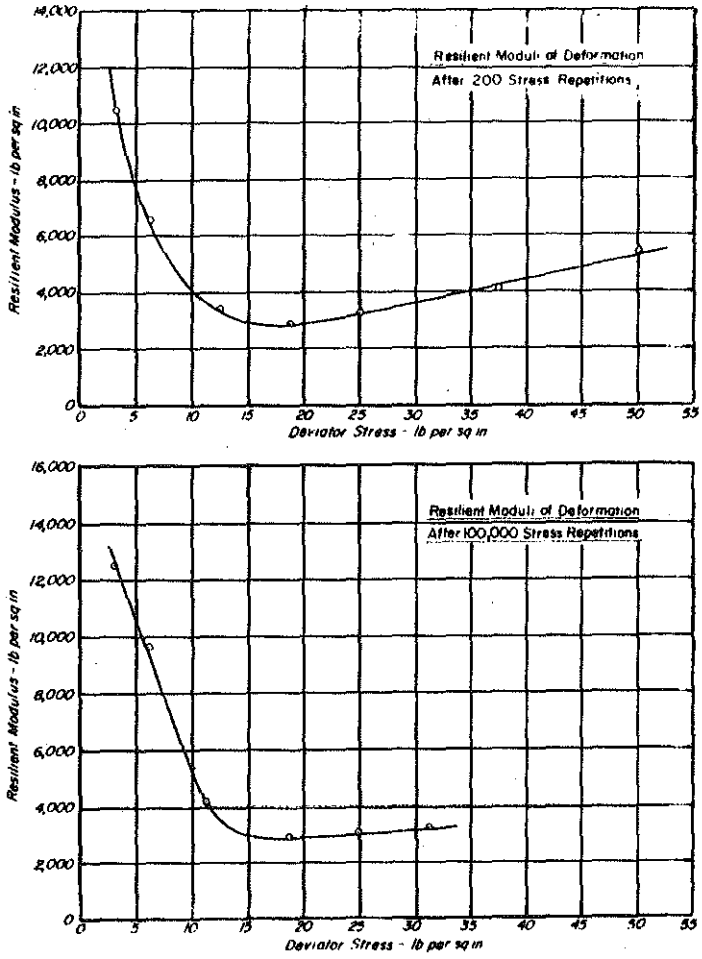

FIGURE 4.5 EFFECT OF STRESS INTENSITY ON RESILIENCE CHARACTERISTICS FOR AASHO ROAD TEST SUBGRADE SOIL, (6).

increases, and the applied deviator stress decreases, there will be an increasing resilient modulus with depth, assuming a uniform soil. Seed et al (43), using repeated plate load tests, and Tanimoto and Nishi (46) have also determined the same relationship.

1.4. Method of Compaction

The method of compaction employed during the preparation of a cohesive soil test specimen has a profound effect on the particle structure and subsequent behavior. Changes in particle structure are related to the shear strain induced in the soil by different methods of compaction.

When cohesive soils are compacted to relatively low degrees of saturation, the shear strain induced in the soil by any method of compaction is not appreciable. Particles assume a random edge to face configuration, which is termed a flocculated structure. The behavior of these samples at low degrees of saturation is similar, no matter what method of compaction is employed (76, 78, 81).

At higher degrees of saturation, such as those on the wet side of the optimum water content, the shear strain induced by various compaction methods may vary greatly. As the hammer or tamping foot penetrates, the soil tends to heave upward around it. The particles tend to align themselves parallel with the surface of shear and with one another. Throughout the sample there are local areas where the particles are situated predominately parallel to each other, termed a dispersed structure (81, 82, 83, 95).

For high degrees of saturation and a static method of compaction, a flocculated structure is retained. Because pressure is applied to the entire surface of the soil, no shear strain, which causes the dispersed structure, is induced. We can obtain the same flocculated structure for a high degree of saturation by soaking the sample. The boundary between the higher and lower degree of saturation appears to be at a degree of saturation of approximately 85 percent. This closely corresponds to the line of optimum water contents. Figure (4.6) shows the different particle structures resulting from kneading and static compaction at different degrees of saturation.

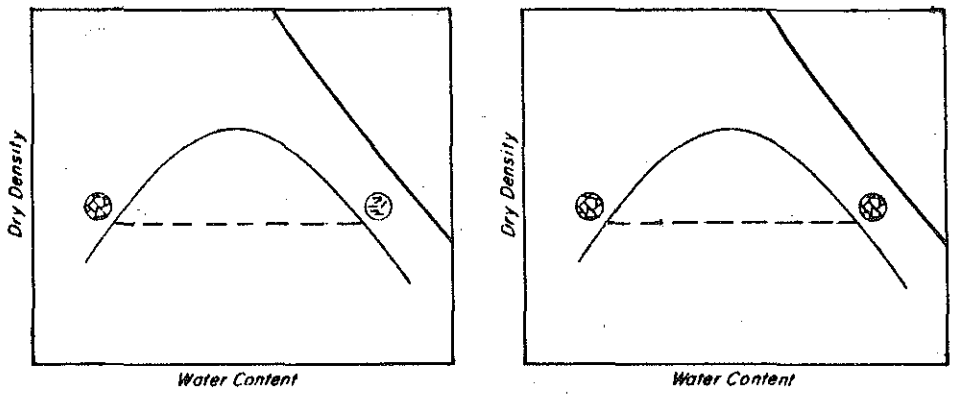

a) Kneading Compaction b) Static Compaction

FIGURE 4.6 PARTICLE ORIENTATIONS IN COMPACTED CLAYS, (6).

For samples compacted dry of optimum, the resilient behavior is essentially the same, regardless of the method of compaction. The resilient behavior of samples compacted wet of optimum varies greatly, depending upon the compaction method. Flocculated structures, obtained by static compaction, produce higher values of resilient modulus and lower resilient deformations than for the dispersed structures obtained by kneading compaction. A comparison of the resilient properties is shown in Figure (4.7) for a degree of saturation of 95 percent.

Using the appropriate method of compaction in preparation, it is possible to simulate field conditions very closely. Seed et al (6) concluded that the particle structures induced by rubber tired rollers in the field, and kneading compaction in the lab, were very similar, since samples from both exhibited similar properties. Clays in the field are typically compacted dry of optimum and thus retain a flocculated structure. To test a critical condition, such as a high degree of saturation, the particle structure tested in the lab must also possess a flocculated structure. This can be obtained in the two ways pointed out above: kneading compaction at a low degree of saturation, and subsequent soaking, or static compaction at the desired degree of saturation. To soak the former would require a great deal of time, whereas static compaction can obtain the required results in much less time.

1.5. Compaction Density and Water Content

All investigators have found that an increasing water content at compaction leads to an increase in resilient deformation, and a decrease in strength and resilient modulus. For a given compactive effort, the resilient deformation is relatively low at water contents dry of optimum, but it increases rapidly as the water content at compaction exceeds the optimum. Seed et al (6) found that for a given dry density, the resilient modulus decreased as the water content at compaction increased. The resilient deformations increased with the water content. Seed et al (43) and Tanimoto and Nishi (46) reported the same results. Figure (4.8), from Monismith and Finn (38), relates the resilient modulus to water content and dry density. It

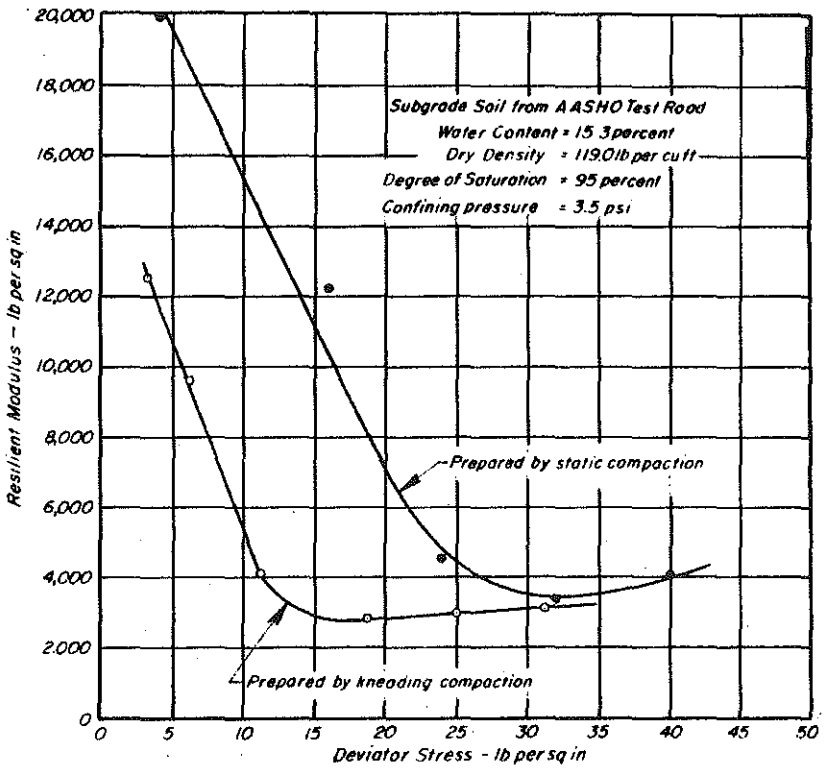

FIGURE 4.7 EFFECT OF METHOD OF COMPACTION ON RELATIONSHIP BETWEEN RESILIENT MODULUS AND STRESS INTENSITY, (6).

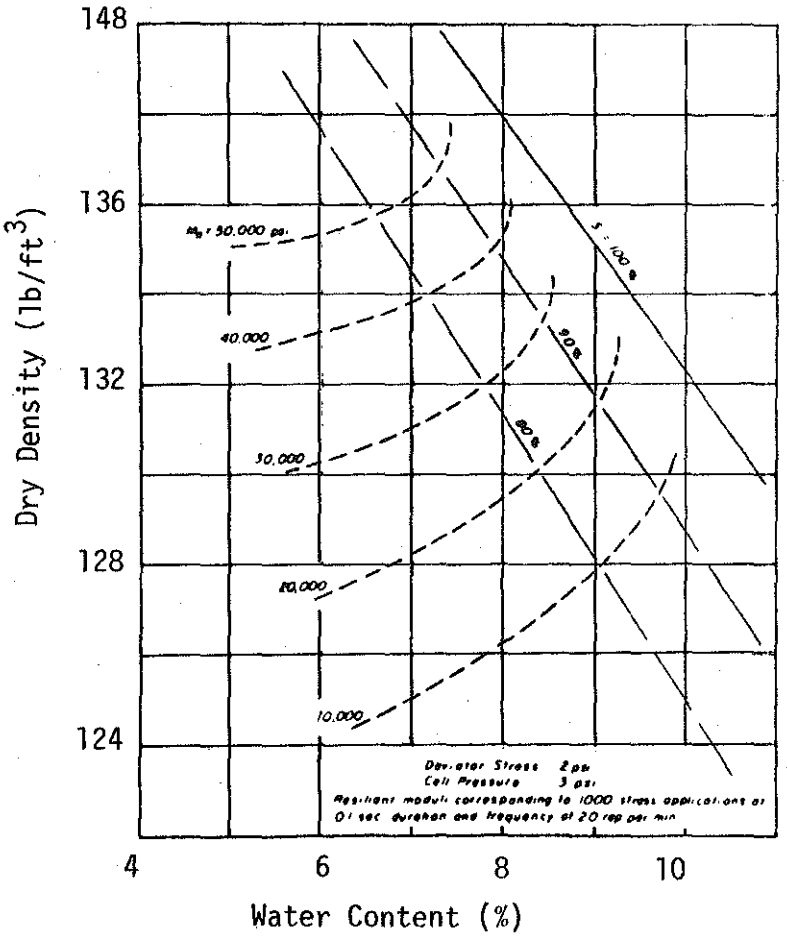

FIGURE 4.8 WATER CONTENT-DRY DENSITY-RESILIENT MODULUS RELATIONSHIP FOR SUBGRADE SOIL, (38).

shows the decrease of M_R with increasing water content. It also shows that for a given water content at compaction, as the dry density increases, the resilient modulus also increases, until it levels off at the optimum condition, then M_R begins to decrease slightly.

At high degrees of saturation, minor changes in dry density or water content have significant effects on the resilient behavior. Seed suggested that this is attributable to the marked change which can take place in the soil structure at this range. He feels that it is desirable to compact samples to a saturation of about 80 percent to avoid this and minimize the resilient deformation. One further caution is also made. Under field conditions, traffic loading of the subgrade soil may tend to densify it, and also reduce the water content. Both of these conditions, along with the large number of repeated loadings, will lead to higher strength and resilient modulus than expected. This is an important consideration in pavement deflection predictions.

Figure (4.9) shows that as the dry density increases, the resilience decreases. If two samples are allowed to absorb water to a degree of saturation of 90% after compaction at an identically lower degree of saturation, the one compacted to a higher density will exhibit much less resilience as shown in this figure. Figure (4.10) shows that the resilient deformation of samples soaked to a higher degree of saturation after being compacted at a low degree of saturation is much smaller than those samples compacted by kneading to the same final condition. The resilient deformation of samples compacted directly to a high degree of saturation may be many times larger than those which attain the same degree of saturation by soaking after compaction at a lower water content.

During construction, a subgrade will most often be compacted to a degree of saturation of approximately 75 percent. This would correspond to a flocculated particle structure as stated previously. After a long period of time, the subgrade may absorb water with no volume change, raising its degree of saturation to about 90 or 95 percent. It is virtually impossible to reproduce this condition by soaking, because the degree of saturation will not be uniform throughout

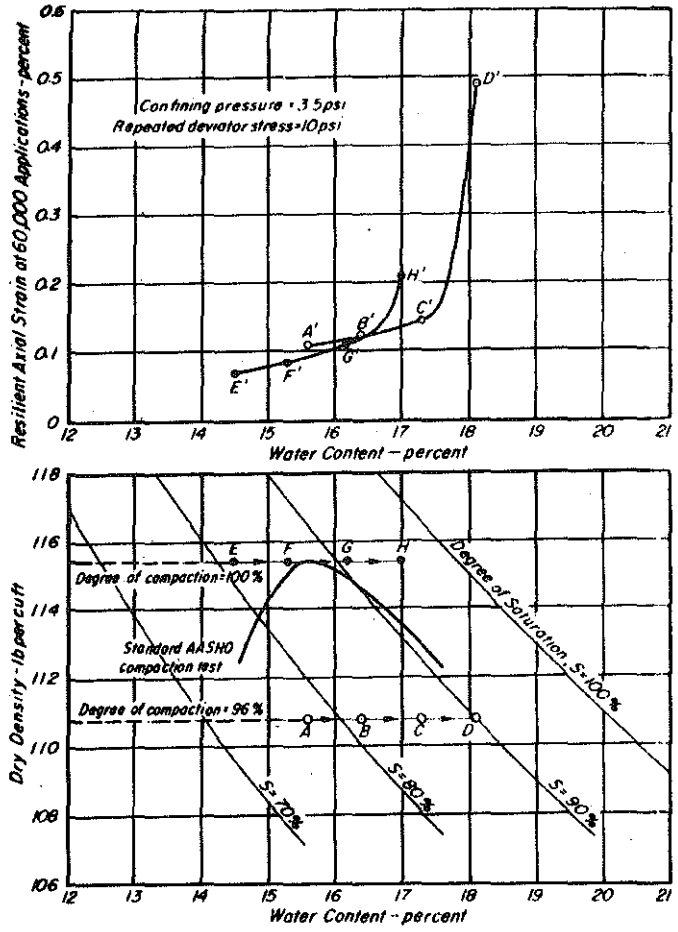

FIGURE 4.9 EFFECT OF INCREASE IN WATER CONTENT AFTER COMPACTION ON RESILIENT DEFORMATIONS, AASHO ROAD TEST SUBGRADE SOIL, (6).

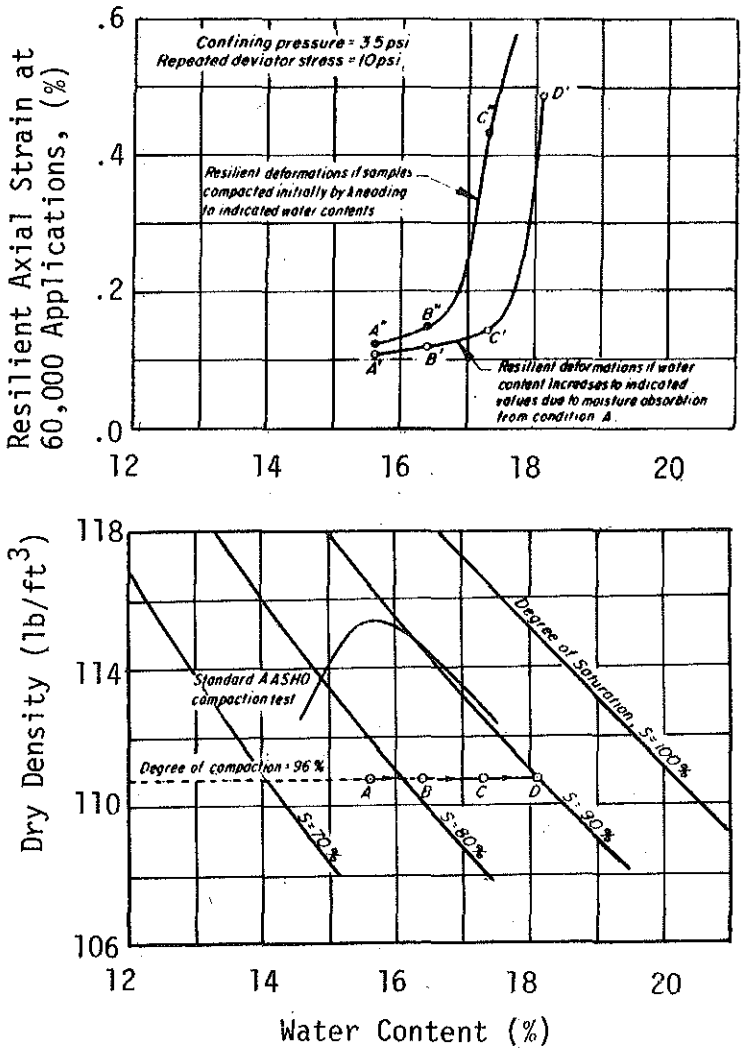

FIGURE 4.10 EFFECT OF METHOD OF ATTAINING FINAL MOISTURE CONDITION ON RESILIENT STRAINS, (6).

the sample. The exterior portions may be saturated 100 percent, while the center may still be only about 80 percent. This is the reason static compaction is used for tests on samples with degrees of saturation greater than 85 percent.

1.6. Confining Pressure

The resilient response of cohesive soils is relatively unaffected by changes in cell pressure during the repeated load triaxial test. In tests on subgrade soils from a prototype pavement, Hicks (28) reported that the stress-strain relationship is little affected by changes in radial stress. This was typical of all samples tested. Table (4.1) illustrates these findings. In tests on silty clays, for the same repeated load, Tanimoto and Nishi (46) reported that the resilient modulus is unaffected by confining pressure, as shown in Figure (4.11). Terrel and Awad (47) also reported similar findings.

1.7. Stress Sequence

Dehlen (75) studied the effects of stress repetitions and sequence on stiff silty clay soil. He found that if 25,000 repetitions were applied at each stress level, the sequence in which the stress levels were applied had a significant effect on the measured resilient modulus, since the sample tended to stiffen due to prior applications of stress. However, if only 100 repetitions were applied at each stress level, the stress sequence had little effect on the resilient modulus measured, provided that the stresses applied were in the range expected under a pavement. In both the 100 and 25,000 repetition tests, Poisson's ratio was relatively unaffected by stress sequence.

2. COHESIONLESS SOILS

The behavior of granular materials found in the base and subbase courses of flexible pavements differs greatly from that of fine-grained soils found in the subgrade. The factors which affect their behavior are more numerous and most of these are related to conditions under which these soils are tested. The state of stress during testing appears to be of much greater importance, and the method of sample preparation seems to be of less importance than previously seen for cohesive soils. In this section, the soil properties and triaxial test parameters which significantly affect the response of cohesionless soils during testing are discussed.

TABLE 4.1 STRESS-STRAIN PAIRS FOR SUBGRADE SAMPLE NO. 2-1, (29).

Repeated Axial Stress	Sustained Radial Stress	Axial Micro Strain	Radial Micro Strain
10.0	3.0	2900.0	1150.0
8.0	3.0	1850.0	750.0
5.0	3.0	900.0	362.0
3.0	3.0	380.0	150.0
1.0	3.0	85.0	26.0
10.0	2.0	2700.0	1100.0
8.0	2.0	1850.0	750.0
5.0	2.0	975.0	387.0
3.0	2.0	390.0	150.0
1.0	2.0	110.0	33.7
10.0	1.0	2700.0	1100.0
8.0	1.0	1850.0	750.0
5.0	1.0	975.0	400.0
3.0	1.0	430.0	168.7
1.0	1.0	95.0	30.0

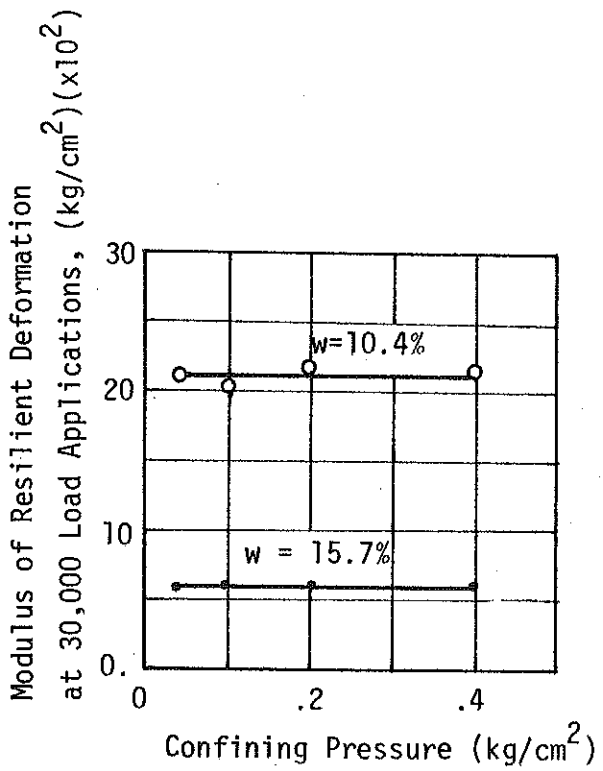

FIGURE 4.11 EFFECT OF CONFINING PRESSURE ON RESILIENCE CHARACTERISTICS OF COMPACTED SUBGRADE MATERIAL, (46)

2.1. Number of Stress Applications

Although researchers are not in full agreement as to the type of effect the number of stress applications has upon the resilient response, they are in agreement that the magnitude of this effect is slight. Some have found that the resilient modulus increases slightly, while still others have observed a decrease in resilient modulus with increasing load applications. Morgan (39) in tests on fine sands, reported that the resilient modulus increases slightly up to about 10,000 load applications, whereafter it remained constant. Tanimoto and Nishi (46) reported similar results, with resilient strain decreasing and resilient modulus increasing slightly, with increasing number of stress applications.

Between 100 and 25,000 stress applications, Hicks (29) found that the values of both the resilient modulus and Poisson's ratio remained fairly constant for dry granular materials. The lower limit of this range was raised slightly for partially saturated materials, where these properties were constant beyond about 100 to 300 stress applications. For saturated granular materials, these properties are constant up to approximately 1,000 stress applications, beyond which the resilient modulus decreases slightly and Poisson's ratio increases slightly. Hicks suggested that this is due to the build-up of pore water pressure and a corresponding decrease in effective confining stress.

Hicks and Monismith (27), and Barksdale and Hicks (23) found that approximately 1,000 stress applications will properly condition the sample and avoid variations in the axial strain due to end imperfections. Once the sample is conditioned, 50 to 100 stress applications can be used to properly characterize the resilient response. They also stated that one sample can be used in this manner to determine the resilient response for many different stress intensities, provided they are in the range of those stresses likely to occur in the pavement. The fact that one sample can be used to study the resilient response under various stress intensities illustrates that a complex stress history has a little effect on the resilient response. For saturated granular materials, they found that the sample response was subject to change due to the build-up

of pore water pressure which causes a reduction in the effective confining stress. This appears to be related to the phenomenon of liquefaction. Studies showed that the possibility of this occurrence was reduced if these samples were conditioned in a drained state.

Kalcheff and Hicks (31) reported that the number of stress applications had little affect on the resilient response of granular materials. For those samples with complex stress histories, they recommended 150 to 200 stress applications to get a good estimate of the resilient properties.

2.2. Stress Intensity

Once again, researchers have failed to find unanimity on the effect the deviator stress on the resilient modulus; however, they do agree that the effect (whatever it is) is slight. Hicks (29) stated that all studies indicate that the resilient modulus is relatively unaffected by the magnitude of the deviator stress. The investigations of Trollope (59), Mitchell (35), Kallas and Riley (63) and Seed et al (43) all came to this conclusion. Morgan (39) found that the resilient modulus decreases and the permanent deformation increases with increasing deviator stress, Figure (4.12). Also, he reported that for a range in deviator stress from 20 to 50 psi, Poisson's ratio appeard to be constant.

Hicks (29) found that for lower levels of axial stress, a slight softening occurred in the axial strain, whereas at high levels of axial stress, the specimens tended to stiffen. A softening pattern was always observed for the radial strains. These points are illustrated by the data in Table (4.2). Figure (4.13) shows the variation of axial and radial strains with axial stress. Hicks also found that Poisson's ratio always increased with increasing deviator stress or principal stress ratio, but this increase appeared to be random.

Hicks and Monismith (27) reported a slight increase in resilient modulus with increasing deviator stress (principal stress ratio), as shown in Figure (4.14). Figure (4.15) shows this increase in Poisson's ratio with deviator stress. Hicks and Monismith also point out that Poisson's ratio can be reasonably approximated by the following equation:

$$\nu_r = A_0 + A_1 \left(\frac{\sigma 1}{\sigma_3}\right) + A_2 \left(\frac{\sigma_1}{\sigma_3}\right)^2 + A_3 \left(\frac{\sigma_1}{\sigma_3}\right)^3 \qquad (4.1)$$

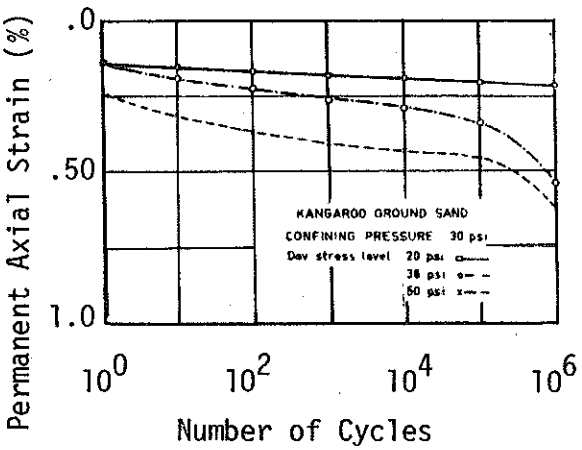

FIGURE 4.12 VARIATION OF PERMANENT AXIAL STRAINS WITH NUMBER OF CYCLES AND DEVIATOR STRESS AT CONSTANT CONFINING PRESSURE, (39).

TABLE 4.2 STRESS-STRAIN PAIRS FOR DRY COARSE AGGREGATE SAMPLE, (29).

REPEATED AXIAL STRESS	SUSTAINED RADIAL STRESS	AXIAL MICRO STRAIN	RADIAL MICRO STRAIN
35.	50.	400.0	102.5
30.	50.	337.5	81.2
20.	50.	235.0	45.0
15.	50.	170.0	23.7
10.	50.	110.0	12.5
35.	30.	550.0	170.0
30.	30.	475.0	145.0
20.	30.	325.0	82.5
15.	30.	245.0	52.5
10.	30.	160.0	25.0
35.	20.	675.0	262.5
30	20.	637.5	235.0
20.	20.	440.0	127.5
15.	20.	335.0	78.7
10.	20.	205.0	41.2
5.	20.	82.5	7.5
35.	10.	1150.0	625.0
30.	10.	1012.5	506.2
20.	10.	712.5	293.7
15.	10.	550.0	195.0
10.	10.	390.0	130.0
5.	10.	150.0	38.7
30.	5.	1325.0	1100.0
20.	5.	1062.5	687.5
15.	5.	825.0	431.2
10.	5.	550.0	237.5
5.	5.	280.0	97.5
3.	5.	145.0	35.0
15.	3.	850.0	562.5
10.	3.	612.5	337.5
5.	3.	350.0	165.0
3.	3.	202.5	80.0
10.	2.	724.0	580.0
5.	2.	435.0	269.0
3.	2.	275.0	145.0
5.	1.	487.5	481.2
4.	1.	420.0	381.2
3.	1.	342.0	293.7

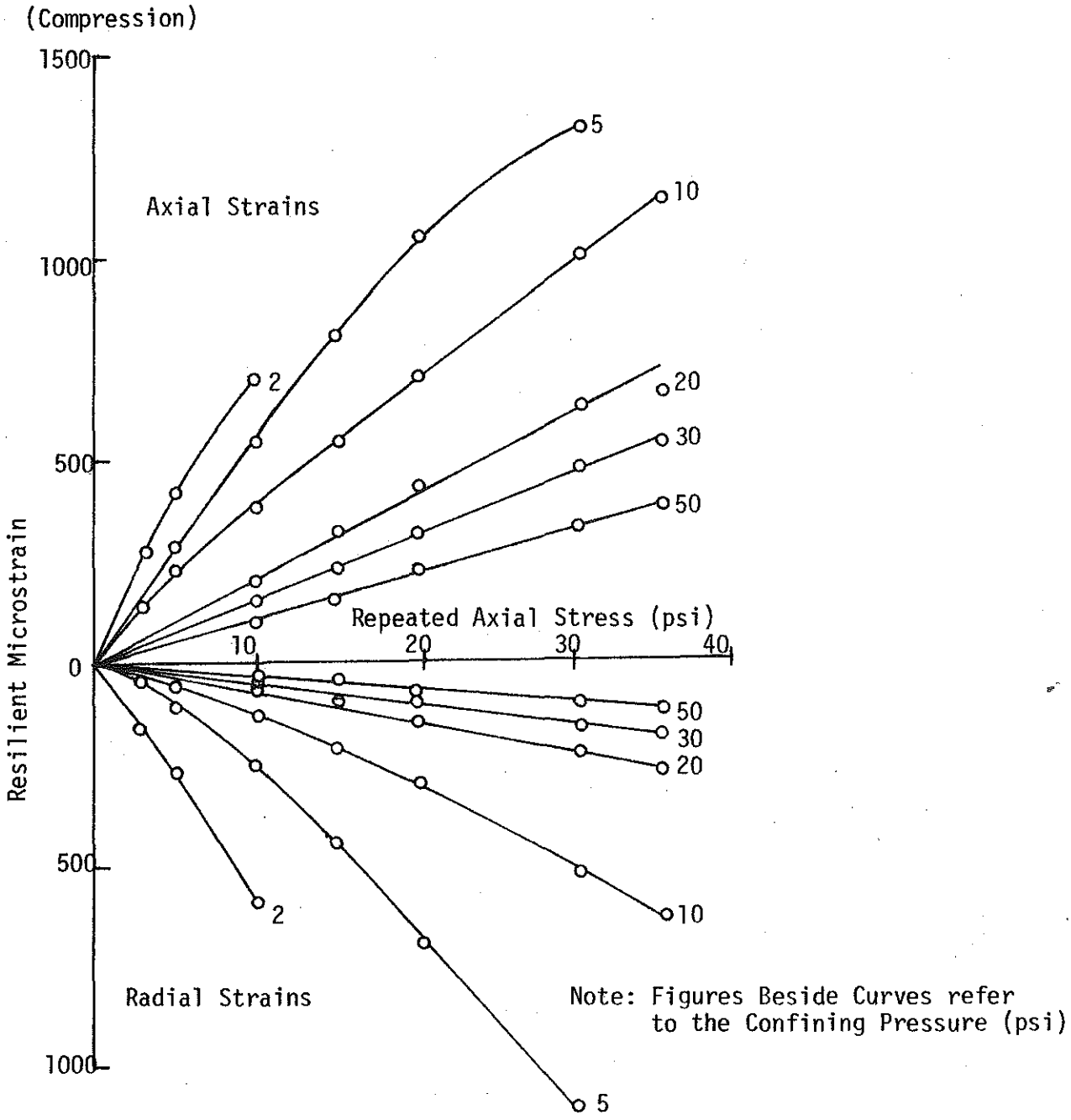

FIGURE 4.13 VARIATION IN AXIAL AND RADIAL STRAINS WITH AXIAL STRESS,(27).

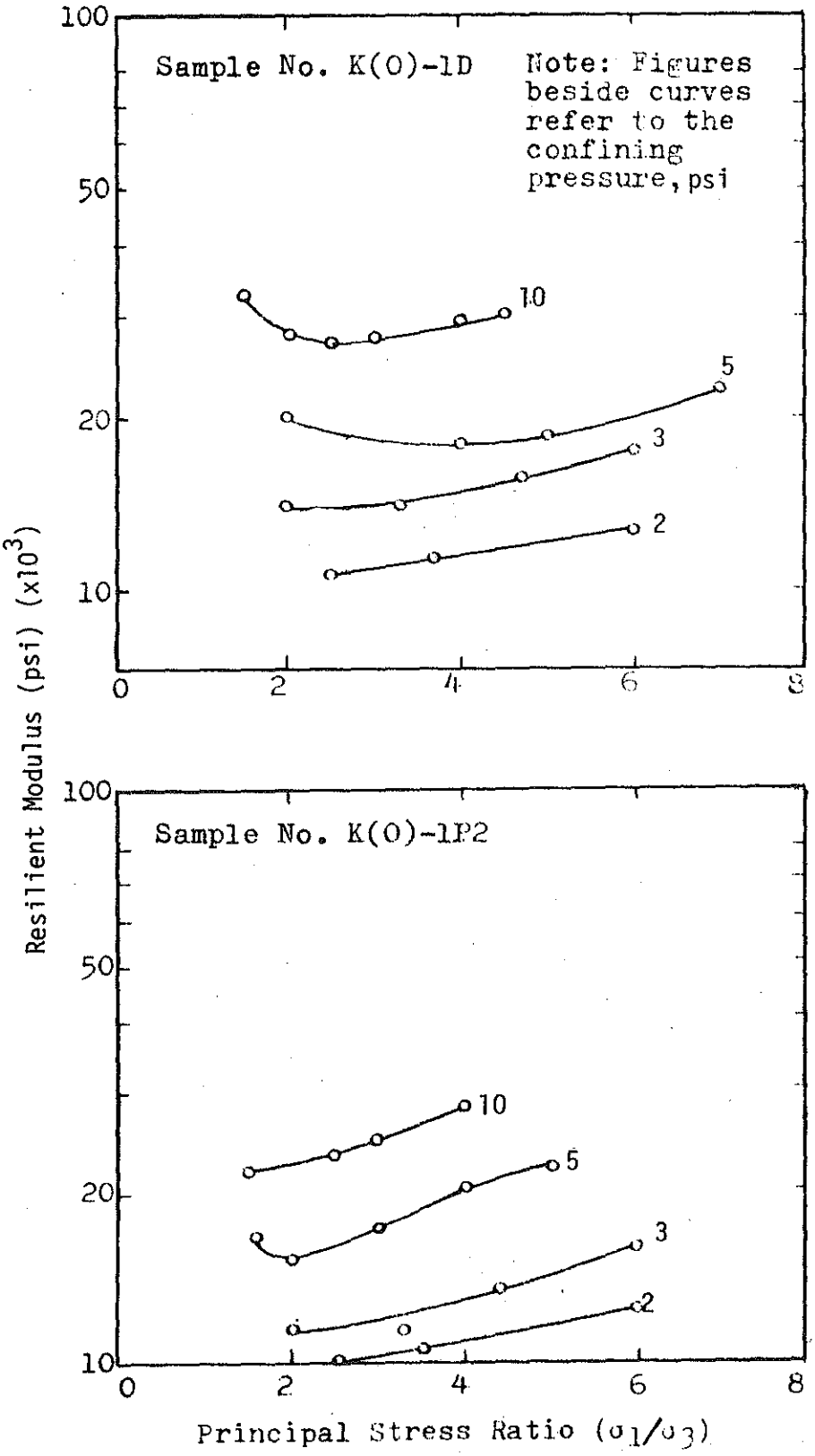

FIGURE 4.14 VARIATION IN RESILIENT MODULUS WITH PRINCIPAL STRESS RATIO, (27).

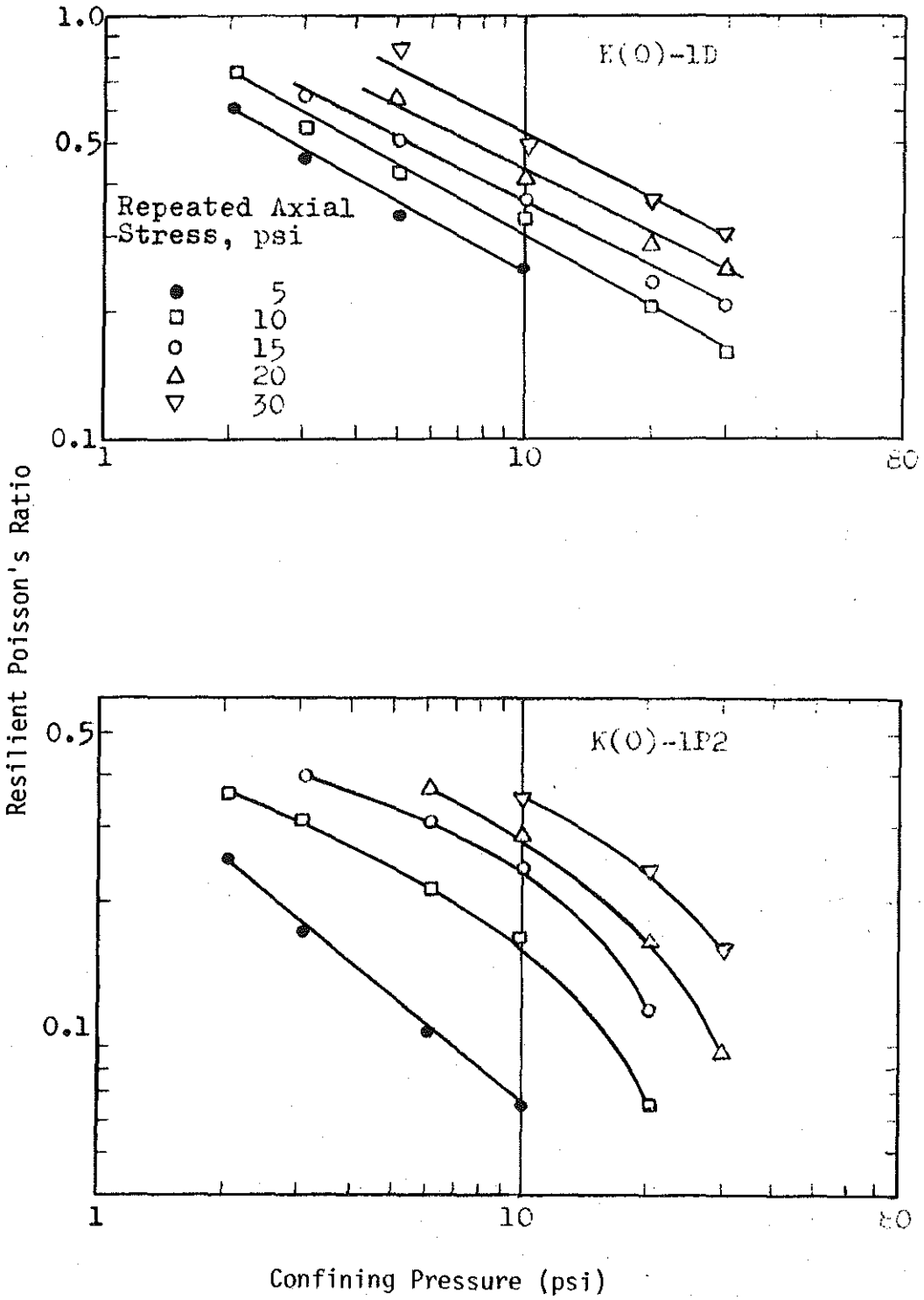

FIGURE 4.15 VARIATION IN RESILIENT POISSON'S RATIO WITH STRESS LEVEL, (27).

Barksdale and Hicks (23) in studies on plastic strain in sands found that at lower values of deviator stress, the rate of accumulation of plastic strain tended to decrease as the number of load applications increased. At higher values of deviator stress, the reverse was found to be true: the rate of accumulation of plastic strain increased as the number of stress applications increased. This is significant in studies of rutting in flexible pavements.

2.3. Stress Sequence

One specimen could be used to test the resilient response of sand over a wide range of stress levels which could be applied in any order without error (27, 31, 22). However, Kalcheff and Hicks (31) reported that the measured plastic properties changed considerably as the stress sequence varied.

2.4. Confining Pressure

There seems to be no question as to the effect of confining pressure, in a triaxial cell, upon the resilient modulus. The higher the confining pressure, the higher the resilient modulus (23, 29, 38, 39, 47, and 61). Tests at the Texas Transportation Institute in 1963 by Dunlap (61) show that the resilient modulus increased by 500% as the confining pressure increased from 3 to 30 psi with the largest increase occurring at confining pressures from 1 to 10 psi. Direct relationships, as introduced earlier, were suggested between the resilient modulus M_R and either of the confining pressure σ_3 or the sum of the principal stresses, θ.

$$M_r = K\,\sigma_3^{\,n} \tag{4.2}$$

$$M_r = K^1\,\theta^{n_1} \tag{4.3}$$

in which K, K^1, n and n^1 are constants determined by a least squares curve fitting method. Figures (4.16), (4.17), (4.18), (4.19), and (4.20) show these relationships for sand, dry gravel and base course aggregates. Morgan (39) attempted to explain these relationships by the elastic compression of the soil skeleton. He stated that as the confining pressure increased, the side portions of the sample would be held more firmly in place. Consequently, the soil resilience will be reduced. He also

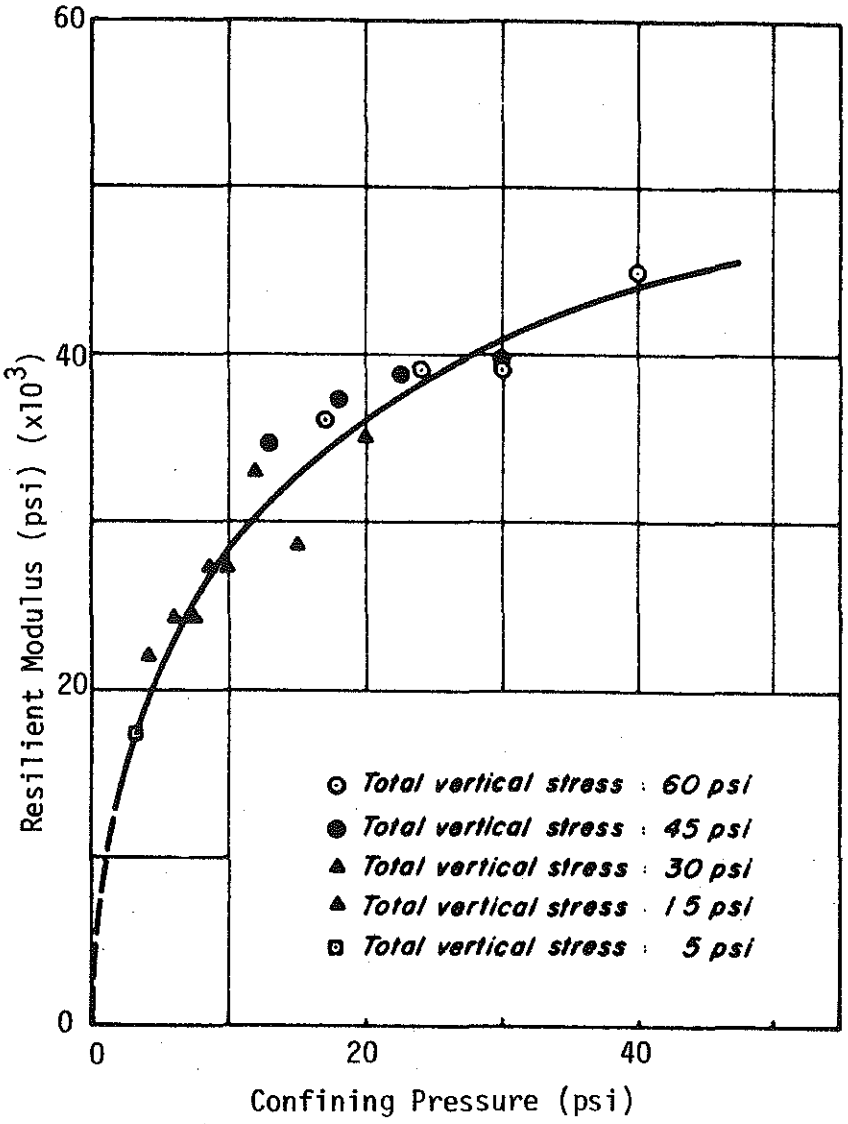

FIGURE 4.16 ARITHMETIC PLOT OF THE RELATIONSHIP BETWEEN RESILIENT MODULUS AND CONFINING PRESSURE FOR SAND, (43).

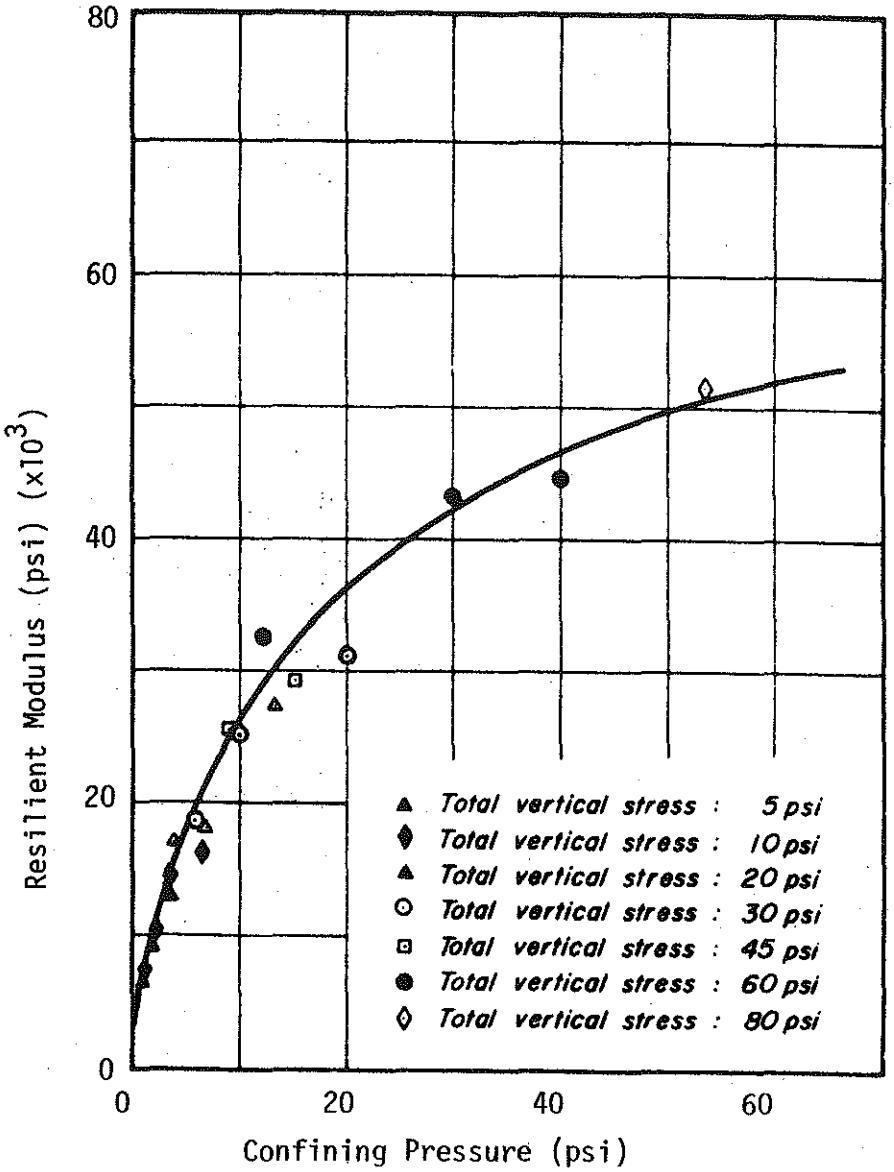

FIGURE 4.17 ARITHMETIC PLOT OF THE RELATIONSHIP BETWEEN RESILIENT MODULUS AND CONFINING PRESSURE FOR GRAVEL,(43).

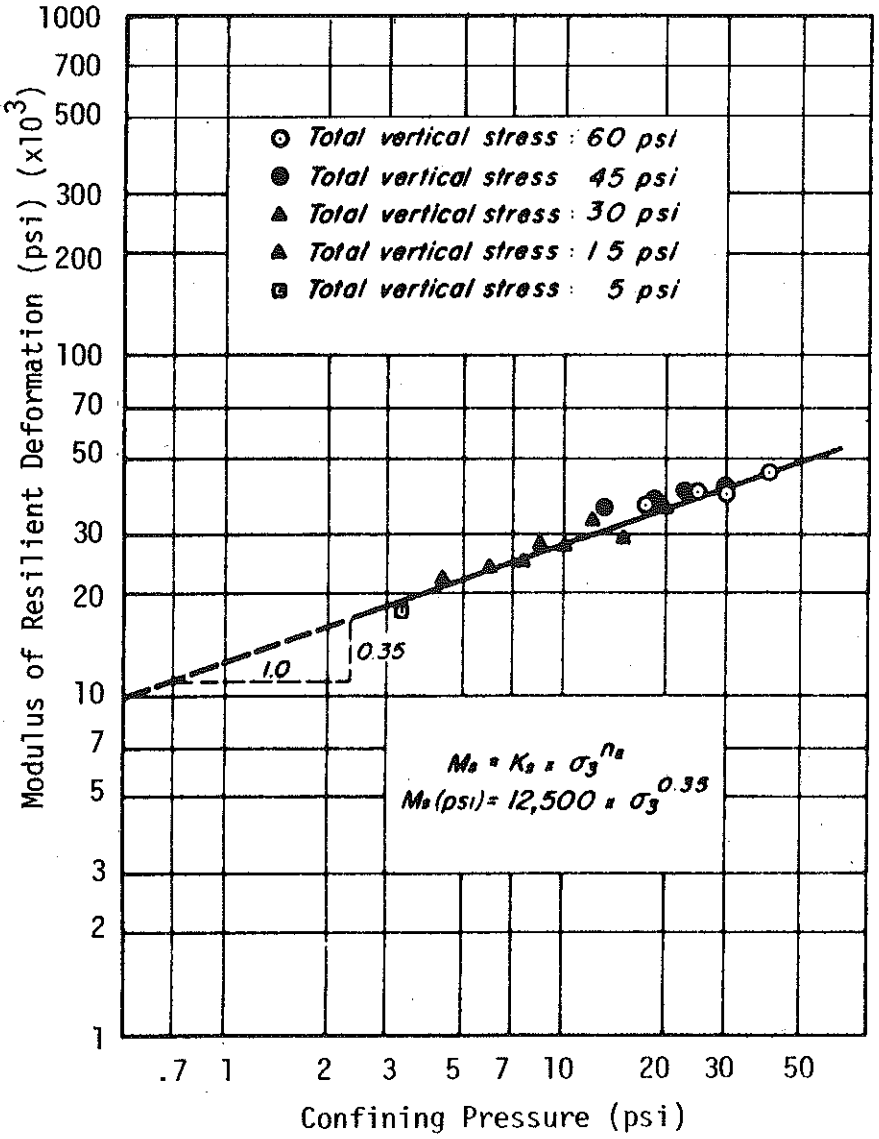

FIGURE 4.18 LOG-LOG PLOT OF THE RELATIONSHIP BETWEEN RESILIENT MODULUS AND CONFINING PRESSURE FOR SAND, (43).

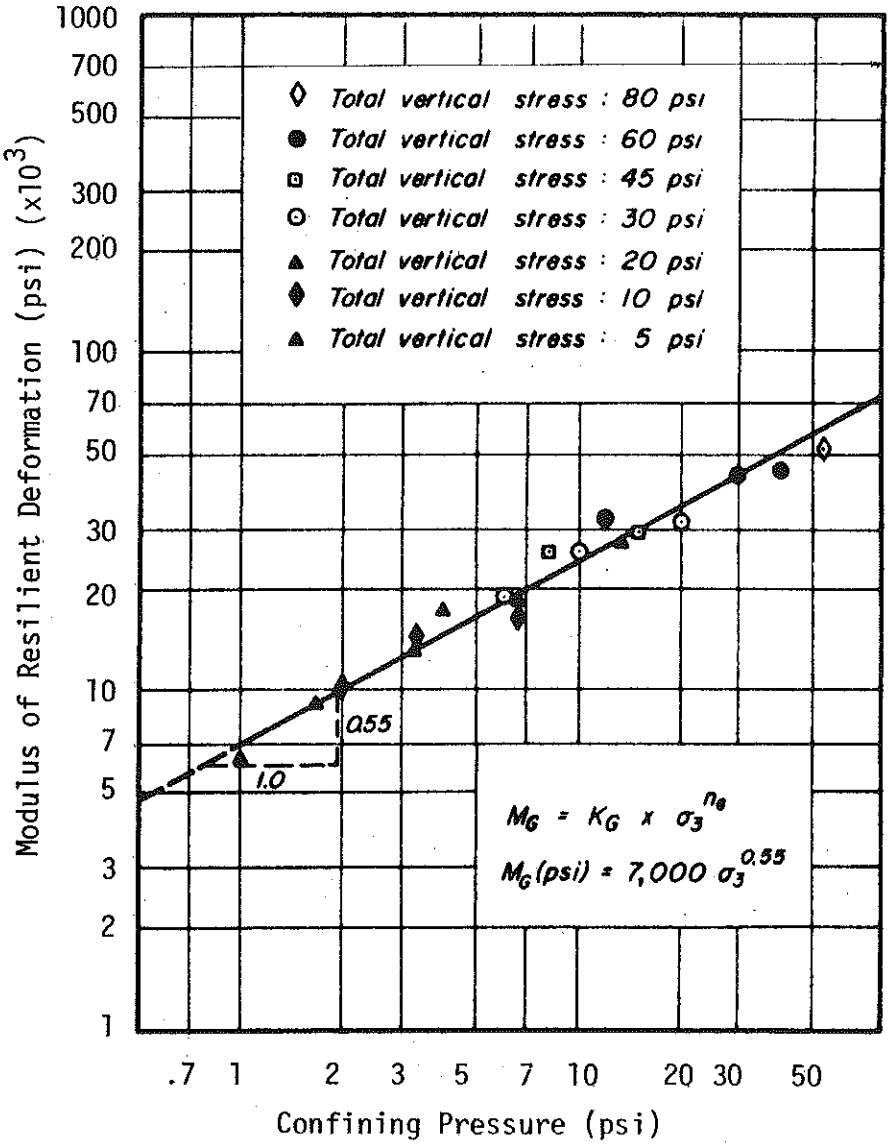

FIGURE 4.19 LOG-LOG PLOT OF THE RELATIONSHIP BETWEEN RESILIENT MODULUS AND CONFINING PRESSURE FOR GRAVEL, (43).

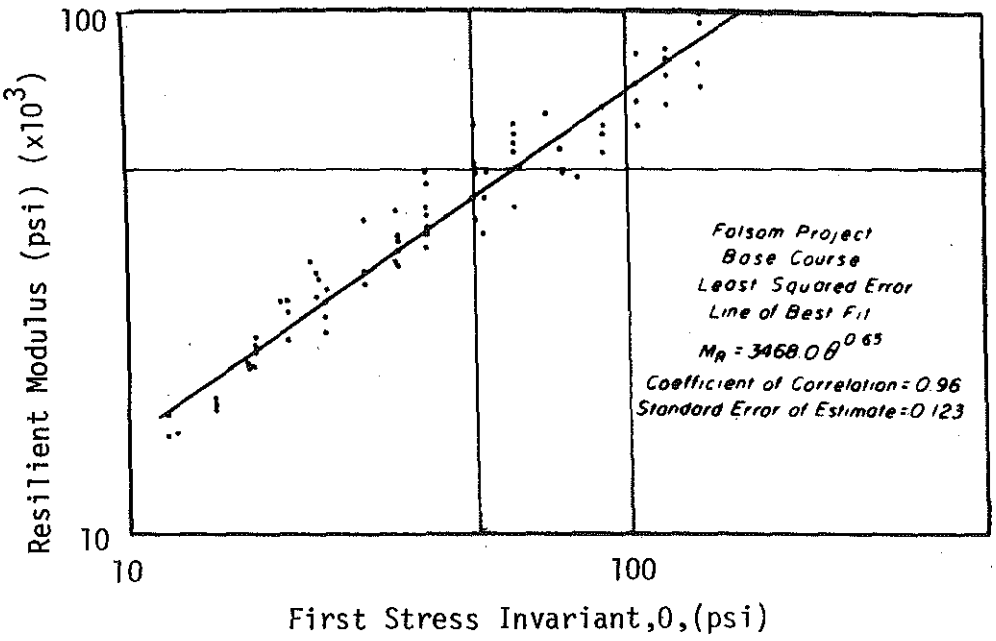

FIGURE 4.20 RELATIONSHIP BETWEEN RESILIENT MODULUS AND SUM OF PRINCIPAL STRESSES, (38).

found that at a constant deviator stress, the axial strain decreased with increasing confining pressure. However, Poisson's ratio did not appear to be related to confining pressure. In contrast to Morgan's results, Hicks and Monismith (27) found that Poisson's ratio increased as the confining pressure decreased. In all cases, they reported the non-linearity of the stress-strain relationship increased as the confining pressure decreased.

Allen and Thompson (22) have compared results based on triaxial testing with a constant confining pressure (CCP), to those with variable confining pressure (VCP). They found that the resilient modulus values for the CCP tests were slightly higher than those for the VCP. Also, the permanent deformation in CCP tests was always greater than that in the VCP. Barksdale (23) found that the plastic strain, permanent deformation, decreased with increasing confining pressure. Tests associated with a current research project, sponsored by the Michigan Department of State Highways and Transportation, conducted by Baladi at Michigan State University, tend to confirm both results. Results obtained from a repeated load triaxial testing with a constant low confining pressure tend to be on the conservative side when they are used to study rutting in the flexible pavement which is associated with the accumulation of plastic strain in the surface and base course layers.

The least squares equation relating M_R to θ was found to be more accurate than that relating M_R to confining pressure. Analysis of test data revealed higher correlation coefficients and a lower standard error for equation (4.3) than for equation (4.2). The explanation for this is believed to be that equation (4.3) accounts for all 3 principal stresses, whereas equation (4.2) accounts for only 2 principal stresses. The constant confining pressure tests tended to overestimate the value of Poisson's ratio, which was believed to be attributable to the anisotropic behavior of the material and the increased volume change of the sample associated with the CCP test. Figures (4.21) and (4.22) show these results for the VCP and CCP tests, respectively. Elastic, isotropic materials cannot have a Poisson's ratio that exceeds 0.5, but this is always the case for the CCP test. Allen and Thompson concluded that the use of a constant value of Poisson's ratio of 0.35 to 0.4 is an adequate representation of this property for pavement deflection analyses.

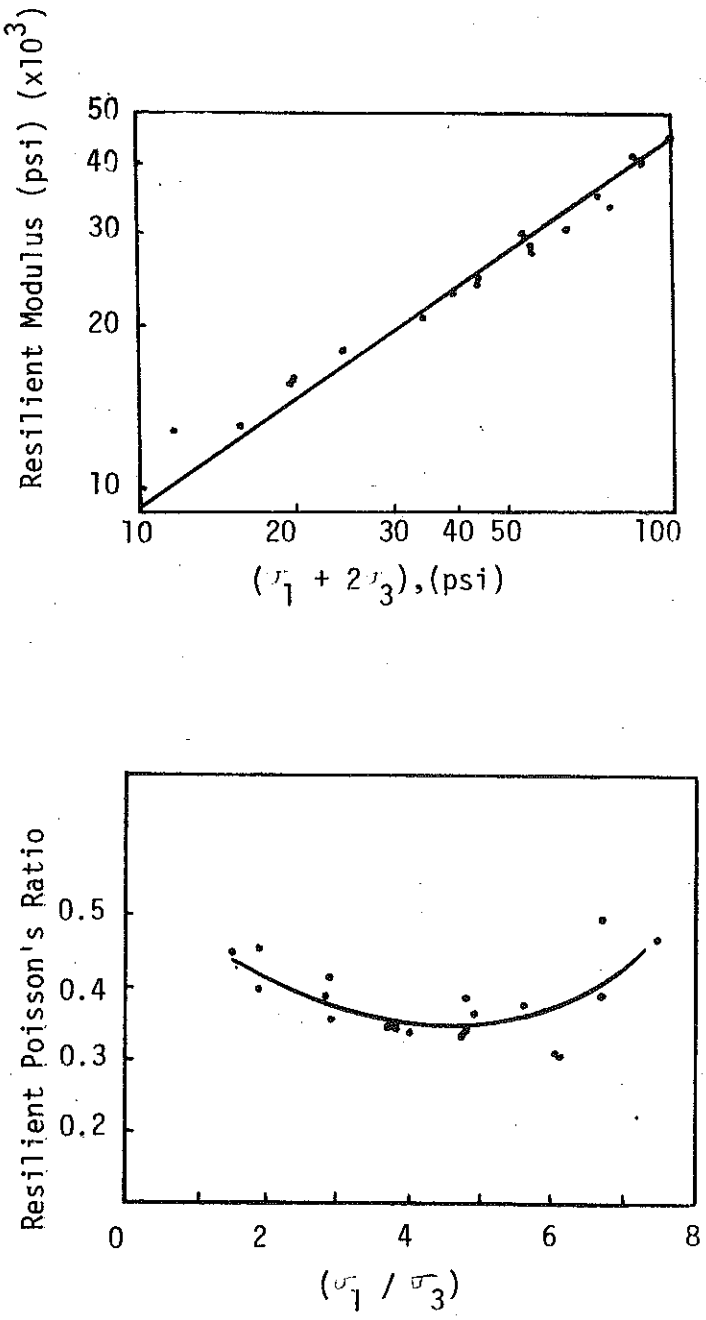

FIGURE 4.21 VARIATION OF RESILIENT MODULUS AND RESILIENT POISSON'S RATIO WITH THE SUM AND THE RATIO OF PRINCIPAL STRESSES RESPECTIVELY,(22).

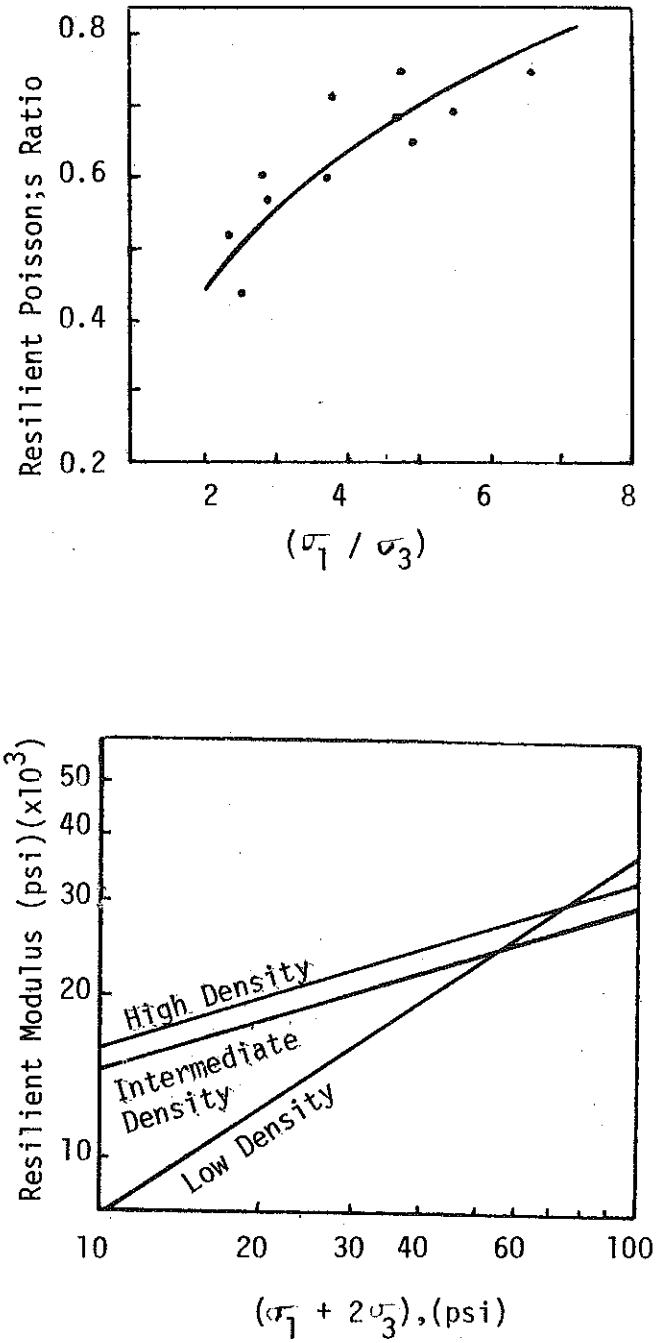

FIGURE 4.22 VARIATION OF RESILIENT POISSON'S RATIO AND RESILIENT MODULUS WITH THE RATIO AND THE SUM OF PRINCIPAL STRESSES RESPECTIVELY, (22).

2.5. Duration of Stress Application

Most investigators have concluded that the effect of the duration of the stress application on resilient response is negligible. Although the resilient modulus tends to increase as the time of load duration decreases, this effect is considered insignificant for the range of load durations encountered in pavement structures.

Hicks and Monismith (27) cite the work of Seed and Chan (6), on studies of the effect of load duration on the sample response for a silty sand. They found that for a decrease in duration from 20 minutes to 1/3 second, the resilient modulus increased from 23000 to 27000 psi, representing a change of 18 percent. They also showed that total deformation of the sample increased, for increases in duration up to 2 minutes. Hicks and Monismith (27) also confirmed the insignificance of load duration of 0.1 to 0.25 seconds.

Barksdale and Hicks (23) found that the resilient response of materials tested was only minimally affected by a variation of load duration from 0.04 to 1.0 second. They concluded that the sample response is independent of the duration of stress application, and that any stress pulse duration in the range of those applied to the pavement by moving wheel loads may be used in the lab with reasonable accuracy.

2.6. Rate of Deformation

It has been determined that resilient modulus tends to increase as the rate of deformation of the sample increases. Trollope (59) found that the resilient modulus increased 20 percent, as the rate of deformation increased from 0.002 to 0.040 inches per minute. Seed et al (43) reported similar findings. Researchers have concluded that effect of this parameter on the resilient response is insignificant, since the change in resilient modulus was negligible for such a large range of variation in the rate of deformation.

2.7. Frequency of Load Application

The effects of varying frequency of load applications also appears to be insignificant. Although the resilient modulus has been found to both increase and decrease with changes in frequency, the magnitude of

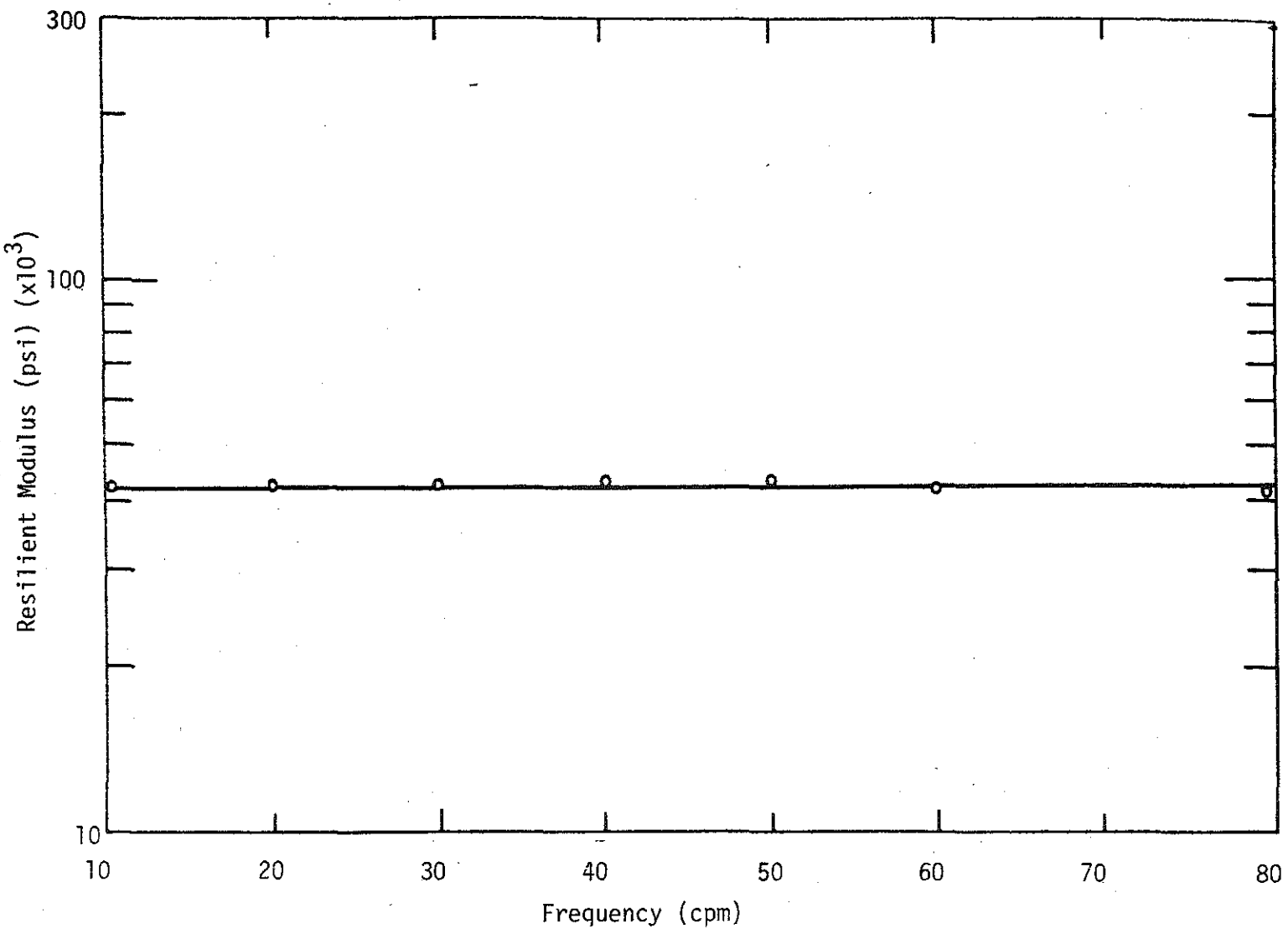

FIGURE 4.23 EFFECT OF LOAD FREQUENCY ON RESILIENT MODULUS FOR σ_3 = 5 psi AND σ_d = 15 psi, (31).

the change is small. In tests on silty sands, Coffman (62) found that the resilient modulus increased with frequency. The increase was on the order of 50 to 100 percent, depending upon the water content and density of the sample. Tanimoto and Nishi (46) reported conflicting results: the increase of resilient axial strain (decrease of the resilient modulus) with increasing frequency of loading. At higher numbers of stress repetitions, approximately 30,000, the effect of frequency was not discernable.

Kalcheff and Hicks (31) found that frequency changes had no effect on the resilient modulus, for tests on coarse aggregate as illustrated in Figure (4.23). They stated that any reasonable frequency of loading may be used to determine the resilient characteristics of cohesionless soils.

2.8. Type of Aggregate and Gradation

It appears that the effects of aggregate type and gradation are fairly insignificant in comparison to the effects of stress state. However, results of testing in this area are inconclusive and not well defined. Haynes and Yoder (26) conducted tests on gravel and crushed stone and found that for a given degree of saturation, the crushed stone samples exhibited greater total and resilient deformations than did the gravel. For both aggregate types, increasing the percent of fines passing the #200 sieve had no effect on the resilient modulus.

The relationship between the resilient modulus and the percent of fines is unclear as reported by Hicks and Monismith (27) and Barksdale and Hicks (23). For a range of confining pressure from 0 to 10 psi, they reported that the resilient modulus for partially crushed aggregate decreases, and that of crushed aggregate increases, as the percent of fines is increased. The changes in the resilient modulus in these cases were slight. Hicks (29) also reported a slight decrease in resilient modulus with increasing fines content for the same test data. In particular, for equation (4.2), Hicks reported that K decreased for partially crushed aggregate and increased for crushed aggregate as the fines content of each was increased. In general, K for the crushed aggregate was greater than K for the partially crushed aggregate, at corresponding relative densities. This too is not clearly defined,

but n was found to decrease slightly as percent of fines increased. Poisson's ratio decreased in most cases as fines content increased, and it was generally greater for the partially crushed aggregate. All of these trends are shown on Table (4.3).

Barksdale and Hicks (23) reported a significant increase in Rut Index and, hence, a tendency to rut as the percent of fines is increased. They suggested to minimize rutting in the surface course and to improve drainage in the base course, that as little fines as practical be used in the base course.

Allen and Thompson (22) also found that aggregate type and gradation had minor effects on the resilient response. Although resilient modulus values were slightly higher for crushed stone samples as compared to gravel, Poisson's ratio was found to vary minimally between materials, and they concluded that the effect of material type and gradation were far surpassed in importance by the effects of stress level.

2.9. Void Ratio

Good agreement has been reached with respect to the effect of this parameter upon the resilient response. The resilient modulus increases as the void ratio decreases (dry density increases) Poisson's ratio is affected slightly, but shows no consistent variation with changes in void ratio.

Trollope (59) noted a 50 percent increase in resilient modulus from loose to dense sand samples. Mitry (36) and Hicks (29) found that Poisson's ratio decreased slightly as the void ratio decreased. However, the effects of density on the resilient modulus were reduced by increasing the fines content as shown in Figure (4.24).

More recently, Barksdale and Hicks (23) found that rutting of the surface increases 1 1/2 to 2 times as a result of a decrease in density from 100 to 95 percent of ASSHO density during construction. Allen and Thompson (22) reconfirmed the established relations between resilience and density in their tests with constant and variable confining pressures. Resilient modulus increased with decreasing void ratio, and Poisson's ratio was not significantly affected.

TABLE 4.3 INFLUENCE OF AGGREGATE GRADATION ON RESILIENT PROPERTIES OF GRANULAR BASE MATERIALS, (27).

Passing # 200 %	Relative Density,%	Degree of Saturation %	$M_R = K_1 \theta^{K_2}$		Mean Poisson's Ratio	Materials
			K_1	K_2		
3	89.2	0	11,752	.53	0.45	Partially
5	85.5	0	10,252	.64	0.45	
8	86.5	0	8,939	.61	0.34	Crushed
3	79.9	100	9,598	.55	0.25	
5	83.8	100	9,430	.50	0.35	
8	81.5	100	9,063	.52	0.25	Aggregate
3	89.3	0	12,338	.55	0.41	Crushed
5	87.0	0	13,435	.56	0.27	
10	86.0	0	14,672	.50	0.27	
5	77.2	0	11,446	.59	0.35	
10	77.0	0	14,313	.52	0.23	Aggregate

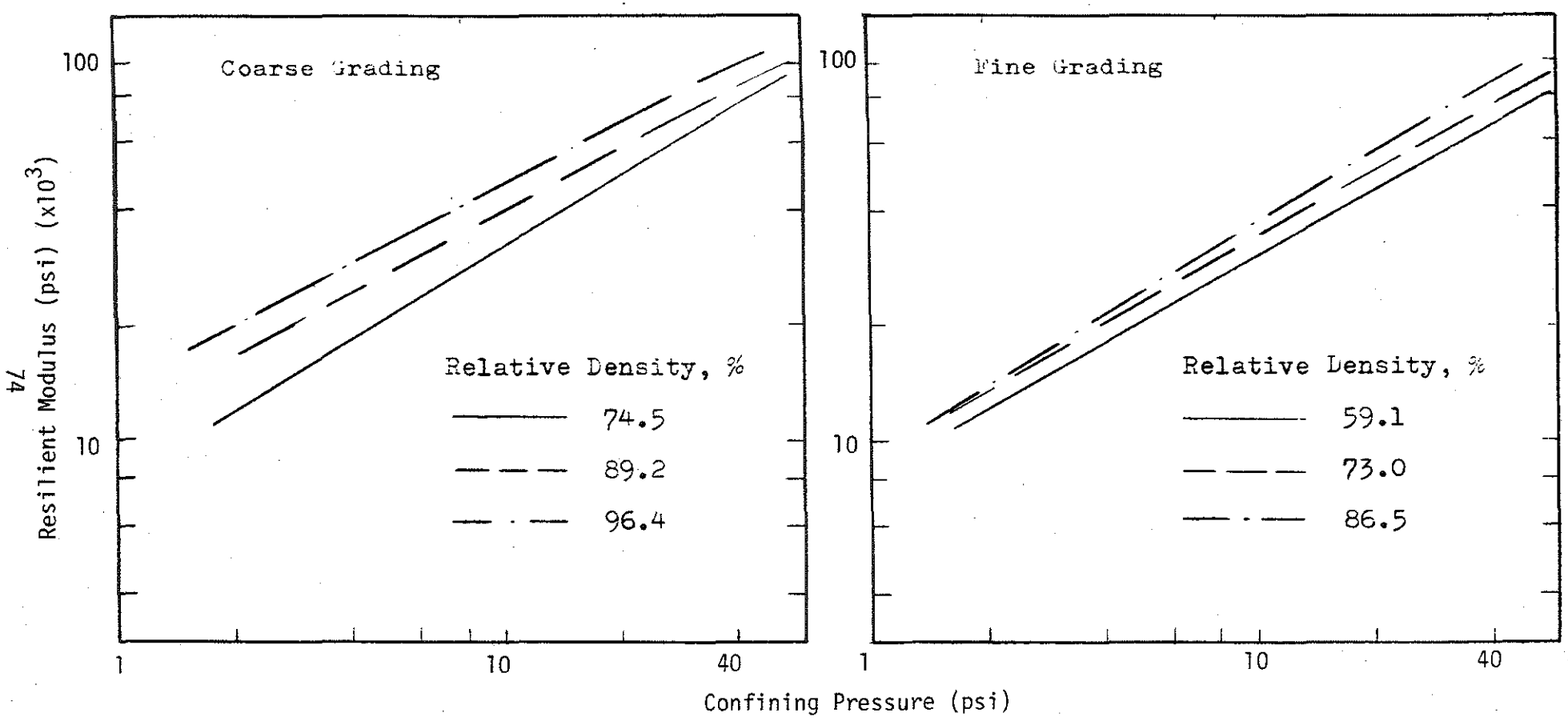

FIGURE 4.24 EFFECT OF DENSITY ON RELATIONSHIP BETWEEN RESILIENT MODULUS AND CONFINING PRESSURE, (27).

2.10. Degree of Saturation

The nature of the effect of the degree of saturation upon the resilient response of test samples is complex, and the extent of its effect appears to be related to many other parameters such as aggregate type and test drainage conditions. In general, as the degree of saturation increases, so does the resilience, and the resilient modulus is reduced. This was determined conclusively by Haynes and Yoder (26). For gravel specimens, they reported that as the degree of saturation increased from 70 to 100 percent, the resilient modulus decreased by 50 percent. For crushed stone, a change of saturation from 70 to 80 percent caused a 20 percent decrease in resilient modulus.

Hicks (29) found that as the degree of saturation increases, Poisson's ratio decreases. It was noted in test results that Poisson's ratio was always less than 0.5. Theoretically, Poisson's ratio should equal 0.5 for undrained test conditions where there is no volume change. Since it was not, Hicks concluded that this was due to improperly functioning LVDT's or sample inhomogeneity. He concluded that based on a total stress analysis, as saturation increased, Poisson's ratio decreased, and the resilient modulus was only slightly affected.

Comparisons of results at a given confining pressure based on effective stresses indicated that the resilient moduli for saturated specimens tested under undrained conditions were approximately the same as those determined for dry specimens. Saturated samples tested under drained conditions had slightly higher resilient moduli than those under undrained conditions. This is believed to be the result of pore water pressure build-up in undrained tests. Partially saturated samples had the lowest moduli of all as shown in Figure (4.25).

It was expected that the resilient modulus would continue to decrease as saturation increased, but this was not shown by the results. Hicks explained that the reason for this inconsistency is related to the manner in which the results were compared. The dry and partially saturated data were compared on the basis of total stresses whereas the dry and saturated data were compared using effective stresses. He stated that if all results were compared in terms of total stresses, the resilient modulus would steadily decrease as the degree of saturation

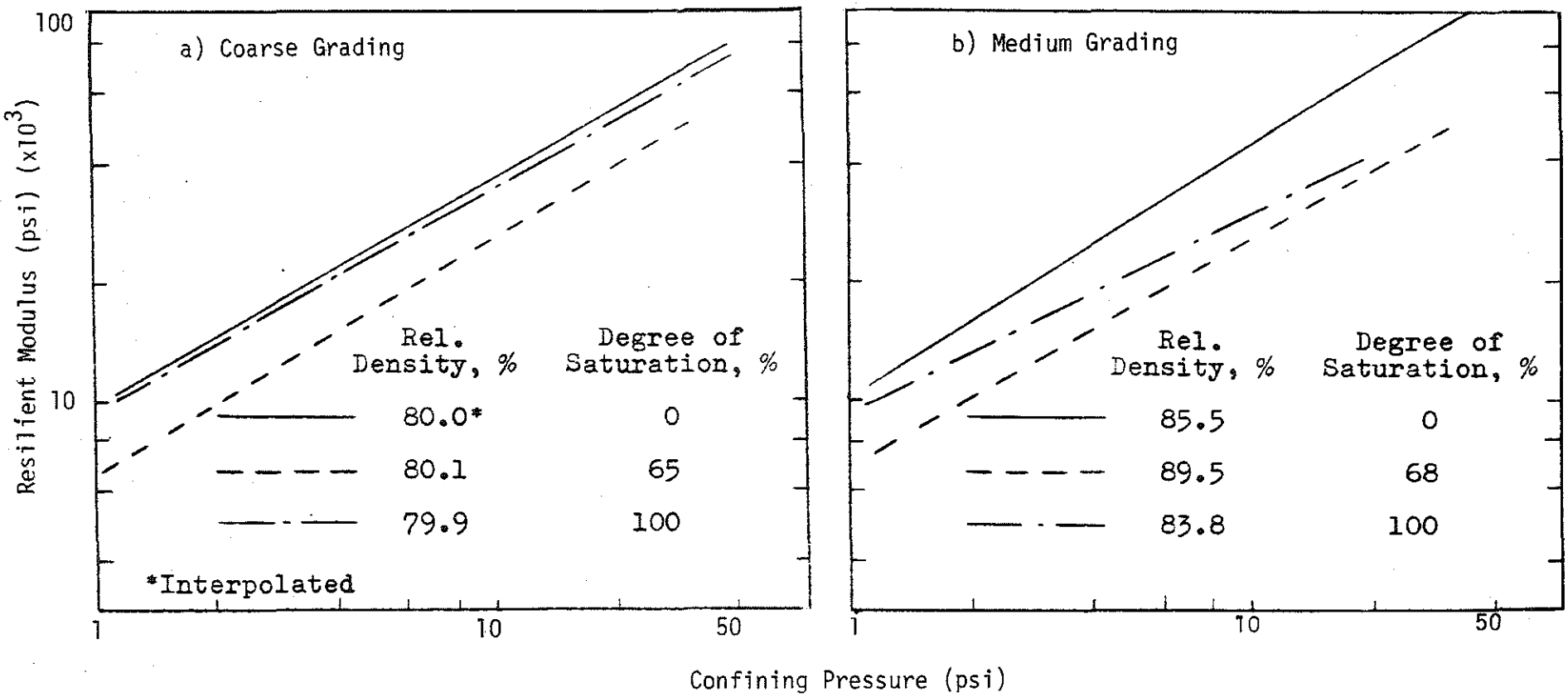

FIGURE 4.25 EFFECT OF DEGREE OF SATURATION ON THE RELATIONSHIP BETWEEN RESILIENT MODULUS AND CONFINING PRESSURE, (27).

increases. Tanimoto and Nishi (46) came up with a different explanation. They stated that the reason is due to a decrease in friction between soil grains, caused by the presence of an adequate amount of water, and possible densification due to repeated loading. The build-up of pore water pressure at full saturation may prevent soil grain movement during rapid loading, causing a rise in stiffness and resilient modulus from the partially saturated to saturated conditions.

Barksdale and Hicks (23) also found that rutting increased with increasing degree of saturation. They pointed out that this emphasizes the importance of a high density at compaction and free drainage for the base and subbase layers.

3. ASPHALT TREATED MATERIALS

In the case of asphalt treated materials, when simulating field conditions in the lab for triaxial testing, the most important factors that must be considered are temperature and stress level. Temperature is very important since asphalt, which typically comprises about 15% by volume of an asphalt concrete layer, is a thermoplastic material. Its stress-strain characteristics are controlled by temperature. At this point in time, researchers are able to accurately predict temperature and stress throughout an asphalt concrete layer. Typical temperature and stress distributions are illustrated by Figure (4.26). Since asphalt is also a viscoelastic material, the response of asphalt treated materials is time dependent. The rate of loading and rest period are also important test parameters. In this section, the most significant parameters for repeated load triaxial testing of asphalt treated materials will be discussed.

3.1. Rate of Loading and Rest Period

The rate of loading and the rest period have no significant effects on the resilient modulus of a bituminous mixture for the conditions of short stress duration and low temperature (48,40,56). However, at higher temperatures when the asphalt treated material is not likely to behave in an elastic manner, they become very important.

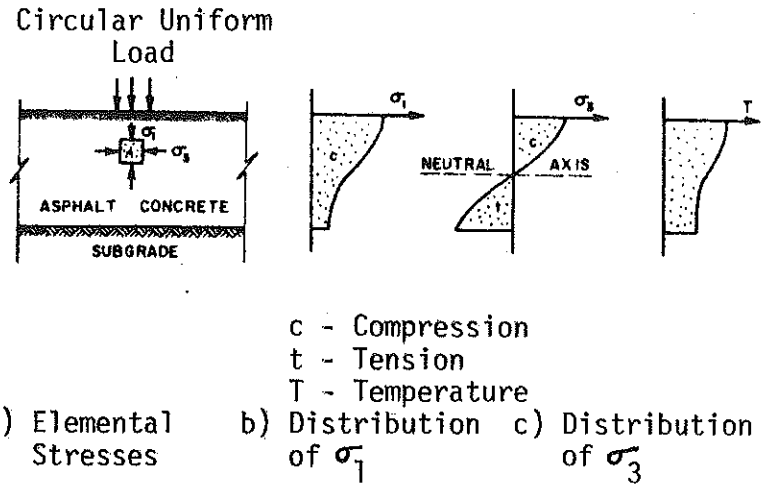

FIGURE 4.26 TYPICAL PAVEMENT STRESS AND TEMPERATURE DISTRIBUTIONS IN CENTER OF WHEEL PATHS UNDER STATIC LOADING, (40).

3.2. Temperature

Terrel and Awad (47) reported that the resilient modulus of asphalt treated materials decreases as temperature increases. They explain that at low temperatures, the asphalt film which surrounds each of the soil grains is stiff enough to behave as a solid. As temperature increases, the asphalt becomes less viscous and loses its "particle cementing" ability. A loss of stiffness and reduction in resilient modulus results. They have also found that Poisson's ratio increases with increasing temperature. At low temperatures, Poisson's ratio was not influenced by asphalt content or gradation, however, at higher temperatures the value of Poisson's ratio had much greater scatter, (Figure 4.27).

3.3. Stress Level and Confining Pressure

The resilient modulus of asphalt mixes is dependent upon confining pressures. The higher the confining pressure, the higher the resilient modulus (48). An increase in the confining pressure and asphalt content, at a given temperature, will result in a reduction in the axial strain as shown in Figures (4.28), (4.29), (4.30), and (4.31). In a variable confining pressure test (VCP), the resilient modulus is independent of the confining pressure. This is shown in Figures (4.32), and (4.33).

The dominant non-linear factor in the behavior of bituminous mixes is the length of the curing time (48, 29).

3.4. Asphalt Content and Load Duration

Examination of Figures (4.34) and (4.35) indicates that the axial strain increases as the asphalt content increases. The axial strain also increases with increasing load duration (47) as indicated in Figures (4.30) and (4.32).

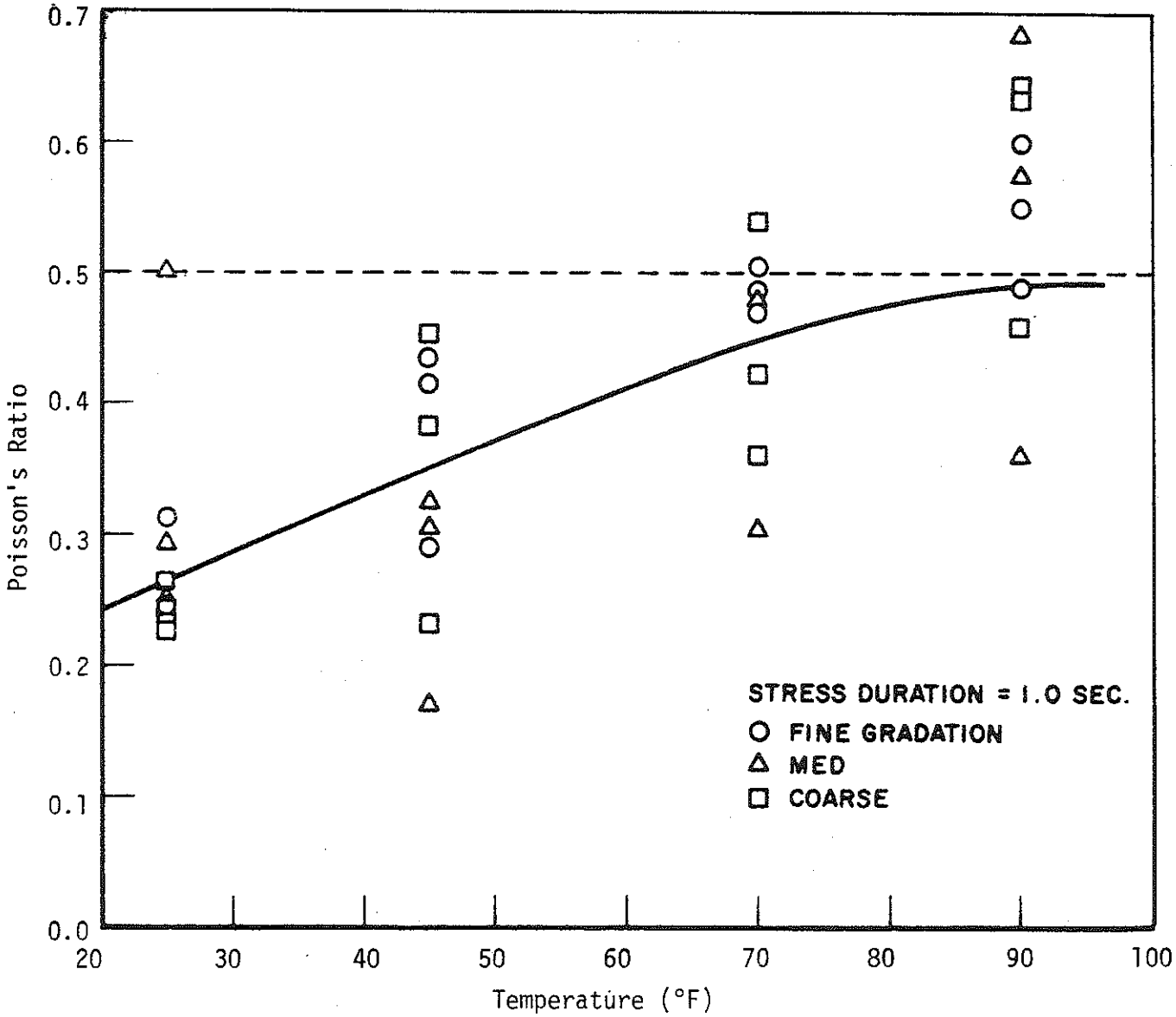

FIGURE 4.27 VARIATION OF POISSON'S RATIO OF DIFFERENT MIXTURES WITH TEMPERATURE, (47).

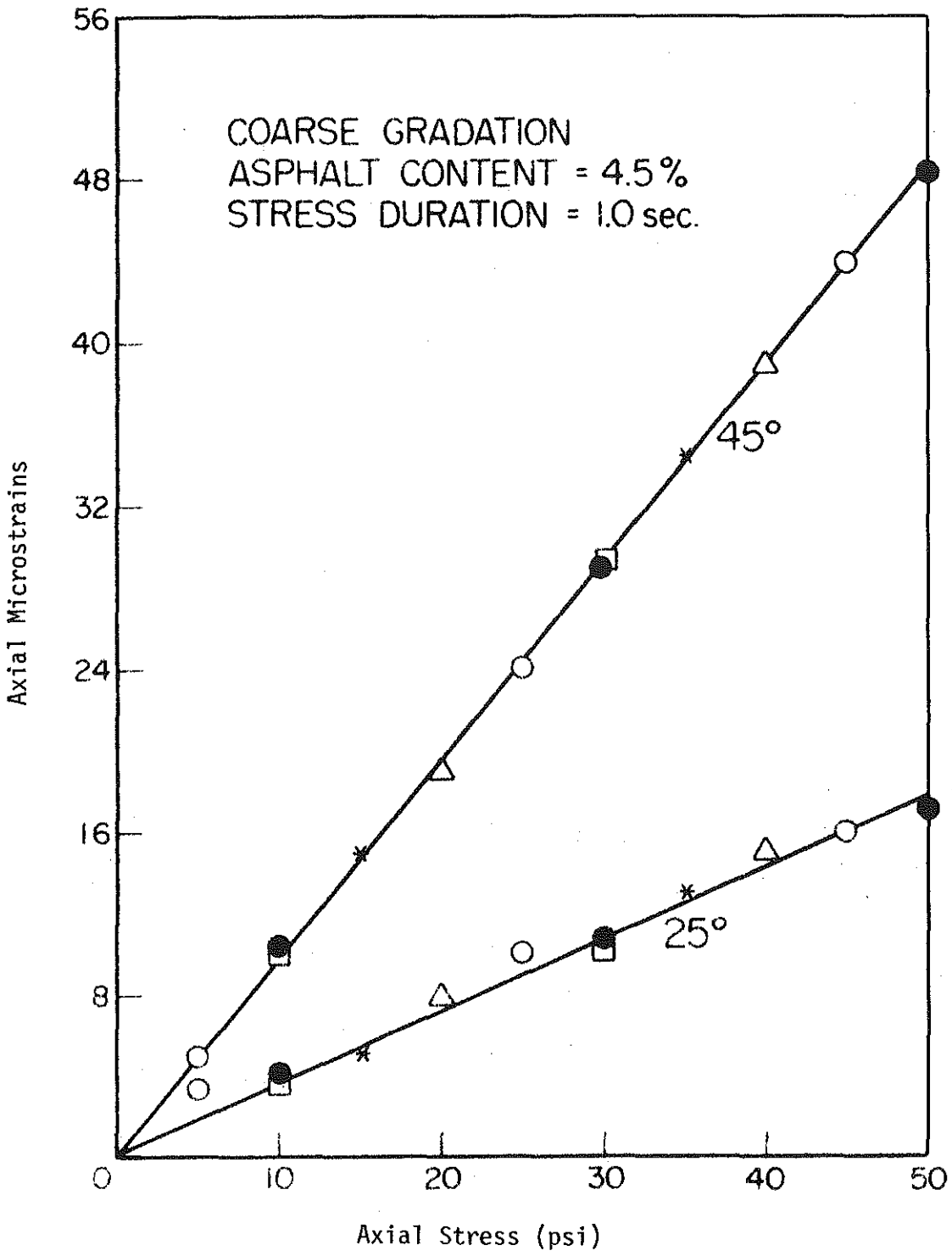

FIGURE 4.28 AXIAL STRESS Vs. AXIAL STRAIN FOR ASPHALT CONCRETE AT 25° AND 45°F WITH 4.5% ASPHALT CONTENT AND 1.0 SECOND STRESS DURATION, (47).

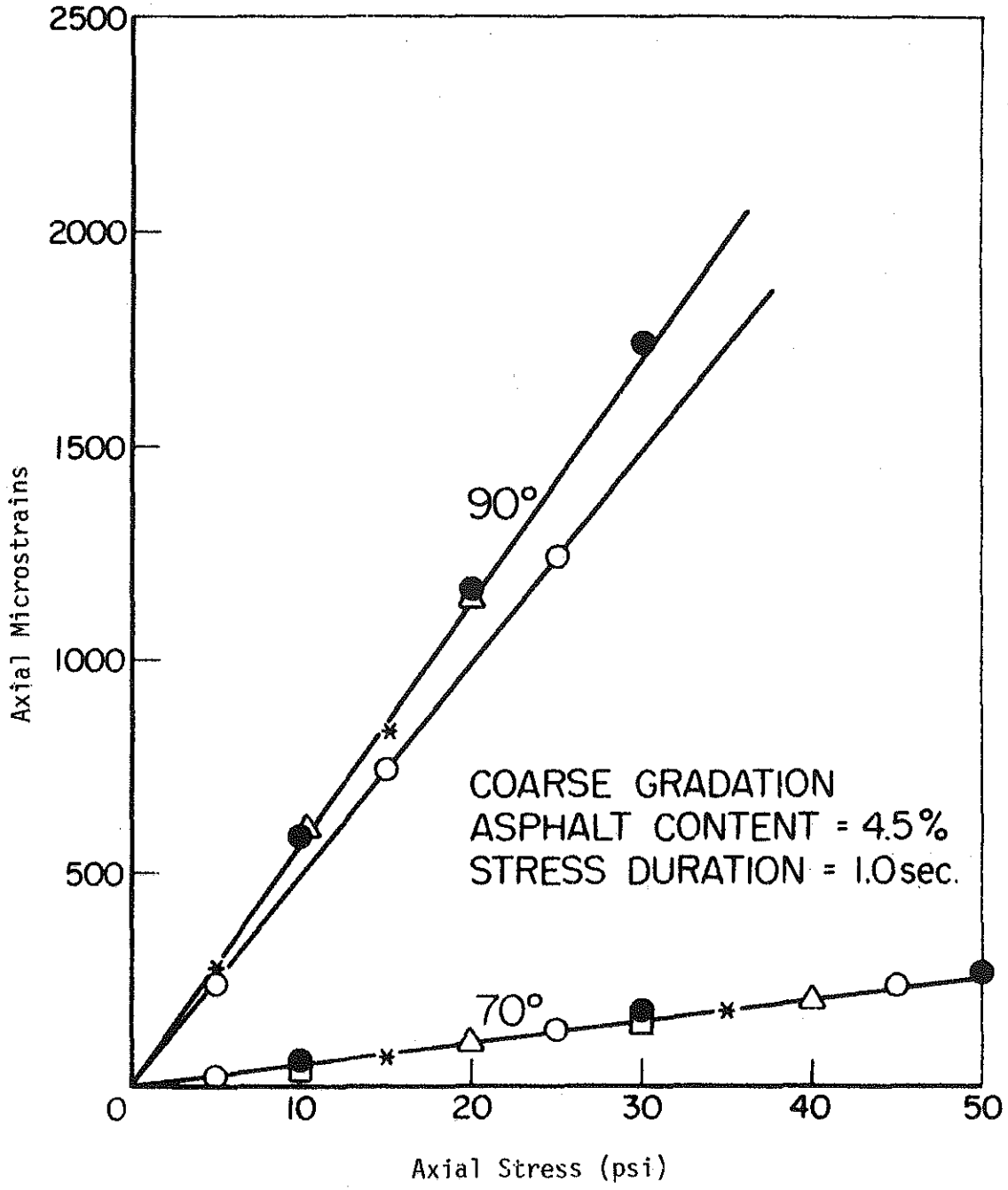

FIGURE 4.29 AXIAL STRESS Vs. AXIAL STRAIN FOR ASPHALT CONCRETE AT 70° AND 90°F WITH 4.5% ASPHALT CONTENT AND 1.0 SECOND STRESS DURATION, (47).

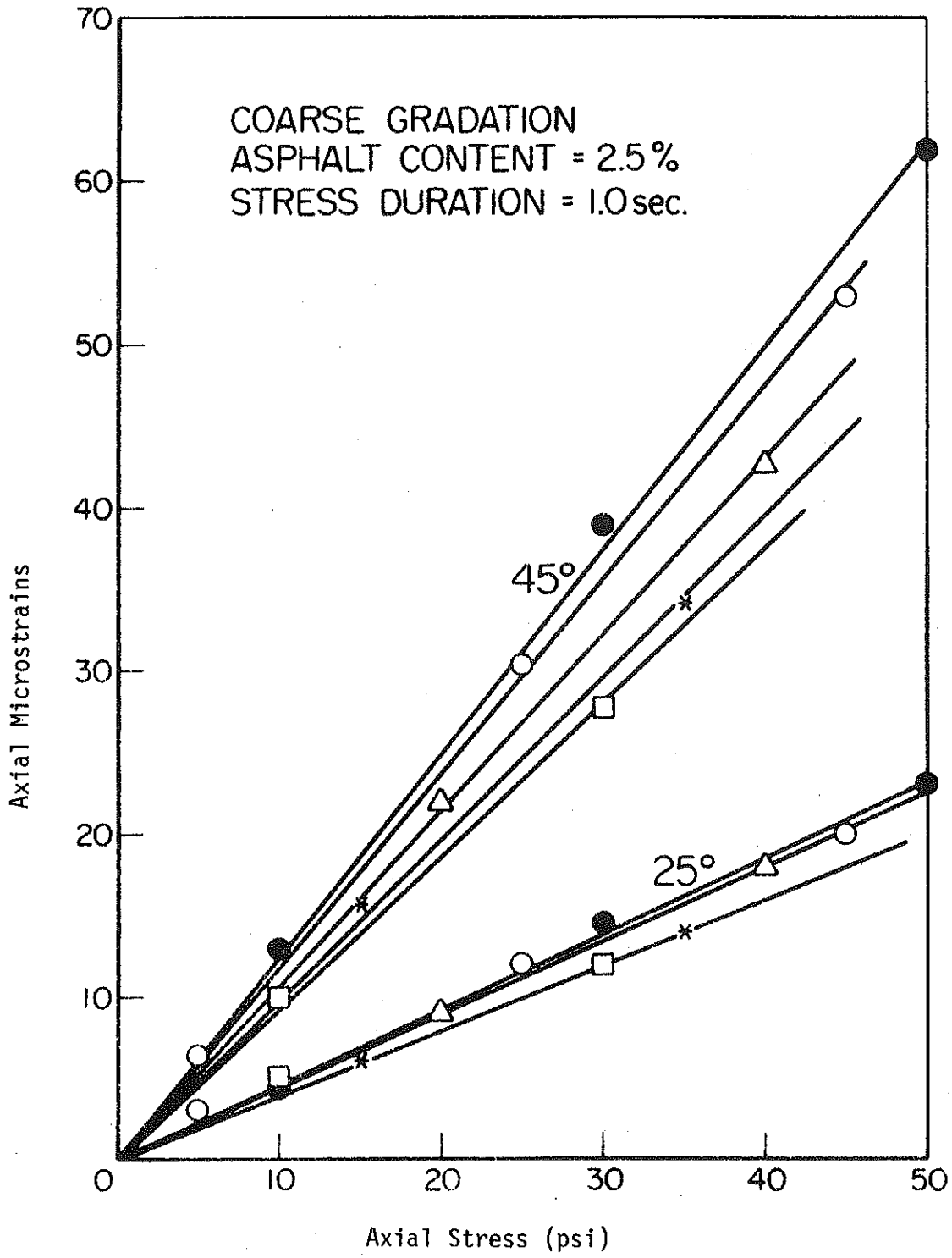

FIGURE 4.30 AXIAL STRESS Vs. AXIAL STRAIN FOR ASPHALT CONCRETE AT 25° AND 45°F WITH 2.5% ASPHALT CONTENT AND 1.0 SECOND STRESS DURATION, (47).

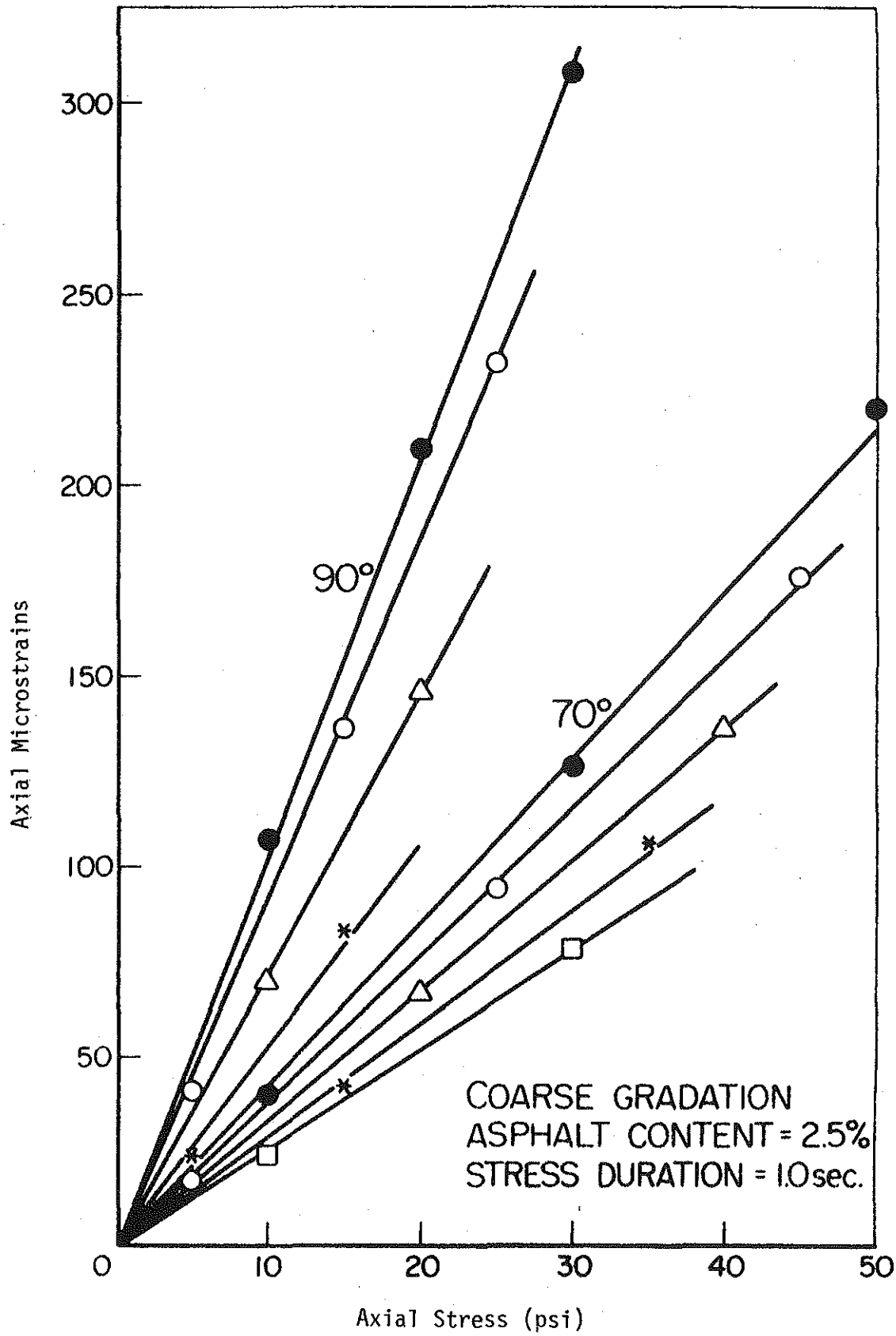

FIGURE 4.31 AXIAL STRESS Vs. AXIAL STRAIN FOR ASPHALT CONCRETE AT 70° AND 90°F WITH 2.5% ASPHALT CONTENT AND 1.0 SECOND STRESS DURATION, (47).

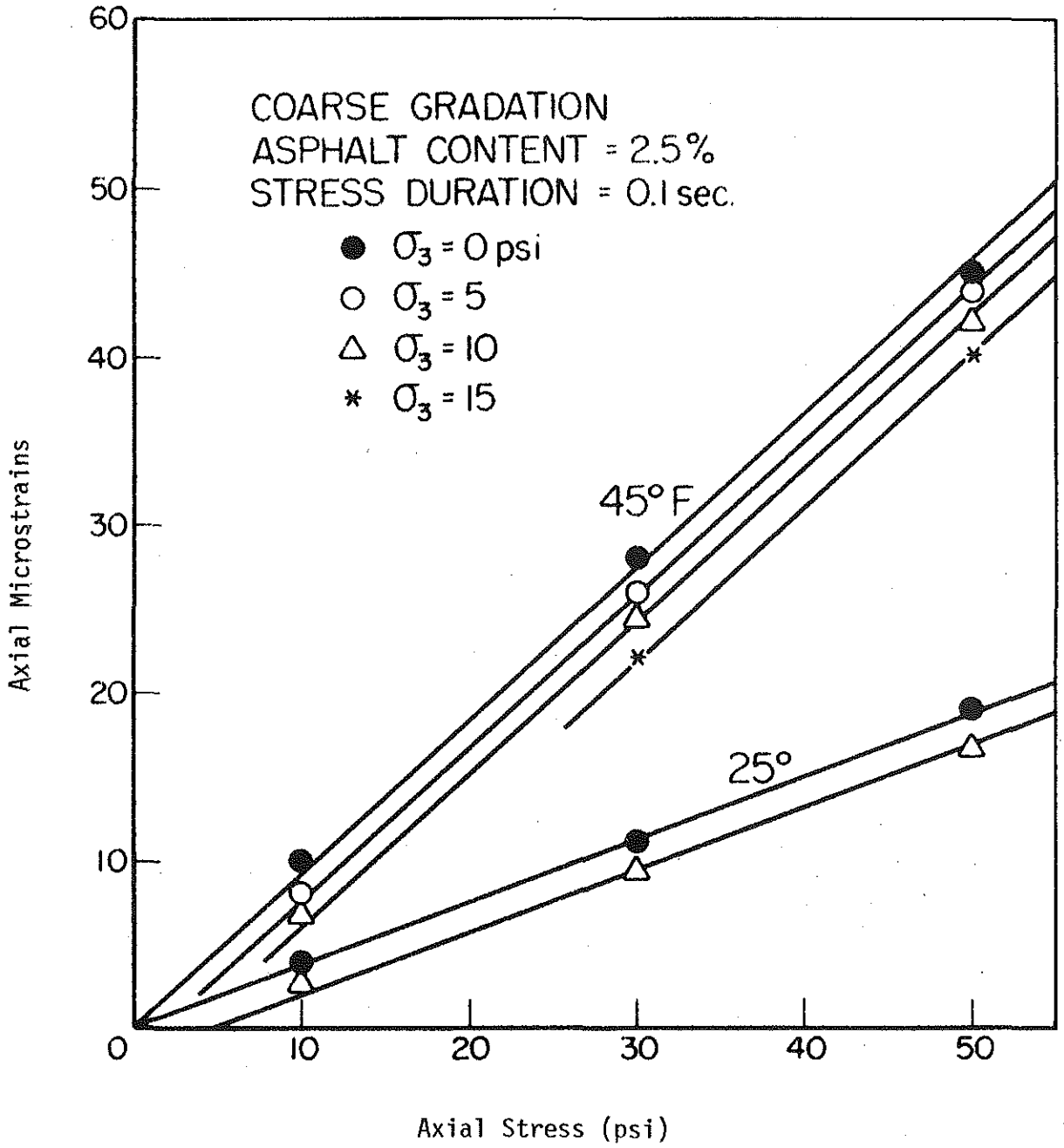

FIGURE 4.32 STRESS-STRAIN STATES UNDER CYCLIC AXIAL AND RADIAL STRESSES, (47).

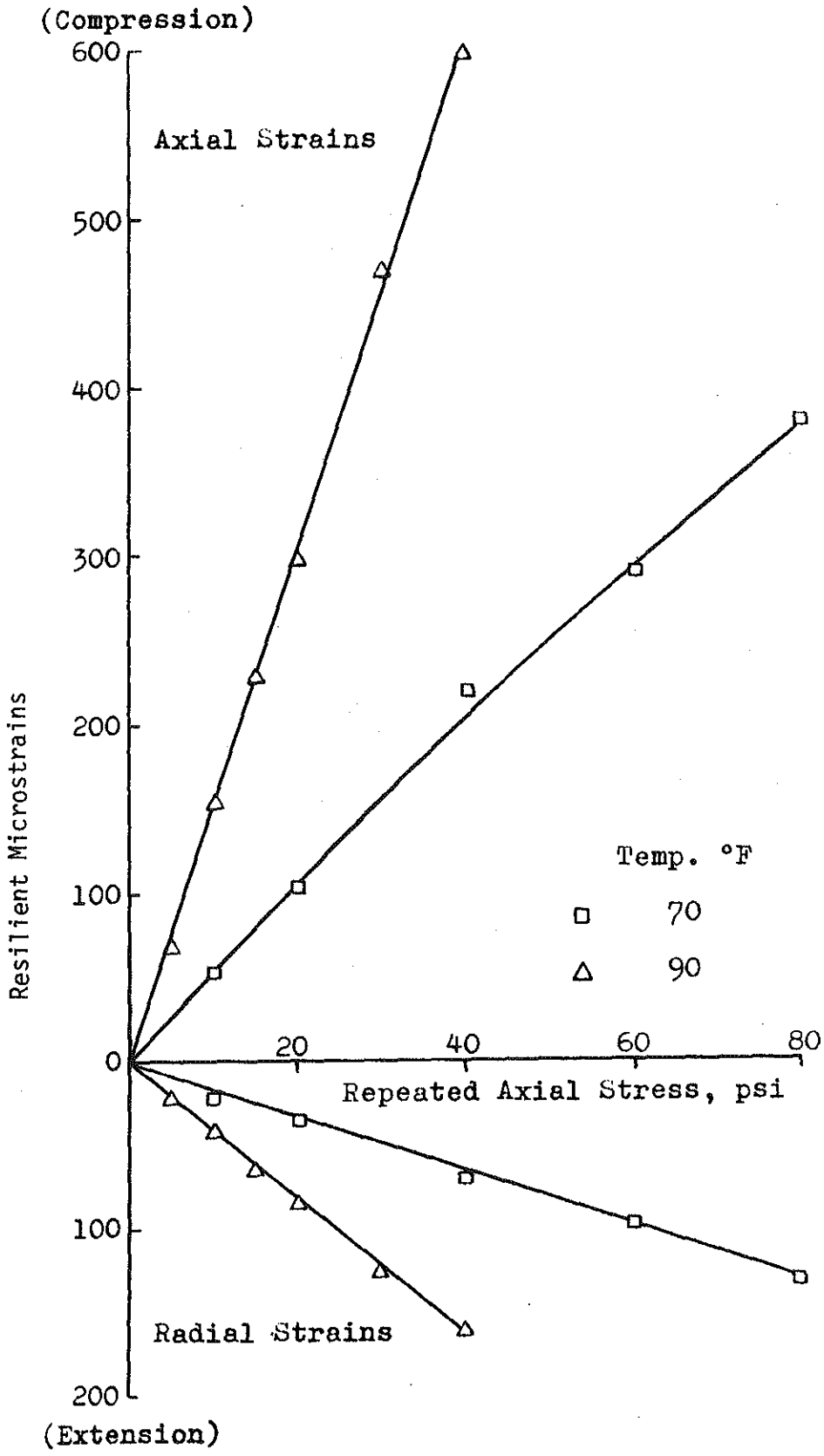

FIGURE 4.33 VARIATION IN RESILIENT AXIAL AND RADIAL STRAINS WITH REPEATED AXIAL STRESS FOR ASPHALT CONCRETE, (29).

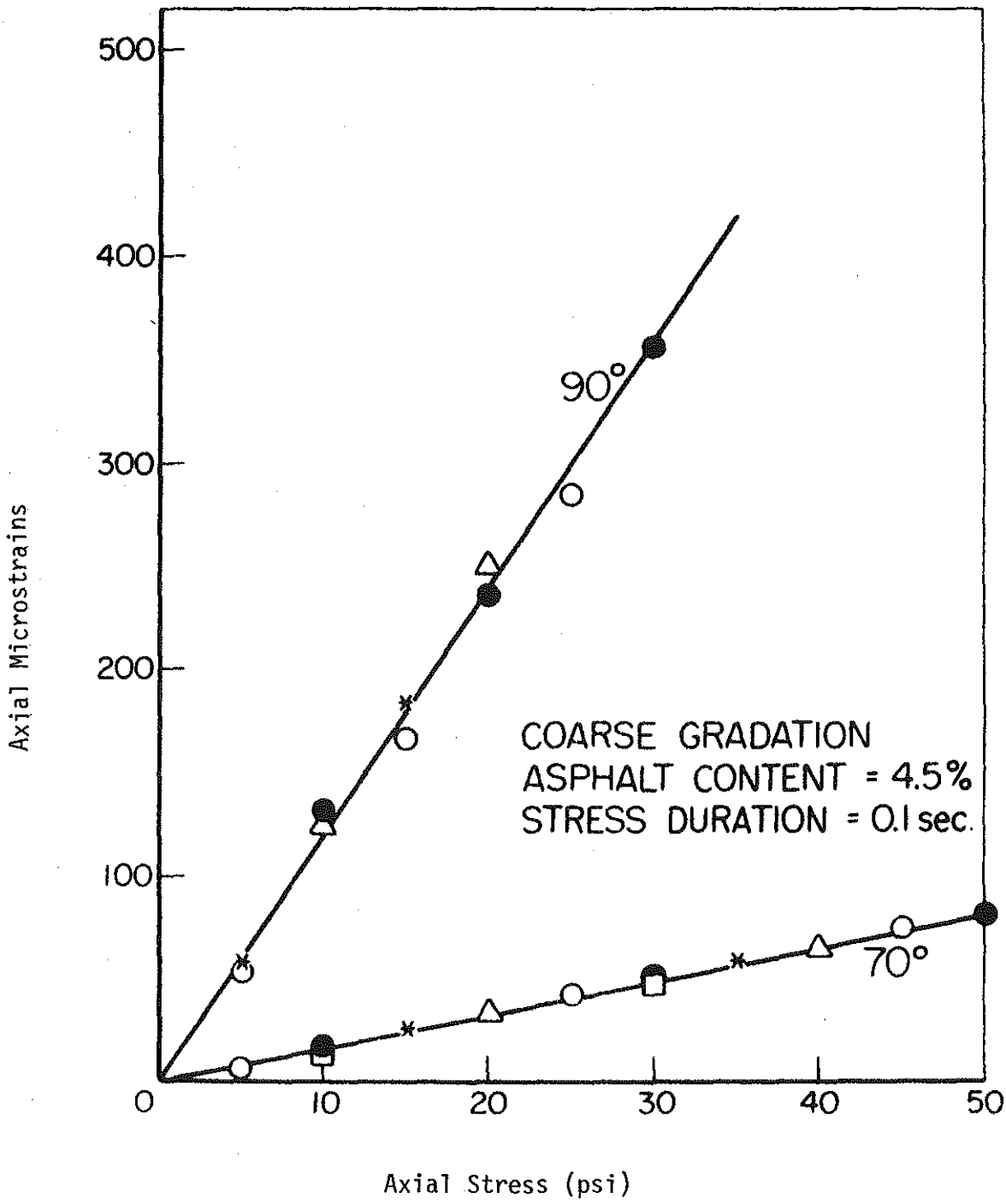

FIGURE 4.34 AXIAL STRESS Vs. AXIAL STRAIN FOR ASPHALT CONCRETE AT 70° AND 90°F WITH 4.5% ASPHALT CONTENT AND 1.0 SECOND STRESS DURATION, (47).

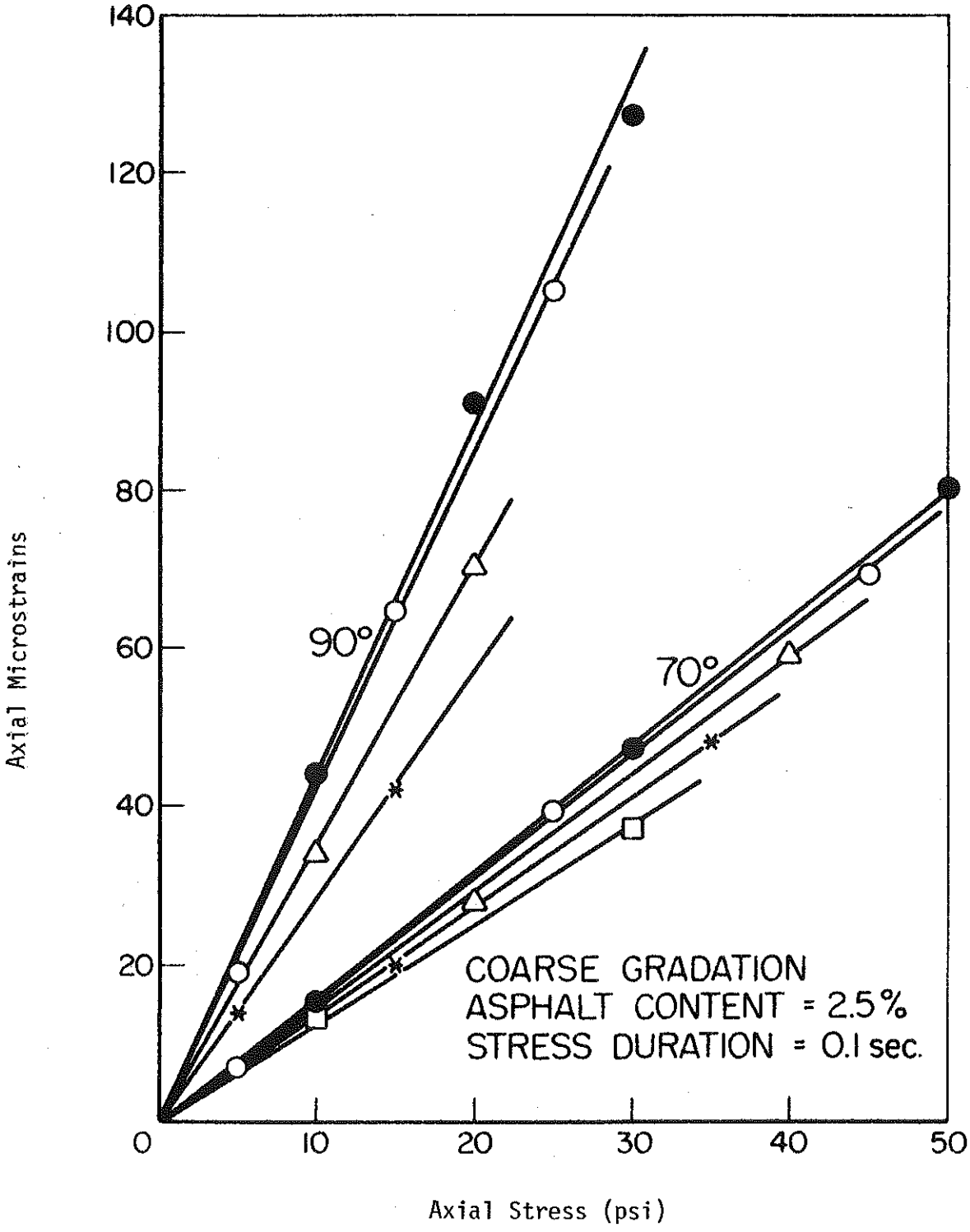

FIGURE 4.35 AXIAL STRESS Vs. AXIAL STRAIN FOR ASPHALT CONCRETE AT 70° AND 90°F WITH 2.5% ASPHALT CONTENT AND 1.0 SECOND STRESS DURATION, (47).

CHAPTER 5

THE STIFFNESS MODULUS OF ASPHALT TREATED MIXES

1. INTRODUCTION

In addition to the repeated load triaxial test, the repeated flexure test has been also used to determine the resilience characteristics of asphalt treated mixes. In this test, beam specimens are repeatedly loaded in a symmetrical fashion about their mid-points, and their responses are monitored. The stiffness modulus "S", for a given temperature "T" and time of loading "t", is given by

$$S(T,t) = \sigma/\varepsilon \qquad (5.1)$$

in which σ = the applied axial stress

ε = the applied axial strain.

This property can be measured directly from the test or it can be estimated by several methods. In this chapter, various aspects of repeated flexure tests will be discussed.

2. EQUIPMENT

Seed et al (44) recognized Deacon (67) for the development of fatigue testing equipment, utilizing repeated flexure, for asphalt treated materials. Deacon determined the stiffness modulus at particular temperatures and times of loading, and found good agreement with values determined by Van der Poel's method.

Mitry (36) performed a significant number of tests using equipment similar to that of Deacon. Beam specimens were taken from a model pavement section using a diamond saw. The specimens were 14 inches long, 1.5 inches wide and 1.5 inches thick. During the test, they were simply supported, symmetrically loaded about the center at two points, 4 inches apart, and subjected to repeated flexure in a temperature controlled chamber with the deflection at the center registered by a linear variable differential transformer (LVDT).

3. TEST PROCEDURE AND PARAMETERS

Like the repeated load triaxial test, attention must be given to the various test parameters associated with repeated flexure to insure accurate

simulation of field conditions. Consideration must be given to the gradation of the aggregate, the density of the mix, the mix temperature, and the time of loading.

Mitry (36) found that a decrease in test temperature from 60 to 45°F increased the stiffness modulus by as much as 300 percent. He tested at temperatures of 45, 52.5, and 60°F, using a load duration of 0.1 seconds and a frequency of 20 cycles per minute. He used 300 load applications in the following sequence: thirty repetitions at 100 psi followed by thirty repetitions at 125 psi. His specimens were 14 inches long, 1.5 inches wide and 1.5 inches thick.

Two modes of loading have been used in the test, the controlled stress and the controlled strain modes. Epps and Monismith (25), based on analyses of pavement sections using linear elastic theory, investigated the relationship of pavement thickness and the mode of load application. They found that for thin asphalt layers, less than 2 inches, the controlled strain mode was representative. For thick asphalt layers, more than 6 inches, they found that the controlled stress mode of loading was more appropriate. A mixed mode of load application was suggested for a range of asphalt layer thicknesses of 2 to 6 inches. Because of the relative ease of testing, and the large amount of available data for comparison, Epps and Monismith recommended the use of a block or haversine wave form for the pattern of stressing in tests using either cantilever or simply supported beams.

Larger beam sizes, 15 inches long, 3.25 inches in width and 3.5 inches in depth, were used for tests conducted by Kallas and Puzinauskas (32). They used approximately 7000 grams of mix material for each beam, which was compacted, using a California kneading compactor, in 2 layers, followed by the application of a static leveling load at the rate of 0.25 inches per minute, see Table (5.1). The tests were conducted using a haversine load wave form, a load duration of 0.1 second and a frequency of 12 cycles per minute. A load of approximately 10 percent of the magnitude of the repeated load was applied to return the beam to its original undeflected position and hold it there during the rest period between loads. Finally, the test temperatures were 55, 70, and 85°F with ranges of stress of 200 to 400 psi, 100 to 300 psi, and 50 to 200 psi being applied at the given temperatures, respectively. On the basis of test results, Kallas and Puzinauskas concluded that the variability of test results is reduced when

TABLE 5.1. SUMMARY OF BEAM COMPACTION PROCEDURES (32)

Project Location	Mix	Temperature, deg F	1st Layer		2nd Layer		2nd Layer-Final		Static load pressure, psi
			Tamps	Pressure, psi	Tamps	Pressure, psi	Tamps	Pressure, psi	
Colorado	A.C. Surface	140	30	200	50	200	50	300	400
Colorado	A.C. Base	140	30	200	50	200	50	300	400
Colorado	L.S. Sand Base	140	30	200	50	200	50	100	400
Colorado	H.S. Sand Base	140	30	200	50	200	50	100	400
Ontario	A.C. Surface	230	100 30	50 200	30	200	90	200	400
California	A.T. Base Sp.	230	100 150 30	50 100 200	100 150 45	50 100 200	45	300	400
Washington State Univ. Test Track Ring 2	A.C. Surface	230	45	200	100	300	...	...	400
Washington State Univ. Test Track Ring 2	A.C. Base	230	130	100	130	100	...	...	400
Laboratory Study	A.C. Asph. A	230	30	200	45	200	45	300	400

the larger beams are used and consequently, less testing is required. Also, their test results tend to agree with those obtained from rotating bending cantilever fatigue tests.

4. FACTORS AFFECTING THE FATIGUE RESPONSE

The variables affecting the fatigue response of asphalt mixes could be placed into three categories (25) as listed in Tables (5.2) and (5.3). The numbers listed after each variable refer to the Bibliography of reference (25).

Figure (5.1) shows that as temperature decreases the number of load applications to failure (fatigue life) increases (30). The stiffness modulus of asphalt mixes is also a function of load duration (41). Figure (5.2) shows that as the loading time or temperature increases, the stiffness modulus decreases. In the range of temperature and load duration encountered in the field, the stiffness modulus may vary from 1,000 to 4,000,000 psi. This underscores the importance of the stiffness modulus and its accurate determination since stresses and strains in the asphalt layer are dependent upon the mixture stiffness.

Generally, as the stiffness modulus increases, the fatigue life of a specimen also increases in the controlled stress mode of loading (25). However, Santucci and Schmidt (100) indicated that for the controlled strain mode of loading, the fatigue life will decrease as the stiffness modulus increases.

Figure (5.3) shows that the fatigue life of an asphalt mix decreases as the percentage of air voids increases (42). The amount of air voids of an asphalt mix is dependent upon the gradation of the aggregate. Open graded aggregates most often lead to a higher air void ratio than that of the well graded aggregates. However, Epps and Monismith (25) concluded that aggregate gradation has little influence on fatigue life that cannot be explained by differences in air voids or asphalt content.

5. MIXTURE DESIGN

Table (5.4) summarizes the effects of mix variables on stiffness modulus and fatigue life which can be used as a guide for asphalt mix design (25). Hard asphalt cement, and rough, angular, and densely graded aggregates should be used in the design of a thick (more than 6 inches) asphaltic layer. On the other hand, soft asphalt and smoother more rounded aggregates would make a better mixture for thin asphalt layer

Table 5.2. LABORATORY TEST VARIABLES AFFECTING FATIGUE BEHAVIOR AS DETERMINED BY CONTROLLED STRESS TESTS, (25)

Load Variables

Load History
- simple loading (6, 9, 12, 14, 21, 23[a], 24, 26, 38, 40, 44, 45, 49)
- compound loading (14)

Rate of Load Application (6, 12, 14, 41, 48)

Pattern of Stressing
- block (6, 9, 12, 14, 21, 45)
- sinusoidal (23, 24, 44, 48)
- haversine (26)

Type of Machine
- bean (flexure)
- rotating cantilever (38, 40)
- diaphragm (23, 24)
- cantilevel (44)

Mixture Variables

Mixture
- stiffness (21, 40, 44, 45)
- air void content (9, 21, 40, 44)
- asphalt content (6, 9, 21, 23)

Asphalt
- type (6, 9, 21)
- hardness (6, 9, 12, 21, 40, 44, 45)

Aggregate
- type (6, 9, 21, 23, 40, 44)
- gradation (6, 9, 21, 40, 44)

Environmental Variables

Temperature (6, 9, 23, 24, 38, 40, 44)

Moisture

Alteration of Material Properties During Service Life (6, 9, 45)

a) neither controlled stress nor strain

TABLE 5.3 LABORATORY TEST VARIABLES AFFECTING FATIGUE BEHAVIOR AS DETERMINED BY CONTROLLED STRAIN TESTS, (37).

Load Variables

Load History
- simple loading (3, 32, 38)
- compound loading

Rate of Load Application (3, 38)

Pattern of stressing
- block (3, 32)
- sinusoidal (38)
- haversine (44, 47)

Type of Machine
- bean (flexure) (32, 46)
- rotating cantilever (38)
- diaphragm
- cantilever (38)
- torsional (38)

Mixture Variables

Mixture
- stiffness (32)
- air void content (32)
- asphalt content (38)

Asphalt
- type (32)
- hardness (3, 32, 44)

Aggregate
- type (3, 38, 46)
- graduation (38, 47)

Environmental Variables

Temperature (3, 38)

Moisture

Alteration of Material Properties During Service Life (32)

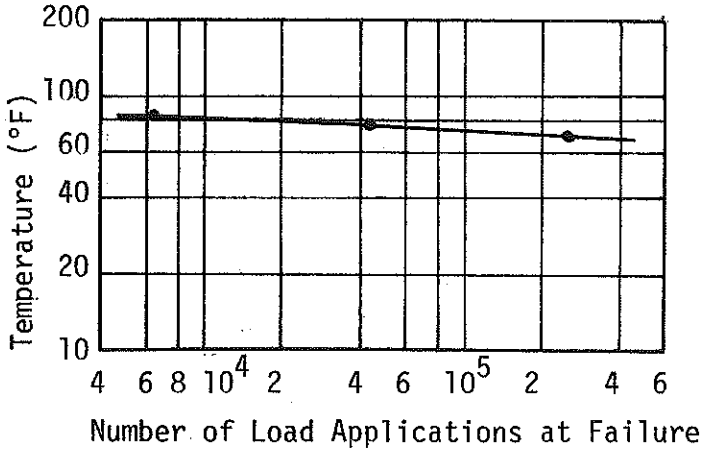

FIGURE 5.1 EQUIVALENT TEMPERATURE VERSUS NUMBER OF LOAD APPLICATIONS AT FAILURE, (30).

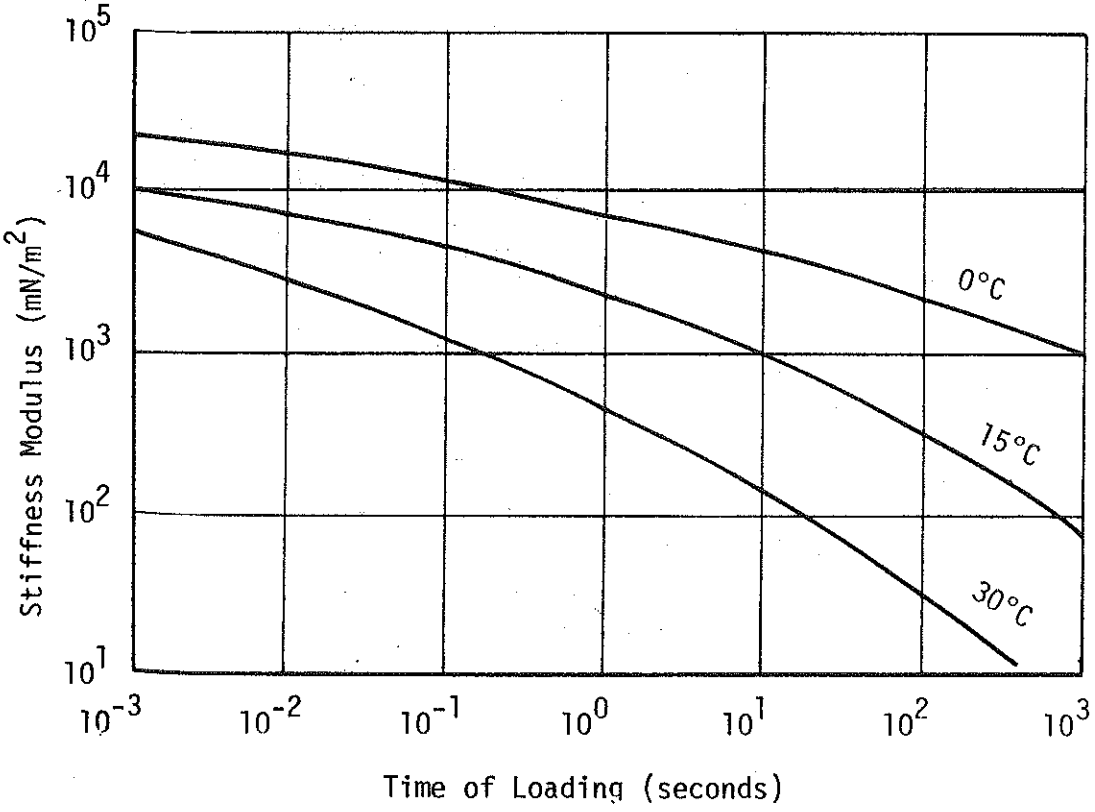

FIGURE 5.2 EFFECT OF TEMPERATURE AND TIME OF LOADING ON THE STIFFNESS OF A TYPICAL ASPHALT BASE COURSE MIX, (41).

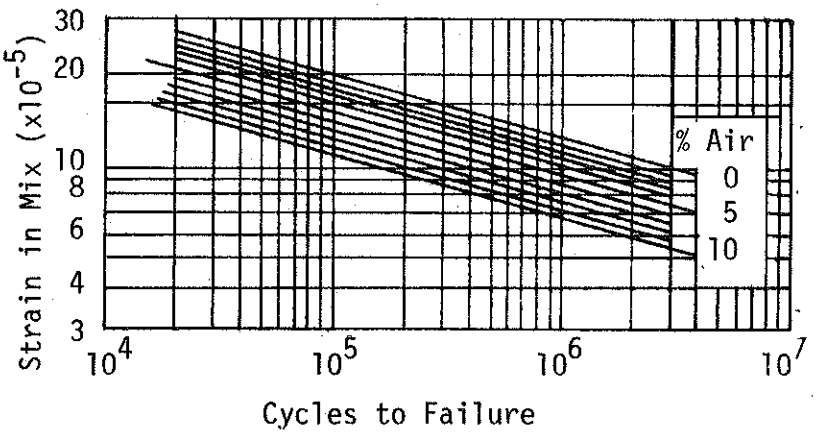

FIGURE 5.3 EFFECT OF VOID CONTENT ON FATIGUE LIFE OF A GAP GRADED BASE COURSE MIX CONTAINING 40/50 PENETRATION BITUMEN, (42).

TABLE 5.4 FACTORS AFFECTING THE STIFFNESS AND FATIGUE BEHAVIOR OF ASPHALT CONCRETE MIXTURES, (37)

Factor	Change in Factor	On Stiffness	On Fatigue Life in Controlled Stress Mode of Test	On Fatigue Life in Controlled Strain Mode of Test
Asphalt penetration	decrease	increase	increase	decrease
Asphalt content	increase	increase[a]	increase[a]	increase[b]
Aggregate type	increase roughness and angularity	increase	increase	decrease
Aggregate gradation	open to dense graduation	increase	increase	decrease[d]
Air void content	decrease	increase	increase	increase[d]
Temperature	decrease	increase[c]	increase	decrease

[a] Reaches optimum at level above that required by stability considerations.

[b] No significant amount of data; conflicting conditions of increase in stiffness and reduction of strain in asphalt make this speculative.

[c] Approaches upper limit at temperature below freezing.

[d] No significant amount of data.

(less than 2 inches). For intermediate thicknesses, an asphalt cement of intermediate hardness (85 to 100) should be used with a high asphalt content and a well compacted mixture.

CHAPTER 6

TEST RESULTS

1. INTRODUCTION

The test results obtained by several investigators will be presented in this Chapter along with the physical properties of the materials and the conditions of testing. This presentation will include the resilience characteristics of various materials tested in repeated load triaxial tests or flexural fatigue tests. It is hoped that this presentation will be useful for comparison with future test results obtained under similar conditions.

2. REPEATED LOAD TRIAXIAL TESTS

2.1. Cohesive Soils

Mitry (36) performed tests on undisturbed cohesive subgrade samples taken from beneath a model pavement section. The samples description and some of their physical properties, the test conditions, and the test results are summarized as follows:

profile and description ..... Figure 6.1

Atterberg limits ..... Figure 6.1

unconfined compressive strength at a rate of strain of 0.058 inches/minute ..... 0.95 kg/cm^2

California Bearing Ratio 6.0

loading frequency ..... 20 cycles/minute

load duration ..... 0.1 second

strains measured at load repetitions of 1000

the resilient modulus for various water contents ..... Table 6.1

the resilient strain for various water contents and axial stresses ..... Figure 6.2

Examination of the results indicates that the resilient modulus increases as the axial stress decreases.

Tanimoto and Nishi (46) tested undisturbed cohesive samples obtained from the upper and lower portions of the subgrade material in the in-service pavement in Kobe City, Japan, using thin walled samplers. Their results are summarized as follows:

material gradation ..... Figure 6.3

specific gravity 2.64

Atterberg limits:

- liquid limit 35.6
- plastic limit 15.8
- plasticity index 19.8

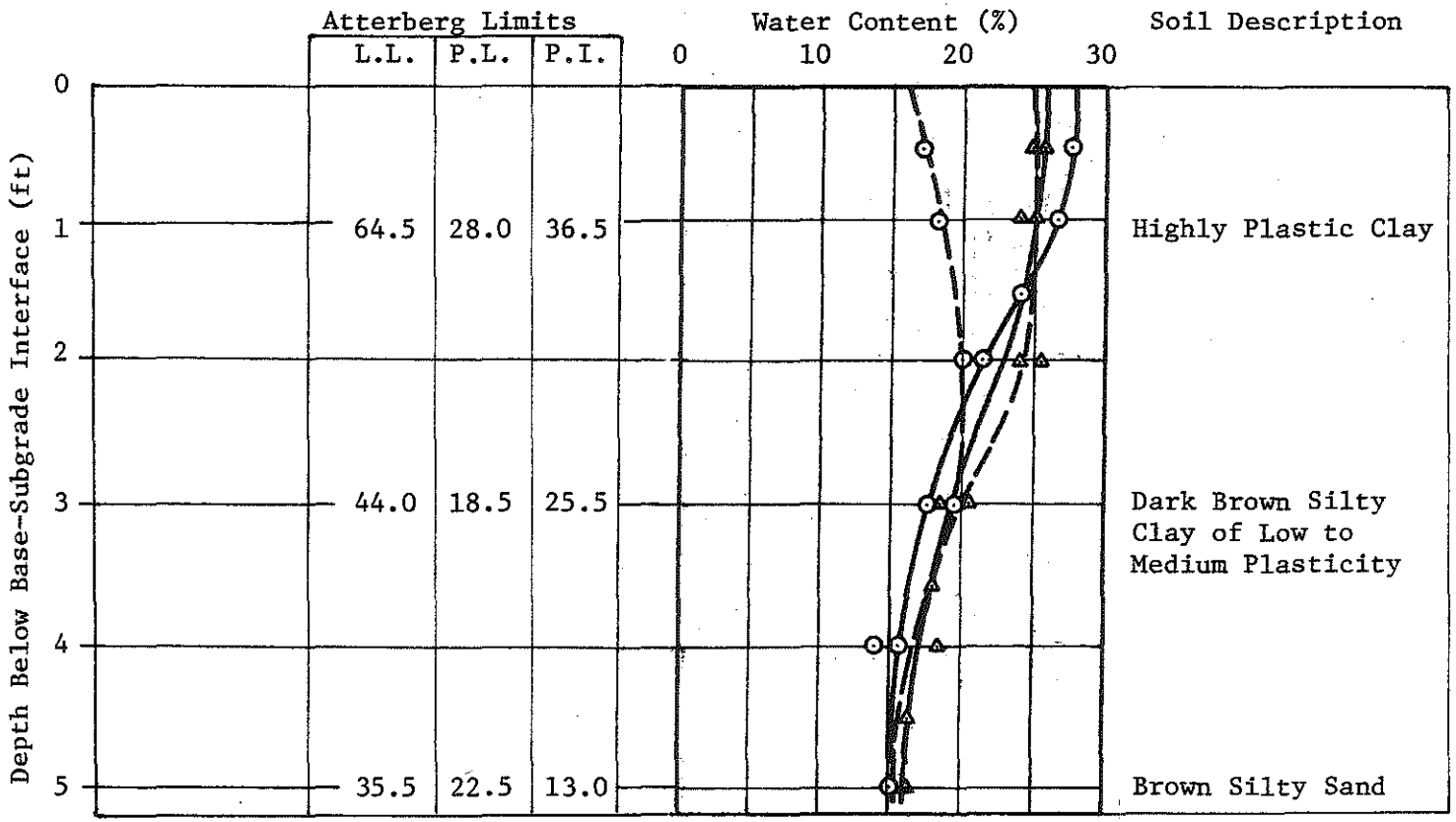

FIGURE 6.1 SUBGRADE CHARACTERISTICS, (36).

TABLE 6.1 RESILIENT MODULI OF UNDISTURBED SPECIMENS OF SUBGRADE SOIL, (36).

Water Content (%)	Axial Stress (psi)	Resilient Axial Strain	Resilient Modulus (psi)
24.6	1.00	0.00024	4,150
25.0	1.72	0.00044	3,900
23.4	3.45	0.00104	3,300
24.2	5.20	0.00162	3,200

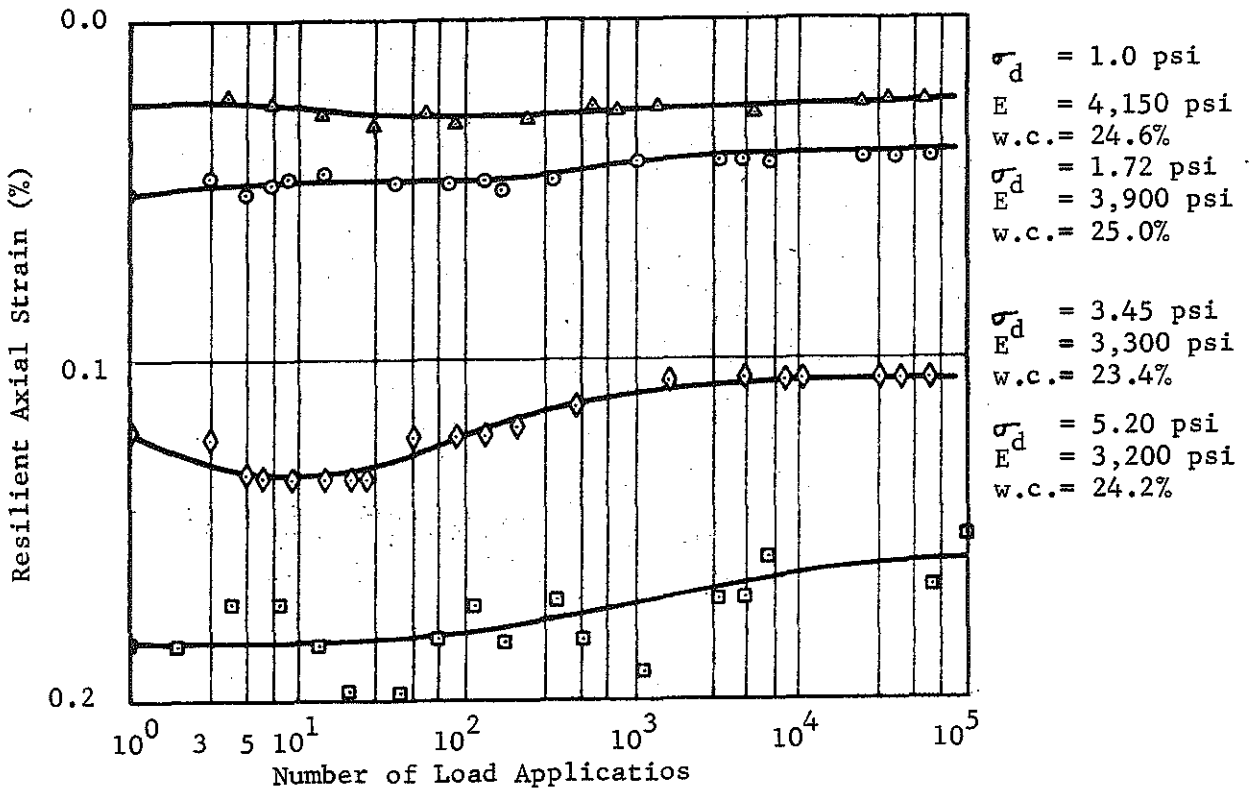

FIGURE 6.2 RESULTS OF REPEATED-LOAD TESTS ON UNCONFINED SPECIMENS OF SUBGRADE, (36).

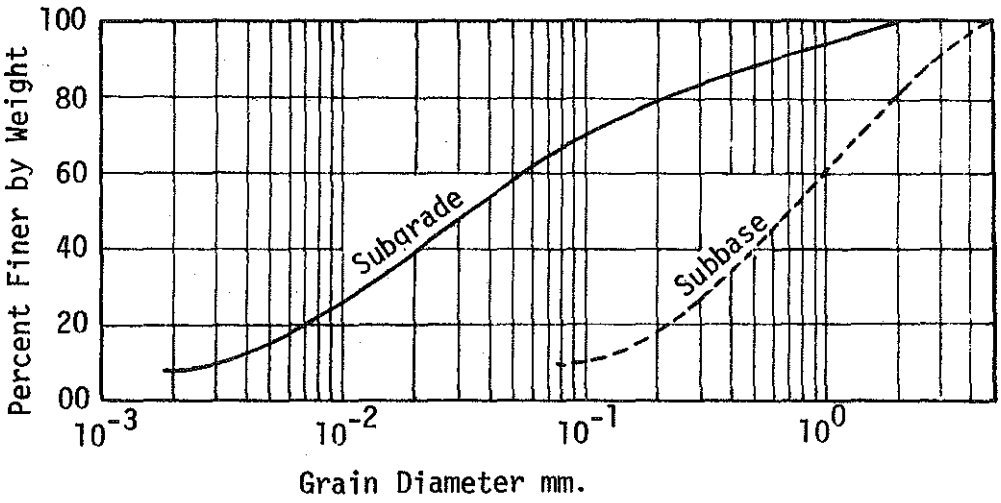

FIGURE 6.3 GRAIN SIZE DISTRIBUTION CURVES OF SAMPLES, (46).

standard AASHO compaction:
- optimum water content (%) 17.6
- maximum dry density ..... 1.75 kg/cm^2

natural water content (%):
- upper layer 25.5
- lower layer 28.5

unconfined compressive strength:
- upper layer ..... 1.20 kg/cm^2
- lower layer ..... 0.80 kg/cm^2

California Bearing Ratio 2.0

loading frequency ..... 20 cycles/minute

load duration ..... 0.1 second

properties determined at load repetitions of 30,000

resilient modulus ..... Figure 6.4

2.2. Cohesionless Soils

Haynes and Yoder (26) performed tests on crushed limestone and gravel materials. The crushed limestone was well graded with sharp angular grains and 11.5 percent passing the #200 sieve, its maximum dry density was 139 pcf. Tests were run with a density of 141 pcf. The gravel was uncrushed and well graded with 9.1 percent passing #200 sieve. The test conditions and results are summarized as follows:

load frequency ..... 40 cycles/minute

load duration ..... 0.04 second

confining pressure ..... 25 psi

deviator stress ..... 70 psi

the deflection history for various water contents and degrees of saturation:
- gravel ..... Figure 6.5
- crushed limestone ..... Figure 6.6

the rebound for various water contents and degrees of saturation:
- gravel ..... Figure 6.7
- crushed limestone ..... Figure 6.8

Mitry (36) tested a Monterey sand with a specific gravity of 2.72 and a CBR value of 21.5, and a Pleasanton gravel with a specific gravity of 2.70 and a CBR value of 103. All tests were run on dry materials. The results are summarized as follows:

load frequency ..... 20 cycles/minute

load duration ..... 0.1 second

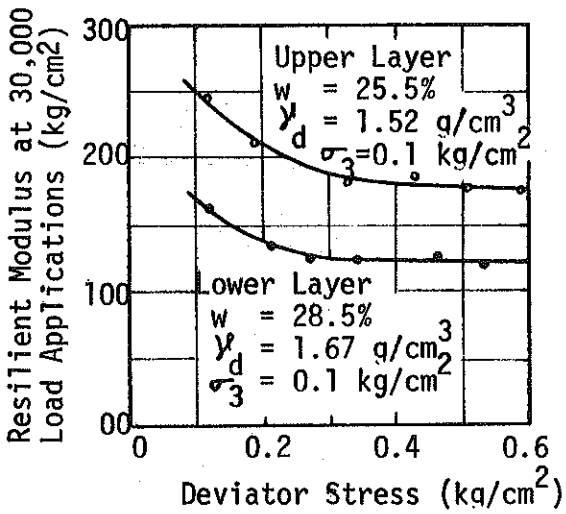

FIGURE 6.4 VARIATION OF RESILIENT MODULUS WITH DEVIATOR STRESS FOR UNDISTURBED SUBGRADE MATERIAL, (46).

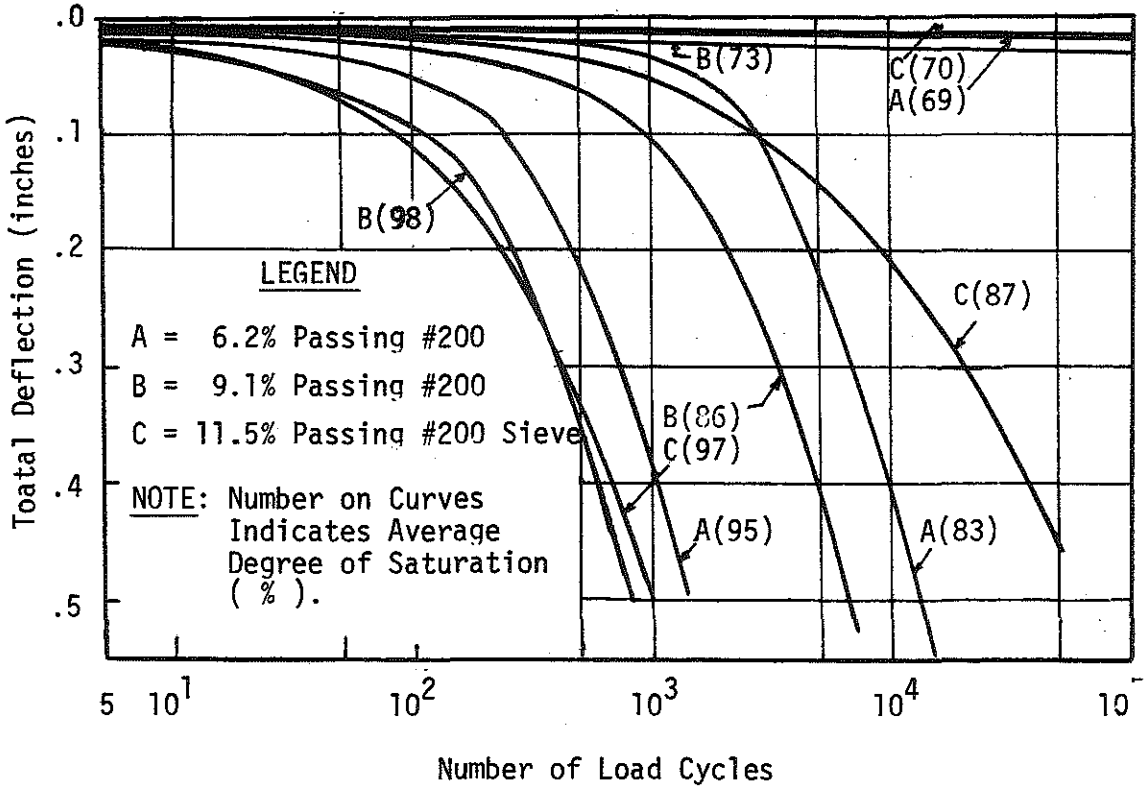

FIGURE 6.5 DEFLECTION HISTORY OF GRAVEL SPECIMENS, (26).

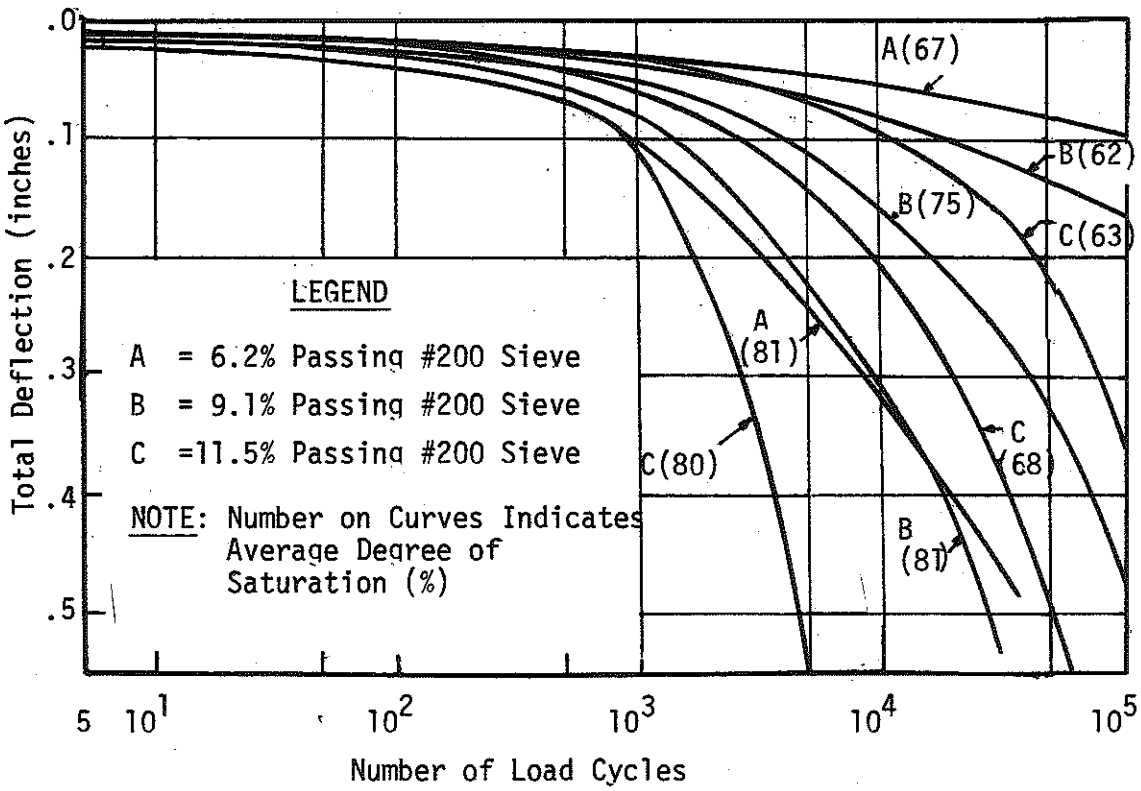

FIGURE 6.6 DEFLECTION HISTORY OF CRUSHED STONE SPECIMENS, (26).

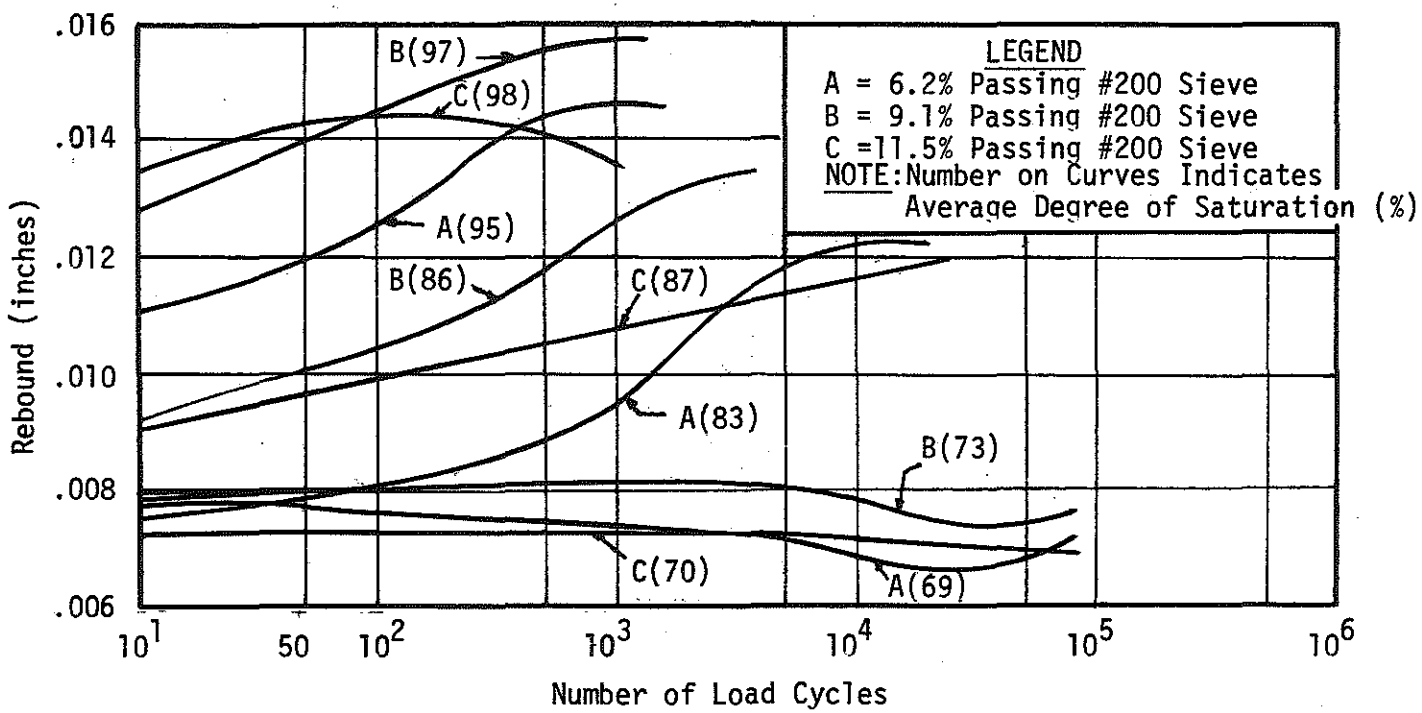

FIGURE 6.7 REBOUND HISTORY OF GRAVEL SPRCIMENS, (26).

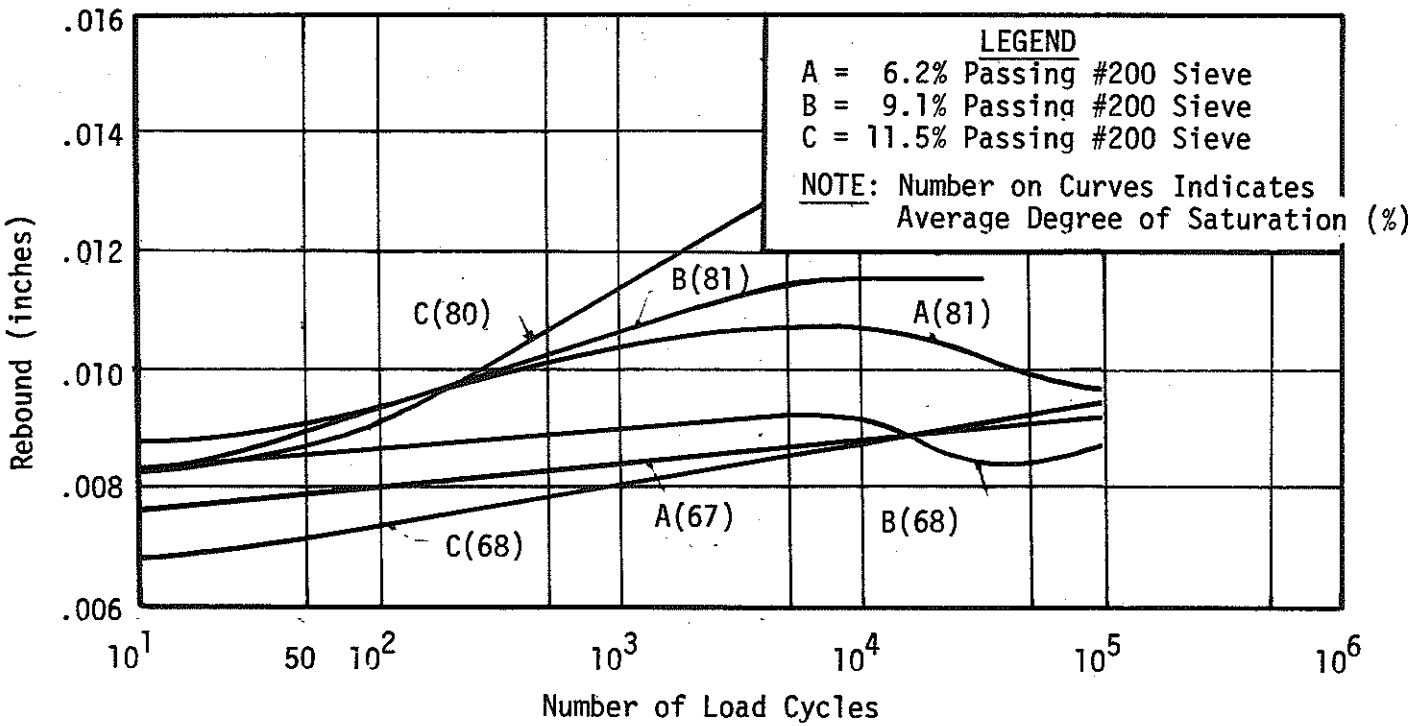

FIGURE 6.8 REBOUND HISTORY OF CRUSHED STONE SPECIMENS, (26).

grain size distribution ..... Table 6.2

resilience characteristics:
- Monterey sand ..... Table 6.3
- Pleasanton gravel ..... Table 6.4

resilient modulus and confining pressure:
- Monterey sand ..... Figure 6.9
- Pleasanton gravel ..... Figure 6.10

Mitry found that these materials exhibited a linear relationship between confining pressure, σ_3, and resilient modulus, M_R, given earlier by equation (2.3). The value of the constants of the equation are illustrated in Figures (6.9) and (6.10) for the Monterey sand and the Pleasanton gravel, respectively.

Partially crushed and crushed aggregates were tested by Hicks (27), the test results are summarized as follows:

sample gradations ..... Table 6.5

load frequency ..... 20 cycles/minute

load duration ..... 0.1 second

principal stresses and their relation to the resilient modulus, and the mean values of Poisson's ratio for various levels of saturation ... Tables 6.6, 6.7, 6.8

Kalcheff and Hicks (31) tested four different aggregates whose gradation and properties are given in Table (6.9). They used stress sequences that are listed in Table (6.10) along with the resilient modulus values. Their tests were run at a load frequency of 30 cycles per minute and a load duration of 0.1 second. The relationship between the confining pressure and the resilient modulus is given in Table (6.11).

Well graded crushed limestone and siliceous gravels and a blend of the two were tested by Allen and Thompson (22). All specimens were prepared at the same gradation and three different levels of density. The test conditions and results are summarized as follows:

density and saturation ..... Table 6.12

load frequency ..... 20 cycles/minute

load duration ..... 0.15 second

sequence of stress conditions ..... Table 6.13

for each stress level, the material properties were determined after load repetitions of ..... 100 cycles

TABLE 6.2 GRAIN SIZE DISTRIBUTION OF MONTEREY SAND AND PLEASANTON GRAVEL, (36).

Sieve Number or Opening	Monterey Sand (Field Test I) Percent Passing	Gravel (Kaiser Randum) (Field Test II) Percent Passing
3/4"		98
1/2"		83
3/8"		65
4		55
8		44.5
16	100	24
30	55	16
50	9	9.5
100	1	5.5
200		3
Specific Gravity	2.72	2.70

TABLE 6.3 RESULTS OF REPEATED LOAD TRIAXIAL TESTS ON MONTEREY SAND, (36).

Specimen Number	Dry Density (pcf)	σ_1 (psi)	$\frac{\sigma_1}{\sigma_3}$	σ_3 (psi)	σ_d (psi)	Resilient Axial Strain (%)	Resilient Modulus (psi)
1	100.0	60	1.5	40	20	0.045	44,500
2	101.5	60	2.0	30	30	0.078	39,600
3	102.0	60	2.5	24	36	0.091	39,600
4	99.5	60	3.5	17	43	0.119	36,100
5	102.0	45	1.5	30	15	0.038	39,500
6	100.0	45	2.0	22.5	22.5	0.058	38,800
7	100.0	45	2.5	18	27	0.073	36,600
8	100.5	45	3.5	13	32	0.093	34,800
9	100.0	30	1.5	20	10	0.029	35,000
10	101.5	30	2.0	15	15	0.053	28,300
11	100.0	30	2.5	12	18	0.054	33,200
12	100.0	30	3.5	8.5	21.5	0.079	27,400
13	101.0	15	1.5	10	5	0.078	27,500
14	101.5	15	2.0	7.5	7.5	0.031	24,200
15	101.7	15	2.5	6	9	0.039	24,100
16	102.5	15	3.5	4.3	10.2	0.045	22,200
17	100.0	5	1.5	3.33	1.67	0.010	17,100

TABLE 6.4 RESULTS OF REPEATED LOAD TRIAXIAL TESTS ON PLEASANTON GRAVEL, (36).

Specimen Number	Dry Density (psf)	σ_1 (psi)	$\frac{\sigma_1}{\sigma_3}$	σ_3 (psi)	σ_d (psi)	Resilient Axial Strain [a] (%)	Resilient Modulus (psi)
1	139.0	5	1.5	3.33	1.67	0.0128	13,050
2	138.5	5	3.0	1.67	3.33	0.0364	9,150
3	138.5	5	5.0	1.00	4.00	0.0635	6,300
4	139.0	10	1.5	6.66	3.33	0.0206	16,200
5	139.0	10	3.0	3.33	6.67	0.0473	14,100
6	140.0	10	5.0	2.00	8.00	0.0775	10,300
7	140.5	10	10.0	1.00	9.00	0.1290	6,960 [b]
8	137.0	20	1.5	13.33	6.67	0.0240	27,700
9	137.2	20	3.0	6.66	13.33	0.0720	18,400
10	139.0	20	5.0	4.00	16.00	0.0925	17,300
11	138.0	30	1.5	20.00	10.00	0.0320	31,200
12	140.0	30	3.0	10.00	20.00	0.0790	25,400
13	138.5	30	5.0	6.00	24.00	0.1280	18,700
14	139.2	45	1.5	30.00	15.00	0.0350	43,400
15	138.5	45	3.0	15.00	30.00	0.1020	29,200
16	138.5	45	5.0	9.00	36.00	0.4420	25,300
17	137.2	60	1.5	40.00	20.00	0.0450	44,500
18	137.5	60	5.0	12.00	48.00	0.1480	32,500
19	137.0	80	1.5	53.30	26.70	0.0510	51,700

[a] At 10,000 load repetitions.
[b] Modulus determined at 500 repetitions; specimen failed at about 1,000 repetitions.

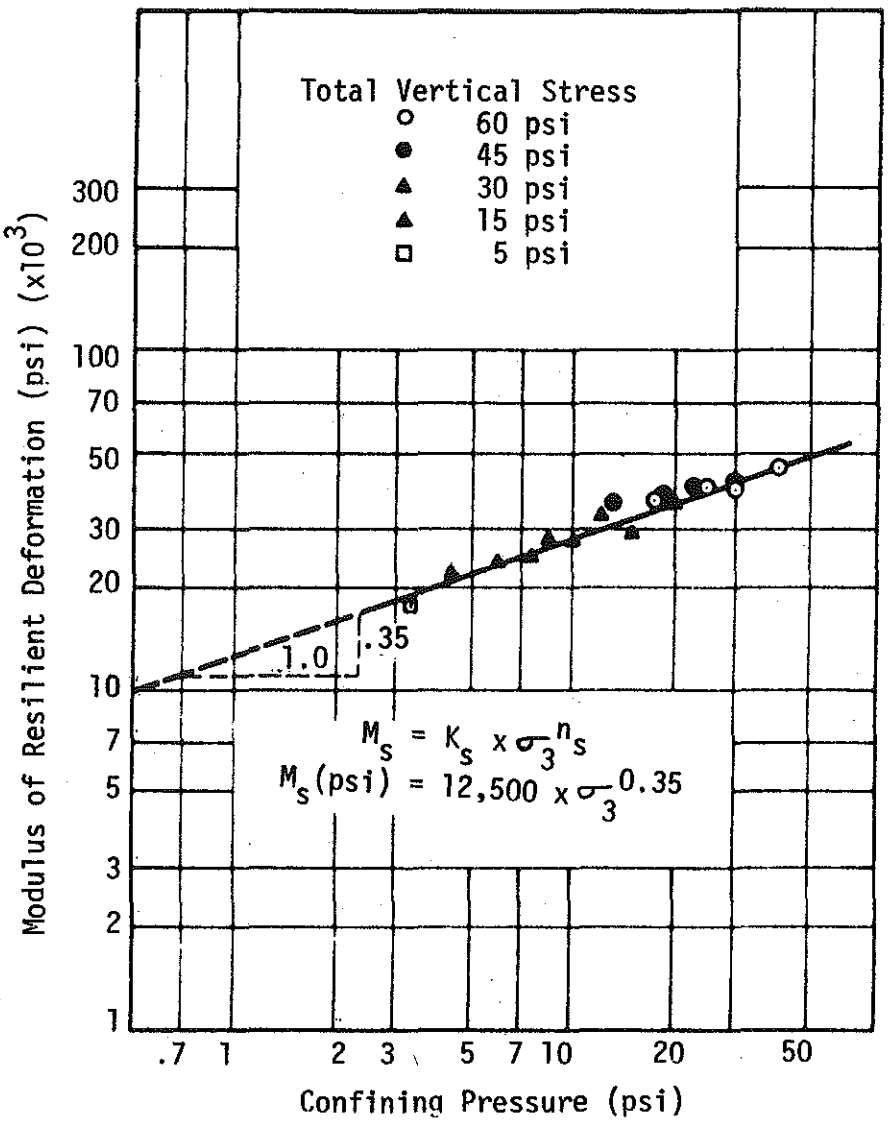

FIGURE 6.9 RELATIONSHIP BETWEEN RESILIENT MODULUS AND CONFINING PRESSURE FOR MONTEREY SAND, (36).

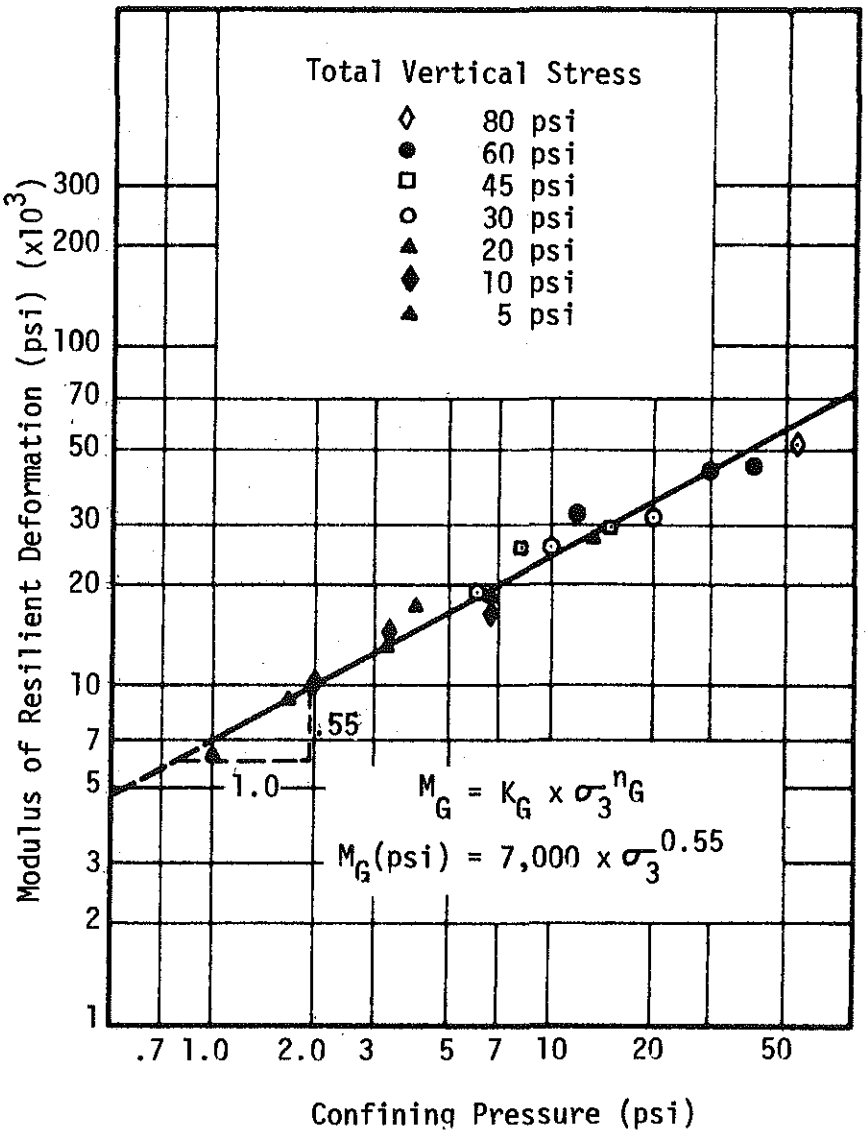

FIGURE 6.10 RELATIONSHIP BETWEEN RESILIENT MODULUS AND CONFINING PRESSURE FOR PLEASANTON GRAVEL, (36).

TABLE 6.5 GRAIN SIZE DISTRIBUTIONS OF AGGREGATE USED IN LABORATORY INVESTIGATION, (27).

Sieve Size	Percent Passing					
	Partially Crushed Aggregate			Crushed Aggregate		
	Coarse	Medium	Fine	Coarse	Medium	Fine
3/4 in.	100	100	100	95	95	95
1/2 in.	83	83	83	81	81	81
3/8 in.	68	68	68	70	70	70
# 4	45	45	45	47	47	47
8	36	36	36	37	37	37
16	28	28	28	30	30	30
30	19	19	19	21	21	21
50	11	13	16	9	12	16.5
100	5	7.5	11.5	4	6.5	13
200	3.3	5	8.2	2.8	5	10

TABLE 6.6 SUMMARY OF MEAN POISSON'S RATIO AND CONSTANTS K_1, K_2 AND K_1', K_2' RELATING RESILIENT MODULUS TO CONFINING PRESSURE (σ_3) AND TO THE SUM OF PRINCIPAL STRESSES (θ) FOR DRY TEST SERIES, (27).

Aggregate Type	% Passing 200	Relative Density(%)	$M_r = K_1 \sigma_3^{K_2}$		$M_r = K_1' \theta^{K_2'}$		Mean Poisson's Ratio *
			K_1	K_2	K_1'	K_2'	
Partially Crushed	3	74.5	8,036	.60	2,156	.71	0.50+
		89.2	11,752	.53	3,977	.61	0.45
		96.4	13,644	.53	4,119	.63	0.47
	5	85.5	10,252	.64	2,780	.73	0.45
		100.2	11,157	.59	3,289	.67	0.32
	8	59.1	7,962	.57	2,447	.66	0.49
		73.0	9,006	.57	2,543	.68	0.45
		86.5	8,939	.61	2,427	.71	0.34
Crushed	3	89.3	12,338	.55	4,368	.60	0.41
		100.3	10,806	.62	3,103	.70	0.35
	5	77.2	11,446	.59	3,572	.66	0.35
		87.0	13,435	.56	4,340	.63	0.27
		91.3	14,874	.51	4,949	.60	0.30
	10	77.0	14,313	.52	5,017	.57	0.23
		86.0	14,672	.50	5,049	.57	0.27

* Average of values at σ_1/σ_3 of 2.0 and 5.0.

TABLE 6.7 SUMMARY OF MEAN POISSON'S RATIO AND CONSTANTS K_1, K_2 AND K_1', K_2' RELATING RESILIENT MODULUS TO CONFINING PRESSURE (σ_3) AND TO THE SUM OF PRINCIPAL STRESSES (θ) FOR PARTIALLY SATURATED TEST SERIES, (27).

Aggregate Type	% Passing 200	Relative Density(%)	Degree of Saturation(%)	$M_r = K_1 \sigma_3^{K_2}$		$M_r = K_1' \theta^{K_2'}$		Mean Poisson's Ratio *
				K_1	K_2	K_1'	K_2'	
Partially Crushed	3	80.7	65	6,786	.59	2,033	.68	0.25
		89.5	67	10,418	.54	3,343	.62	0.34
	5	89.5	68	6,937	.57	2,068	.66	0.39
		102.0	85	7,119	.62	2,039	.70	0.45
		107.0	90	9,795	.56	3,122	.64	0.38
	8	82.8	75	5,204	.64	1,608	.71	0.50+
		92.9	83	7,302	.62	1,901	.73	0.42
Crushed	3	86.1	70	8,818	.57	2,714	.65	0.29
		104.0	74	9,821	.57	2,710	.68	0.25
	5	78.2	76	7,833	.58	2,351	.66	0.35
		78.8	74	8,563	.56	2,589	.65	0.34
		87.3	81	9,032	.58	2,678	.66	0.22
	10	91.8	94	7,759	.57	2,231	.67	0.45
		98.0	92	9,863	.55	3,038	.64	0.45

* Average of values at σ_1/σ_3 of 2.0 and 5.0.

TABLE 6.8 SUMMARY OF MEAN POISSON'S RATIO AND CONSTANTS K_1, K_2 AND K_1', K_2' RELATING RESILIENT MODULUS TO CONFINING PRESSURE (σ_3) AND TO THE SUM OF PRINCIPAL STRESSES (θ) FOR SATURATED TEST SERIES, (27).

Aggregate Type	% Passing 200	Relative Density(%)	$M_r = K_1 \sigma_3^{K_2}$		$M_r = K_1' \theta^{K_2'}$		Mean Poisson's Ratio *
			K_1	K_2	K_1'	K_2'	
Partially Crushed	3	79.9	9,598	.55	2,681	.67	0.25
		88.7	10,396	.54	3,278	.63	0.20
		90.1	10,771	.50	3,616	.60	0.33
	5	74.2	8,080	.54	2,481	.65	0.36
		83.8	9,430	.50	3,208	.59	0.35
		95.0	9,801	.58	2,612	.71	0.34
	8	81.5	9,063	.52	2,967	.62	0.25
		92.0	12,015	.49	4,068	.58	0.25

* Average values at σ_1/σ_3 of 2.0 and 5.0.

TABLE 6.9 PHYSICAL PROPERTIES OF MATERIALS TESTED, (31).

Material Source Identification	A Penna. 2A Subbase 1.5" x 0 Grey Dolomitic	B AASHO Base 1.5" x 0 White Dolomitic	C Md. DGA Base 1" x 0 Grey Siliceous	D Va. 21A Base 1" x 0 Diabase
Description				
Sieve Size	Total Percent Passing the Sieve Indicated*			
1.5"	100	100		
1.0"	97	89	100	100
3/4"	82	82	88	88
3/8"	43	64	63	64
No. 4	30	49	47	51
No. 30	11	23	17	20
No. 200	5.6	12.6	7.7	9.0
Specific Gravity				
bulk dry	2.80	2.68	2.72	2.91
apparent	2.85	2.79	2.74	3.00
Absorption, %	0.6	1.5	0.3	0.8
Los Angeles Abrasion Loss, ASTM C131				
% Wear	22	23	20	15
Moisture Density Tests, ASTM D1557 Method D (plus 3/4" removed)				
Optimum Moisture	5.0	5.4	5.5	6.0
Maximum Density, pcf	144.0	144.2	144.0	152.5
Solids, %	82.5	83.5	85.0	84.0

*Gradation after Compaction (Wet Sieving).

TABLE 6.10 EFFECT OF STRESS SEQUENCE ON RESILIENT MODULUS, (31).

Material: Source A, Penna. 2A Subbase, (144 pcf)

Test Conditions: Partially Saturated
Load Duration: 0.10 sec.
Rate of Application: 30 Cycles per minute

Confining Pressure / Deviator Stress	Resilient Modulus, M_r, 1,000 psi				
	#1	#2	#3	#4	Average
2/6	c* 25	a 30	a 30	c 27	28
2/10	30	30	30		30
2/4	20	23	23		22
2/6	26	28	28		27
5/15	a 46	b 45	b 48	b 41	45
5/25	49	48	48		48
5/10	38	36	37		37
5/15	40	42	39		41
20/60	b 116	c 114	c 104	a 103	109
20/80	127	116			121
20/40	97	92			94
20/60	105	104		d 122	110

*The Order of Test Sequence Was a, b, c, d.

TABLE 6.11 SUMMARY OF CONSTANTS K, C, K', n AND n' FOR THREE OF THE AGGREGATES TESTED, (31).

Aggregate Source	Density % of ASTM D 1557	$M_r^* = K(\sigma_3)^n + C$			$M_r = K'(\theta)^{n'}$	
		K	n	C**	K'	n'
A	99.8	23,000	0.458	23,000	9,400	0.486
	93.9	20,000	0.476	20,000	9,000	0.463
C	99.9	22,000	0.498	22,000	7,300	0.549
	94.2	22,000	0.490	22,000	7,300	0.541
D	100.9	13,300	0.608	15,000	4,200	0.642
	95.4	13,000	0.592	14,000	4,000	0.625

* The equation $M_r = K(\sigma_3)^n + C$ is suggested in place of $M_r = K(\sigma_3)^n$ because $M_r \neq 0$ when $\sigma_3 = 0$. The limits for these constants are as follows:

$K = 0$ for $\sigma_3 < 1$ $\qquad$ $C = 0$ for $\sigma_3 \geq 1$

** In this investigation, C was determined on specimens at $\sigma_3 = 0$ and $\sigma_d = \sigma_1 = 5$ psi.

TABLE 6.12 TEST SPECIMEN DATA, (22).

Specimen	Material	Material	Moisture (percent)	Saturation (percent)
HD-1	Crushed Stone	138.0 High	5.7	78
MD-1	Crushed Stone	134.0 Intermediate	6.3	73
LD-1	Crushed Stone	130.0 Low	7.0	70
HD-2	Gravel	139.4 High	6.3	82
MD-2	Gravel	134.0 Intermediate	6.5	74
LD-2	Gravel	131.0 Low	6.7	69
HD-3	Blend	139.5 High	6.3	88
MD-3	Blend	134.5 Intermediate	6.8	78
LD-3	Blend	131.0 Low	7.2	74

TABLE 6.13 TEST SCHEDULE DATA, (22).

Stress Level (psi)			Confining Pressure
σ_3	σ_1	σ_1/σ_3	
2	8	4	Variable
2	12	6	Variable
2	16	8	Variable
2	8	4	Constant
2	12	6	Constant
2	16	8	Constant
5	10	2	Constant
5	15	3	Constant
5	25	5	Constant
5	35	7	Constant
5	45	9	Constant
5	10	2	Variable
5	15	3	Variable
5	25	5	Variable
5	35	7	Variable
5	45	9	Variable
8	12	1.5	Variable
8	24	3	Variable
8	40	5	Variable
8	56	7	Variable
8	12	1.5	Constant
8	24	3	Constant
8	40	5	Constant
8	56	7	Constant
11	22	2	Constant
11	44	4	Constant
11	66	6	Constant
11	22	2	Variable
11	44	4	Variable
11	66	6	Variable
15	25	1.6	Variable
15	45	3	Variable
15	60	4	Variable
15	75	5	Variable
15	25	1.6	Constant
15	45	3	Constant
15	60	4	Constant
15	70	4.7	Constant

Note: All stress levels were applied for 100 repetitions.
One pulse duration of 0.15 seconds was used.

the regression equation constants ..... Table 6.14

the regression equation constants for the resilient Poisson's ratio, equation (2.4) ..... Table 6.15

Based on the test results, Allen and Thompson concluded that the regression equation with θ, the sum of principal stresses, was found to be more accurate in relating θ to the resilient modulus than the one relating confining pressure to the resilient modulus.

2.3. Asphalt Treated Materials

Terrel and Awad (47) conducted tests on asphalt treated materials. They used an asphalt binder having 85 - 100 penetration asphalt cement, and tested three different asphalt contents: 2.5, 3.5, and 4.5 percent. Table (6.16) provides a listing of the results of tests made on this binder. Three different gradations of a pit run gravel were also used for testing, the test results and the sample conditions are summarized as follows:

gradations ..... Table 6.17

specific gravity 2.65

specimens were conditioned, for all possible states of stress, at a load repetition of ..... 50 cycles

load frequency ..... 20 cycles/minute

load durations ..... 0.1 and 1.0 seconds

the constants of equations (3.6) and (3.7) ..... Tables 6.18, 6.19, 6.20

the modulus of total deformation ..... Tables 6.21, 6.22, 6.23

the variation of resilient modulus for different asphalt contents ..... Figures 6.11, 6.12, 6.13

The dashed lines in Figures (6.11), (6.12), and (6.13) represent values determined by the Heukelom and Klomp method (69). The solid lines in the figures represent values that were determined by a curve fitting technique using the following equation:

$$\log_{10} M_R = 6.8203 - 2.9944(10^{-6})(a/c)^2(T)^2 - 1.1927(10^{-4})(T) - \frac{1.414\ (\%air)}{(T)}$$

in which, (a/c) = the asphalt content in percent by weight

T = the temperature in degrees Fahrenheit

% air = the percent of air voids by volume.

TABLE 6.14 REGRESSION EQUATION CONSTANTS FOR RESILIENT MODULUS FROM PRIMARY TEST DATA, (22).

Specimen	Type of Test	Model: $M_r = f(\theta)$			Model: $M_r = f(\sigma_3)$		
		Equation	Correlation[a] Coefficient	Standard Error	Equation	Correlation Coefficient	Standard Error
HD-1	VCP	$6{,}635\theta^{0.40}$	0.930	3,144	$18{,}010\sigma_3^{0.28}$	0.669[b]	6,338
MD-1	VCP	$1{,}793\theta^{0.70}$	0.992	1,463	$8{,}556\sigma_3^{0.57}$	0.794[a]	7,014
LD-1	VCP	$2{,}113\theta^{0.66}$	0.982	2,058	$8{,}410\sigma_3^{0.57}$	0.819[a]	6,227
HD-2	VCP	$7{,}766\theta^{0.32}$	0.767	3,996	$18{,}480\sigma_3^{0.19}$	0.515[c]	5,338
MD-2	VCP	$6{,}995\theta^{0.33}$	0.906	2,202	$15{,}738\sigma_3^{0.25}$	0.664[b]	3,897
LD-2	VCP	$1{,}613\theta^{0.69}$	0.973	2,033	$7{,}924\sigma_3^{0.51}$	0.781[a]	5,473
HD-3	VCP	$6{,}891\theta^{0.45}$	0.980	2,035	$18{,}951\sigma_3^{0.35}$	0.832[a]	5,638
MD-3	VCP	$7{,}725\theta^{0.33}$	0.981	1,042	$15{,}806\sigma_3^{0.26}$	0.841[a]	2,890
LD-3	VCP	$4{,}562\theta^{0.43}$	0.856	3,367	$14{,}516\sigma_3^{0.24}$	0.498[c]	5,648

TABLE 6.14 CONTINUED

Specimen	Type of Test	Model: $M_r = f(\theta)$			Model: $M_r = f(\sigma_3)$		
		Equation	Correlation[a] Coefficient	Standard Error	Equation	Correlation Coefficient	Standard Error
HD-1	CCP	$2{,}376\theta^{0.69}$	0.997	1,149	$12{,}454\sigma_3^{0.55}$	0.845[a]	7,896
MD-1	CCP	$4{,}928\theta^{0.46}$	0.973	1,950	$14{,}254\sigma_3^{0.39}$	0.872[a]	4,115
LD-1	CCP	$3{,}083\theta^{0.59}$	0.962	3,132	$11{,}068\sigma_3^{0.53}$	0.909[a]	4,813
HD-2	CCP	$4{,}596\theta^{0.50}$	0.741	8,063	$11{,}128\sigma_3^{0.54}$	0.803[a]	7,157
MD-2	CCP	$8{,}016\theta^{0.31}$	0.803	3,551	$14{,}729\sigma_3^{0.31}$	0.838[a]	3,247
LD-2	CCP	$2{,}849\theta^{0.56}$	0.882	4,289	$8{,}517\sigma_3^{0.55}$	0.916[a]	3,641
HD-3	CCP	$5{,}989\theta^{0.48}$	0.932	4,254	$16{,}433\sigma_3^{0.45}$	0.922[a]	4,542
MD-3	CCP	$6{,}459\theta^{0.37}$	0.829	3,977	$13{,}379\sigma_3^{0.37}$	0.873[c]	3,471
LD-3	CCP	$2{,}966\theta^{0.60}$	0.882	4,962	$9{,}079\sigma_3^{0.53}$	0.914[a]	4,260

[a] Significant at $\alpha = 0.001$. [b] Significant at $\alpha = 0.01$. [c] Significant at $\alpha = 0.05$.

TABLE 6.15 REGRESSION EQUATION CONSTANTS FOR RESILIENT POISSON'S RATIO FROM PRIMARY TEST DATA, (22).

$$\nu_r = A_0 + A_1 (\sigma_1/\sigma_3) + A_2 (\sigma_1/\sigma_3)^2 + A_3 (\sigma_1/\sigma_3)^3$$

Specimen	Type of Test	A_0	A_1	A_2	A_3	Correlation Coefficient	Standard Error
HD-1	VCP	0.62	-0.19	0.040	-0.0020	0.907[a]	0.026
MD-1	VCP	0.47	-0.07	0.020	-0.0010	0.838[a]	0.045
LD-1	VCP	0.60	-0.14	0.020	-0.0007	0.881[a]	0.036
HD-2	VCP	-0.12	0.45	-0.090	0.0050	0.645[b]	0.085
MD-2	VCP	0.46	0.01	-0.010	0.0020	0.889[a]	0.026
LD-2	VCP	0.70	-0.22	0.040	-0.0020	0.925[a]	0.027
HD-3	VCP	0.49	0.01	-0.010	0.0010	0.766[a]	0.037
MD-3	VCP	0.50	-0.02	-0.003	0.0006	0.561[c]	0.048
LD-3	VCP	0.52	-0.07	0.006	0.0002	0.840[a]	0.026
HD-1	CCP	-0.17	0.30	-0.040	0.0020	0.895[a]	0.047
MD-1	CCP	0.29	0.12	-0.010	0.0006	0.746[a]	0.060
LD-1	CCP	-0.01	0.28	-0.040	0.0020	0.723[a]	0.096
HD-2	CCP	-0.14	0.46	-0.060	0.0030	0.429[d]	0.208
MD-2	CCP	0.95	-0.22	0.040	-0.0020	0.654[b]	0.144
LD-2	CCP	-0.04	0.32	-0.050	0.0030	0.953[a]	0.056
HD-3	CCP	-0.16	0.37	-0.050	0.0030	0.868[a]	0.073
MD-3	CCP	-0.02	0.27	-0.030	0.0010	0.828[a]	0.091
LD-3	CCP	-0.09	0.36	-0.050	0.0030	0.729[a]	0.121

[a] Significant at = 0.001. [b] Significant at = 0.01. [c] Significant at = 0.02.
[d] Significant at = 0.1.

TABLE 6.16 TEST RESULTS ON ASPHALT CEMENT, (47).

Test	Result
Specific Gravity (ASTM D70)	0.990
Penetration (ASTM D5)	88 dmm
Recovered Penetration (ASTM)	67 dmm
Flash Point (ASTM D93)	480°F
R & B Softening Pt. (ASTM D36)	108°F
Ductility (ASTM D113)	100 + cm

TABLE 6.17 GRADATION OF THE AGGREGATE, (47).

Sieve	Fine Cumulative % Passing	Individual % Retained	Note
3/4"	100	0	
1/2"	100	0	F
1/4"	78	22	I
#10	57	21	N
#40	32	25	E
#200	9	23	
-#200	0	9	
3/4"	100	0	M
1/2"	83	16	I
1/4"	61	23	D
#10	36	25	D
#40	18	18	L
#200	8	10	E
-#200	0	8	
3/4"	100	0	C
1/2"	56	44	O
1/4"	40	16	A
#10	22	18	R
#40	8	14	S
#200	2	6	E
-#200	0	2	

TABLE 6.18 SUMMARY OF RESILIENT MODULUS TESTS FOR 0.1 AND 1.0 SECOND STRESS DURATIONS ON SAMPLES OF FINE GRADATION, (47).

GRADATION	ASPHALT CONTENT	PERCENT VOIDS	PERCENT AIR	TEMPERATURE	COEFFICIENT				RESILIENT MODULUS-PSI	POISSON'S RATIO
					B1	B2	B3	B4		
FINE	2.25	15.37	13.71	25	.600	-.070	-.752	1.112	1.007E+06	.276
FINE	2.25	15.37	13.71	45	1.000	-.212	-1.100	1.530	1.017E+06	.445
FINE	2.25	15.37	13.71	70	1.700	-.490	-4.600	4.000	3.127E+05	.536
FINE	2.25	15.37	13.71	90	4.360	-1.475	-4.800	5.450	2.531E+05	.529
FINE	2.37	11.70	7.18	25	.440	-.105	-.185	.300	2.390E+06	.231
FINE	2.37	11.70	7.18	45	.450	-.118	-.320	.528	1.779E+06	.260
FINE	2.37	11.70	7.18	70	.870	-.354	-.825	.980	8.917E+05	.350
FINE	2.37	11.70	7.18	90	2.350	-.900	-1.900	3.270	4.392E+05	.410
FINE	2.46	9.46	1.97	25	.142	-.060	-.160	.268	4.138E+06	.303
FINE	2.46	9.46	1.97	45	.220	-.123	-.200	.406	2.726E+06	.294
FINE	2.46	9.46	1.97	70	.680	-.445	-.910	1.020	9.295E+05	.420
FINE	2.46	9.46	1.97	90	1.720	-1.410	-3.400	3.370	3.513E+05	.563
FINE	2.25	15.37	13.71	25	.780	-.105	-.900	1.410	7.921E+05	.265
FINE	2.25	15.37	13.71	45	1.390	-.344	-1.910	2.320	5.778E+05	.434
FINE	2.25	15.37	13.71	70	3.800	-1.140	-6.800	7.080	1.900E+05	.503
FINE	2.25	15.37	13.71	90	9.800	-3.130	-9.750	10.400	1.291E+05	.554
FINE	2.37	11.70	7.18	25	.440	-.134	-.208	.370	2.165E+06	.247
FINE	2.37	11.70	7.18	45	.450	-.172	-.430	.735	1.443E+06	.290
FINE	2.37	11.70	7.18	70	1.700	-.795	-1.900	2.140	5.350E+05	.481
FINE	2.37	11.70	7.18	90	6.200	-2.670	-5.500	8.270	1.787E+05	.487
FINE	2.46	9.46	1.97	25	.182	-.097	-.185	.325	3.328E+06	.313
FINE	2.46	9.46	1.97	45	.270	-.207	-.500	.625	1.769E+06	.417
FINE	2.46	9.46	1.97	70	1.550	-1.170	-1.450	2.270	5.415E+05	.473
FINE	2.46	9.46	1.97	90	5.900	-4.120	-8.400	8.840	1.437E+05	.600

TABLE 6.19. SUMMARY OF RESILIENT MODULUS TESTS FOR 0.1 AND 1.0 SECOND STRESS DURATIONS ON SAMPLES OF MEDIUM GRADATION, (47).

GRADATION	ASPHALT CONTENT	PERCENT VOIDS	PERCENT AIR	TEMPERATURE	COEFFICIENT B1	B2	B3	B4	RESILIENT MODULUS PSI	POISSON'S RATIO
MEDIUM	2.36	12.69	9.94	25	.332	-.068	-.385	.720	1.663E+06	.251
MEDIUM	2.36	12.69	9.94	45	.655	-.104	-.450	1.050	1.058E+06	.195
MEDIUM	2.36	12.69	9.94	70	1.100	-.264	-1.070	1.540	9.594E+05	.427
MEDIUM	2.36	12.69	9.94	90	1.720	-.450	-1.600	3.480	4.096E+05	.280
MEDIUM	2.49	8.71	2.43	25	.125	-.085	-.100	.240	4.687E+06	.289
MEDIUM	2.49	8.71	2.43	45	.133	-.090	-.170	.356	3.474E+06	.301
MEDIUM	2.49	8.71	2.43	70	.255	-.256	-.640	.840	1.435E+06	.429
MEDIUM	2.49	8.71	2.43	90	1.440	-.960	-2.000	2.430	5.186E+05	.512
MEDIUM	2.50	9.32	1.03	25	.255	-.070	-.150	.284	3.266E+06	.240
MEDIUM	2.50	9.32	1.03	45	.375	-.200	-.205	.288	2.506E+06	.338
MEDIUM	2.50	9.32	1.03	70	1.250	-.960	-1.520	2.020	6.459E+05	.534
MEDIUM	2.50	9.32	1.03	90	4.600	-5.830	-10.700	12.100	1.098E+05	.605
MEDIUM	2.36	12.69	9.94	25	.520	-.092	-.490	.840	1.287E+06	.250
MEDIUM	2.36	12.69	9.94	45	.600	-.107	-.450	1.400	9.151E+05	.170
MEDIUM	2.36	12.69	9.94	70	1.680	-.448	-1.200	2.360	5.572E+05	.306
MEDIUM	2.36	12.69	9.94	90	3.550	-1.060	-3.300	6.000	2.499E+05	.363
MEDIUM	2.49	8.71	2.43	25	.180	-.086	-.360	.266	3.363E+06	.500
MEDIUM	2.49	8.71	2.43	45	.310	-.130	-.338	.490	2.092E+06	.326
MEDIUM	2.49	8.71	2.43	70	.860	-.720	-1.880	1.880	5.545E+05	.481
MEDIUM	2.49	8.71	2.43	90	4.520	-3.000	-5.650	6.600	1.999E+05	.576
MEDIUM	2.50	9.32	1.03	25	.275	-.096	-.235	.360	2.683E+06	.296
MEDIUM	2.50	9.32	1.03	45	.650	-.390	-.450	.880	1.105E+06	.309
MEDIUM	2.50	9.32	1.03	70	9.200	-4.100	-13.100	7.800	1.435E+05	.823
MEDIUM	2.50	9.32	1.03	90	30.200	-36.300	-39.500	48.250	2.713E+04	.686

TABLE 6.20. SUMMARY OF RESILIENT MODULUS TESTS FOR 0.1 AND 1.0 SECOND STRESS DURATIONS ON SAMPLES OF COARSE GRADATION, (47).

GRADATION	ASPHALT CONTENT	PERCENT VOIDS	PERCENT AIR	TEMPERATURE	COEFFICIENT				RESILIENT MODULUS PSI	POISSON'S RATIO
					B1	B2	B3	B4		
COARSE	2.41	12.80	9.21	25	.320	-.086	-.130	.362	2.653E+06	.191
COARSE	2.41	12.80	9.21	45	.431	-.140	-.372	1.000	1.249E+06	.213
COARSE	2.41	12.80	9.21	70	.947	-.485	-.682	1.530	6.978E+05	.271
COARSE	2.41	12.80	9.21	90	2.140	-.850	-1.785	4.120	3.892E+05	.342
COARSE	2.43	12.99	5.79	25	.200	-.085	-.132	.390	2.946E+06	.262
COARSE	2.43	12.99	5.79	45	.400	-.124	-.290	.384	2.169E+06	.299
COARSE	2.43	12.99	5.79	70	.750	-.384	-.773	1.480	7.646E+05	.295
COARSE	2.43	12.99	5.79	90	2.350	-1.610	-3.370	3.500	3.630E+05	.603
COARSE	2.47	12.42	3.50	25	.304	-.125	-.100	.265	3.106E+06	.233
COARSE	2.47	12.42	3.50	45	.241	-.174	-.361	.522	2.125E+06	.379
COARSE	2.47	12.42	3.50	70	1.030	-.632	-1.446	1.280	9.987E+05	.692
COARSE	2.47	12.42	3.50	90	5.110	-5.050	-12.000	10.320	1.241E+05	.705
COARSE	2.41	12.80	9.21	25	.416	-.100	-.239	.460	2.022E+06	.229
COARSE	2.41	12.80	9.21	45	.642	-.176	-.550	1.200	9.597E+05	.232
COARSE	2.41	12.80	9.21	70	2.830	-1.580	-2.450	4.170	3.153E+05	.424
COARSE	2.41	12.80	9.21	90	4.200	-1.620	-4.000	6.120	2.441E+05	.457
COARSE	2.43	12.99	5.79	25	.300	-.100	-.192	.444	2.377E+06	.231
COARSE	2.43	12.99	5.79	45	.449	-.222	-.496	.562	1.600E+06	.383
COARSE	2.43	12.99	5.79	70	1.800	-1.020	-2.040	3.830	3.540E+05	.361
COARSE	2.43	12.99	5.79	90	7.300	-4.670	-10.100	10.100	1.305E+05	.643
COARSE	2.47	12.42	3.50	25	.372	-.113	-.181	.344	2.457E+06	.241
COARSE	2.47	12.42	3.50	45	.410	-.374	-.781	.900	1.180E+06	.454
COARSE	2.47	12.42	3.50	70	1.650	-1.940	-2.810	3.620	3.417E+05	.541
COARSE	2.47	12.42	3.50	90	28.000	-26.900	-59.700	54.000	2.201E+04	.635

TABLE 6.21. SUMMARY OF MODULUS OF TOTAL DEFORMATIONS FOR 0.1 AND 1.0 SECOND STRESS DURATIONS ON SAMPLES OF FINE GRADATION, (47).

GRADATION	ASPHALT CONTENT	PERCENT VOIDS	PERCENT AIR	TEMPERATURE	COEFFICIENT				MODULUS OF TOTAL DEFORMATIONS	POISSON'S RATIO
					B1	B2	B3	B4		
FINE	2.25	15.37	13.71	25	.600	-.070	-.752	1.112	1.007E+06	.276
FINE	2.25	15.37	13.71	45	1.000	-.212	-1.250	1.550	6.585E+05	.321
FINE	2.25	15.37	13.71	70	2.160	-.520	-5.330	5.200	2.148E+05	.419
FINE	2.25	15.37	13.71	90	4.960	-1.735	-5.500	6.250	1.468E+05	.354
FINE	2.37	11.70	7.18	25	.440	-.105	-.185	.300	2.390E+06	.231
FINE	2.37	11.70	7.18	45	.450	-.118	-.320	.528	1.779E+06	.260
FINE	2.37	11.70	7.18	70	1.020	-.380	-.920	1.030	8.054E+05	.349
FINE	2.37	11.70	7.18	90	2.600	-1.140	-2.250	3.670	2.703E+05	.305
FINE	2.46	9.46	1.97	25	.142	-.060	-.160	.258	4.138E+06	.303
FINE	2.46	9.46	1.97	45	.220	-.123	-.200	.420	2.675E+06	.288
FINE	2.46	9.46	1.97	70	.810	-.675	-1.160	1.255	7.472E+05	.457
FINE	2.46	9.46	1.97	90	2.420	-1.840	-3.630	3.900	2.456E+05	.448
FINE	2.25	15.37	13.71	25	.780	-.105	-.900	1.410	7.921E+05	.265
FINE	2.25	15.37	13.71	45	1.510	-.376	-2.000	2.400	4.254E+05	.337
FINE	2.25	15.37	13.71	70	4.320	-1.290	-10.000	9.000	1.171E+05	.441
FINE	2.25	15.37	13.71	90	11.500	-4.030	-10.500	11.301	7.235E+04	.350
FINE	2.37	11.70	7.18	25	.440	-.134	-.208	.370	2.165E+06	.247
FINE	2.37	11.70	7.18	45	.450	-.180	-.430	.760	1.415E+06	.288
FINE	2.37	11.70	7.18	70	2.040	-.915	-2.350	2.370	3.637E+05	.396
FINE	2.37	11.70	7.18	90	7.900	-3.330	-7.100	9.750	9.467E+04	.329
FINE	2.46	9.46	1.97	25	.182	-.097	-.185	.325	3.328E+06	.313
FINE	2.46	9.46	1.97	45	.292	-.223	-.500	.650	1.691E+06	.407
FINE	2.46	9.46	1.97	70	2.400	-1.800	-3.000	3.220	2.770E+05	.443
FINE	2.46	9.46	1.97	90	8.600	-6.630	-12.000	11.401	7.631E+04	.474

TABLE 6.22. SUMMARY OF MODULUS OF TOTAL DEFORMATIONS FOR 0.1 AND 1.0 SECOND STRESS DURATIONS ON SAMPLES OF MEDIUM GRADATION, (47).

GRADATION	ASPHALT CONTENT	PERCENT VOIDS	PERCENT AIR	TEMPERATURE	COEFFICIENT				MODULUS OF TOTAL DEFORMATIONS	POISSON'S RATIO
					B1	B2	B3	B4		
MEDIUM	2.36	12.69	9.94	25	.332	-.068	-.385	.720	1.663E+06	.251
MEDIUM	2.36	12.69	9.94	45	.655	-.104	-.450	1.050	1.058E+06	.195
MEDIUM	2.36	12.69	9.94	70	1.100	-.264	-1.075	1.580	6.397E+05	.286
MEDIUM	2.36	12.69	9.94	90	1.850	-.465	-1.700	3.650	3.215E+05	.232
MEDIUM	2.49	8.71	2.43	25	.125	-.085	-.100	.240	4.687E+06	.289
MEDIUM	2.49	8.71	2.43	45	.133	-.090	-.180	.370	3.373E+06	.304
MEDIUM	2.49	8.71	2.43	70	.285	-.256	-.660	.860	1.379E+06	.421
MEDIUM	2.49	8.71	2.43	90	1.550	-1.090	-2.300	2.620	3.774E+05	.426
MEDIUM	2.50	9.32	1.03	25	.255	-.070	-.185	.284	3.205E+06	.272
MEDIUM	2.50	9.32	1.03	45	.420	-.208	-.300	.320	2.199E+06	.372
MEDIUM	2.50	9.32	1.03	70	1.380	-1.070	-2.000	2.200	4.345E+05	.445
MEDIUM	2.50	9.32	1.03	90	5.500	-6.500	-14.400	16.600	6.881E+04	.479
MEDIUM	2.36	12.69	9.94	25	.520	-.092	-.490	.840	1.287E+06	.250
MEDIUM	2.36	12.69	9.94	45	.600	-.107	-.470	1.440	8.959E+05	.172
MEDIUM	2.36	12.69	9.94	70	1.750	-.460	-1.300	2.400	4.222E+05	.248
MEDIUM	2.36	12.69	9.94	90	3.900	-1.150	-4.200	6.600	1.628E+05	.290
MEDIUM	2.49	8.71	2.43	25	.180	-.086	-.360	.266	3.363E+06	.500
MEDIUM	2.49	8.71	2.43	45	.350	-.134	-.380	.500	1.958E+06	.336
MEDIUM	2.49	8.71	2.43	70	1.000	-.748	-2.000	2.000	5.107E+05	.468
MEDIUM	2.49	8.71	2.43	90	5.100	-3.450	-6.650	7.370	1.263E+05	.425
MEDIUM	2.50	9.32	1.03	25	.275	-.096	-.250	.370	2.630E+06	.303
MEDIUM	2.50	9.32	1.03	45	.690	-.446	-.700	.960	9.843E+05	.376
MEDIUM	2.50	9.32	1.03	70	9.500	-4.160	-13.900	8.350	8.379E+04	.504
MEDIUM	2.50	9.32	1.03	90	31.500	-37.300	-46.500	52.600	1.785E+04	.499

TABLE 6.23. SUMMARY OF MODULUS OF TOTAL DEFORMATIONS FOR 0.1 AND 1.0 SECOND STRESS DURATIONS ON SAMPLES OF COARSE GRADATION, (47).

GRADATION	ASPHALT CONTENT	PERCENT VOIDS	PERCENT AIR	TEMPERATURE	COEFFICIENT				MODULUS OF TOTAL DEFORMATIONS	POISSON'S RATIO
					B1	B2	B3	B4		
COARSE	2.41	12.80	9.21	25	.320	-.086	-.130	.362	2.653E+06	.191
COARSE	2.41	12.80	9.21	45	.431	-.140	-.372	1.000	1.249E+06	.213
COARSE	2.41	12.80	9.21	70	.947	-.520	-.870	1.580	6.688E+05	.310
COARSE	2.41	12.80	9.21	90	2.030	-.923	-1.910	4.310	2.746E+05	.259
COARSE	2.43	12.99	5.79	25	.200	-.085	-.270	.390	2.824E+06	.334
COARSE	2.43	12.99	5.79	45	.400	-.124	-.290	.384	2.169E+06	.299
COARSE	2.43	12.99	5.79	70	1.073	-.400	-.821	1.615	6.462E+05	.263
COARSE	2.43	12.99	5.79	90	2.810	-1.910	-5.230	4.070	2.160E+05	.514
COARSE	2.47	12.42	3.50	25	.304	-.125	-.100	.265	3.106E+06	.233
COARSE	2.47	12.42	3.50	45	.325	-.174	-.395	.522	1.929E+06	.366
COARSE	2.47	12.42	3.50	70	1.084	-.780	-1.730	1.630	5.633E+05	.471
COARSE	2.47	12.42	3.50	90	5.110	-5.490	-12.400	11.800	8.744E+04	.521
COARSE	2.41	12.80	9.21	25	.416	-.100	-.205	.460	2.046E+06	.208
COARSE	2.41	12.80	9.21	45	.642	-.189	-.565	1.250	9.331E+05	.235
COARSE	2.41	12.80	9.21	70	2.830	-1.670	-2.240	4.260	2.383E+05	.311
COARSE	2.41	12.80	9.21	90	5.420	-2.050	-5.420	7.620	1.288E+05	.321
COARSE	2.43	12.99	5.79	25	.300	-.100	-.192	.444	2.377E+06	.231
COARSE	2.43	12.99	5.79	45	.522	-.236	-.496	.576	1.490E+06	.364
COARSE	2.43	12.99	5.79	70	2.290	-1.160	-3.310	4.360	2.457E+05	.366
COARSE	2.43	12.99	5.79	90	7.850	-5.430	-13.800	11.901	7.645E+04	.490
COARSE	2.47	12.42	3.50	25	.372	-.113	-.181	.344	2.457E+06	.241
COARSE	2.47	12.42	3.50	45	.574	-.375	-.853	.970	1.022E+06	.422
COARSE	2.47	12.42	3.50	70	3.150	-2.670	-6.460	5.380	1.728E+05	.526
COARSE	2.47	12.42	3.50	90	28.800	-28.000	-61.600	57.300	1.725E+04	.515

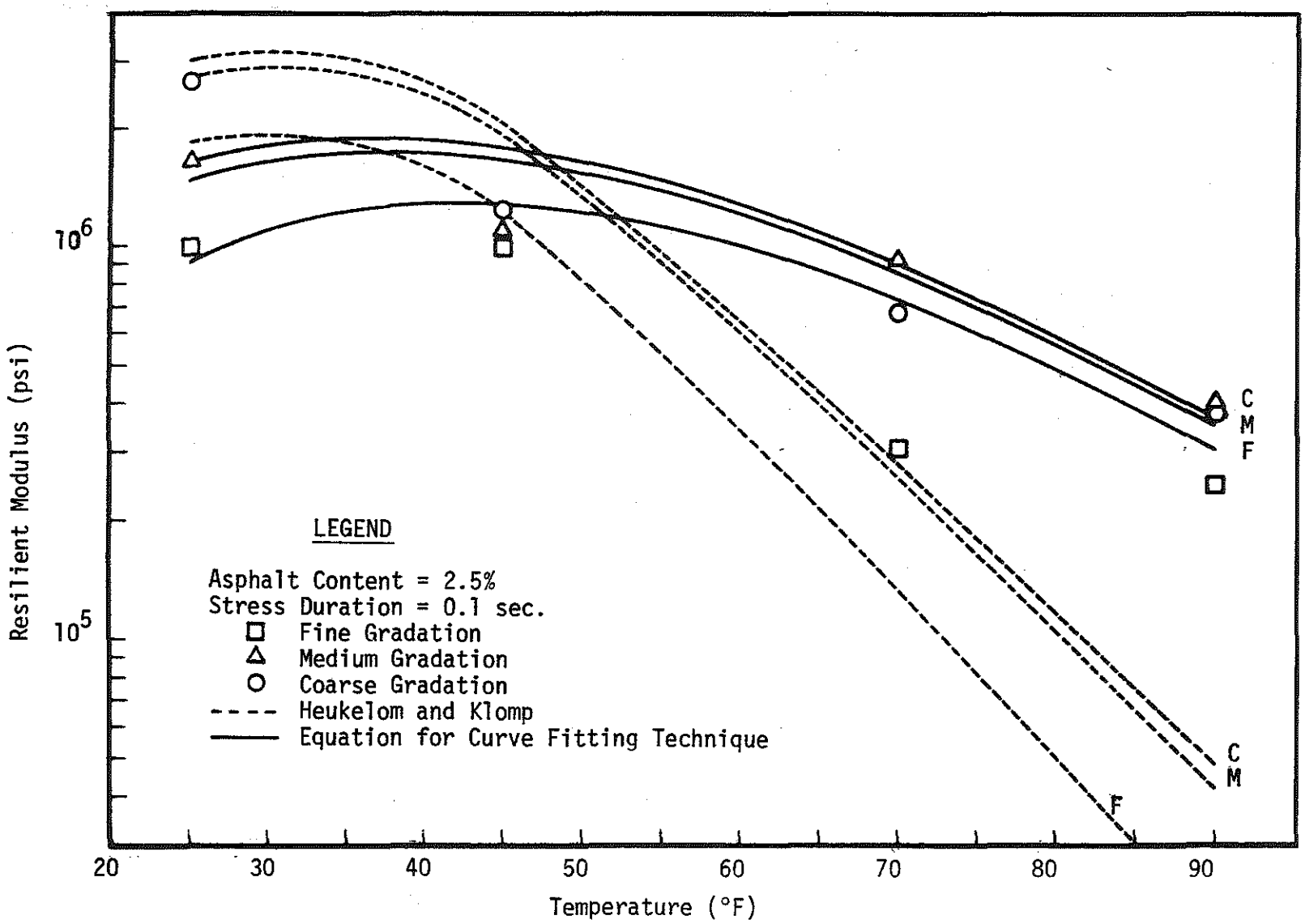

FIGURE 6.11 RESILIENT MODULUS COMPUTED FROM TEST DATA, THE REGRESSION EQUATION, AND HEUKELOM AND KLOMP FOR ASPHALT CONTENT OF 2.5%, (47).

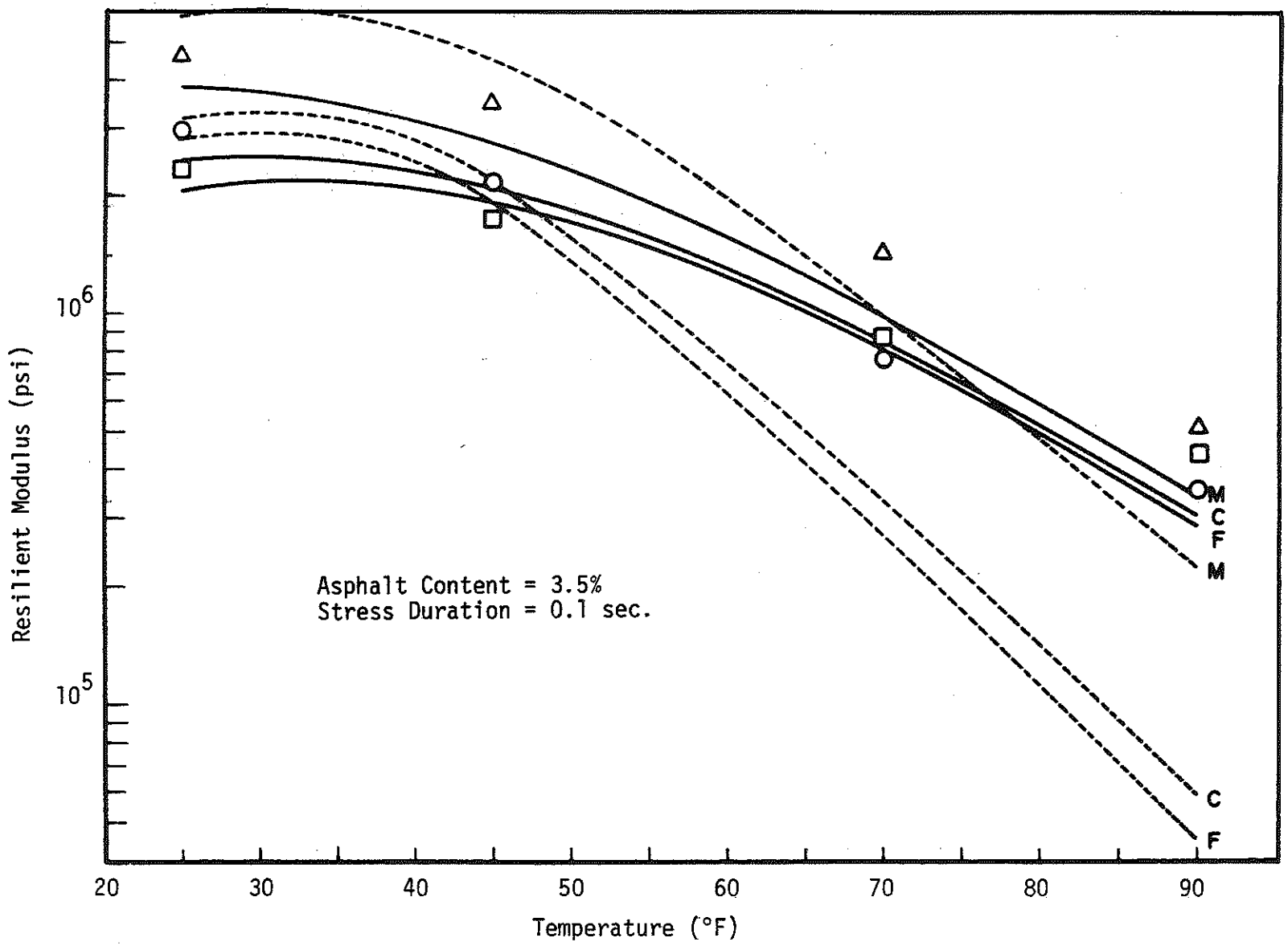

FIGURE 6.12 RESILIENT MODULUS COMPUTED FROM TEST DATA, THE REGRESSION EQUATION, AND HEUKELOM AND KLOMP FOR ASPHALT CONTENT OF 3.5%, (47).

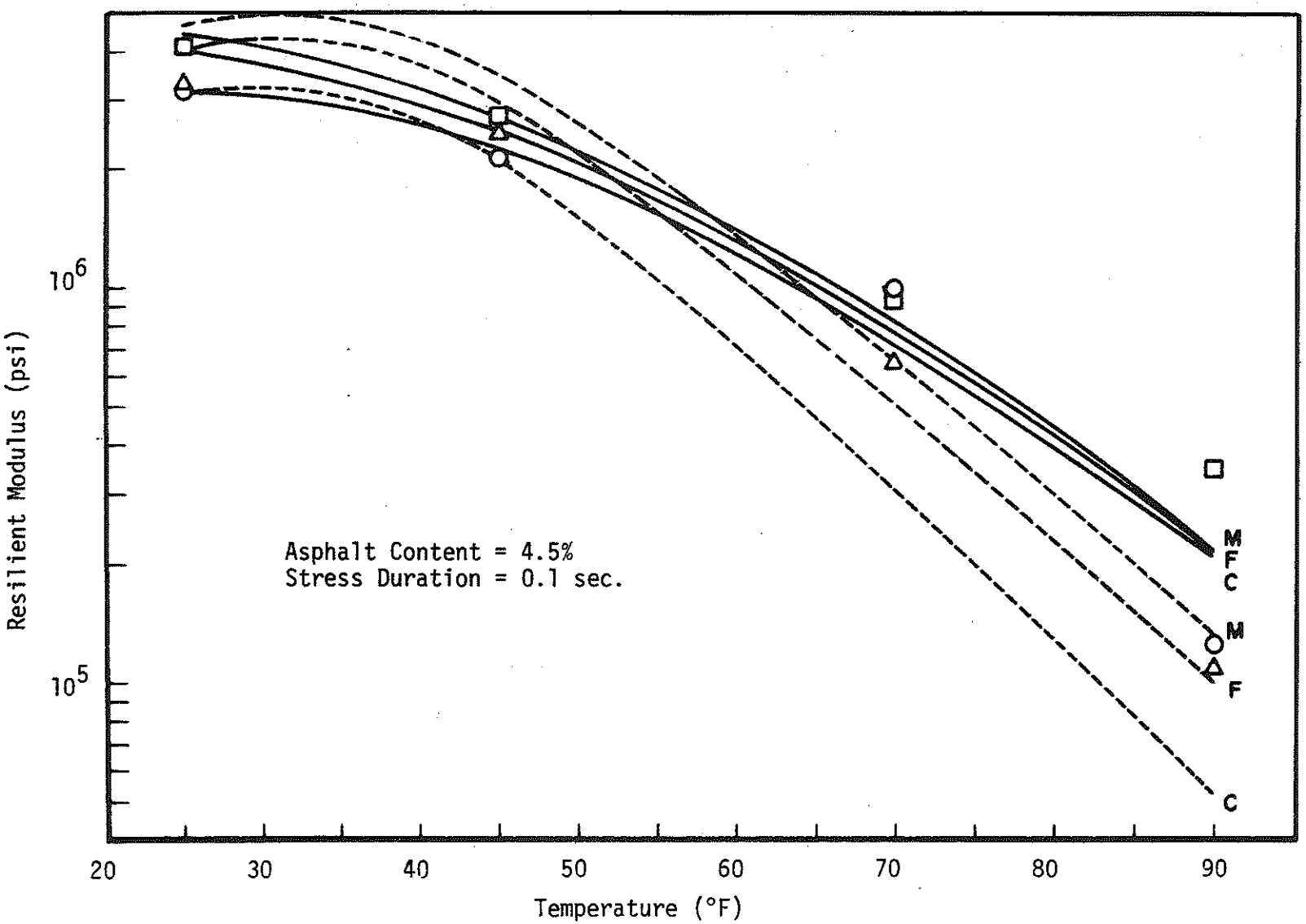

FIGURE 6.13 RESILIENT MODULUS COMPUTED FROM TEST DATA, THE REGRESSION EQUATION, AND HEUKELOM AND KLOMP FOR ASPHALT CONTENT OF 4.5%, (47).

It should be noted that the best agreement between the different methods occurred at low asphalt contents.

3. FLEXURAL FATIGUE TEST ON ASPHALT TREATED MATERIALS

Mitry (36) performed beam flexure tests on asphalt concrete specimens taken from the surface layer of a model pavement section. The sample conditions and the test results are summarized as follows:

average density of the mix	145 pcf
specimens consisted of penetration asphalt cement of	85 - 100
beam dimensions	14 inches long 1.5 inches wide 1.5 inches deep
test temperatures	45, 52.5, and 60°F
load frequency	20 cycles/minute
load duration	0.1 second
applied stress sequence	30 cycles at 100 psi 30 cycles at 125 psi 30 cycles at 100 psi . . . . . . until fracture
the stiffness modulus values for different temperatures	Table 6.24

Kallas and Puzinauskas (32) tested larger numbers of different mixes (see Table 6.25) at a temperature of 70°F, with the exception of the laboratory study mix which was also tested at 55 and 85°F. Stresses ranged from 200 to 400 psi for tests at 55°F, from 100 to 300 psi for tests at 70°F, and from 50 to 200 psi for tests at 85°F. The asphalt beams were 15 inches long, 3.5 inches deep, and 3.25 inches in width. The load frequency was 12 cycles per minute and its duration was 0.1 second. Table (6.26) provides a list of the flexural test data including values of the stiffness modulus, and number of cycles to fracture for each of the mixes tested.

A relationship, least squares regression equation, was found between the initial bending strain, ε, and the number of cycles to fracture, N_f. This relationship is such

$$N_f = K_1 (1/\varepsilon)^{n_1} \qquad (6.1)$$

in which, K_1 = constant dependent on the mix

n_1 = the slope of the regression line on a logarithmic scale plot.

TABLE 6.24 VARIATIONS OF STIFFNESS MODULUS WITH TEMPERATURE OF ASPHALT CONCRETE BEAM SPECIMENS, (36).

Temperature of Testing, in °F	45	52.5	60
Specimen No.	Stiffness Modulus, (psi)		
1	550,000	358,500	209,000
2	376,500	260,000	151,700
3	367,500	254,000	143,000
4	374,000	220,000	111,500
Average	414,500	273,100	153,800

TABLE 6.25 PROPERTIES OF MIXTURES, ASPHALTS, AND AGGREGATES, (32).

Project Location	Mix	Asphalt Content (%)	Asphalt Penetration 77°F, dmm	Asphalt Viscosity		Specifig Gravity of Aggregate[a]			
				60°F Poises	140°F poises	Bulk		Apparent	
						Coarse	Fine	Coarse	Fine
Colorado	A.C. Surface	5.6	57	19.1×10^6	2.84×10^3	2.617	2.588	2.658	2.662
	A.C. Base	5.6	57	19.1	2.84	2.593	2.588	2.646	2.640
	H.S. Sand Base	8.0	57	19.1	2.84		2.601		2.648
	L.S. Sand Base	8.6	57	19.1	2.84		2.605		2.647
Ontario	A.C. Surface	5.7	84	7.85	1.76	3.166	2.652	3.202	2.727
California	A.C. Base	5.2	65	11.3	2.50	2.607	2.581	2.678	2.686
	A.T. Base-Sp.	5.7	65	11.3	2.50	2.526	2.540	2.674	2.672
Washington State Univ.	A.C. Surface	5.2	90	5.25	1.22	2.884	2.651	3.018	2.781
Test Track-Ring 2	A.T. Base	3.0	59	16.0	2.68	2.713	2.669	2.723	2.638
Lab. Study	A.C. Asph. A	6.0	84	7.2	2.67	2.691	2.654	2.763	2.710

[a] Determined by ASTM test methods C127 and C128.

TABLE 6.26 FLEXURAL FATIGUE DATA FOR ASPHALT PAVING MIXES, (32).

Project Location	Mix	Test Temperature deg F	Stress, psi	Fracture Life, N_f	Initial Stiffness Modulus, psi	Initial Strain, μ in./in.	Bulk Specific Gravity	Air Voids, %
Colorado	A.C. Surface	70	278	10	1.27×10^5	2185	2.287	5.2
			254	390	1.15	2198	2.293	4.8
			228	460	1.14	1985	2.285	5.2
			197	840	1.34	1463	2.290	5.0
			185	1110	1.60	1155	2.290	5.0
			165	4275	2.87	573	2.292	4.9
			137	7320	2.22	615	2.289	5.1
			115	17580	2.78	459	2.285	5.2
			91	127500	3.15	287	2.285	5.2
Colorado	A.C. Base	70	255	510	1.23×10^5	2083	2.278	5.0
			243	925	2.17	1120	2.283	4.7
			217	875	1.49	1454	2.287	4.5
			189	3140	2.41	786	2.282	4.7
			168	4115	2.09	806	2.280	4.9
			144	6010	2.47	590	2.280	4.9
			119	30625	2.76	432	2.283	4.7
			96	89970	3.26	275	2.281	4.8
Colorado	L.S. Sand Base	70	191	20040	2.83×10^5	675	2.200	5.0
			144	64900	3.45	421	2.211	6.1
			99	439800	3.78	261	2.211	6.1
Colorado	H.S. Sand Base	70	200	10450	2.95×10^5	679	2.133	8.8
			101	263600	3.00	336	2.169	7.4

TABLE 6.26 CONTINUED

Project Location	Mix	Test Temperature deg F	Stress, psi	Fracture Life, N_f	Initial Stiffness Modulus, psi	Initial Strain, μ in./in.	Bulk Specific Gravity	Air Voids, %
Ontario	A.C. Surface	70	274	462	1.12×10^5	2445	2.489	4.3
			255	769	1.04	2465	2.489	4.3
			237	1345	1.30	1828	2.496	4.0
			212	2715	1.55	1365	2.499	4.0
			200	2505	1.67	1210	2.491	4.3
			174	7015	1.80	966	2.494	4.1
			150	17050	1.72	868	2.504	3.7
			124	16965	1.74	710	2.492	4.2
			98	144381	1.82	538	2.414	4.1
California	A.T. Base-Sp.	70	306	35	0.97×10^5	3152	2.009	16.4
			294	75	1.09	2613	2.025	15.8
			265	100	0.83	2995	2.020	16.0
			233	340	1.11	2101	2.028	15.6
			190	294	0.83	2296	2.016	16.0
			152	970	1.23	1273	2.019	16.0
			125	1630	1.15	1089	2.005	16.5
			103	3573	1.18	873	2.017	16.1
California	A.C. Base	70	265	269	0.75×10^5	3508	2.218	8.2
			287	169	1.38	2085	2.227	7.9
			244	328	1.41	1732	2.234	7.6
			222	332	1.28	1725	2.210	8.5
			199	891	1.36	1459	2.217	8.3
			179	1820	1.88	953	2.210	8.5
			154	3335	1.80	856	2.230	7.7
			127	10675	1.95	649	2.213	8.4
			112	23700	2.02	554	2.201	9.0

Figures (6.14) through (6.18) illustrate this relationship for several different mixes. Figure (6.19) shows that the slope of the regression line, n_1 in equation (6.1), is dependent upon the test temperature. The values of the constants K_1 and n_1, their estimated standard error, and the correlation coefficients for different mixes are listed in Table (6.27). A similar relationship was also noted between bending stresses, σ, and N_f

$$N_f = K_2 \ (1/\sigma)^{n_2} \qquad (6.2)$$

in which, K_2 = constant dependent on the mix

n_2 = the slope of the regression line on a logarithmic scale plot.

Figures (6.20) and (6.21) show this relation and its dependence upon the test temperature. Table (6.28) provides a list of values of the constants K_2 and n_2 along with the estimated standard error and the correlation coefficients.

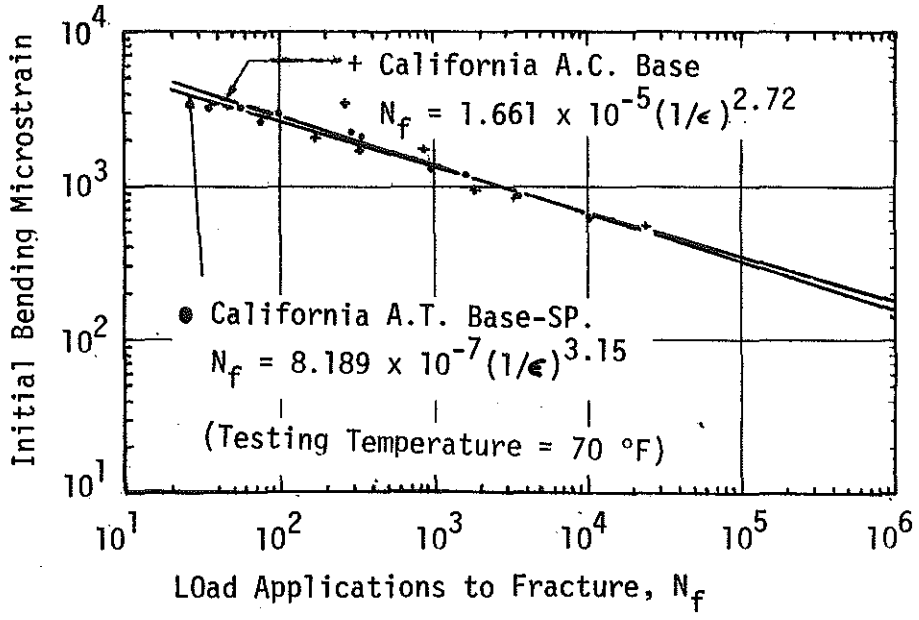

FIGURE 6.14 STRAIN-FRACTURE LIFE FATIGUE RESULTS FOR CALIFORNIA ASPHALT CONCRETE AND ASPHALT TREATED BASE MIXES, (32).

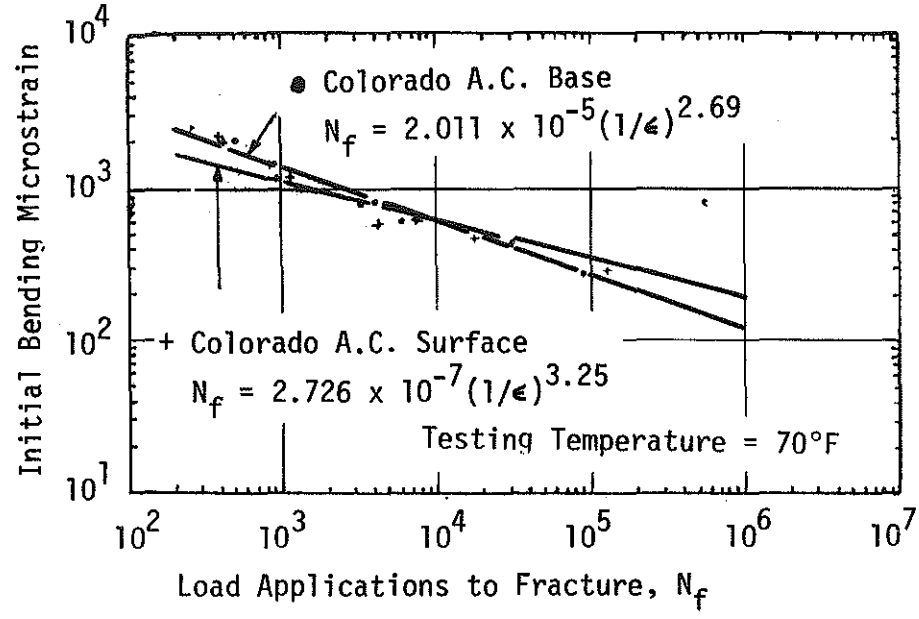

FIGURE 6.15 STRAIN-FRACTURE LIFE FATIGUE RESULTS FOR COLORADO ASPHALT CONCRETE BASE AND SURFACE MIXES, (32).

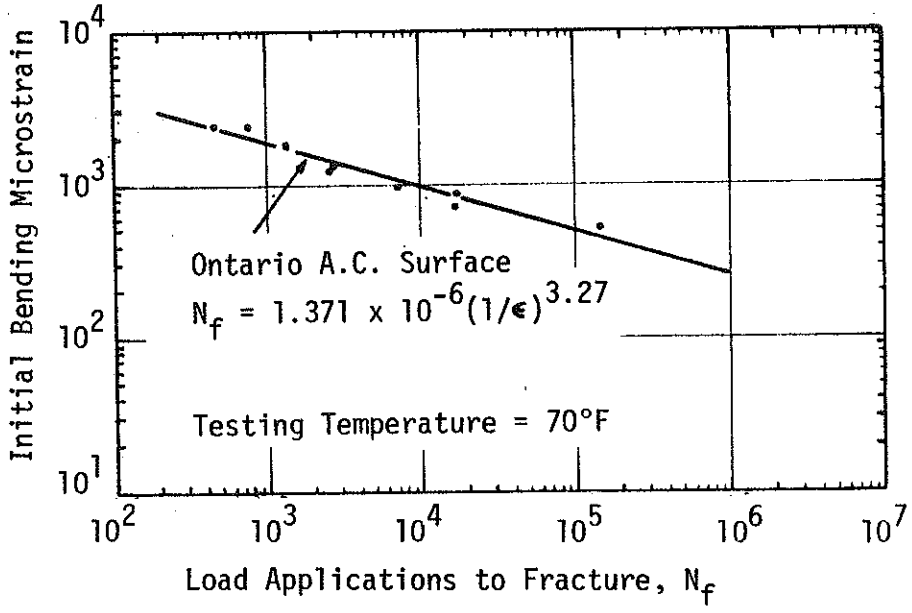

FIGURE 6.16 STRAIN-FRACTURE LIFE FATIGUE RESULTS FOR ONTARIO ASPHALT CONCRETE SURFACE MIX, (32).

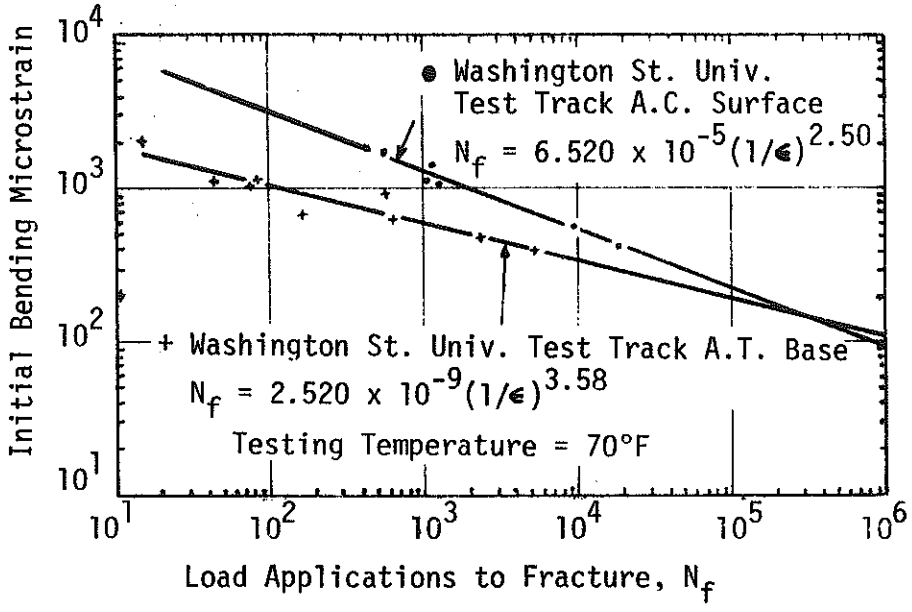

FIGURE 6.17 STRAIN-FRACTURE LIFE FATIGUE RESULTS FOR WASHINGTON STATE UNIVERSITY TEST TRACK ASPHALT CONCRETE SURFACE AND ASPHALT TREATED MIXES, (32).

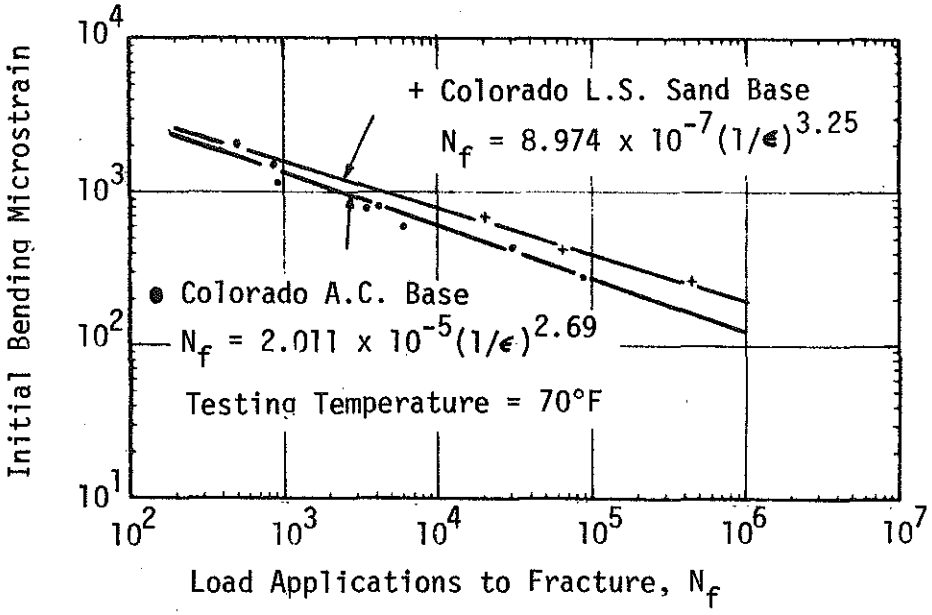

FIGURE 6.18 STRAIN-FRACTURE LIFE FATIGUE RESULTS FOR COLORADO ASPHALT CONCRETE AND LOW STABILITY SAND ASPHALT BASE MIXES, (32).

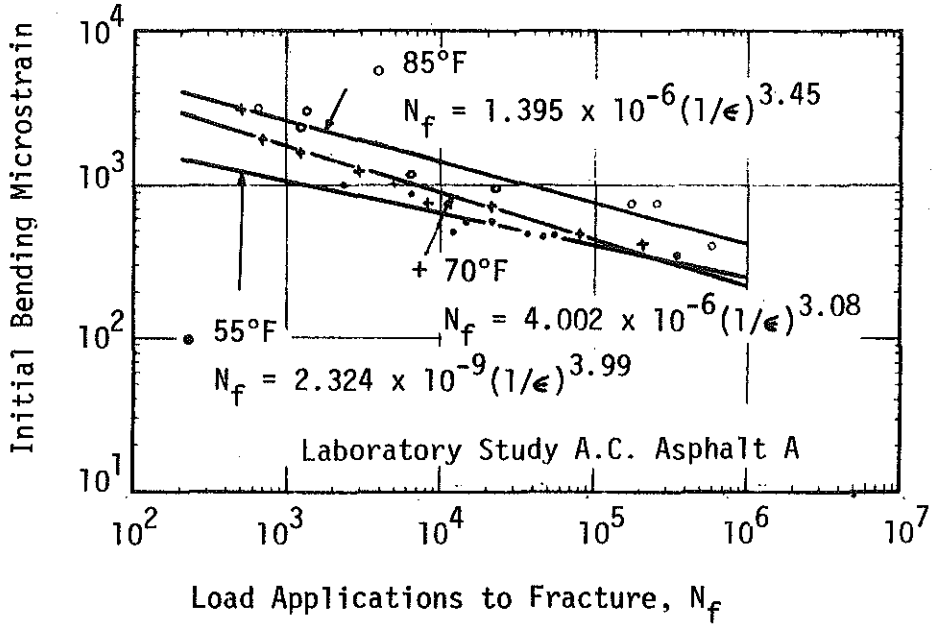

FIGURE 6.19 STRAIN-FRACTURE LIFE FATIGUE RESULTS FOR VARIOUS TEMPERATURES FOR LABORATORY STUDY OF ASPHALT CONCRETE MIX, (32).

TABLE 6.27 CONSTANTS, CORRELATION COEFFICIENTS, AND STANDARD DEVIATION ERRORS FOR LEAST SQUARES REGRESSION $N_f = K_1 (1/\varepsilon)^n$ FOR ASPHALT PAVING MIXES, (32).

Project Location	Mix	Number of Specimens	Temperature, deg F	Constant, K_1	Constant, n_1	Correlation Coefficient	Standard Deviation Error
Colorado	A.C. Surface	9	70	2.73×10^{-7} 2.73×10^{-7}	3.25	0.91	0.52
Colorado	A.C. Base	8	70	2.01×10^{-5} 2.01×10^{-5}	2.69	0.98	0.18
Colorado	L.S. Sand Base	3	70	8.97×10^{-7}	3.25	0.99	0.13
Colorado	H.S. Sand Base	2	70	2.82×10^{-11}	4.60	....	....
Ontario	A.C. Surface	9	70	1.37×10^{-6}	3.27	0.97	0.21
California	A.T. Base-Sp.	8	70	8.19×10^{-7}	3.15	0.97	0.19
California	A.C. Base	9	70	1.66×10^{-5}	2.72	0.93	0.29
Washington State Univ. Test Track-Ring 2	A.C. Surface	6	70	6.52×10^{-5}	2.50	0.98	0.13

TABLE 6.27 CONTINUED

Project Location	Mix	Number of Specimens	Temperature, deg F	Constant, K_1	Constant, n_1	Correlation Coefficient	Standard Deviation Error
Washington State Univ. Test Track-Ring 2	A.T. Base	9	70	2.52×10^{-9}	3.58	0.93	0.32
Laboratory Study	A.C. Asph. A	9	55	2.32×10^{-9}	3.99	0.92	0.26
Laboratory Study	A.C. Asph. A	9	70	4.00×10^{-9}	3.08	0.97	0.24
Laboratory Study	A.C. Asph. A	8	85	1.40×10^{-6}	3.45	0.96	0.35
Combined		58	70	1.70×10^{-5}	2.66	0.78	0.58

[a] N_f = dependent variable

[b] All A.C. and A.T. surface and base mixes except L.S. and H.S. sand bases, and A.C. laboratory study mixes.

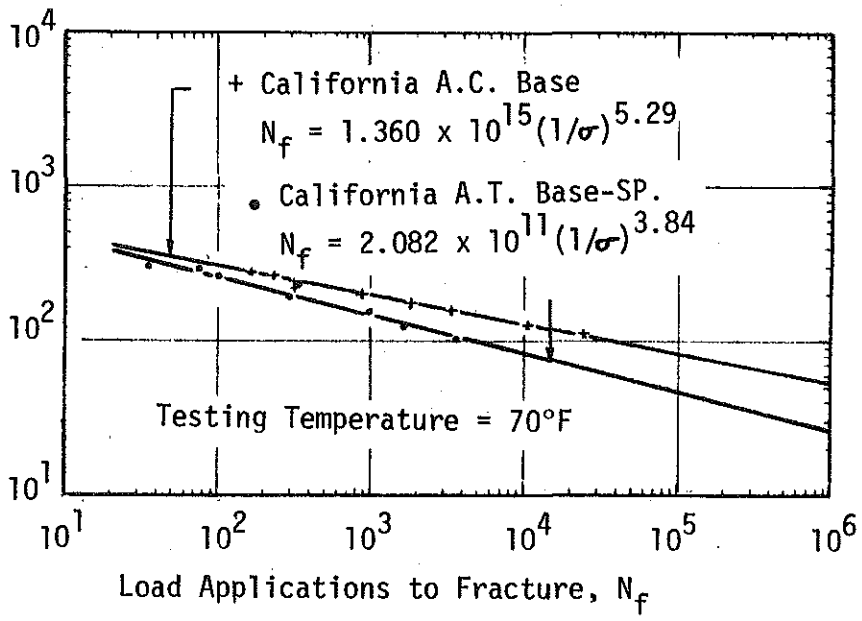

FIGURE 6.20 STRESS-FRACTURE LIFE FATIGUE RESULTS FOR CALIFORNIA ASPHALT CONCRETE AND ASPHALT TREATED BASE MIXES, (32).

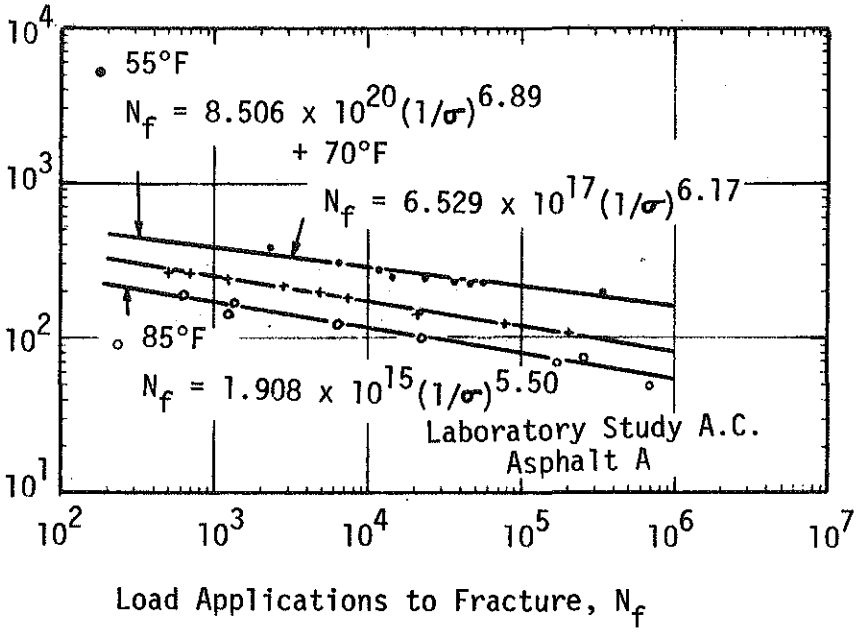

FIGURE 6.21 STRESS-FRACTURE LIFE FATIGUE RESULTS FOR VARIOUS TEMPERATURES FOR LABORATORY STUDY OF ASPHALT CONCRETE MIX, (32).

TABLE 6.28 CONSTANTS, CORRELATION COEFFICIENTS, AND STANDARD DEVIATION ERRORS FOR LEAST SQUARES REGRESSION EQUATION $N_f = K_2 (1/\sigma)^{n}$ FOR ASPHALT PAVING MIXES, (32).

Project Location	Mixes	Number of Specimens	Temperature, deg F	Constant, K_2	Constant n_2	Correlation Coefficient	Standard Deviation Error
Colorado	A.C. Surface	9	70	3.90×10^{18}	6.87	0.95	0.40
Colorado	A.C. Base	8	70	1.02×10^{15}	5.11	0.99	0.14
Colorado	L.S. Sand Base	3	70	9.04×10^{14}	4.68	0.99	0.05
Colorado	H.S. Sand Base	2	70	7.07×10^{14}	4.71	....	....
Ontario	A.C. Surface	9	70	2.08×10^{15}	5.16	0.99	0.15
California	A.T. Base-Sp.	8	70	2.08×10^{11}	3.84	0.98	0.16
California	A.C. Base	9	70	1.36×10^{15}	5.29	0.99	0.10
Washington State Univ. Test Track-Ring 2	A.C. Surface	6	70	7.53×10^{14}	5.21	0.98	0.12

TABLE 6.28 CONTINUED

Project Location	Mixes	Number of Specimens	Temperature, deg F	Constant, K_2	Constant n_2	Correlation Coefficient	Standard Deviation Error
Washington State Univ. Test Track-Ring 2	A.T. Surface	6	70	7.88×10^{15}	5.93	0.94	0.31
Laboratory Study	A.C. Asph. A	9	55	8.51×10^{20}	6.89	0.94	0.22
Laboratory Study	A.C. Asph. A	9	70	6.52×10^{17}	6.17	1.00	0.07
Laboratory Study	A.C. Asph. A	9	85	1.91×10^{15}	5.50	0.98	0.26
Combined		58	70	4.28×10^{15}	5.55	0.86	0.47

[a] N_f = dependent variables.

[b] All A.C. and A.T. surface and base mixes except L.S. and H.S. sand base, and A.C. laboratory study mixes.

CHAPTER 7

SAMPLE PREPARATION, TEST PROCEDURES AND EQUIPMENT

1. SAMPLE PREPARATION

A vast number of methods have been employed by researchers for the preparation of specimens for triaxial testing. A number of them are presented here, but these in no way are meant to represent the best or recommended way of sample preparation. Indeed, the number of sample preparation methods is as many as the various forms of apparatus in which samples are tested.

Two different methods were noted for the compaction of fine-grained soils: one using static compaction, the other employs a dynamic compaction method. Ahmed and Larew (21) conducted tests on silty clays and used a method of static compaction as previously employed by Leonards in 1955. Soil cakes were prepared in steel molds which were 3.5 inches in height and 20 inches in diameter. The soil in these molds were compacted with a static load, then specimens were obtained and sealed in aluminum foil and wax before testing. Tanimoto and Nishi (46) used the CBR compaction apparatus for the preparation of silty clay soils which they tested. The specimens were made by compacting 5 equal layers with 10 blows of the CBR hammer per layer. The samples were compacted to a low degree of saturation so as to retain the desired flocculated particle structure.

Impact and vibration techniques are most often used for compaction of more coarsely grained soils. Haynes and Yoder (26) and Mitry (36) employed impact methods for tests conducted on sands. Haynes and Yoder used a 5.5 lbs hammer falling 12 inches but did not specify layer numbers or sample size. Mitry compacted his sand specimens in 12 equal layers. The final sample size was 6.5 inches in height and 3.8 inches in diameter. To insure a more uniform sample density, the number of blows to each layer was increased as each was added, the first layer receiving 3 blows, and second layer 4 blows, and so on.

Hicks (27) employed 3 different methods to achieve 3 different degrees of saturation. For dry specimens, vibration compaction was used. The soil was placed in layers into a split mold, 3.19 inches in diameter and 8 inches in height. Vibrations were induced by the insertion of an air hammer which reacted against the rigid cap placed on the soil surface. All layers were

vibrated for 15 seconds. Partially saturated samples were prepared in the same manner, with the only exception being the addition and thorough mixing of water with oven-dried materials just prior to compaction. Saturated samples likewise were compacted using vibration techniques. Once completed, the samples were mounted in the cell, and de-aired water was allowed to percolate up through the sample, such that it took 30 minutes to fill the cell. Once the air was removed, the sample was placed under a vacuum all night. Back pressure techniques were also used to insure complete saturation.

Mitry (36) found the use of the air hammer unsatisfactory for course aggregates. Initially, an air hammer was used, but this lead to the crushing of soil grains and punctures in the membrane which encased the sample during testing. Alternatively, the soils were placed in steel molds and vibrated on a shaking table. The specimens were compacted in 2 equal layers, with each being vibrated for 15 seconds. A 15 lbs. weight was placed on top during the vibration.

Allen and Thompson (22) prepared specimens of coarse aggregate on the triaxial chamber base plate by impact methods. They were formed using a 6 inch diameter and 12 inch tall split mold. The hammer had a striking face 2 inches in diamter, weighed 10 lbs. and dropped 18 inches. The specimens were encased in 2 latex membranes to prevent leakage, which proved successful.

The most complete description of the preparation of asphalt treated materials is given by Terrel et al (47). These specimens were prepared using a mechanical mixer and the Triaxial Institute kneading compactor. First, the asphalt and aggregate were heated to 300^{o}F and mixed mechanically. This mix cured for 15 hours at 140^{o}F, and was then placed in plastic bags for storage at room temperature until compaction. The samples were compacted in 3 layers, with the bottom layer receiving 130 tamps, the middle 140, and the top layer getting 150 tamps at 500 psi. After this, the compacted specimens were placed in the oven at 140^{o}F for 90 minutes. A static pressure of 1000 psi was then applied to the samples at the rate of 0.05 inches per minute, followed by storage in plastic bags at 40^{o}F until testing.

Hicks (27) obtained specimens of asphalt treated materials from model pavement sections using a diamond core barrel of 4 inches in diameter. These

samples were trimmed to a height of 8 inches before the installation of strain gages. These gages were 2.5 inches long and were bonded near the middle of the sample. Two were oriented axially at opposite sides, and two were placed circumferentially, also at opposite sides.

Seed et al (43) conclude that even though estimates must be made for the void ratio, degree of saturation and density expected in the field, these can be duplicated with good accuracy in the laboratory. The selection of a representative stress condition still remains as the major problem in materials characterization.

2. TEST PROCEDURE

Van Til et al (50) have suggested the following procedure for the resilient modulus test:

2.1. Apparatus

a) Loading Piston.

b) Triaxial cell of suitable size.

c) Cyclic air supply.

d) An LVDT suitably mounted for measuring the deformation due to the applied load.

e) Controller to regulate speed of testing at frequences up 3 cps.

f) Load cell.

g) Recording equipments.

h) Rubber membranes.

i) O-rings of suitable sizes.

2.2. Procedure

a) Measure and record weight and height of specimen.

b) Place suitable membrane around specimen.

c) Secure membrane to top and base caps with O-rings.

d) Place specimen with membrane in triaxial cell.

e) Apply predesignated confining pressure.

f) Apply the cyclic stress as desired.

g) Record applied load and deflection at the following number cycles: 10, 50, 500, 1000, 2000, 5000, 10,000, 20,000.

2.3. Calculations

From the data reported calculate the following:

a) Damping coefficient.

b) Resilient modulus.

c) Poisson's ratio.

For testing the resilient response of a single specimen of granular material at several different stresses, Kalcheff and Hicks (31) suggested the following sequence of stresses:

$\frac{\sigma_1}{2 \text{ psi}}$	$\frac{\sigma_1 - \sigma_3}{6 \text{ psi}}$
5	15
10	30
20	60
2	6
0	5

They have recommended a load duration time of 0.1 seconds and a frequency of 30 cycles per minute. Readings should be taken once the number of load applications at each stress condition reaches 150 to 200.

The Transportation Research Board has published a manual which outlines test preprations and procedures for various roadbed materials. Released in 1975, Special Report No. 162, entitled "Test Procedures for Characterizing Dynamic Stress-Strain Properties of Pavement Materials," includes specimen preparation processes, and testing procedures for all types of materials. Because of its value, it is presented in its entirety as Appendix A.

3. TEST EQUIPMENT

Very complex equipment systems have evolved for the characterization of roadbed materials. Among the components of these systems are the triaxial cell, the load application and control systems, the measurement and data acquisition systems and, in the case of asphalt mix testing, the temperature control systems. Investigators have witnessed the ever-increasing use of pneumatic loading systems first described by Seed and Fead in ASTM Special Technical Publication No. 154, 1959. The proving ring has been replaced by the load cell, and the strain gage by the LVDT. As an aid to future investigations, a description of some of the equipment systems used, with emphasis upon those components noted above, follows.

The loading system employed by Seed et al (43) is shown in Figure (7.1). This system operated by compressed air in separate tanks at the required pressure for the seating and peak applied loads. Using a 3-way solenoid

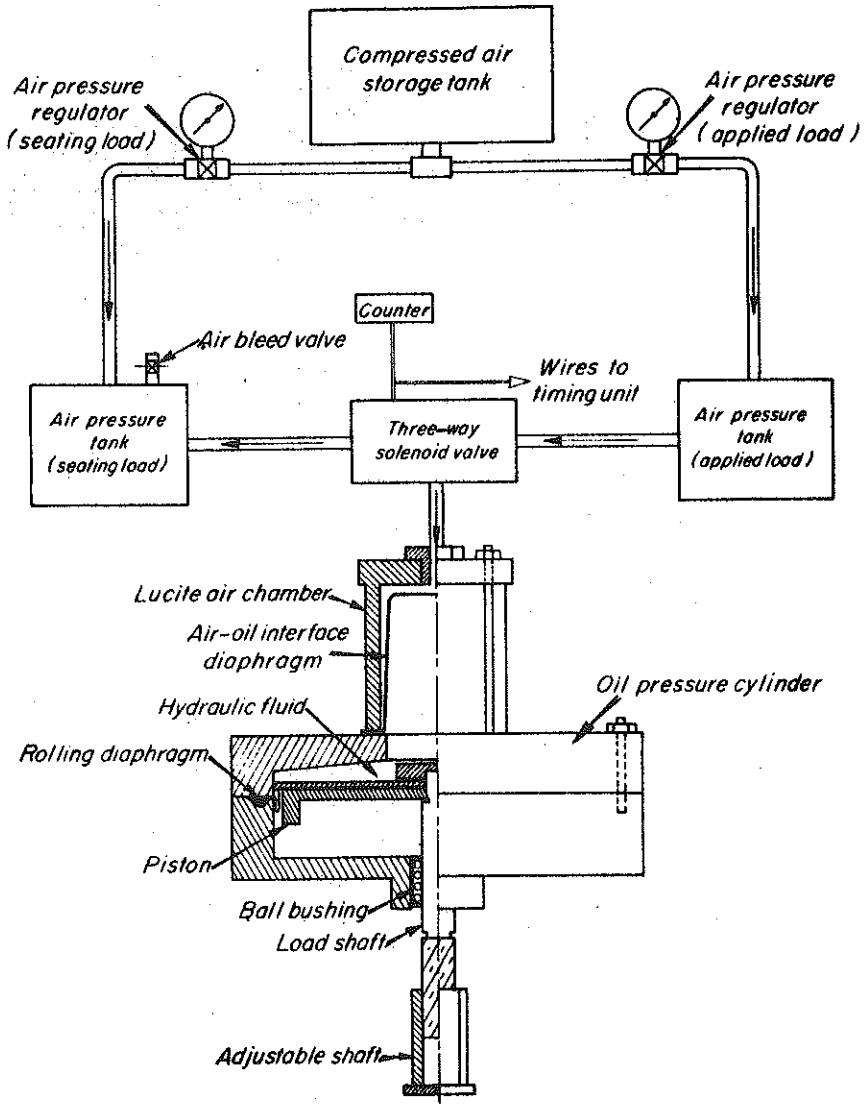

FIGURE 7.1 LARGE LOADING PISTON AND CONTROL MECHANISM, (43).

valve, the appropriate pneumatic pressure was supplied through a bellofram seal to oil above the main piston. A ball-bushing guide was used to reduce friction and a neoprene rolling diaphragm to prevent loss of oil. The peak load applied to the specimen was varied by regulating the air pressure, as recorded by the pressure gage. Loads up to 5 kips could be obtained with this system.

A pneumatic loading system was also used by Hicks (29). Axial and radial deformations were measured with LVDT's. Dual LVDT's were clamped onto each specimen outside the membrane to measure the radial strain at the quarter points and the axial strains over the middle 4 inches. Air was used as the cell "fluid", as the presence of the LVDT's and load cell inside the chamber ruled out the use of water. The circumferential clamps were held in place by light springs instead of rigid screws to permit free movement. Horizontal LVDT's were mounted on the clamps to measure the radial strain. Two Sanbron 595 DT 100 LVDT's were mounted between the clamps to measure the axial strain. A DC powered Serta model 200 pressure transducer was used in all tests. The pressure monitoring system is shown in Figure (7.2).

Terrel and Awad (47) conducted tests on asphalt mixes for the Washington State Highway Department. The axial loads were applied to test specimens by a closed-loop servo-hydraulic system made by MTS, with the following features:

1. stress or strain controlled loading
2. 12 kip capacity
3. a hydraulic power supply capable of 20 gpm at 300 psi
4. maximum stroke of 5 inches
5. frequency range of 0.001 to 1100 cps
6. 12 loading modes

The axial load was monitored by a load cell which was fixed to the upper side of the test specimen, inside the triaxial cell, to eliminate the effects of piston friction. This set-up is shown in Figure (7.3).

Figure (7.4) shows the system used to pulse the chamber pressure. The pressure is kept in two tanks (σ_3 and $\Delta\sigma_3$). The pressure σ_3 is equivalent to the in-situ lateral pressure and alternatively applied with $\Delta\sigma_3$, which corresponds to the total lateral pressure during the load pulse.

The triaxial cell provides continuous circulation of oil at a constant temperature, under the required pressure. The cell is shown in Figure (7.5).

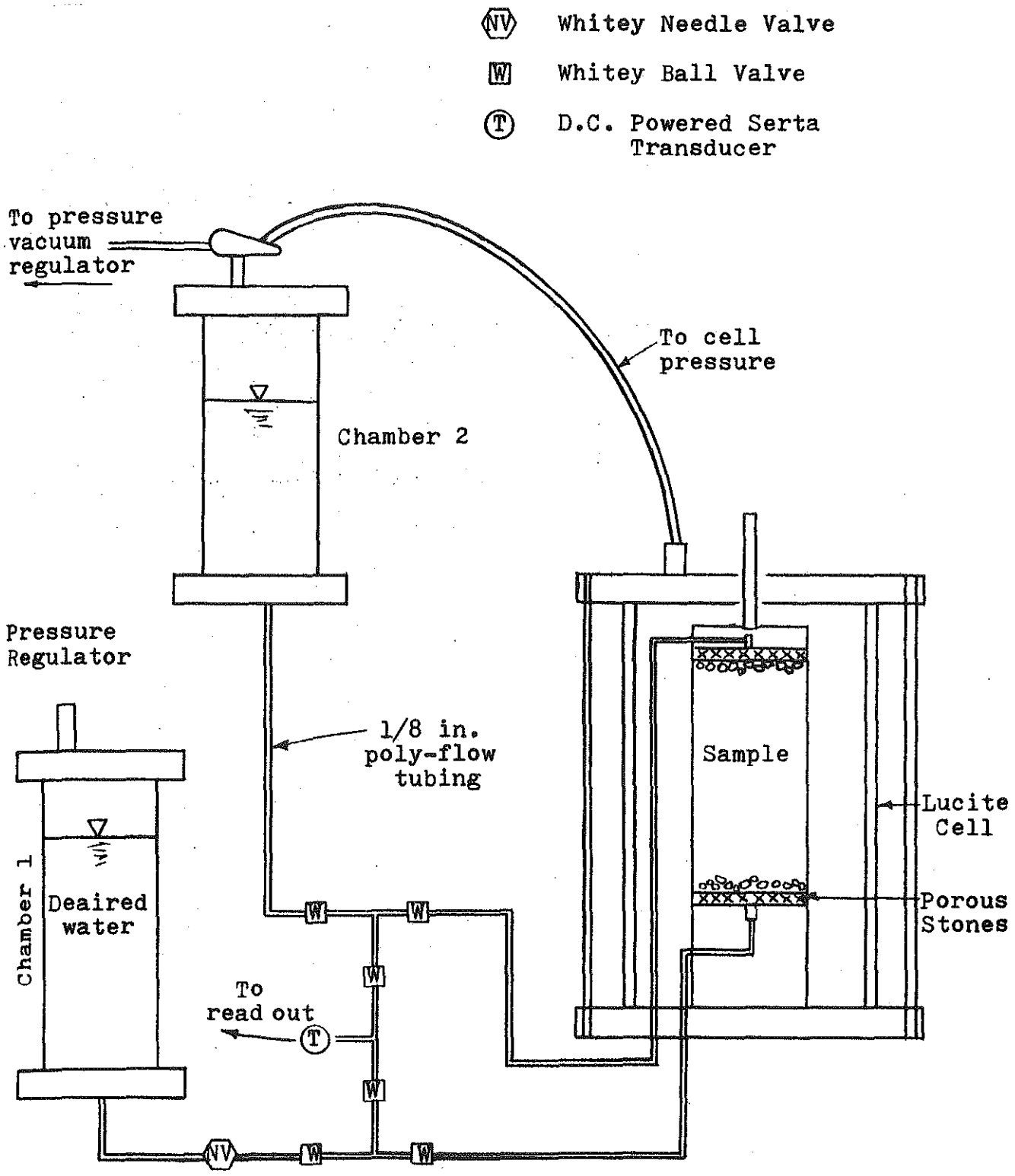

FIGURE 7.2 PORE PRESSURE MEASURING SYSTEM, (29).

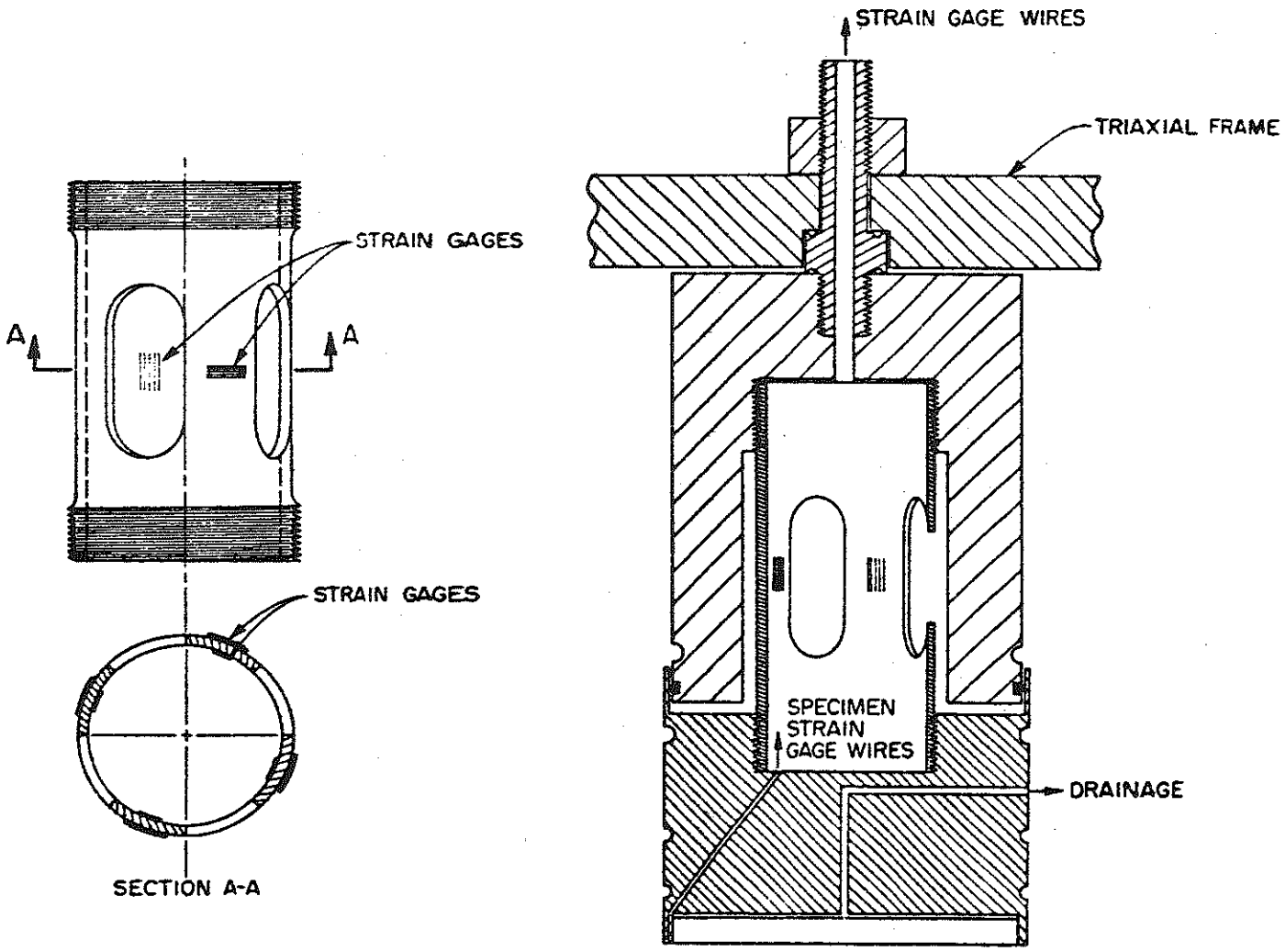

FIGURE 7.3 THE LOAD CELL USED INSIDE THE TRIAXIAL CHAMBER, (47).

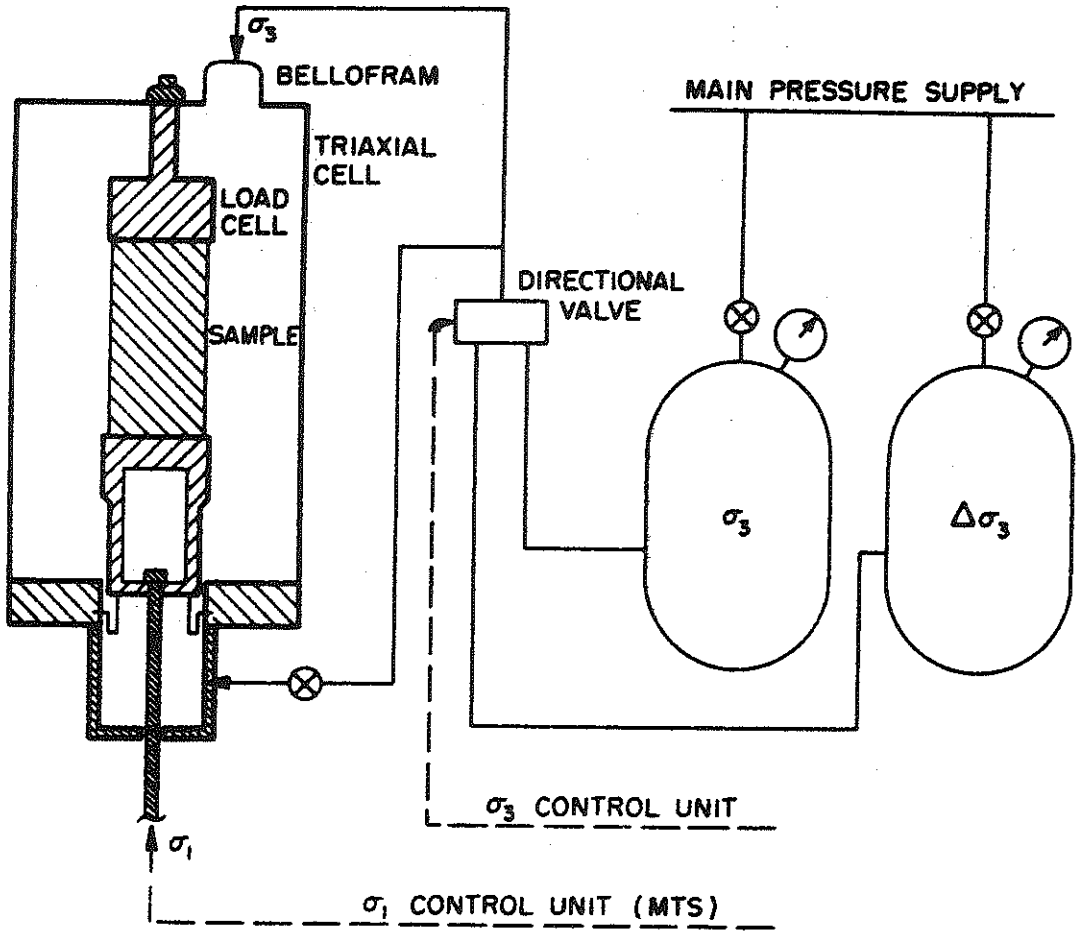

FIGURE 7.4 THE SYSTEM USED FOR PULSING THE CHAMBER PRESSURE, (47).

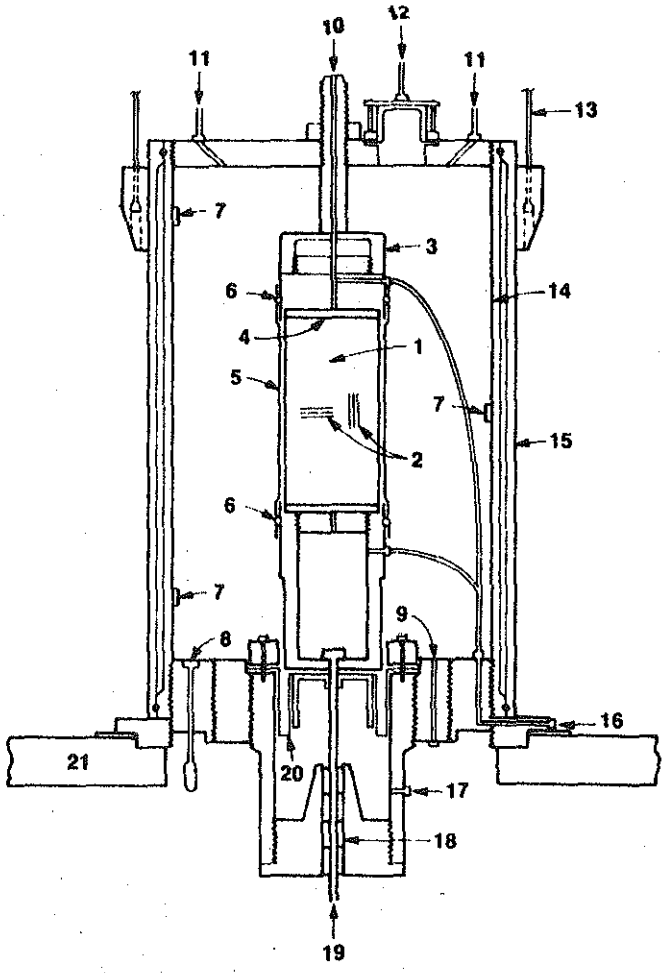

(1) 4 x 8 Inch Sample
(2) Strain Gages
(3) Controlling Load Cell
(4) Porous Stone
(5) Rubber Membrane
(6) O - Rings
(7) Temperature Sensors
(8) Pressure Cell
(9) Oil Circulation Outlet
(10) Outlet of Electric Wiring
(11) Oil Circulation Inlet
(12) Chamber Pressure (σ_3)
(13) Plastic Cylinder Lifting Device
(14) Aluminum Frame With Three Openings
(15) Plastic Cylinder
(16) Drainage Outlet
(17) Pressure (σ_3) Bottom Inlet
(18) Rectilinear Ball Bearings
(19) Axial Loads (MTS)
(20) Special Bellofram
(21) 2" Aluminum Platform

FIGURE 7.5 THE TRIAXIAL CHAMBER, (47).

This was accomplished by having the entire temperature control system under the same pressure. The heating tank, and the triaxial cell were equipped with belloframs, connected to two pressure reservoirs which provide two levels of pressure, static and pulsating.

The temperature control system used by Terrel and Awad is shown in Figure (7.6). It is a closed-loop system. The refrigerator and heating units worked opposite of each other to maintain a constant temperature in the tank. A centrifugal pump circulated the oil through the triaxial cell, where the temperature was measured by 3 sensors located at different elevations. The refrigerator and heat are activated by a thermostat to maintain a constant temperature. The temperature control system consisted of these items:

1. One H.P. Copelametic refrigeration unit using an R-12 refrigerant.
2. 4000 watt calrod merchant heater
3. Thermac power controller 6000, model D30.

Slippage between the rubber membrane and the specimen, and variations in output due to the circulating oil ruled out the use of LVDT's. Instead, two axial and two circumferential strain gages were used. SR4, A-1, wire gages, 0.75 inches long and M.M. EA-13-19CDK foil gages, 2 inches long proved satisfactory, though the 2 inch long gages were later selected for used. Other components of this system include:

1. A digital voltmeter, model 251-A
2. Tektronix - 564 memo-oscilloscope with 3A6 vertical amplifier and type 2B67 time base.
3. Dixson Southern 10-212 light beam ultra-violet oscilloscope recorder.
4. Daytronic 300D carrier amplifier with type 93 input module and type P output module.
5. Daytronic 870 data module.

Allen and Thompson (22) performed tests in which the triaxial chamber confining pressure was varied simultaneously with the axial load. This was done using a closed-loop testing system. Axial stress was applied through a hydraulic actuated piston. The chamber pressure was varied using a hydraulic actuated piston which reacted directly upon the chamber fluid, which in this case was water. Program input was provided by two function generators, one to the axial load, and one to the chamber pressure. Two were necessary to allow for the slight delay in the confining pressure pulse. This delay was caused by chamber fluid compression and friction

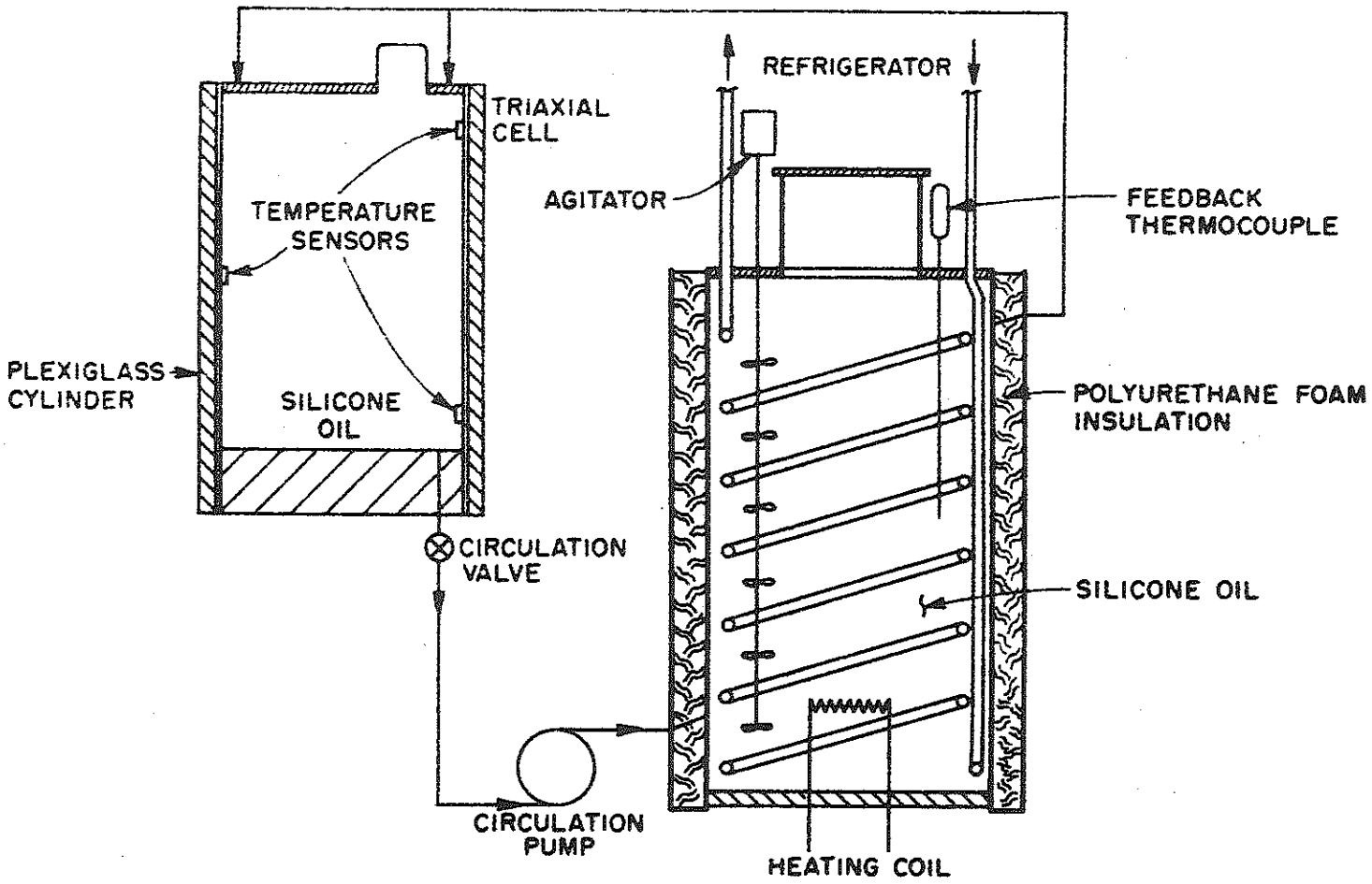

FIGURE 7.6 THE TEMPERATURE CONTROL SYSTEM, (47).

losses in the line. By delaying the axial load, it was possible to apply both pulses simultaneously.

The axial load was monitored by a load cell mounted on the test frame above the chamber. The chamber pressure was monitored by a pressure transducer located at the chamber base. Axial deformations were measured over the central half of the specimen by two optical trackers. Radial deformations were measured by sensors (4 inch diameter disk shaped coils of wire) that were mounted at midheight of the specimen and held in place by a 2 inch wide rubber strip. A dial gage mounted on top of the chamber, and an LVDT on the actuator of the test frame were used to measure non-recoverable and resilient deformations. All stress and deformation data were recorded on an 8-track oscillograph printer.

Morris and Haas (40) also employed an electrohydraulic closed-loop system for tests on asphalt mix specimens. Clear, additive free, mineral oil was used as the chamber fluid. Rubber membranes and O-rings were used to seal the specimen. Axial and lateral pressure systems consisted of hydraulic actuators and servovalves fed by a 70 gal/min, 300 psi hydraulic power supply. The axially loading actuator was 1-1/2 inches in diameter and had a 3 kip capacity.

The axial and lateral actuator systems were regulated independently by means of two servocontrollers. These compare the desired (command) and measured (feedback) load level signals, and produce an error signal which causes the actuator to stroke in the direction which reduces the error. Feedback signals for the axial and lateral pressures are obtained by a loadcell and a pressure transducer, respectively. The load cell is located inside the triaxial cell below the specimen to ensure that piston friction does not affect the load measurement.

Just as Allen and Thompson had found, Morris and Haas saw that the confining pressure pulse was delayed when the axial and lateral pulses were triggered together, so the axial pulse was delayed such that a simultaneous application of axial and lateral stress was obtained.

The temperature of the surrounding oil was maintained within $\pm 0.5^{\circ}F$ of desired values. This temperature control system consisted of 3 components:

1. Chromel heating element
2. Iron-constantin thermocouple
3. Indicating thermocouple controller

BIBLIOGRAPHY

1. ————————, "AASHO INTERIM GUIDE FOR DESIGN OF PAVEMENT STRUCTURES 1972", American Association of State Highway Officials, AASHO Committee on Design, Washington, D.C., 1972.

2. HIGHTER, W.H., "THE APPLICATION OF ENERGY CONCEPTS TO PAVEMENTS", Joint Highway Research Project, Purdue University and Indiana State Highway Commission, November 1972, No. 38.

3. YODER, E.J., and WITCZAK, M.W.,"PRINCIPLE OF PAVEMENT DESIGN", John Wiley and Sons, Inc., New York, 1975.

4. BOYER, R.E.,"PREDICTING PAVEMENT PERFORMANCE USING TIME DEPENDENT TRANSFER FUNCTIONS", Joint Highway Research Project, Purdue University and Indiana State Highway Commission, September 1972, No. 32.

5. BALADI, G.Y.,"INVARIANT PROPERTIES OF FLEXIBLE HIGHWAY PAVEMENTS", Ph.D. Thesis, Purdue University, December 1976.

6. SEED, H.B., CHAN, C.K., and LEE, C.E., "RESILIENCE CHARACTERISTICS OF SUBGRADE SOILS AND THEIR RELATION TO FATIGUE FAILURES IN ASPHALT PAVEMENTS", Proceedings, International Conference on the Structural Design of Asphalt Pavements, University of Michigan, 1962.

7. LARENCE, H.G., and LEONARDS, G.A.," A STRENGTH CRITERION FOR REPEATED LOADS", Proceedings of the Highway Research Board, Vol. 41, 1962.

8. RAO, H.A. BALEKRISHNA, "EVALUATION OF FLEXIBLE PAVEMENTS BY NONDESTRUCTIVE TESTS", Proceedings, Third International Conference on the Structural Design of Asphalt Pavements, London,1972.

9. GUILLEMIN, R. and GRAMSAMMER, J.C., "DYNAMIC NONDESTRUCTIVE TESTING OF PAVEMENTS IN FRANCE", Proceedings, Third International Conference on the Structural Design of Asphalt Pavements, London, 1972.

10. WISEMAN, GDALYAH, "THE INTERPRETATION OF SURFACE DEFLECTION MEASUREMENTS USING THE MODEL OF AN INFINITE PLATE ON AN ELASTIC FOUNDATION", Symposium

on Nondestructive Test and Evaluation of Airport Pavements, Vicksburg, Mississippi, November 1975.

11. WEISS, R.A., "NONDESTRUCTIVE VIBRATORY TESTING OF AIRPORT PAVEMENTS", Vol. II, Report No. FAA-RD-73-205-II, United State Department of Transportation, Federal Highway Administration, Washington, D.C. April 1975.

12. HAAS, R., "SURFACE EVALUATION OF PAVEMENTS", State of the Art, Report No. FHWA-RD-74-60, Transportation Research Board, Washington, D.C., June 1970.

13. GREEN, J.L., and HALL, J.W., "NONDESTRUCTIVE VIBRATORY TESTING OF EVALUATION METHODOLOGY AND PROCEDURE", Vol. 1, Report No. FAA-RD-73-205-1, United States Department of Transportation, Federal Aviation Administration, Washington, D.C., September 1975.

14. HALL, J.W., "NONDESTRUCTIVE TESTING OF FLEXIBLE PAVEMENTS - A LITERATURE REVIEW", Technical Report, AFWL-TR-68-147, Kirtland Air Force Base, New Mexico, May 1970.

15. NAIR, K., "PAVEMENT EVALUATION BY WAVE PROPAGATION", ASCE, Vol. 97, Note 1, February 1971.

16. ————, "SOIL MANUAL FOR DESIGN OF ASPHALT PAVEMENT STRUCTURE", The Asphalt Institute, 2nd. Edition, 3rd. Printing, February 1969.

17. BURMISTER, D.M., "EVALUATION OF PAVEMENT SYSTEMS OF THE WASHO ROAD TEST BY LAYERED SYSTEM METHODS", Highway Research Board, Bulletin 177, 1958.

18. ————, "DETERIORATING AIRPORT PAVEMENTS SPUR EFFORT TO HEAD OFF CRISIS", Engineering News Record, November 1971.

19. ————, "DEVELOPMENT OF CBR FLEXIBLE PAVEMENT DESIGN METHODS FOR AIRFIELDS", Symposium, Transactions, American Society of Civil Engineering, Vol. 115, 1950.

20. CASAGRANDE, A., and SHANNON, W.L., "RESEARCH ON STRESS-DEFORMATION AND STRENGTH CHARACTERISTICS OF SOILS AND SOFT ROCKS UNDER TRANSIENT LOADING", Publication Harvard Grad. Sch., Engineering Soil Mechanics, Series 31, 1948.

21. AHMED, S.B., and LAREW, H.G., "A STUDY OF THE REPEATED LOAD STRENGTH MODULI OF SOILS", Proceedings, International Conference on the Structural Design of Asphalt Pavements, University of Michigan, 1962.

22. ALLEN, J.J., and THOMPSON, M.R., "RESILIENT RESPONSE OF GRANULAR MATERIALS SUBJECTED TO TIME-DEPENDENT LATERAL STRESSES", Transportation Research Board 510, Soil Mechanics, 1974.

23. BARKSDALE, R.D., and HICKS, R.G., "EVALUATION OF MATERIALS FOR GRANULAR BASE COURSES", Proceedings, Third International Conference on Materials Technology, Rio De Janeiro, Brazil, August 1972.

24. BARKSDALE, R.D., "COMPRESSIVE STRESS PULSE TIMES IN FLEXIBLE PAVEMENTS FOR USE IN DYNAMIC TESTING", Highway Research Board 345, 1971.

25. EPPS, J.A., and MONISMITH, C.L., "FATIGUE OF ASPHALT CONCRETE MIXTURES - SUMMARY OF EXISTING INFORMATIONS", Fatigue of Compacted Bituminous Aggregate Mixtures. ASTM STP 508, American Society of Testing and Materials, 1972.

26. HICKS, R.G., and MONISMITH, C.L., "FACTORS INFLUENCING THE RESILIENT RESPONSE OF GRANULAR MATERIALS", Highway Research Board Record 345, Washington, D.C., 1970.

27. HAYNES, J.H., and YODER, E.J., "EFFECTS OF REPEATED LOADING ON GRAVEL AND CRUSHED STONE BASE COURSE MATERIALS USED IN THE AASHO ROAD TEST", Highway Research Board 39, Washington, D.C., 1963.

28. HICKS, R.G., and MONISMITH, C.L., "PREDICTING OF THE RESILIENT RESPONSE OF PAVEMENTS CONTAINING GRANULAR LAYERS USING NON-LINEAR ELASTIC THEORY", Proceedings, Third International Conference on the Structural Design of Asphalt Pavements, London, England, 1972.

29. HICKS, R.G., "FACTORS INFLUENCING THE RESILIENT PROPERTIES OF GRANULAR MATERIALS", Ph.D. Thesis, University of California, Berkeley, 1970

30. JIMENEY, R.A., and GALLAWAY, B.M., in Proceedings, Association of Asphalt Paving Technologists, PRPTA, Vol. 31, 1962.

31. KALCHEFF, I.V., and HICKS, R.G., "A TEST PROCEDURE FOR DETERMINING THE RESILIENT PROPERTIES OF GRANULAR MATERIALS", 76th Annual Meeting of the ASTM, Philadelphia, June 1973.

32. KALLAS, B.F., and PUZINAUSKAS, V.P., "FLEXURE FATIGUE TESTS ON ASPHALT PAVING MIXTURES", Fatigue of Compacted Bituminous Aggragate Mixtures, ASTM STP 508, American Society for Testing and Materials, 1972.

33. LUO, WEN-KUH, "THE CHARACTERISTICS OF SOILS SUBJECTED TO REPEATED LOADS AND THEIR APPLICATIONS TO ENGINEERING PRACTICE", Soila and Foundations, Vol. 13, No. 1, March 1973.

34. MCLEAN, D.B., and MONISMITH, C.L., "ESTIMATION OF PERMANENT DEFORMATION IN ASPHALT CONCRETE LAYERS DUE TO REPEATED TRAFFIC LOADING", Paper Presented at Annual Meeting of Highway Research Board, January 1974.

35. MITCHELL, J.K., SHEN, C.K., and MONISMITH, C.L., "BACKGROUND,EQUIPMENT, PRELIMINARY INVESTIGATION, REPEATED COMPRESSION AND FLEXURE TESTS ON CEMENT-TREATED SILTY CLAY", Report No. 1, University of California, Berkeley, December 1965.

36. MITRY, F.G., "DETERMINATION OF THE MODULUS OF RESILIENT DEFORMATION OF UNTREATED BASE COURSE MATERIALS", Ph.D. Thesis, University of California, Berkely, 1964.

37. MONISMITH, C.L., "SOME APPLICATIONS OF THEORY IN DESIGN OF ASPHALT PAVE MENTS", Fifth Annual Nevada Streets and Highway Conference, University of Nevada, March 1970.

38. MONISMITH, C.L., and FINN, F.N., "FLEXIBLE PAVEMENT DESIGN: A STATE OF THE ART - 1975", Proceedings, Pavement Design for Practicing Engineers, Specialty Conference, Georgia Institute of Technology, June 1975.

39. MORGAN,J.R., "THE RESPONSE OF GRANULAR MATERIALS TO REPEATED LOADINGS", Proceedings, Third Conference, Australian Road Research Board, Part 2, 1966.

40. MORRIS, J., and HAAS, R.C.G., "DYNAMIC TESTING OF BITUMINOUS MIXTURES FOR PAVEMENT DEFORMATION RESPONSE", Fatigue and Dynamic Testing of

Bituminous Mixtures, ASTM STP 561, American Society of Testing and Materials, 1974.

41. PELL, P.S., and BROWN, S.F., "THE CHARACTERISTICS OF MATERIALS FOR THE DESIGN OF FLEXIBLE PAVEMENT STRUCTURES", Proceedings, Third International Conference on the Structural Design of Asphalt Pavements, London, England, 1972.

42. PELL, P.S., and TAYLOR, I.F., in Proceedings, Association of Asphalt Paving Technologists, PRPTA, Vol. 38, 1969.

43. SEED, H.B., MITRY, F.G., MONISMITH, C.L., and CHAN, C.K., "FACTORS INFLUENCING THE RESILIENT DEFORMATIONS OF UNTREATED AGGREGATE BASE IN TWO-LAYER PAVEMENTS SUBJECTED TO REPEATED LOADING", Highway Research Board 190, Washington, D.C., 1967.

44. SEED, H.B., MITRY, F.G., MONISMITH, C.L., and CHAN, C.K., "PREDICTION OF FLEXIBLE PAVEMENT DEFLECTIONS FROM LABORATORY REPEATED LOAD TESTS", NCHRP Report No. 35, Washington, D.C., 1967.

45. SHACKEL, B., "A RESEARCH APPARATUS FOR SUBJECTING PAVEMENT MATERIALS TO REPEATED TRIAXIAL LOADING", Australian Road Research, Vol. 4, June 1970.

46. TANIMOTO, K. and NISHI, M., "ON RESILIENCE CHARACTERISTICS OF SOME SOILS UNDER REPEATED LOADING", Soils and Foundations, Vol. 10, No. 1, 1970.

47. TERREL, R.L., and AWAD, I.S., "RESILIENT BEHAVIOR OF ASPHALT TREATED BASE COURSE MATERIALS", Washington State Highway Department Research Program Report 6.1, August 1972.

48. TERREL, R.L., AWAD, I.S., and FOSS, L.R., "TECHNIQUES FOR CHARACTERIZING BITUMINOUS MATERIALS USING A VERSATILE TRIAXIAL TESTING SYSTEM", Fatigue and Dynamic Testing of Bituminous Mixtures, ASTM STP 561, American Society for Testing and Materials, 1974.

49. TERREL, R.L., AWAD, I.S., and FOSS, L.R., "INVESTIGATING STRESS-STRAIN CHARACTERISTICS OF ASPHALT TREATED MATERIALS", Closed Loop, Vol.4, No. 1 1973.

50. VAN TIL, C.J., MCCULLOUGH, B.F., VALLERGA, B.A., and HICKS, R.G., "EVALUATION OF AASHO INTERIM GUIDES FOR DESIGN OF PAVEMENT STRUCTURES", NCHRP Report No. 128, Washington, D.C., 1972.

51. WANG, M.C., MITCHELL, J.K., and MONISMITH, C.L., "STRESSES AND DEFLECTIONS IN CEMENT-STABILIZED PAVEMENTS", Contract Report No. 3-145, Behavior of Stabilized Soils under Repeated Loading, U.S. Army Engineer Waterways Experiment Station, October 1970.

52. WISSA, A.E.Z., and PANIAGUA, J.G., "EQUIPMENT FOR STUDYING THE EFFECT OF REPEATED LOADING ON THE STRESS-STRAIN BEHAVIOR OF STABILIZED SOILS", Contract Report No. 3-63, Soil Stabilization, U.S. Army Engineer Waterways Experiment Station, June 1972.

53. YODER, E.J., "PRINCIPLES OF PAVEMENT DESIGN", John Wiley and Sons, Inc. New York, 1955.

54. ————, "TEST PROCEDURES FOR CHARACTERIZING DYNAMIC STRESS-STRAIN PROPERTIES OF PAVEMENT MATERIALS", Transportation Research Board, Special Report 162, Washington, D.C., 1975.

55. CAMPEN, W.C., and SMITH, J.R., "USE OF LOAD TESTS IN THE DESIGN OF FLEXIBLE PAVEMENTS", Special Technical Publication No. 79, ASTM, 1947.

56. MCLEOD, N.W., "A CANADIAN INVESTIGATION OF LOAD TESTING APPLIED TO PAVEMENT DESIGN", Special Technical Publication No. 79, ASTM, 1947.

57. PHILLIPE, R.R., "FIELD BEARING TESTS APPLIED TO PAVEMENT DESIGN", Special Technical Publication No. 79, ASTM, 1947.

58. HITTLE, J.E., and GOETZ, W.H., "A CYCLIC LOAD TEST PROCEDURE", Special Technical Publication No. 79, ASTM, 1947.

59. TROLLOPE, D.H., LEE, I.K., and MORRIS, J., "STRESSES AND DEFORMATION IN TWO-LAYER PAVEMENT STRUCTURES UNDER SLOW REPEATED LOADING", Proceedings, Australian Road Research Board, Vol. 1, Part 2, 1962.

60. BIAREZ, J., "CONTRIBUTION ET L'ETUDE DES PROPERIETES MECANIQUES DES SOLS ET DES MATERIAU PULVERULENTS", D.Sc. Thesis, Universite de Grenoble, France, 1962.

61. DUNLAP, W.A., "A REPORT ON A MATHEMATICAL MODEL DESCRIBING THE DEFORMATION CHARACTERISTICS OF GRANULAR MATERIALS", Technical Report No. 1, Texas Transportation Institute, Texas A&M University, 1963.

62. COFFMAN, B.S., KRAFT, D.C., and TAMAYO, J., "A COMPARISON OF CALCULATED AND MEASURED DEFLECTIONS FOR THE AASHO ROAD TEST", Proceedings, Association of Asphalt Paving Technologists, Vol. 33, 1964.

63. KALLAS, B.F.,and RILEY, J.C., Proceedings, Second International Conference on the Structural Design of Asphalt Pavements, University of Michigan, Ann Arbor, Michigan, 1967.

64. KASIANCHUK, D.A., TERREL, R.L., and HAAS, C.G., "A DESIGN SUBSYSTEM FOR MINIMIZING FATIGUE, PERMANENT DEFORMATION, AND SHRINKAGE FRACTURE DISTRESS OF ASPHALT PAVEMENTS", Proceedings, Vol. 1, Third International Conference on the Structural Design of Asphalt Pavements, London, September 1972.

65. NIJBOER, L.W., and METCALF, C.T., "DYNAMIC TESTING AT THE AASHO ROAD TEST", Proceedings, International Conference on Structural Design of Asphalt Pavements, University of Michigan, Ann Arbor, Michigan, 1963.

66. NIJBOER, L.W. and VAN DER POEL, C., "A STUDY OF VIBRATION PHENOMENA IN ASPHALTIC ROAD CONSTRUCTION", Proceedings, Association of Asphalt Paving Technologists, Vol. 22, 1953.

67. DEACON, J.A., "FATIGUE OF ASPHALT CONCRETE", Ph.D. Thesis, University of California, Berkeley, 1965.

68. DEACON, J.A., "EQUIVALENT PASSAGES OF AIRCRAFT WITH RESPECT TO FATIGUE DISTRESS OF FLEXIBLE AIRFIELD PAVEMENTS", Proceedings, AAPT, Vol. 40, 1971.

69. HEUKELOM, W. and KLOMP, A.J.G., "ROAD DESIGN AND DYNAMIC LOADINGS", Proceedings, Association of Paving Technologists, Vol. 33, 1964.

70. VAN DER POEL, C., "ROAD ASPHALT", In Building Materials, their Elasticity and Inelasticity, Edited by REINER M. Interscience, 1954.

71. VAN DER POEL, C., "A GENERAL SYSTEM DESCRIBING THE VISCO-ELASTIC PROPERTIES OF BITUMENS AND ITS RELATION TO ROUTINE TEST DATA", Journal, Applied Chem. Vol. 4, 1954.

72. ALI, G.A., "A LABORATORY INVESTIGATION OF THE APPLICATION OF TRANSFER FUNCTIONS TO FLEXIBLE PAVEMENTS", Ph.D. Thesis, Purdue University, August 1972.

73. HARR, M.E., and BOYER, R.E., "PREDICTING PAVEMENT PERFORMANCE USING TIME-DEPENDENT TRANSFER FUNCTIONS", AFWL-TR-72-204, Kirtland Air Force Base, New Mexico, January 1973.

74. NG-A-QUI, N.T., "NONCONTACT NONDESTRUCTIVE EVALUATION OF FLEXIBLE PAVEMENTS USING PROTOTYPE LOADS", Ph.D. Thesis, Purdue University, December 1976.

75. CANNON, R.H. JR., "DYNAMIC OF PHYSICAL SYSTEM", McGraw Hill Book Company, 1967.

76. LEONARDS, G.A., EDITOR, "FOUNDATION ENGINEERING", McGraw Hill Book Company, 1962

77. PERLOFF, W.H., and BARON, W., "SOIL MECHANICS - PRINCIPLES AND APPLICATIONS", The Ronald Press Company, New York, 1976.

78. HEUKELOM, W. and FOSTER, C.R., "DYNAMIC TESTING OF PAVEMENTS", Proceedings, ASCE, Vol. 86, 1960.

79. MENDELSON, A., "PLASTICITY - THEORY AND PRACTICE", Macmillan Publishing Company, River Side, N.J., 1968.

80. KENIS, W.J., and MCMAHON, T.F., "ADVANCE NOTICE OF FHWA PAVEMENT DESIGN SYSTEM AND A DESIGN CHECK PROCEDURE", Presented at AASHO Design Committee Meeting, October 1969.

81. HEUKELOM, W., and KLOMP, A.J.G., "CONSIDERATION OF CALCULATED STRAINS AT VARIOUS DEPTHS IN CONNECTION WITH THW STABILITY OF ASPHALT PAVEMENTS", Proceedings, Second International Conference on Structural Design of Asphalt Pavements, University of Michigan, Ann Arbor, Michigan, 1967.

82. ROMAIN, J.E., "RUT DEPTH PREDICTION IN ASPHALT PAVEMENTS", Proceedings, Third International Conference on Structural Design of Asphalt Pavements, University of Michigan, Ann Arbor, Michigan, 1972.

83. BURMISTER, D.M., "THEORY OF STRESSES AND DISPLACEMENTS IN LAYERED SYSTEMS AND APPLICATIONS TO THE DESIGN OF AIRPORT RUNWAYS", Proceedings, Highway Research Board, Vol. 23, 1943.

84. BURMISTER, D.M., "THE GENERAL THEORY OF STRESSES AND DISPLACEMENTS IN LAYERSD SOIL SYSTEMS", Journal, Applied Physics, Vol. 16, No. 2, 3, and 5, 1945.

85. BURMISTER, D.M., "APPLICATIONS OF LAYERED SYSTEM CONCEPTS AND PRINCIPLES TO INTERPRETATIONS AND EVALUATIONS OF ASPHALT PAVEMENT PERFORMANCES AND TO DESIGN AND CONSTRUCTION", Proceedings, International Conference on Structural Design of Asphalt Pavements, University of Michigan, Ann Arbor, Michigan, 1963.

86. MITCHELL, J.K., FOSSBERG, P.E., and MONISMITH, C.L., "BEHAVIOR OF STABILIZED SOILS UNDER REPEATED LOADING, REPEATED COMPRESSION AND FLEXURE TESTS ON CEMENT AND LIME-TREATED BUCKSHOT CLAY, CONFINING PRESSURE EFFECTS IN REPEATED COMPRESSION FOR CEMENT-TREATED SILTY CLAY", Contract Report No. 3-145, U.S. Army Engineers Waterway Experiment Station, CE, Vicksburg, Mississippi, May 1966.

87. WITCZAK, M., "DESIGN OF FULL-DEPTH ASPHALT AIRFIELD PAVEMENTS", Proceedings, Third International Conference on the Structural Design of Asphalt Pavements, University of Michigan, Ann Arbor, Michigan, 1972

88. HAAS, R.C.G., KAMEL, N.I., and MORRIS, J., "BRAMPTON TEST ROAD: ANALYSIS OF PERFORMANCE BY ELASTIC LAYER THEORY AND ITS APPLICATION TO PAVEMENT DESIGN AND MANAGEMENT IN ONTARIO", Ontario Joint Transportation and Communication Program, Report RR 182, Ontario, Canada, November 1972.

89. ELLIOT, J.F., MOAVENZADEH, F., and FINKADLY, H., "MOVING LOAD ON VISCOELASTIC LAYERED SYSTEMS", Phase II-Addendum, Departmant of Civil Engineering, Massachusetts Institute of Technology, Cambridge, Massachusetts, Res. Report R70-20, April 1970.

90. HOFSTRA, A., and KLOMP, A.J.G., "PERMANENT DEFORMATION OF FLEXIBLE PAVEMENTS UNDER SIMULATED ROAD TRAFFIC CONDITIONS", Proceedings, Third International Conference on Structural Design of Asphalt Pavements, university of Michigan, Ann Arbor, Michigan, 1972.

91. DEHLEN, G.L., "THE EFFECT OF NON-LINEAR MATERIAL RESPONSE ON THE BEHAVIOR OF PAVEMENTS SUBJECTED TO TRAFFIC LOADS", University of California, Ph.D. Thesis, 1969.

92. ACUM, W.E.A., and FOX, L., "COMPUTATION OF LOAD STRESSES IN A THREE LAYER ELASTIC SYSTEM", Geotechnique, December 1951.

93. JONES, A., "TABLES OF STRESSES IN THREE-LAYER ELASTIC SYSTEMS", Paper Presented at Annual Meeting of Highway Research Board, Washington, D.C., January 1962.

94. PEATTIE, K.R., "STRESS AND STRAIN FACTORS FOR THREE-LAYER ELASTIC SYSTEMS", Wood River Research Laboratory, Shell Oil Company, 1962.

95. SKEMPTON, A.W., "THE BEARING CAPACITY OF CLAYS", Soil Mechanics Paper Presented at the Building Research Congress, 1951, Technical Memorandum No. 25, National Research Council of Canada, Associate Committee on Soil and Snow Mechanics, Ottawa, Canada, November, 1952.

96. ————, "NONDESTRUCTIVE TESTING OF PAVEMENTS", Tests on Multiple-Wheel Heavy Gear Load Sections at Eglin and Hurlburt Airfields, Air Force Weapons Laboratory, Albuquerque, New Mexico, Technical Report No. AFWL-TR-71-64, March 1972.

97. SWAMI, S.A., "THE RESPONSE OF BITUMINOUS MIXTURES TO DYNAMIC AND STATIC LOADS USING TRANSFER FUNCTIONS", Ph.D. Thesis, Purdue University, 1969.

98. NORMAN, P.J., SNOWDON, R.A., and JACOBS, J.C., "PAVEMENT DEFLECTION MEASUREMENTS AND THEIR APPLICATION TO STRUCTURAL MAINTENANCE AND OVERLAY DESIGN", Transport and Road Research Laboratory, Department of the Environment, TRRL Report LR 571, 1973.

99. THOMPSON, O.O., "EVALUATION OF FLEXIBLE PAVEMENT BEHAVIOR WITH EMPHASIS ON THE BEHAVIOR OF GRANULAR LAYERS", Ph.D. Thesis, University of Illinois, 1969.

100. SANTUCCI, L.E. and SCHMIDT, R.J., Proceedings, Association of Asphalt Paving Technologists, PRPTA, Vol. 38, 1969.

101. SCHMIDT, R.J., and SANTUCCI, L.E., Proceedings, Association of Asphalt Paving Technologists, PRPTA, Vol. 38, 1969.

102. ALLEN, J.J., "THE EFFECTS OF NON-CONSTANT LATERAL PRESSURES ON THE RESILIENT RESPONSE OF GRANULAR MATERIALS", Ph.D. Thesis, University of Illinois at Urbana-Champaign, May 1973.

103. GRAY, J.E., "CHARACTERISTICS OF GRADED BASE COURSE AGGREGATES DETERMINED BY TRIAXIAL TESTS", National Crushed Stone Association, Washington, D.C., Engineering Bulletin 12, 1962.

104. LAREW, H.G., "THE STRENGTH AND DEFORMATION CHARACTERISTICS OF COMPACTED FINE-GRAINED SOILS UNDER THE ACTION OF REPEATED APPLICATIONS OF STRESS", Ph.D. Thesis, Purdue University, January 1960.

105. AHMED, S.B., "EVALUATION OF THE STRENGTH MODULUS OF SOILS UNDER THE ACTION OF REPEATED LOADING", M.S.C.E. Thesis, University of Virginia, August 1961.

106. ————, "DESIGN OF FLEXIBLE PAVEMENTS USING THE TRIAXIAL COMPRESSION TEST", State Highway Commission of Kansas, Highway Research Board, Bulletin No. 8, 1955.

107. ————, "ENGINEERING AND DESIGN OF FLEXIBLE AIRFIELD PAVEMENTS", U.S. Army, Corps of Engineers, Waterway Experiment Station, Vicksburg, Mississippi, EM 1110-45-302, 1958

108. ————, "SYSTEMS APPROACH TO PAVEMENT DESIGN, SYSTEM FORMULATION, PERFORMANCE DEFINITION, AND MATERIAL CHARACTERISATION", Materials Research and Development, Inc., NCHRP Project 1-10, 1968b.

109. BISHOP, A.W., and HENKEL, D.J., "THE MEASUREMENT OF SOIL PROPERTIES IN THE TRIAXIAL TEST", Edward Arnold, Ltd., London, 1962.

110. CHANG, CHIN-YUNG, "MODULUS OF RESILIENT DEFORMATION OF UNTREATED BASE COURSE MATERIALS", M.S.C.E., University of California, Berkeley, March 1969.

111. BOUSSINESQ, J.W., "APPLICATION DES POTENTIALS A L'ÈTUDE DE L'ÈQUILIBRIUM ET DU MOUVEMENT DES SOLIDS ELASTIQUES", Paris, Bauthier-Villiers, 1885.

112. SHIFLEY, L.H., "THE INFLUENCE OF SUBGRADE CHARACTERISTICS ON THE TRANSIENT DEFLECTIONS OF ASPHALT CONCRETE PAVEMENTS", Ph.D. Thesis, University of California, Berkeley, 1967.

113. HICKS, R.G., and FINN, F.N., "ANALYSIS OF RESULTS FROM THE DYNAMIC MEASYREMENTS PROGRAM ON THE SAN DIEGO TEST ROAD", Hicks, R.G., Ph.D. Thesis, Reference List, University of California, Berkeley, 1970.

APPENDIX A

Test Procedures for Characterizing Dynamic Stress-Strain Properties of Pavement Materials

SPECIAL REPORT 162
Transportation Research Board, National Research Council
National Academy of Sciences
Washington, D.C., 1975

CONTENTS

FOREWORD

The purpose of this document is to compile for the highway engineer and researcher the dynamic testing procedures for evaluating the resilient moduli of highway materials that have been found to give reasonable results. It is hoped that such a document will encourage the eventual establishment of standard test procedures for use by researchers and practicing engineers. The use of standardized test procedures would permit the direct comparison of experimental test results obtained by various research organizations.

Some of the various test methods described in this report may give considerably different results. No attempt is made to recommend the most appropriate test method for specific conditions. Caution therefore should be exercised in selecting appropriate test methods for characterizing in the laboratory the material properties representative of field conditions.

This report was written as a part of the activities of the Transportation Research Board's Committee on Strength and Deformation Characteristics of Pavement Sections. John A. Deacon, who was at the time committee chairman, appointed a subcommittee cochaired by Eugene L. Skok, Jr., and Bernard F. Kallas to prepare this report. The report was completed under the committee chairmanship of Richard D. Barksdale. The report was written by Bernard F. Kallas, Carl L. Monismith, Eugene L. Skok, Jr., Q. L. Robnett, Richard D. Barksdale, Thomas W. Kennedy, and Kamran Majidzadeh and was edited by Richard D. Barksdale. Other committee members helped review this document and assisted in its development. Appreciation is extended also to W. M. Sangster, Director of the School of Civil Engineering, Georgia Institute of Technology, for the financial support necessary for the preparation of most of the figures.

INTRODUCTION

During the past 10 to 15 years, people have shown considerable interest in the use of various elastic and viscoelastic layered system theories to predict the physical response of structural pavement sections. Use of such models has become more common because, by using modern high-speed digital computers, one can rapidly solve more complicated layered pavement system models than one could in the past. When an elastic layered theory is used to predict pavement response, one must either evaluate experimentally or estimate the modulus of elasticity and Poisson's ratio of each layer in the system. Therefore, the problem of determining the critical conditions for design and the pertinent material properties for each layer still remains.

The stress-strain properties of materials used in highway construction can vary greatly because of a number of factors including stress state, pulse rate and duration, temperature, degree of saturation, density, age, and method of testing. A variety of different methods for evaluating the dynamic material properties of pavement materials have been developed in recent years by a number of researchers. A review of many of the testing procedures for evaluating the modulus of elasticity and Poisson's ratio of highway materials and an extensive list of references have been presented elsewhere (1).

Because of the wide variation in measured material properties that can occur with variations in test conditions and procedures, procedures should be specified and described carefully when one presents and uses the test results. Standardized test procedures are especially desirable if the test results are to be used by several different agencies. The purpose of this document is to present several acceptable methods currently being used for determining the stress-strain properties of pavement materials for use in elastic layered theories.

The laboratory testing techniques given in this Special Report include both the test procedure and a description of sample preparation and the type of equipment that is necessary to perform the tests. Testing procedures are given for determining the dynamic modulus of elasticity by using the following tests: (a) repeated load triaxial test, (b) complex modulus test, (c) flexural bending test, (d) indirect tensile test, and (e) resonant column method. In addition, a simplified, approximate test procedure is given for determining the dynamic modulus for cohesive soils. The procedures presented should be considered as somewhat standardized; eventually, after some modifications, it is hoped that these procedures can be developed into standard test methods for determining the elastic modulus and Poisson's ratio for use with layered theories. This Special Report also defines some of the problems involved in the dynamic testing of highway materials and suggests methods of sample preparation and test procedures that tend to minimize these problems.

FUNDAMENTAL CONSIDERATIONS

Proper evaluation of pavement material properties requires careful consideration of many factors including (a) magnitude, speed, and nature of traffic loading; (b) short- and long-term environmental conditions; (c) construction variables; and (d) nature of materials being tested (stabilized, cohesive, granular). That the test should simulate as closely as practical in situ environmental conditions and the stress state occurring under the action of the moving (or static) wheel loads is the basic philosophy that should be used in evaluating material properties. Considerable judgment must be used in estimating the overall long-term environmental effects such as degree of saturation and density of pavement materials. Work should be done according to degree of saturation rather than moisture content because the former appears to be a more basic variable.

Under field service conditions, variation in the dynamic modulus and, to a lesser extent, Poisson's ratio that is due to changes in environmental factors such as degree of saturation and temperature can have significant effects on the overall performance of the pavement. Even though reasonably accurate values of the dynamic modulus of pavement materials may be obtained in the laboratory under carefully controlled conditions, extreme care must be exercised in incorporating these data into mechanistic design procedures.

SELECTION OF STRESS PULSE

When a wheel load moves past an element of material located within the pavement system, the element is subjected to a simultaneous buildup in both the major and minor principal stresses. Currently, for routine laboratory testing, only the major principal stress (axial stress in a triaxial test) needs to be varied if care is taken in selecting the confining pressure. The actual stress pulse applied by a moving wheel load is close to half sine in shape. Preliminary results, however, indicate that triangular, sinusoidal, and half sine pulses all can be used to simulate actual in situ stress provided care is taken in selecting the magnitude and duration of the pulse. For conventional flexible pavement structures and spring and summer temperatures, the duration of the stress pulse varies primarily with element location on point of loading and with vehicle speed. The data shown in Figure 1 are suggested as a practical guide for use in selecting the duration of the stress pulse that should be used in performing a dynamic laboratory test.

DYNAMIC MODULI

For moderate stress levels, the elastic response of most subgrade soils, unstabilized granular materials, and stabilized materials becomes relatively constant after

Figure 1. Variation of equivalent vertical stress pulse time with vehicle velocity and depth (3).

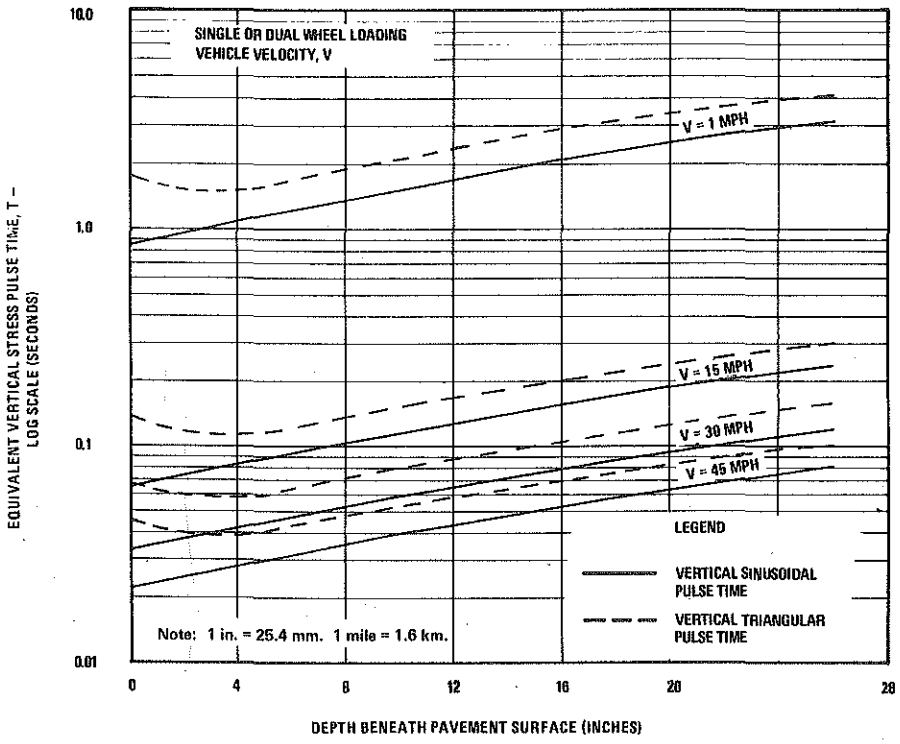

approximately 100 to 200 load repetitions. Studies also indicate that a single test specimen usually can be used to characterize the nonlinear elastic response of most paving materials. This can be accomplished with 1 specimen by determining the elastic bounce at several different confining pressures and deviator stresses, or temperature in the case of asphalt concrete, provided care is exercised to increase gradually the severity of the stress level.

For triaxial testing, results indicate that, when the dynamic modulus is greater than about 15,000 lbf/in.^{2} (103 500 kPa), special measuring clamps or special optical tracking equipment should be attached to the specimen to eliminate end effects and slop in the system. Clamps suitable for use on cylindrical specimens will be described in another section of this Special Report.

A specimen tested in a triaxial cell probably should be tested with the drainage valves leading to the inside of the specimen open because of the conditions of a material sample beneath pavement subjected to many load repetitions. In determining dynamic modulus when only 100 to 200 load applications are to be applied, the method of drainage probably will not have a significant effect on the resultant dynamic modulus in most instances. If the test is performed over a period of days and drainage is permitted, then the specimen may dry out and become hard because of the development of significant amounts of capillary tension.

POISSON'S RATIO

Because of problems associated with reliable measurements of Poisson's ratio and because the response of pavement is relatively insensitive to reasonable variations in this parameter, estimated values of Poisson's ratio can be used at this time as an engineering approximation for the mechanistic design procedure. Typical ranges in the

variation of Poisson's ratio have been found to be as follows:

Material	Poisson's Ratio
Asphalt concrete	0.25 to 0.35
Unstabilized granular subgrades, subbases, and bases	0.30 to 0.40
Silty subgrades	0.35 to 0.45
Clay subgrades	0.40 to 0.50
Soil cement	0.10 to 0.25

If Poisson's ratio is to be measured, measuring clamps that fit around the cylindrical triaxial specimen can be used.

INFLUENCE OF TYPE OF MATERIAL

One should carefully consider the type of material when selecting both the test method and test conditions such as stress level. For unbound cohesive and granular materials, either the repeated load triaxial test or the complex modulus test is well suited for evaluating elastic properties.

In general, the dynamic modulus of cohesive soils decreases rapidly with increasing magnitude of repeated axial stress up to a point; then it increases at a greatly reduced rate. For some types of soils, dynamic modulus is relatively unaffected by small changes in confining pressure. The effect of confining pressure on the dynamic modulus appears to become greater as clay content decreases or the material becomes stiffer. Numerous studies of the dynamic modulus of sands, gravels, and crushed stones have shown that the dynamic modulus significantly increases with increases in confining pressure and is only slightly affected by reasonable variations in the magnitude of the repeated axial stress.

Results of dynamic triaxial tests have indicated that temperature and rate or frequency of loading have a significant effect on the stiffness of asphalt-bound materials. Asphalt content, type of asphalt, air voids, aggregate grading, and type of aggregate have a considerably smaller effect on stiffness. The dynamic modulus determined from flexural and indirect tensile tests has been found to be as small as half the value determined from triaxial tests. Probably the actual in situ modulus for asphalt concrete is somewhere between the values determined from flexural and triaxial tests.

Repeated load tests performed on cylindrical specimens of cement-bound materials have shown that the dynamic modulus of soil cement decreases with increases in confining pressure. Furthermore, laboratory results indicate that the dynamic modulus measured by using the triaxial test may be as much as 10 times greater than that obtained in repeated flexural tests. Results of the flexural tests probably should be used for stabilized materials in layered theories because this test more closely simulates conditions of bending, which occurs in very stiff base layers. Also, because of cracking with time in cement-treated and asphalt concrete bases, the effective modulus will tend to decrease significantly over time.

SPECIMEN PREPARATION AND COMPACTION PROCESSES

To obtain specimens that are representative of field conditions, one must use great care in preparing, handling, and storing the test specimens. Furthermore, use of different materials and different methods of compaction in the field will require the use of varying compaction techniques in the laboratory. This section will describe methods that can be used to prepare cohesive soils, granular soils, and asphalt concrete for laboratory use. Typical equipment required is as follows:

1. Compaction apparatus;
2. Loading equipment [static machine with a 10- to 30-ton (9- to 27-Mg) capacity, kneading compactor for cohesive soils and stabilized materials, and vibratory compactor for granular soils];
3. Calipers, micrometer gauge, and steel rule [calibrated to 0.01 in. (0.254 mm)];
4. Rubber membranes from 0.01 to 0.025 in. (0.254 to 0.635 mm) in thickness;
5. Rubber O-rings;
6. Vacuum source with bubble chamber and regulator;
7. Membrane stretcher;
8. Scales;
9. Weighing pans; and
10. Porous stones.

COMPACTED COHESIVE SPECIMENS

The resilient character of compacted clays is dependent on the structure imparted to the soil particles by the compaction process. (The unified soil classification system is used to define a clay soil.) Laboratory compaction processes must be selected in accordance with the expected field compaction conditions. Any compaction process that causes shearing deformation in a clay soil having a degree of saturation greater than 80 percent results in a dispersed (or parallel) clay structure. Clays with a dispersed structure exhibit greater deformation than would the same soil with a flocculated (random) structure tested under identical conditions. Some general criteria can be used to guide selection of the appropriate compaction conditions for clay soils.

1. If the field compaction conditions will be at a water content corresponding to less than 80 percent of the saturation water content and the in-service water content is expected to remain less than the 80 percent saturation value, then any of the standard impact, gyratory, kneading, or static procedures may be used to simulate the in-service condition.
2. If the field compaction will be at a water content corresponding to greater than 80 percent of the saturation water content and the in-service water content is expected

to remain greater than the 80 percent saturation value, then the compaction process must be of the shearing type. That is, an impact, gyratory, or kneading process must be used to simulate the dispersed structure in service.

3. If the field compaction conditions will be at a water content corresponding to less than 80 percent of the saturation water content and the in-service conditions are expected to result in a degree of saturation greater than 80 percent, then static compaction must be used to simulate the flocculated structure in service.

In Figure 2, resilient modulus is shown as isograms on a chart of dry density versus water content. The form shown in Figure 2 has general application to compacted clay soils and may be used to guide the selection of a test program.

1. If the range of compaction conditions and the range of in-service conditions are known, select an appropriate laboratory compaction method. Prepare and test samples at dry densities and water contents within the in-service range such as that shown in Figure 2.
2. If the service conditions are not well defined, then prepare and test specimen over a substantial range of dry densities and water contents. Display the results as shown in Figure 2 and use the resilient modulus in conjunction with other properties such as rutting and swelling to select the range of field placement conditions.

Specimen Size

The diameter of the specimen to be tested is determined by a lower bound of approximately 2.5 in. (63.5 mm) or by 4 to 5 times the maximum size of particle in the material. This lower bound represents a minimum size that can be expected to provide a reasonable representation of the larger mass of material in a pavement. Specimen length should not be less than 2 times the diameter.

Moisture-Density Relationship

Four steps should be followed to determine moisture-density relationship.

1. Establish the moisture-density relationship for the soil according to 1 of the following procedures: (a) ASTM D1557-AASHO T-180, (b) ASTM D698-AASHO T-99, (c) California 216F, or (d) some other standard method. Prepare a graph showing dry density and water content as described in the standard procedure chosen.
2. Determine the specific gravity of the soil according to the appropriate procedure (ASTM D854 or California 209A).
3. Use the data obtained in steps 1 and 2 to determine 100 percent and 80 percent of saturation at various densities. Place this information on the graph drawn in step 1; that is, draw a 100 percent and an 80 percent saturation line.
4. Select the densities, water contents, and compaction method to be used to prepare specimen.

Preparation of Soil for Compaction

Ten steps should be followed to prepare soil for compaction.

1. Determine the water content W_1 percent of the soil (if other than oven-dried material is to be used).
2. Determine the volume V_s of the compacted specimen to be prepared. For other than static compaction methods, the height of the compacted specimen must be greater than that required for resilience testing to allow for trimming of the specimen ends. An excess of 0.5 in. (13 mm) generally will be adequate.

3. Determine the sample weight of the oven-dried soil W_s and water W_w required to obtain the desired dry density γ_d and water content W percent as follows:

W_s in pounds = γ_d in pounds per cubic foot × V_s in cubic feet

W_s in grams = W_s in pounds × 453

$$W_w \text{ in pounds} = \gamma_d \text{ in pounds per cubic foot} \times \frac{W \text{ percent}}{100}$$

W_w in grams = W_w in pounds × 453

4. Determine the sample weight of other than oven-dried soil (W_{ss}) required to obtain W_s. An additional amount of approximately 500 g should be allowed, and the excess should be used to determine the water content at the time of compaction.

$$W_{ss} \text{ in grams} = (W_s \text{ in grams} + 500)\left(1 + \frac{W_1}{100}\right)$$

5. Determine the weight of water (W_{aw}) required to increase the weight from the existing (W_{1w}) to the desired (W_w).

$$W_{1w} \text{ in grams} = (W_s + 500)\left(\frac{W_1}{100}\right)$$

W_{aw} in grams = $W_w - W_{1w}$

6. Determine the wet weight of soil (W_{wet}) to be compacted.

$$W_{wet} \text{ in grams} = W_s \times \left(1 + \frac{W \text{ percent}}{100}\right)$$

7. Place the mass of soil determined in step 3 into a mixing pan.
8. Add the water to the soil in small amounts and mix thoroughly after each addition.
9. Place the mixture in a plastic bag. Seal the bag and knead the soil with the fingers to obtain uniform dispersion of water throughout the soil. The mixture should be stored in the plastic bag in an atmosphere of 75 percent relative humidity for 12 to 24 h. Ensure a complete seal by using 2 or more bags.
10. After mixing and storage, weigh the wet soil and bag to the nearest gram and record this value on a form for compacted clays as shown in Figure 3.

Compaction by Impact or Kneading Methods

Specimens prepared in standard molds associated with impact or kneading methods

Figure 2. Result of resilience tests on compacted clays, variation of dry density with water content.

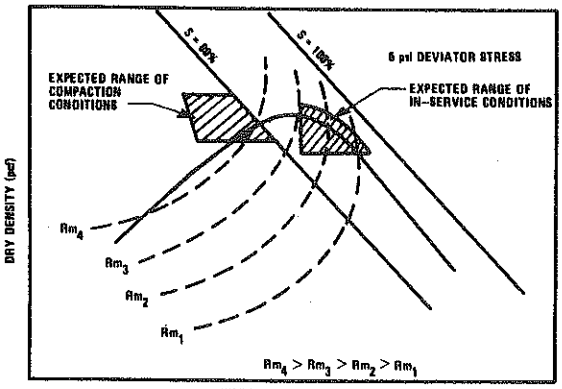

Note: 1 lb/ft^3 = 16.02 kg/m^3. 1 lbf/in.^{2} = 6.9 kPa.

Figure 3. Sample data recording form for compacted clays.

Soil sample_____
Location_____
Sample no._____
Specific gravity_____

Soil Specimen Measurements
Diameter
Top_____
Middle_____
Bottom_____
Average_____
Membrane thickness_____
Net diameter_____
Height of specimen plus cap and base_____
Height of cap and base_____
Initial length_____

Soil Specimen Weight
Initial weight of container plus wet soil, g_____
Final weight of container plus wet soil, g_____
Weight of wet soil used_____

Soil Specimen Volume
Initial area, in.^{2}_____
Volume,[a] in.^{3}_____
Wet density, lb/ft^3_____
Water content, percent_____
Percent saturation_____
Dry density, lb/ft^3_____

Date_____
Compaction method_____
Vertical spacing between LVDT clamps, in._____
Chamber pressure, lbf/in.^{2}_____

Constants
Vertical LVDT_____
Horizontal LVDT_____
Load cell_____
Comments_____

			Vertical Values				Horizontal Values			
Load Cell Chart Reading	Deviator Load (lb)	σ_d (lbf/in.^{2})	LVDT Chart Reading	Deformation (in.)	ϵ_{R1} (in./in.)	$M_R = \sigma_d/\epsilon_{R1}$ (lbf/in.^{2})	LVDT Chart Reading	Deformation (in.)	ϵ_{R3} (in./in.)	$\nu_R = \epsilon_{R3}/\epsilon_{R1}$

[a]Initial area times initial length.

(ASTM D1557, ASTM D698, California 216F, Harvard miniature compaction, or California or Triaxial Institute kneading compaction) may not be of the correct dimensions for direct use in resilience testing. However, molds of the correct dimensions can be obtained, and the methods can be adapted to the new mold sizes. This generally will require adjustments in the number of compacted layers or the number of tamps per layer or both. Large compacted specimens can be prepared and the correct size trimmed from these.

1. Establish the number of layers N to be used to compact the soil. Determine the weight of wet soil required per layer W_L.

$$W_L \text{ in grams} = \frac{W_{wet}}{N}$$

2. Place the mass of soil determined in step 1 in the mold. Compact according to the standard procedure. Scarify the surface of the layer.
3. Repeat step 2.
4. After compaction, use approximately 200 g of the remaining wet soil to determine water content.
5. Carefully remove the specimen from the mold. Trim the ends to provide plane surfaces.
6. Weigh the specimen to the nearest gram. Determine the average height and diameter to the nearest 0.01 in. (0.254 mm). Record these values on a form for compacted clays as shown in Figure 3.

The specimen is now ready for resilience testing. If there will be a delay of more than a few minutes before beginning the resilience testing, the specimen should be carefully wrapped in plastic to prevent evaporation. Note that fine-grained cohesive soils compacted wet of optimum (especially when a dispersed structure is developed) exhibit thixotropic strength gains with time. The limited data reported in the literature (2) indicate that a curing period of 1 to 7 days (depending on the soil) is usually sufficient to minimize the thixotropic strength gain effects on the resilient modulus. Limited results also indicate that a few hundred "conditioning" stress applications may be sufficient to eliminate or minimize this effect when the specimens are immediately tested after preparation.

Compaction by Static Loading

In the absence of standard methods for static compaction, the following procedure may be used. The process is one of compacting a known weight of wet soil to a volume that is fixed by the configuration of the mold assembly. A typical mold assembly for the preparation of a specimen with a 2.8-in. (71.12-mm) diameter and 6-in. (152.4-mm) height by using 3 layers is shown in Figure 4. To meet specific needs, equipment of differing size and number of layers can be developed.

1. Establish the number of layers N to be used to compact the soil. Determine the weight of wet soil per layer.

$$W_L \text{ in grams} = \frac{W_{wet}}{N}$$

2. Place 1 of the loading rams into the sample mold.
3. Place the mass of soil determined in step 1 in the sample mold. Use a spatula

Figure 4. Apparatus for compaction by static loading.

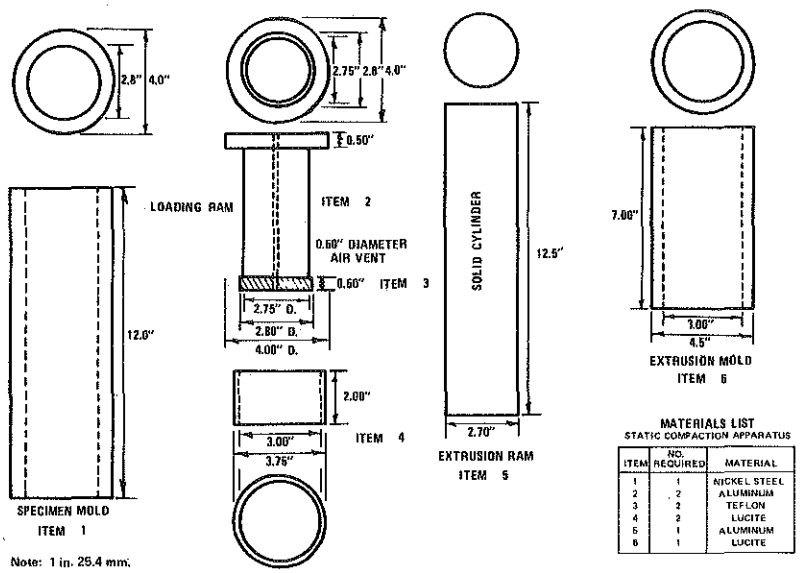

MATERIALS LIST
STATIC COMPACTION APPARATUS

ITEM	NO. REQUIRED	MATERIAL
1	1	NICKEL STEEL
2	2	ALUMINUM
3	2	TEFLON
4	2	LUCITE
5	1	ALUMINUM
6	1	LUCITE

to draw the soil away from the edge of the mold and form a slight mound in the center.

4. Insert the second loading ram and place the assembly in the loading machine. Apply a small load. Adjust the mold so that it rests equidistant between the CLAMPS of the loading rams. Soil pressures developed by the initial loading will serve to hold the mold in place. By having both loading rams reach the 0-volume change positions simultaneously, one can obtain more uniform layer densities.

5. Slowly increase the load until the loading ram caps rest firmly against the mold. Hold the load at or near the maximum load for a period of time. The rate of loading and load duration depend on the amount of soil rebound. The slower the rate of loading is and the longer the load is held, the less the rebound is.

6. Decrease the load to 0 and remove the assembly from the loading machine.

7. Remove a loading ram. Scarify the surface of the compacted layer, put the correct weight of soil for a second layer in place, and adjust the soil as in step 3. Add a spacer ring and insert the loading ram.

8. Invert the assembly and repeat step 7.

9. Place the assembly in the loading machine. Load slowly while holding the load at or near maximum when the spacer disk firmly contacts the mold.

10. Repeat steps 6, 7, 8, and 9 as required.

11. Use approximately 200 g of the remaining soil for a measurement of water content.

12. Place the extruder ram into the sample mold and force the specimen out of the sample mold into the extruder mold.

13. Use the extruder mold to carefully slide the compacted specimen onto a glass plate.

14. Determine the weight of the compacted specimen to the nearest gram. Measure the height and diameter to the nearest 0.1 in. (2.54 mm). Record these values on a form for compacted clays as shown in Figure 3.

The specimen is now ready for resilience testing. If there will be a delay of more than a few minutes before beginning the resilience testing, the specimen should be carefully wrapped in plastic to prevent evaporation. (Refer to the note on thixotropic effects given after step 7 under compaction by impact or kneading methods.)

COMPACTED GRANULAR SPECIMENS

Of particular concern in the preparation of granular soil specimens is the extent to which these materials can be handled (in removing them from a mold and transporting and placing them in the triaxial cell). Granular soils that exhibit sufficient cohesion to permit handling can be prepared by the methods described for compacted clay soils; however, it is generally not necessary to consider soil structure effects. The exception is some silts that also may exhibit strength properties that are dependent on compaction conditions.

This section contains some items that can be applied generally to compacted granular soils, but this section mainly is directed to compaction of materials that cannot be handled between compaction and testing.

Specimen Size

The diameter of the specimen to be tested is determined by a lower bound of approximately 2.5 in. (63.5 mm) or by 4 to 5 times the maximum size of particle in the material. This lower bound represents a minimum size that can be expected to provide a reasonable representation of the larger mass of material in a pavement.

Specimen length should not be less than 2 times the diameter.

Moisture-Density Relationship

Four steps should be followed to determine moisture-density relationship.

1. Establish the moisture-density relationship for the soil according to 1 of the following procedures: (a) ASTM D 1557-AASHO T-180, (b) ASTM D 698-AASHO T-99, (c) California 216F, or (d) some other standard method. Prepare a graph of dry density and water content.
2. Determine the specific gravity of the soil by using 1 of the following procedures: (a) ASTM D 854, (b) ASTM C 127, (c) California 206D, (d) California 207D, or (e) some other standard.
3. Use the data from steps 1 and 2 to determine 100 percent of saturation at various densities. Draw the curve for 100 percent saturation on the graph drawn in step 1.
4. Select the densities and water contents at which specimens are to be prepared. These usually will consist of several values covering the expected in-service range. Note that material that has a moderately high permeability and is to be tested at 100 percent saturation generally is prepared in an oven-dried or air-dried state and saturated by back-pressure techniques or capillary saturation.

Preparation of Soil for Compaction

Cohesionless granular materials are compacted most readily by use of a split mold mounted on the base of the triaxial cell as shown in Figure 5. Compaction forces are generated by a vibrator, such as a small, hand-operated air hammer. Nineteen steps should be followed to prepare soil for compaction.

1. Determine the water content (W_1 percent) of the soil (if other than oven-dried material is to be used).
2. Tighten the sample base into place on the triaxial cell base. It is essential that an airtight seal be developed.
3. Place the porous stone plus the sample cap on the sample base. (Two stones are required for saturated specimens, but generally only the lower stone would be used for tests at lower water contents unless drainage from both ends is desired.) Determine the height of base, cap, and stone to the nearest 0.01 in. (0.254 mm), and record

this value on a form for granular soils as shown in Figure 6.

4. Remove the sample cap and upper porous stone. Measure the thickness of the rubber membrane with a micrometer gauge. Record this value on a form for granular soils as shown in Figure 6.

5. Place the rubber membrane over the sample base and lower porous stone. Fix the membrane in place with an O-ring seal.

6. Place the split-mold sample former around the sample base and draw the rubber membrane up through the mold. Tighten the split mold firmly into place. Exercise care to avoid pinching the membrane.

7. Stretch the membrane tightly over the rim of the mold. Apply a vacuum to the mold to remove all membrane wrinkles. The membrane now should fit smoothly around the inside perimeter of the mold. The vacuum is maintained throughout the compaction procedure.

8. Use calipers to determine to the nearest 0.01 in. (0.254 mm) the inside diameter of the membrane-lined mold. Determine to the nearest 0.01 in. (0.254 mm) the distance from the top of the porous stone to the rim of the mold.

9. Determine the volume of specimen to be prepared. The diameter of the specimen is the diameter determined in step 8, and the height is a value less than that determined in step 8 but at least 2 times the diameter.

10. Determine the weight of material that must be compacted into the volume determined in step 9 to obtain the desired density and water content. (The section on preparing clay soils for compaction contains further information on this.)

11. Determine the number of layers to be used for compaction. Normally, layer depths will be 1 to 1.5 in. (25.4 to 38.1 mm). Determine the weight of soil required for each layer and the thickness of each layer.

12. Place the required mass of soil into a mixing pan. (Allow approximately 300 g more than required for compaction; the excess is to be used for determining the water content.) Add the required amount of water and mix thoroughly.

13. Determine the weight of wet soil plus water and record on a form for granular soils as shown in Figure 6.

14. Place the amount of wet soil required for 1 layer into the mold. Exercise care to avoid spillage. Use a spatula to draw the material away from the edge of the mold and form a small mound at the center of the mold.

15. Insert the vibrator head and vibrate the soil until the distance from the surface of the compacted layer to the rim of the mold is equal to the distance measured in step 8 minus the thickness of the lift determined in step 11. This may require removal and reinsertion of the vibrator head several times until experience is obtained in gauging the required vibration time.

16. Repeat steps 14 and 15 for each new lift. The measured distance from the surface of the compacted layer to the rim of the mold is successively reduced by the thickness of each new lift from step 11. The final surface should be a smooth, horizontal plane.

17. When compaction is completed, observe the weight of the mixing pan plus excess soil and record it on a form for granular soils as shown in Figure 6. The weight determined in step 13 less the weight observed now is the weight of wet soil incorporated in the specimens. Use approximately 200 g of the excess material to determine water content.

18. Place the porous stone and sample cap on the surface of the specimen. Roll the rubber membrane off the rim of the mold and over the sample cap. If the sample cap projects above the rim of the mold, the membrane should be sealed tightly against the cap with an O-ring seal. If it does not, the seal can be applied later.

19. Disconnect the vacuum supply from the mold. Place the entire assembly on the loading machine in preparation for resilience testing.

COMPACTED CYLINDRICAL ASPHALT CONCRETE SPECIMENS

This method, which is similar to that which is to be published as an ASTM test method,

Figure 5. Apparatus for vibratory compaction of granular materials.

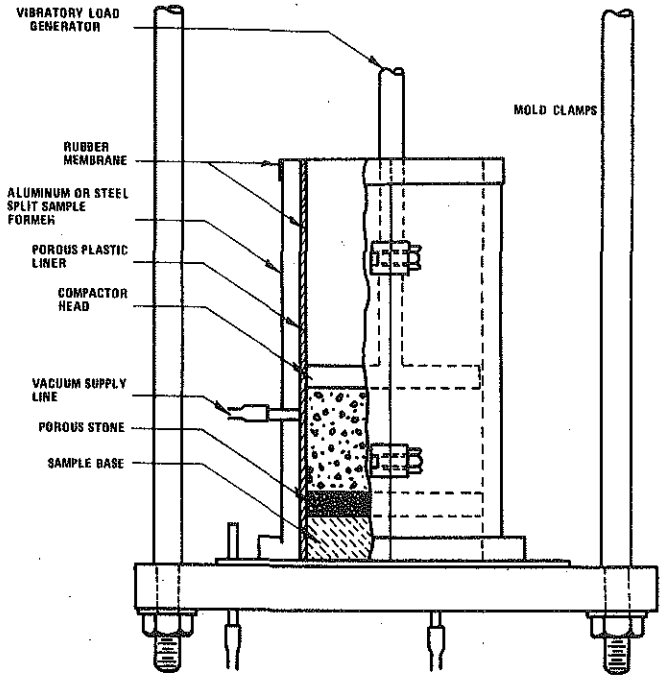

Figure 6. Sample data recording form for granular soils.

Soil sample_____
_____
Location_____
Sample no._____
Specific gravity_____

Soil Specimen Measurements
Diameter
Top_____
Middle_____
Bottom_____
Average_____
Membrane thickness_____
Net diameter_____
Height of specimen plus cap and base_____
Height of cap and base_____
Initial length_____

Soil Specimen Weight
Initial weight of container plus wet soil, g_____
Final weight of container plus wet soil, g_____
Weight of wet soil used_____

Soil Specimen Volume
Initial area, $in.^2$_____
Volume,[a] $in.^3$_____
Wet density, lb/ft^3_____
Water content, percent_____
Percent saturation_____
Dry density, lb/ft^3_____
Void ratio_____

Date_____
Compaction method_____
_____
Vertical spacing between LVDT clamps, in._____

Constants
Vertical LVDT_____
Horizontal LVDT_____
Load cell_____
Comments_____
_____
_____
_____

						Vertical Values				Horizontal Values			
σ_3 ($lbf/in.^2$)	Load Cell Chart Reading	Deviator Load (lb)	$\sigma_d = \sigma_1 - \sigma_3$ ($lbf/in.^2$)	$\frac{\sigma_1}{\sigma_3}$	θ ($lbf/in.^2$)	LVDT Chart Reading	Deformation (in.)	ϵ_{R1} (in./in.)	$M_R = \sigma_d/\epsilon_{R1}$ ($lbf/in.^2$)	LVDT Chart Reading	Deformation (in.)	ϵ_{R3} (in./in.)	$\nu_R = \epsilon_{R3}/\epsilon_{R1}$

[a] Initial area times initial length.

covers the preparation of cylindrical specimens 4 in. (101.6 mm) in diameter and approximately 8 in. (203.2 mm) high of bituminous paving mixture suitable for complex and resilient modulus tests. The method is intended for dense-graded bituminous concrete mixtures containing aggregate up to 1 in. (25.4 mm) maximum size.

Test Specimens

Prepare 3900 g of the bituminous mixture as specified by ASTM D 1560.

Apparatus

An apparatus should be used that meets the specifications given by ASTM D 1561 except that steel molding cylinders with 0.25-in. (6.35-mm) wall thickness, 4-in. (101.6-mm) inside diameter, and 10-in. (254-mm) height should be used.

Procedure

Three steps should be followed for determining compaction temperature, molding specimens, and applying static load.

1. Use the compaction temperature for bituminous mixtures as specified by ASTM D 1561.
2. Heat the compaction mold to the temperature specified in step 1. Place the compaction mold in position in the mold holder and insert a paper disk 4 in. (101.6 mm) in diameter to cover the baseplate of the mold holder. Weigh out half the required amount of bituminous mixture for 1 specimen at the specified temperature and place uniformly in the insulated feeder trough, which has been preheated to the compaction temperature for the mixture. By means of the variable transformer that controls the heater, maintain a sufficiently hot compactor foot to prevent the mixture from adhering to it. By means of a paddle of suitable dimensions to fit the cross section of the trough, push 30 approximately equal portions of the mixture continuously and uniformly into the mold while applying 30 tamping blows at a pressure of 250 lbf/in.^{2} (1725 kPa). Immediately place the remaining half of the mixture uniformly in the feeder trough. Push 30 approximately equal portions of the mixture continuously and uniformly into the mold while applying 30 tamping blows at pressure of 250 lbf/in.^{2} (1725 kPa). If sandy or unstable material is involved and there is undue movement of the mixture under the compactor foot, reduce the compaction temperature and compactor foot pressure until kneading compaction can be accomplished.
3. Immediately after compaction with the California kneading compactor, apply a static load to the specimen by using a compression testing machine. Apply the load by the double plunger method in which metal followers are employed as free-fitting plungers on the top and bottom of the specimen. Apply the load on the specimen at a rate of 0.05 in./min (0.021 mm/s) until an applied pressure of 1,000 lbf/in.^{2} (6900 kPa) is reached. Release the load immediately. After the compacted specimen has cooled to the point at which it will not deform on handling, remove it from the mold. Place the specimen on a smooth flat surface and allow it to cool to room temperature. The cylindrical sample will have approximately the same bulk specific gravity as specimens prepared according to ASTM D 1559 and ASTM D 1561.

COMPACTED ASPHALT CONCRETE BEAM SPECIMENS

This method, which is similar to that which is to be published as an ASTM test method, covers the preparation of beam specimens of bituminous paving mixture suitable for flexural modulus and flexural fatigue tests. The method is intended for dense-graded

bituminous concrete mixtures containing aggregate up to 1.5 in. (38.1 mm) maximum size.

Test Specimens

The beam test specimens should have a rectangular cross section of 3.25 in. (82.5 mm) by approximately 3.5 in. (88.9 mm) and a length of 15 in. (381 mm). Prepare approximately 7000 g of the bituminous mixture as specified by ASTM D 1560.

Apparatus

The apparatus shall be as specified by ASTM D 1561 except that the compactor shall be equipped with a specially modified compaction mold assembly and tamping foot as shown in Figure 7.

Procedure

Three steps should be followed for determining compaction temperature, molding specimens, and applying static load.

1. Use the compaction temperature for bituminous mixtures as specified by ASTM D 1561.
2. Heat the compaction mold to the compaction temperature specified in step 1. Place the mold on the sliding base assembly of the California kneading compactor and place a paper that is 3.25 in. (82.5 mm) wide and 15 in. (381 mm) long on the mold baseplate. Weigh out half of the required amount of bituminous mixture for 1 specimen and place it in the compaction mold in a layer of uniform thickness. By means of the variable transformer that controls the heater, maintain a sufficiently hot compactor foot to prevent the mixture from adhering to it. When applying tamping blows to the mixture, turn the base assembly table hand wheel $\frac{1}{8}$ revolution to move the mold laterally 0.75 in. (19 mm) after each tamping blow. Apply 20 tamping blows at a foot pressure of 200 lbf/in.^{2} (1380 kPa). Place the remaining half of the bituminous mixture in the compaction mold in a layer of uniform thickness. Apply 45 tamping blows at a foot pressure of 200 lbf/in.^{2} (1380 kPa). Apply the final 45 tamping blows at a foot pressure of 300 lbf/in.^{2} (2070 kPa). If sand or unstable material is involved and there is undue movement of the mixture under the compactor foot, reduce the compaction temperature and compactor foot pressure until kneading compaction can be accomplished.

Figure 7. California kneading compactor equipped with modified tamping foot and compaction mold assembly.

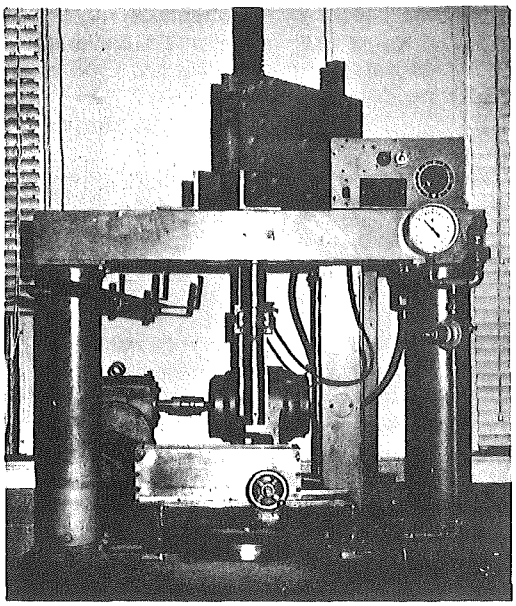

3. Immediately after compaction in the California kneading compactor, place the leveling bar on top of the specimen. By means of a compression testing machine, apply a static load on the specimen

at the rate of 0.05 in./min (0.021 mm/s) until an applied pressure of 1,000 lbf/in.^{2} (6900 kPa) is reached. Release the load immediately. After the compacted specimen has cooled sufficiently so that it will not deform on handling, remove it from the mold. Place the specimen on a smooth flat surface and allow it to cool to room temperature. The beam specimens have approximately the same bulk specific gravity as specimens prepared according to ASTM D 1559 and ASTM D 1561.

RESILIENCE TESTING OF UNSTABILIZED SOILS

The objective of this method is to define the resilient characteristics of untreated granular and cohesive soils for conditions that represent a reasonable simulation of the in situ state of stress in pavements subjected to moving wheel loads. Procedures described define resilient character in a triaxial state of stress when pressure in the triaxial chamber acts as a static all-around stress and when a repeated axial deviator stress of fixed magnitude, frequency, and load duration is applied to the soil from a force generator located outside the triaxial chamber. A simplified approximate procedure for testing unstabilized cohesive soils will be presented in another section of this Special Report. The notations used in this section are as follows:

σ_1 = total axial stress applied to the cylindrical specimen,
σ_2 = total radial stress applied to the cylindrical specimen,
σ_3 = confining pressure for the triaxial test,
$\sigma_d = \sigma_1 - \sigma_3$ = deviator stress (repeated axial stress for the procedure),
ϵ_1 = total axial strain due to σ_d,
ϵ_3 = total radial strain due to σ_d,
ϵ_{R1} = recovered axial strain,
ϵ_{R3} = recovered radial strain,
$M_R = \frac{\sigma_d}{\epsilon_{R1}}$ = resilient modulus,
$\nu_R = \frac{\epsilon_{R3}}{\epsilon_{R1}}$ = resilient Poisson's ratio,
$\theta = \sigma_1 + 2\sigma_3 = \sigma_d + 3\sigma_3$ = sum of the principal stresses in the triaxial state of stress,
σ_1/σ_3 = principal stress ratio,
$\gamma_d = \frac{G \cdot \gamma_w}{1 + (wG/S)}$ = unit weight of dry soil,
γ_w = unit weight of water,
G = specific gravity of soil,
W = water content of soil,
S = degree of saturation, and
$e = \frac{G}{\gamma_d}\gamma_w - 1$ = void ratio.

Load duration is the time interval the sample is subjected to a stress deviator. Cycle duration is the time interval between successive applications of a stress deviator.

TEST EQUIPMENT

Triaxial Test Cell

A triaxial cell suitable for use in resilience testing of soils is shown in Figure 8. This equipment is similar to most standard cells except that it is somewhat larger to facilitate the internally mounted load and deformation measuring equipment and has additional outlets for the electrical leads from the measuring devices. For the type of equipment shown in Figure 8, air would be used as the cell fluid.

The external loading source may be any device capable of providing a variable load of fixed cycle and load duration. The device can range from simple cam and switch control of static weights or air pistons to closed loop electrohydraulic systems. A load duration of 0.1 s and a cycle duration of 3 s have been found to be satisfactory for many applications.

Deformation Measurement

Deformation-measuring equipment consists of linear variable differential transformers (LVDTs) attached to the soil specimen by a pair of clamps. Four LVDTs are used; 2 are for the measurement of axial deformation, and 2 are for the measurement of horizontal or radial deformation. The clamps and LVDTs are shown in position on a soil specimen in Figure 8. Details of the clamps are shown in Figure 9. Load is measured by placing a load cell between the sample cap and the loading piston as shown in Figure 8.

Use of the type of measuring equipment that has just been described offers several advantages.

1. It is not necessary to reference deformations to the equipment that deforms during loading.
2. The effect of end-cap restraint on soil response is virtually eliminated.
3. The horizontally mounted LVDTs permit the measurement of the resilient Poisson effect.
4. Any effect of piston friction is eliminated by measuring loads at the caps of the sample.

It is necessary to maintain suitable recording equipment in addition to the measuring devices. It is desirable to have simultaneous recording of load and deformations. The number of recording channels can be reduced by wiring the leads from the LVDTs so that only the average signal from each pair is recorded. By introducing switching and balancing units, one can use a single-channel recorder. Use of a single-channel recorder, however, will not permit the making of simultaneous recordings.

RESILIENCE TESTING OF COHESIVE SOILS

Test Method

Twenty steps make up the test method for resilience testing of cohesive soils.

1. Place the triaxial cell base assembly on the platform of the loading machine. Tighten the sample base firmly to obtain an airtight seal.
2. Close the valve on the vacuum lead to the sample cap. (This line is not required for testing clays; closing the valve will prevent loss of air from the chamber during testing.)
3. Carefully place the specimen on the sample base. (Porous stones are not

Figure 8. Apparatus for resilience testing of soils.

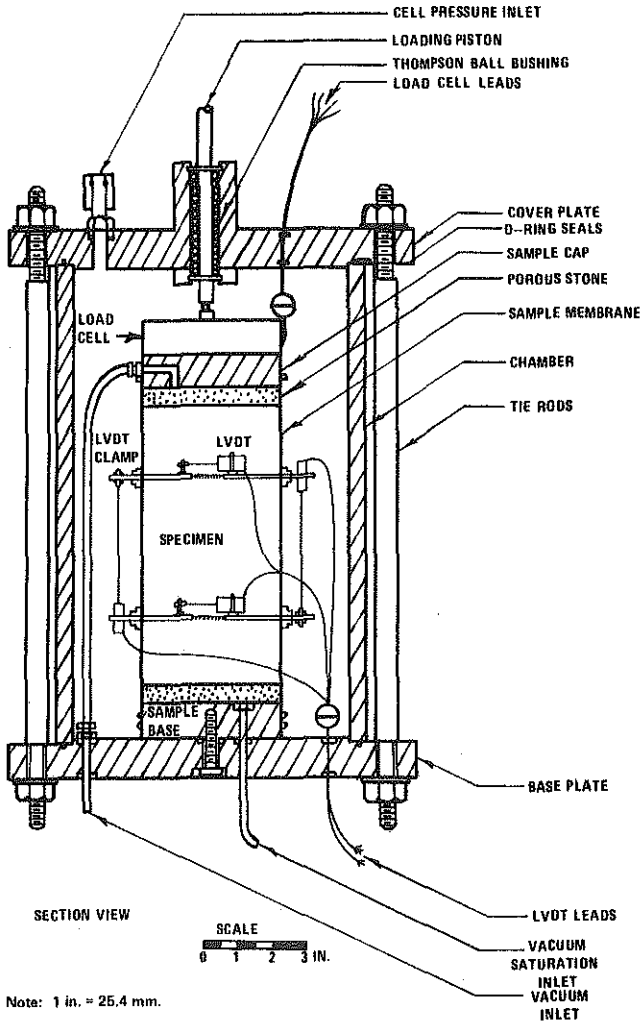

Note: 1 in. = 25.4 mm.

Figure 9. Clamps for holding linear variable differential transformers in measuring axial deformation and diameter change.

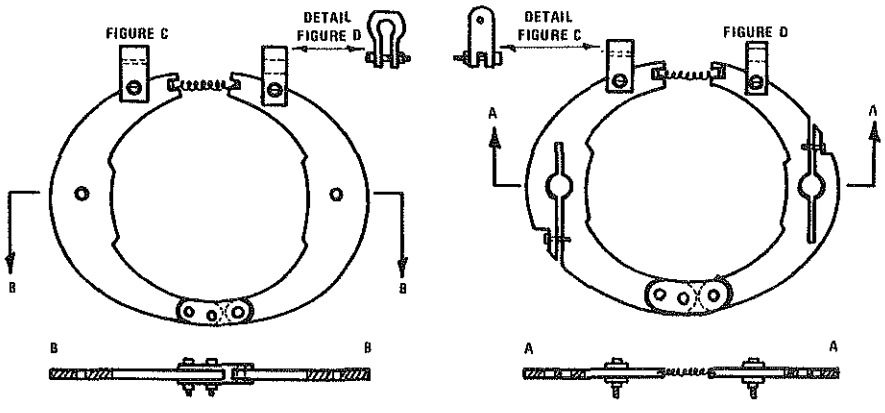

Note: 1 in. = 25.4 mm.

necessary for testing clay soils unless a drained condition is desired.)

4. Place the sample cap on the specimen.

5. Stretch a membrane tightly over the interior surface of the membrane stretcher. Slip the stretched membrane carefully over the specimen. Roll the membrane off the stretcher onto the sample base and cap. Remove the stretcher. Place O-ring seals around the base and cap.

6. Connect the vacuum-saturation line to the vacuum source through the medium of a bubble chamber [a vacuum of 5 to 10 lbf/in.^{2} (34.5 to 69 kPa) generally is adequate]. If bubbles are absent, an airtight seal has been obtained. If bubbles are present, check for leakage caused by poor connections, holes in the membrane, or imperfect seals at the cap and base. The existence of an airtight seal ensures that the membrane will remain firmly in contact with the specimen. This is essential for use of the clamp-mounted LVDTs. Leakage through holes in the membrane can frequently be eliminated by coating the surface of the membrane with a rubber latex or by using a second membrane.

7. When leakage has been eliminated, disconnect the vacuum supply.

8. Extend the lower LVDT clamp and slide it carefully down over the specimen to approximately the lower quarter point of the specimen.

9. Repeat step 8 for the upper clamp and place it at the upper quarter point. Ensure that both clamps lie in horizontal planes.

10. Connect the LVDTs to the recording unit and balance the recording bridges. This will require recorder adjustments and adjustment of the LVDT stems. When a recording bridge balance has been obtained, determine to the nearest 0.01 in. (0.254 mm) the vertical spacing between the LVDT clamps and record this value on a form for compacted clays as shown in Figure 3.

11. Place the triaxial chamber into position. Set the load cell in place on the sample cap.

12. Place the cover plate on the chamber. Insert the loading piston and obtain a firm connection with the load cell.

13. Tighten the tie rods firmly.

14. Slide the assembled apparatus into position under the axial loading device. Bring the loading device to a position where it nearly contacts the loading position.

The resilient properties of compacted clays are affected only slightly by the magnitude of the confining pressure. For most applications, the effect of confining pressure can be disregarded. For silty soils, however, the effect of confining pressure is much greater. The confining pressure used should approximate the expected in situ horizontal stresses. These generally will be on the order of 1 to 5 lbf/in.^{2} (6.9 to 34.5 kPa). A chamber pressure of 3 lbf/in.^{2} (20.7 kPa) would be a reasonable value for most testing. Resilient properties of cohesive soils are greatly dependent on the magnitude of the deviator stress (repeated axial stress). It is, therefore, necessary to conduct the test for a range in deviator stress values. For example, test at 0.5, 1.0, 2.0, 3.0, 4.0, 5.0, 7.5, 10, and 15 lbf/in.^{2} (3.45, 6.9, 13.8, 20.7, 27.6, 34.5, 51.75, 69, and 103.5 kPa).

15. Connect the chamber pressure supply line and apply confining pressure (equal to chamber pressure).

16. Rebalance the recording bridges for the LVDTs and balance the load-cell recording bridge.

17. Begin the test by applying 200 repetitions of a deviator stress of approximately 1 lbf/in.^{2} (6.9 kPa) and then 200 repetitions each at 3, 5, 7.5, and 10 lbf/in.^{2} (20.7, 34.5, 51.75, and 69 kPa). The foregoing stress sequence constitutes sample conditioning, that is, the elimination of the effects of the interval between compaction and loading and the elimination of the effects of initial loading versus reloading.

18. Decrease the deviator load to the lowest value to be used. Apply 200 repetitions of load and record both the horizontal and vertical recovered deformations at or near the 200th repetition. [The deformation measured by the horizontal LVDTs is approximately twice the actual deformation on the diameter because of the locations

of the hinge and the LVDT (Figure 9).]

19. Increase the deviator load and record deformations as in step 18. Repeat over the range of deviator stresses to be used.

20. At the completion of the loading, reduce the chamber pressure to 0. Remove the chamber LVDTs and load cell. Use the entire specimen for determining water content.

Calculations and Presentation of Results

The results of resilience tests can be presented in a summary table such as that given in a form for compacted clays as shown in Figure 3. The results also can be presented graphically as shown in Figure 10. A form similar to that of Figure 10 may be used to display the resilient Poisson's ratio.

RESILIENCE TESTING OF GRANULAR SOILS

Test Method

A number of steps make up the test method for resilience testing of granular soils.

1. Connect the vacuum-saturation inlet to a vacuum source and apply 5 to 10 lbf/in.^{2} (34.5 to 69 kPa) of vacuum through the medium of a bubble chamber. The vacuum serves a dual purpose in testing granular material. It serves to detect leakage and to impart a stress-induced rigidity to the material to prevent collapse when the sample mold is removed. This vacuum supply is maintained until step 9.

2. Carefully remove the sample mold. Seal the membrane to the sample cap if this has not been done. Determine to the nearest 0.1 in. (2.54 mm) the height of specimen plus cap and base and the diameter of the specimen plus membrane. Record these values on a form for granular soils as shown in Figure 6.

3. Observe the presence or absence of air bubbles in the bubble chamber. Eliminate system leakage by using methods previously described for compacted clays.

4. When leakage has been eliminated, place the LVDT clamps on the specimen and balance the recorder bridges as described previously for clay soils.

5. Connect the vacuum inlet line to the sample cap if the specimen is to be tested in a saturated state. If the specimen is not to be tested in a saturated state, this line is not connected and is sealed to prevent loss of air from the chamber.

6. Determine to the nearest 0.01 in. (0.254 mm) the spacing between the LVDT clamps and record this value.

7. Place the load cell on the sample cap, assemble the remainder of the cell, and tighten the tie rods firmly. Slide the assembly under the axial loading assembly.

8. Connect the chamber pressure supply line and apply a pressure of 5 lbf/in.^{2} (34.5 kPa).

9. Remove the vacuum supply from the vacuum-saturation inlet and open this line to the atmosphere.

If the specimen is to be saturated before testing, steps 10 through 13 are required. If the specimen is not to be saturated before testing, the test continues with step 14.

10. Connect the vacuum supply to the vacuum inlet (at top of specimen) and connect the vacuum-saturation inlet to a source of deaired, distilled water.

11. Apply a vacuum of 2 to 3 lbf/in.^{2} (13.8 to 20.7 kPa), open the water supply valve, and allow water to be drawn slowly upward through the sample.

12. Continue to flush water through the system to remove all entrapped air. To evaluate the presence or absence of air from the sample requires that one observe pore pressures. When all air has been eliminated, an increase in chamber pressure

Figure 10. Result of resilience tests on compacted clays, typical variation in resilient modulus with deviator stress.

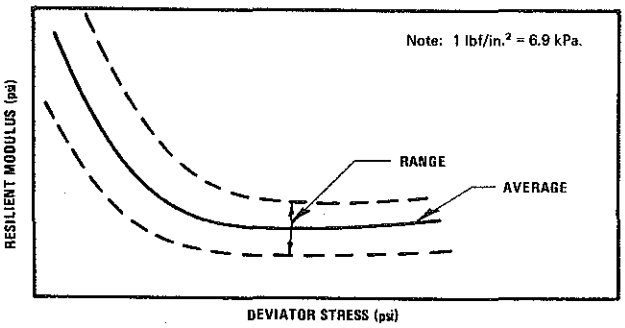

Figure 11. Results of resilience tests on granular soils, regression constants.

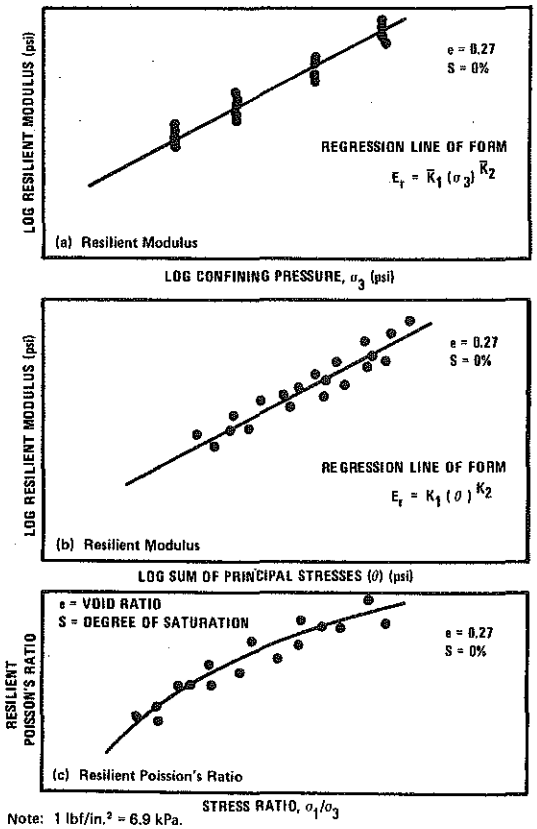

Note: 1 lbf/in.² = 6.9 kPa.

Figure 12. Results of resilience tests on granular soils, void ratio.

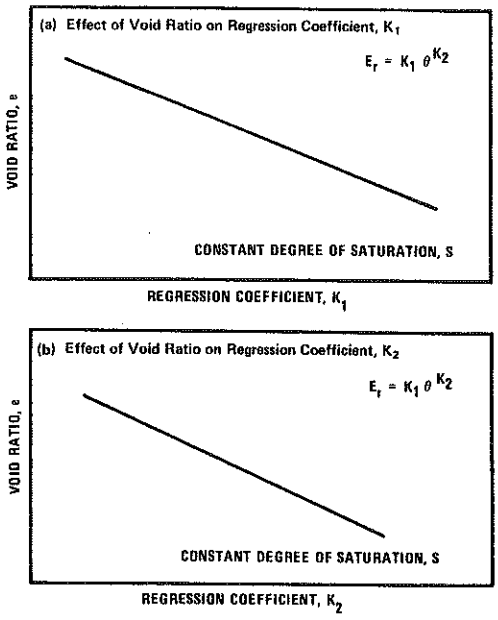

Figure 13. Results of resilience tests on granular soils, axial stress and confining pressure.

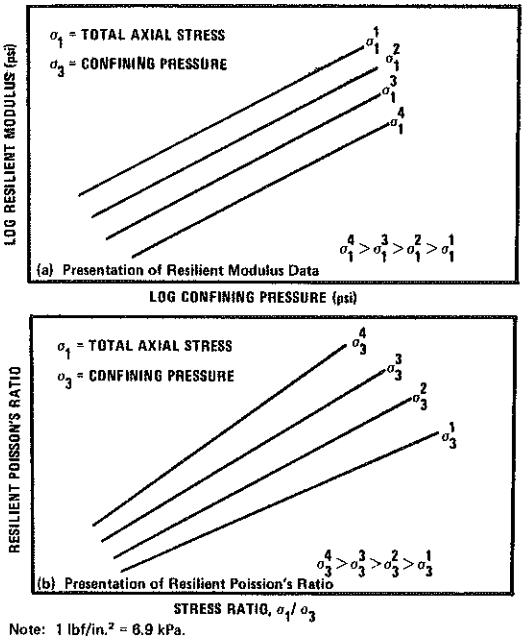

Note: 1 lbf/in.^{2} = 6.9 kPa.

(with valves to the water supply and vacuum supply closed) will result in an equal increase in pore pressure. (In view of the wide variety of pore-pressure measuring devices, no attempt will be made in this report to describe a procedure.)

13. Increase the chamber pressure to 10 lbf/in.^{2} (69 kPa); apply a 5-lbf/in.^{2} (34.5-kPa) back pressure to the water supply while closing the vacuum inlet valve. The effective confining pressure [5 lbf/in.^{2} (34.5 kPa)] on the specimen is now equal to the chamber pressure [10 lbf/in.^{2} (69 kPa)] minus the back pressure [5 lbf/in.^{2} (34.5 kPa)].
14. Rebalance the recorder bridges to the load cell and LVDTs.
15. Select the range of stresses at which the test is to be performed.

The resilient modulus of granular soils is dependent on the magnitude of the confining pressure and nearly independent of the magnitude of the repeated axial stress. The resilient Poisson's ratio is largely dependent on the principal stress ratio. Therefore, it is necessary to test granular materials over a range of confining and axial stresses. (The confining pressure is equal to the chamber pressure for dry and wet specimens and is equal to the chamber pressure less the back pressure for saturated specimens.) A suggested stress range for confining pressures is 1, 3, 5, 7.5, 10, 15, and 20 lbf/in.^{2} (6.9, 20.7, 34.5, 51.7, 69, 103.5, and 138 kPa). At each confining pressure, test at 5 values of deviator stress corresponding to multiples (1, 2, 3, 4, 5) of the cell pressure.

16. Before beginning to record deformations, apply a series of conditioning stresses to the material to eliminate initial loading effects. The greatest amount of volume change occurs during the application of the conditioning stresses. Simulation of field conditions suggests that drainage of saturated samples be permitted during the application of these loads but that the test loading (beginning with step 20) be conducted in an undrained state.
17. Set the axial load generator to apply a deviator stress of 10 lbf/in.^{2} (69 kPa) (that is, a stress ratio equal to 3). Activate the load generator and apply 200 repetitions of this load. Stop the loading.
18. Set the axial load generator to apply a deviator stress of 25 lbf/in.^{2} (172.5 kPa) (that is, a stress ratio equal to 6). Activate the load generator and apply 200 repetitions of this load. Stop the loading.
19. Repeat step 18 while maintaining a stress ratio equal to 6 by using the following order and magnitude of confining pressures: 10, 20, 10, 5, 3, and 1 lbf/in.^{2} (69, 138, 69, 34.5, 20.7, and 6.9 kPa).
20. Begin the recorded test by using a confining pressure of 1 lbf/in.^{2} (69 kPa) and an equal value of deviator stress. Record the resilient deformations after 200 repetitions. Increase the deviator stress to twice the confining pressure and record the resilient deformations after 200 repetitions. Repeat until a deviator stress of 5 times the confining pressure is reached (stress ratio of 6).
21. Repeat step 20 for each value of confining pressure.
22. When the test is completed, decrease the back pressure to 0, reduce the chamber pressure to 0, and dismantle the cell. Remove the LVDT clamps and so forth. Remove the soil specimen and use the entire amount of soil to determine the water content.

Calculations and Presentations of Results

Calculations can be performed by using the tabular arrangement from a form for granular soils as shown in Figure 6.

Individual test results and series are most readily presented in graphical form, such as that shown in Figure 11. Plotting the regression constants of Figure 11 versus void ratio as shown in Figure 12 provides a convenient means of interpolating for particular field conditions.

Materials such as fine sands, silts, and those with only small amounts of clay may display properties somewhat different than those shown in Figure 11, which demonstrates their dependence on both cell pressure and deviator stress. Graphical displays such as those shown in Figure 13 would then be more appropriate.

COMPLEX MODULUS TESTING OF PAVEMENT MATERIALS

Laboratory procedures are discussed below for determining the complex modulus of paving materials for conditions that represent a reasonable simulation of the in situ state of stress in pavements subjected to moving wheel loads. This test can be performed inside a triaxial cell at appropriate continuing pressures.

TEST EQUIPMENT

Loading and Load Measurement Equipment

An electrohydraulic testing system with a proper function generator capable of generating a sine or half sine function at frequencies between 1 to 20 cycles/s is suitable for complex modulus testing. However, a much less expensive eccentric-cam mechanical testing system also can be used to apply a sinusoidal loading to the specimen. Any recording device that can follow the output from the testing system can be used for recording the load and deformation to which the specimen is subjected.

A sample cap as shown in Figure 14 is required to transfer the load to the sample as well as to help in the measurement of axial deformation. Clamps such as those shown in Figures 8 and 9 also can be used to eliminate end effects in stiff materials.

Deformation Measurement Equipment

An LVDT attached to a suitable support (Figure 15) can be used for measurement of sample deformations. Leg A or leg B or both leg A and leg B of this support can be used for clamping with the testing machine platform (Figure 16). Figure 17 shows a complex modulus test apparatus.

A fast-responding 2-channel recorder capable of recording load on one channel and deformations on another channel is preferable so that load and deformation may be recorded simultaneously.

Additional Equipment

Additional equipment necessary for complex modulus testing includes the following:

1. Scales;
2. Weighing pans;
3. Mixer;

Figure 14. Sample cap for complex modulus test..

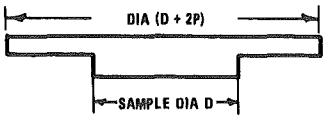

Figure 15. Linear variable differential transformer support for complex modulus test.

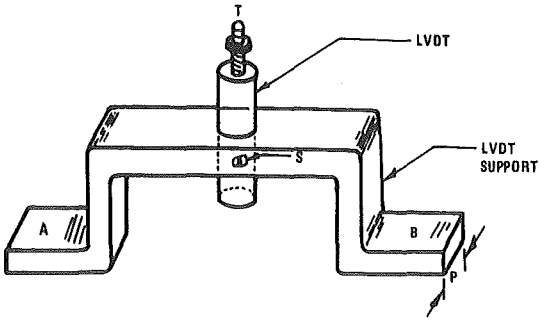

Figure 16. Experimental setup for complex modulus testing.

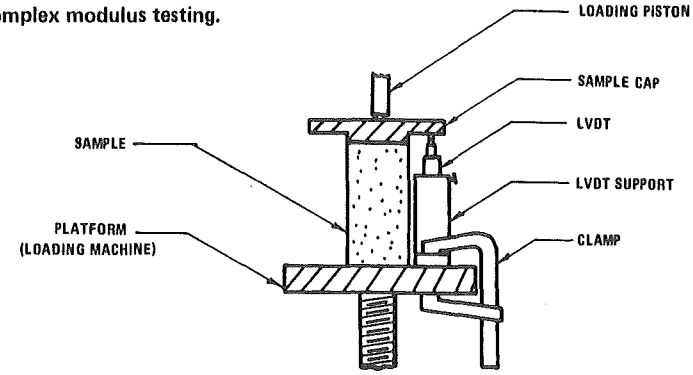

Figure 17. Complex modulus test apparatus.

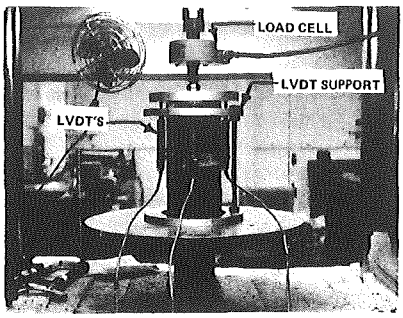

Figure 18. Sample data recording form for complex modulus testing.

Sample no._____ Date_____
Load Temperature, deg F_____
Static, lb_____ σ^*, lbf/in.^{2}_____
Dynamic, lb_____ Sample height, in._____

Frequency of Loading (cycles/s)	Deformations of Sample (in.) Position 1	Position 2	Position 3	Position 4	Position 5	Position 6	Position 7	Position 8	Avg Deformation (in.)	E^*
1										
5										
8										
10										
12										
15										
20										

4. Compaction apparatus;
5. Calipers, micrometer gauge, and steel rule calibrated to 0.01 in. (0.254 mm); and
6. Thermometer.

COMPACTION

The laboratory compaction process for specimens should be selected in accordance with the expected field compaction conditions as discussed in the section on specimen preparation and compaction processes.

SPECIMEN SIZE

Specimen length should not be less than 2 times the diameter. Minimum diameter of the specimen should not be less than 4 times the maximum size of aggregate used in the mix as recommended in ASTM standards. Specimens 2.75 in. (69.8 mm) in diameter and 5.5 in. (139.7 mm) high are recommended for all mixes having maximum size aggregates less than 0.5 in. (12.7 mm). For methods of preparing the specimens, refer to the section on specimen preparation and compaction processes.

COMPLEX MODULUS TESTING

Fifteen steps make up the test method for complex modulus testing.

1. Mark the center of the load axis on the loading machine platform. Mark 8 radial lines passing through this center so that they are equally spaced at 45-deg intervals. Number these radial lines from 1 to 8.
2. Carefully place the specimen on the platform of the loading machine and center it.
3. Place the sample cap on the specimen and center it. Place a ball bearing between the loading piston and this cap.
4. Place the LVDT with its support over position number 1 as marked on the platform so that the tip T (Figure 15) of LVDT touches the cap on the specimen but so that the LVDT support does not touch any part of the specimen (Figure 16).
5. Adjust the height of the LVDT with the help of screw S (Figure 15) so that it is close to null position. Balance the recording pen according to the procedure specified for the recorder operation.
6. Apply a small load [say, 1 lb (0.45 kg)] on the sample to take care of any machine instability during testing.
7. Select an appropriate frequency of loading as discussed under fundamental considerations.
8. Increase the cyclic load on the sample to the desired level and apply 100 cycles. (A separate experiment should be performed to establish the linearity range for the specimen. The load level is to be selected so that it is always below the limit for the upper point in linear range.)
9. Record the load and deformation on the sample and record the frequency of loading on the form.
10. Increase the frequency of loading to the next desired value and record the response. Repeat this procedure by increasing the frequency each time until all the frequencies have been tested.
11. Move the LVDT to the next position and repeat steps 4 through 10, but there is no need to apply the load for 100 cycles as specified in step 8.
12. Make readings for all 8 positions marked on the platform. The observations and results may be recorded conveniently in a table such as that shown in Figure 18.
13. Calculate the complex modulus E* shown in the last column of the sample form

shown in Figure 18 as follows:

$$\epsilon^* = \frac{\text{average axial dynamic deformation of the sample in 8 positions}}{\text{height of the sample}}$$

$$\sigma^* = \frac{\text{maximum axial dynamic load on the sample}}{\text{area of sample top}}$$

$$E^* = \frac{\sigma^*}{\epsilon^*}$$

14. Use special care for field samples to get the top and bottom on a plane at a right angle to the loading axis. Cap with a suitable material if the surfaces are not parallel.
15. Plot the results on an E* versus frequency graph.

FLEXURAL MODULUS TESTING OF STABILIZED MATERIALS

Laboratory procedures for the determination of flexural modulus of bituminous paving layers containing aggregate with maximum sizes up to 1.5 in. (38.1 mm) are described in this section. The flexural modulus of a simply supported beam specimen subjected to 2 symmetrical concentrated loads applied near the center is determined during the controlled-stress mode of flexural fatigue testing. The flexural modulus is determined immediately after 200 load applications and is a measure of the initial stiffness of the bituminous paving.

The extreme-fiber stress σ, extreme-fiber strain ϵ, and flexural stiffness modulus E_s of simply supported beam specimens subjected to the 2-point loading that produces uniaxial bending stresses are calculated by the following formulas:

$$\sigma = \frac{3aP}{bt^2}$$

$$\epsilon = \frac{12td}{(3\ell^2 - 4a^2)}$$

$$E_s = \frac{Pa(3\ell^2 - 4a^2)}{48Id}$$

where

a = 0.5 (reaction span length - 4) in inches (millimeters),
P = dynamic load applied to deflect beam upward in pounds (kilograms),
b = specimen width in inches (millimeters),
t = specimen depth in inches (millimeters),
d = dynamic deflection of beam center in inches (millimeters),
ℓ = reaction span length in inches (millimeters), and
I = specimen moment of inertia in inches^4 (m^4).

TEST EQUIPMENT

The repeated flexure apparatus is shown in Figure 19. It accommodates beam specimens 15 in. (381 mm) long with widths and depths that do not exceed 3 in. (76.2 mm). A 3,000-lb-capacity (1350-kg-capacity) dynamic testing system capable of applying

Figure 19. Repeated flexure apparatus for testing stabilized materials.

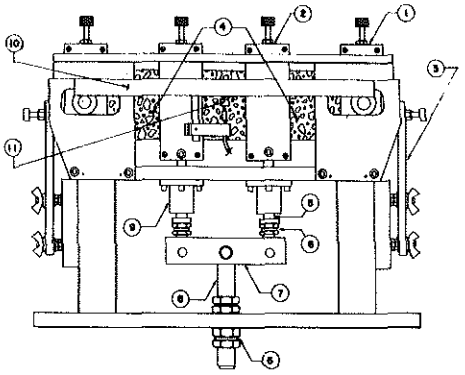

KEY:

1. REACTION CLAMP
2. LOAD CLAMP
3. RESTRAINER
4. SPECIMEN
5. LOADING ROD
6. STOP NUTS
7. LOAD BAR
8. PISTON ROD
9. THOMPSON BALL BUSHING
10. LVDT HOLDER
11. LVDT

repeated tension-compression loads in the form of sine or half sine waves of 0.1-s duration and rest periods of about 4 to 9 times the load duration provides suitable loading for flexural modulus determinations during flexural fatigue tests. Both pneumatic and electrohydraulic testing systems have been found to be suitable for this type of testing. The 2-point loading produces an approximately constant bending moment over the center 4 in. (101.6 mm) of a 15-in.-long (381-mm-long) beam specimen with widths and depths not exceeding 3 in. (76.2 mm). A sufficient load, approximately 10 percent of which will deflect the beam upward, is applied in the opposite direction, which forces the beam to return to its original horizontal position and holds it at the position during the rest period. Adjustable stop nuts installed on the flexure apparatus loading rod prevent the beam from bending below the initial horizontal position during the rest period.

The dynamic deflection of beam center is measured with an LVDT. A Shaevitz 100 MHR is an LVDT that has been found suitable. The LVDT core is attached to a nut bonded with epoxy cement to the center of the specimen. Outputs of the LVDT and the load cell of the electrohydraulic testing machine through which loads are applied and controlled are fed to any suitable recorder. The repeated flexure apparatus is enclosed in a controlled-temperature cabinet capable of controlling temperatures within 0.5 F (0.28 C). A Missimer Model-100 x 500-CO_2 plug-in temperature conditioner has been found to provide suitable temperature control.

SPECIMEN PREPARATION

Beam specimens 15 in. (381 mm) long, 3.5 in. (88.9 mm) deep, and 3.25 in. (82.5 mm) wide are prepared according to ASTM D 3202 or the asphalt concrete beam preparation method described under the specimen preparation and compaction processes section of this Special Report. If there is undue movement of the mixture under the compactor foot during beam compaction, then temperature, foot pressure, and number of tamping blows should be reduced. Similar modifications to compaction procedures should be made if specimens with less density are desired. A diamond blade masonry saw is used to cut test specimens 3 in. (76.2 mm) or slightly less deep and 3 in. (76.2 mm) or slightly less wide from the 15-in.-long (381-mm-long) beams. Specimens with suitable dimensions also may be cut from pavement samples. The widths and depths of the specimens are measured to the nearest 0.01 in. (0.254 mm) at the center and at 2 in. (50.8 mm) on both sides from the center. Mean values are determined and used for subsequent calculations.

TEST PROCEDURES

The repeated flexure apparatus loading clamps are adjusted to the same level as the reaction clamps. The specimen is clamped in the fixture by using a jig to position the centers of the 2 loading clamps 2 in. (50.8 mm) from the center of the beam and to position centers of the 2 reaction clamps 6.5 in. (165.1 mm) from beam center. Double layers of Teflon sheets are placed between the specimen and the loading clamps to reduce friction and longitudinal restraint caused by the clamps.

After the beam has reached the desired test temperature, repeated loads are applied. The duration of a load application is 0.1 s; the rest period between loads is 0.4 s. The applied load should be that which produces an extreme-fiber stress level suitable for flexural-fatigue tests. For fatigue tests on typical bituminous concrete paving, the following ranges of extreme-fiber stress levels are suggested:

1. 55 F (12.78 C) and 150 to 400 lbf/in.^{2} (1035 to 2760 kPa),
2. 70 F (21.11 C) and 75 to 300 lbf/in.^{2} (517.5 to 2070 kPa), and
3. 85 F (29.44 C) and 35 to 200 lbf/in.^{2} (241.5 to 1380 kPa).

The beam center-point deflection and applied dynamic load are measured immediately after 200 load applications for calculation of ϵ, σ, and E_s.

The flexural modulus may be determined for other extreme-fiber stress levels and for other temperatures. The described apparatus and procedures have been found suitable for flexural modulus tests at temperatures ranging from 40 to 100 F (4.44 to 37.78 C) and for extreme fiber levels up to 400 lbf/in.^{2} (2760 kPa). The extreme-fiber stress level for flexural modulus tests at any temperature should not exceed that which causes specimen fracture before at least 1,000 loads are applied.

PRESENTATION OF RESULTS

The report of flexural stiffness modulus test results should include the following:

1. Density of test specimens;
2. Length, width, and depth of specimens;
3. Number of load applications if other than 200;
4. Specimen temperature;
5. σ;
6. ϵ; and
7. E_s.

E_s is strongly dependent on temperature and also quite dependent on stress. This behavior may be shown graphically by plotting E_s versus σ for each test temperature.

INDIRECT TENSILE TEST

Procedures for the determination of Poisson's ratio ν, modulus of elasticity E, and tensile strength S_T of pavement materials by using the indirect tensile test are described in this section. The indirect tensile test involves loading a cylindrical specimen with compressive loads that act parallel to and along the vertical diametrical plane as shown in Figure 20. To distribute the load and maintain a constant loading area, the compressive load is applied through a 0.5-in.-wide (12.7-mm-wide) steel loading strip that is curved at the interface with the specimen and has a radius equal to that of the specimen.

This loading configuration develops a relatively uniform tensile stress perpendicular to the direction of the applied load and along the vertical diametrical plane that ultimately causes the specimen to fail by splitting or rupturing along the vertical diameter (Figure 21). By measuring the applied load at failure and by continuously monitoring the loads and the horizontal and vertical deformations of the specimen, one can estimate S_T, ν, and E.

TEST EQUIPMENT

The basic testing apparatus includes a loading system and a means of measuring the applied loads, horizontal deformations of the specimens, and vertical deformations of the specimens.

The loading system consists of loading equipment, a loading device, and loading strips. The external load can be supplied by any loading system that can apply compressive loads preferably at a prescribed loading rate. Ideally, a closed loop electrohydraulic system should be used to accurately control the loading rate. A relatively high deformation rate should be used to simulate rapidly applied pavement loadings. A deformation rate of 2 in./min (0.84 mm/s) has been used although difficulties with measuring and recording loads and deformations have been experienced.

Some type of loading device should be used to ensure that the loading platens and strips remain parallel during the test. A loading device that has proved to be satisfactory is a modified, commercially available die set with upper and lower platens constrained to remain parallel during the test. Mounted on the upper and lower platens are 0.5-in.-wide (12.7-mm-wide) steel loading strips with a curved loading surface whose radius of curvature is equal to the radius of the specimen.

DEFORMATION- AND LOAD-MEASURING EQUIPMENT

Preferably, the load should be measured by a load cell to obtain electrical readouts that can be recorded continuously. Horizontal deformations of the specimens are

Figure 20. Cylindrical splitting test specimen with compressive load being applied.

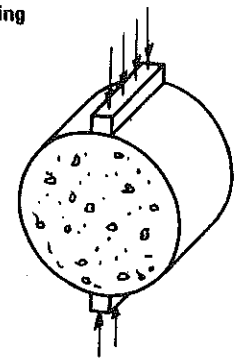

Figure 21. Cylindrical splitting test specimen failing under compressive load.

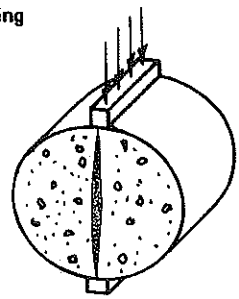

measured by using a device basically consisting of 2 cantilevered arms with attached strain gauges. Deformation of the specimen or deflection of the arms at points of contact with the specimen has been calibrated with the output from the strain gauges mounted on the arms.

Vertical deformations are measured by a direct-current LVDT. The LVDT also can be used to control the vertical deformation rate during the test by providing an electrical signal related to the relative movements of the upper and lower platens if a closed-loop electrohydraulic load system is used.

SPECIMEN PREPARATION

Cylindrical laboratory specimens or field cores can be tested. However, care should be exercised to ensure that the specimen does not have significant surface irregularities that will interfere with the proper seating contact between the specimen and the loading strips. The maximum size of the specimen is limited by the clearance in the loading device. The largest diameter specimen that can be tested in the device is approximately 6 in. (152.4 mm).

TEST PROCEDURE

Six steps make up the indirect tensile test procedure.

1. Determine the height and diameter of the specimen.
2. Carefully center the specimen on the lower loading strip.
3. Slowly lower the upper platen until light contact is made between the specimen and the upper loading strip.
4. Place the horizontal deformation measuring device with light contact between the arms and the specimen.
5. Load the specimen at a constant deformation rate.
6. Record the load versus horizontal deformation and load versus vertical deformation.

CALCULATION OF TENSILE PROPERTIES

The theoretical relationships used in calculating E, ν, and S_T are complex and require integration of various mathematical functions. However, by assuming a specimen diameter, one can make the required integrations and simplify the relationships. These simplified relationships for calculating E, ν, S_T, and total tensile strain at failure ϵ_T for

4-in.-diameter (101.6-mm-diameter) and 6-in.-diameter (152.4-mm-diameter) specimens with a 0.5-in.-wide (12.7-mm-wide) curved loading strip are as follows (1 in. = 25.4 mm; 1 lbf/in.^{2} = 6.9 kPa):

Tensile Property	4-In.-Diameter Specimen	6-In.-Diameter Specimen
S_T, lbf/in.^{2}	$0.156 \frac{P_{fail}}{h}$	$0.105 \frac{P_{fail}}{h}$
ν	$\frac{0.0673DR - 0.8954}{-0.2494DR - 0.0156}$	$\frac{0.04524DR - 0.6804}{-0.16648DR - 0.00694}$
E, lbf/in.^{2}	$\frac{S_H}{h}[0.9976\nu + 0.2692]$	$\frac{S_H}{h}[0.9990\nu + 0.2712]$
ϵ_T	$X_{TF}\left[\frac{0.1185\nu + 0.03896}{0.2494\nu + 0.0673}\right]$	$X_{TF}\left[\frac{0.0793\nu + 0.0263}{0.1665\nu + 0.0452}\right]$

where

P_{fail} = total load at failure in pounds (kilograms),
h = height of specimen in inches (millimeters),
DR = deformation ratio $\frac{Y_T}{X_T}$ = the slope of line of best fit between vertical deformation Y_T and the corresponding horizontal deformation X_T up to P_{fail},
S_H = horizontal tangent modulus $\frac{P}{X_T}$ = the slope of the line of best fit between load P and X_T for loads up to P_{fail}.

It is recommended that the line of best fit be determined by the least squares method.

TESTING FOR SHEAR MODULUS AND DAMPING OF SOILS BY THE RESONANT COLUMN METHOD

The resonant column method of testing has been described in detail elsewhere (3). This method covers the determination of the shear modulus and damping capacity of cylindrical specimens of soils either in undisturbed or remolded conditions by vibration by means of the resonant column technique. The vibration apparatus and specimen may be enclosed in a triaxial chamber and subjected to an all-around pressure and axial load. The test is considered nondestructive when the strain amplitude caused by vibration is less than about 10^{-4} in./in. (mm/mm). Thus many measurements may be made on the same specimen for various states of confining pressure. Because the modulus of pavement materials is strain (and stress) dependent, the materials should be tested at strain levels similar to those existing in the pavement.

A resonant column is defined as a cylindrical specimen or column of soil attached to a rigid pedestal of sufficient inertia to make the motion of the attached end of the specimen essentially 0 during vibration of the specimen. An apparatus is attached to produce sinusoidal excitation and measure the vibration amplitude of the end of the specimen. The frequency of excitation is adjusted to produce resonance of the system (column), which is composed of the specimen and the attached excitation apparatus. The system resonant frequency in this test is the frequency at which the sinusoidal excitation force is in phase with the velocity of the vibration end of the specimen. For low damping, it is permissible to assume that this frequency will correspond to a value that produces maximum amplitude of displacement. The dynamic shear modulus and damping capacity can be calculated from the results of the resonant column test. The shear modulus is assumed to be the elastic shear modulus of a uniform, linearly elastic specimen of the same mass, density, and dimensions as the soil specimen used in the resonant column test. The modulus of elasticity E is determined

$$E = 2G(1 + \nu)$$

where

G = dynamic shear modulus, and
ν = dynamic Poisson's ratio.

When using this method, one should remember that the E of paving materials is significantly influenced by the strain amplitude at which the test is performed. Therefore, a strain amplitude should be used that is representative of what the specimen will be subjected to in the field.

SIMPLIFIED TEST METHOD FOR DETERMINING THE RESILIENT MODULUS OF COHESIVE SOILS

The simplified test method described in this chapter is similar to the method for cohesive soils described in the section on resilience testing of unstabilized soils. This simplified method is part of a production-type resilience testing procedure that has been developed for and used extensively with fine-grained cohesive soils. A more complete description of the simplified testing procedure is given elsewhere (4).

In general, the procedure consists of preparing sets of at least three 2-in.-diameter (50.8-mm-diameter) by 4-in.-high (101.6-mm-high) cylindrical specimens by using a miniature kneading compactor. The specimen sets are prepared at moisture and density conditions representative of expected field conditions and then are tested by using the simplified method.

The method takes advantage of the simplicity, ease of testing, and minimal equipment requirements normally associated with an unconfined compression-type repeated load test (i.e., $\sigma_3 = 0$). Because no confining pressure is required, a triaxial cell is not needed.

Justification for not using a confining pressure during the testing of cohesive soils lies in the fact that (a) the magnitude of confining pressure normally encountered in a subgrade is typically in the range of 1 to 5 lbf/in.^{2} (6.9 to 34.5 kPa) and (b) the effect of small magnitudes of confining pressure on the resilient response of fine-grained cohesive soils is very slight and typically is less than "between specimen" testing variability.

An additional advantage inherent in the simplified method is the use of an LVDT mounted in line with the longitudinal axis of the test specimen, which eliminates the need for mounting deformation measuring equipment on the specimen. It is important that the LVDT be mounted in this position because of the effect that eccentricity has if the LVDT is mounted to the side. A schematic diagram of the mounting position of the LVDT and the resilience testing equipment is shown in Figure 22.

As indicated in the section on fundamental considerations, something such as LVDT clamps or optical tracking equipment should be used for deformation measurement if the resilient modulus is greater than about 15,000 lbf/in.^{2} (103 500 kPa). However, for fine-grained cohesive soils, the axially mounted LVDT is satisfactory provided a sufficiently rigid machine is used.

It is suggested that at least 3 specimens be tested for a given set of variables and that the results be averaged. The reason for this is that "between specimen" variability for typical laboratory resilient testing is substantial (typical coefficients of variation of 10 to 15 percent or higher are not uncommon for cohesive soils and this type of test); thus the results from 1 specimen may be substantially different from the average of the results from a number of specimens.

Figure 22. Repeated load testing apparatus for simplified resilient modulus test.

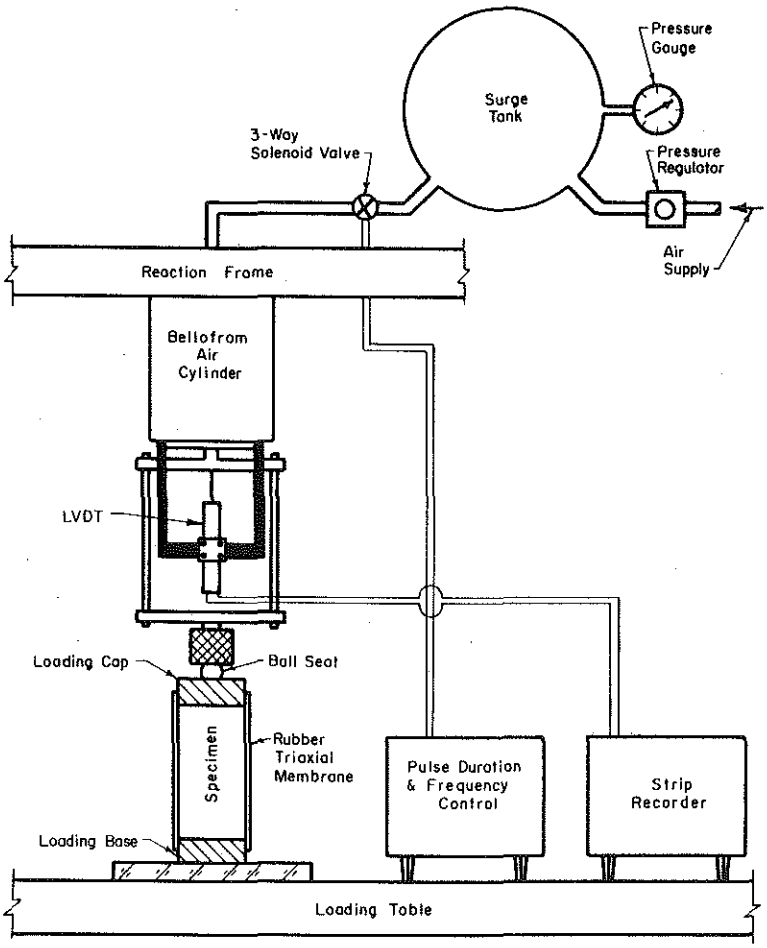

SIMPLIFIED TEST METHOD

Ten steps make up the simplified test method.

1. Carefully place the specimen on the loading base.
2. Carefully place the loading cap on top of the specimen.
3. Stretch a rubber membrane tightly over the interior surface of a membrane stretcher. Carefully slip the stretched membrane over the specimen. Roll the membrane off the stretcher onto the base and cap. Remove the stretcher. Place O-ring seals or rubber bands around the base and cap. (The purpose of the membrane is to prevent loss of moisture during the test.)
4. Place the membrane-encapsulated specimen into position in the loading machine as shown in Figure 22. A steel ball bearing is placed between the top loading cap and the axial loading device. It is important to obtain proper alignment of the specimen and axial loading device to minimize eccentricities.

Resilient properties of cohesive soils are greatly dependent on the magnitude of the deviator stress (total repeated axial stress in this case). It is therefore necessary to conduct the test over a range of deviator stress values, for example: 3, 5, 7.5, 10, 15

lbf/in.^{2} (20.7, 34.5, 51.75, 69, 103.5 kPa) and possibly higher values.

A conditioning phase is used to properly seat the loading cap and base and eliminate or minimize initial loading effects.

5. Condition the specimen with 1,000 applications (load duration of 0.060 s and cycle duration of 3 s) of an axial stress equal to about 7 lbf/in.^{2} (48.3 kPa) followed by 20 applications each of an axial stress of 3, 5, 7.5, 10, and 15 lbf/in.^{2} (20.7, 34.5, 51.75, 69, and 103.5 kPa). (Observe permanent axial deformation during the latter stages of the conditioning phase. If appreciable permanent deformation starts to accumulate, then eliminate the higher values of axial conditioning stress from the conditioning phase.)

6. Decrease the deviator stress to about 3 lbf/in.^{2} (20.7 kPa).

7. Apply approximately 10 to 20 deviator stress applications and record the resilient axial deformation.

8. Increase the axial stress level incrementally about 3 lbf/in.^{2} (20.7 kPa).

9. Repeat step 7.

10. Repeat step 8 and step 7 until the desired upper value of axial stress is reached. An upper value of at least 20 to 25 lbf/in.^{2} (138 to 172.5 kPa) is recommended.

CALCULATIONS AND PRESENTATION OF RESULTS

The results of the resilience test can be presented in the form of a summary table or graphically as in Figures 2 and 10.

REFERENCES

1. R. D. Barksdale and R. G. Hicks. Material Characterization and Layered Theory for Use in Fatigue Analyses. HRB Special Rept. 140, 1973, pp. 20-48.
2. H. B. Seed et al. Prediction of Flexible Pavement Deflections From Laboratory Repeated-Load Tests. NCHRP Rept. 35, 1967.
3. B. O. Hardin. Suggested Methods of Test for Shear Modulus and Damping of Soils by Resonant Column. ASTM Special Technical Publication 479, 1970.
4. Q. L. Robnett and M. R. Thompson. Resilient Properties of Subgrade Soils, Phase 1—Development of Testing Procedure. Univ. of Illinois at Urbana-Champaign, Interim Rept., Civil Engineering Studies, Series 139, May 1973.